REPORT NO. FRA/ORD-78/43A

CLAIRE
OR TOSS

X TRP

VSS Demo Program Part 2
Model Development & Data Anal.

VSS DEMONSTRATION PROGRAM

PART 2
MODEL DEVELOPMENT AND DATA ANALYSIS

WYLE LABORATORIES
SCIENTIFIC SERVICES AND SYSTEMS GROUP
4620A EDISON AVENUE
COLORADO SPRINGS, COLORADO 80915

FEBRUARY, 1979

FINAL REPORT

Document is available to the U.S. public
through the National Technical Information Service
Springfield, Virginia 22161

Prepared for

U.S. DEPARTMENT OF TRANSPORTATION
FEDERAL RAILROAD ADMINISTRATION
OFFICE OF RESEARCH AND DEVELOPMENT
WASHINGTON, D.C. 20590

VSS DEMONSTRATION PROGRAM

PART 2
MODEL DEVELOPMENT AND DATA ANALYSIS

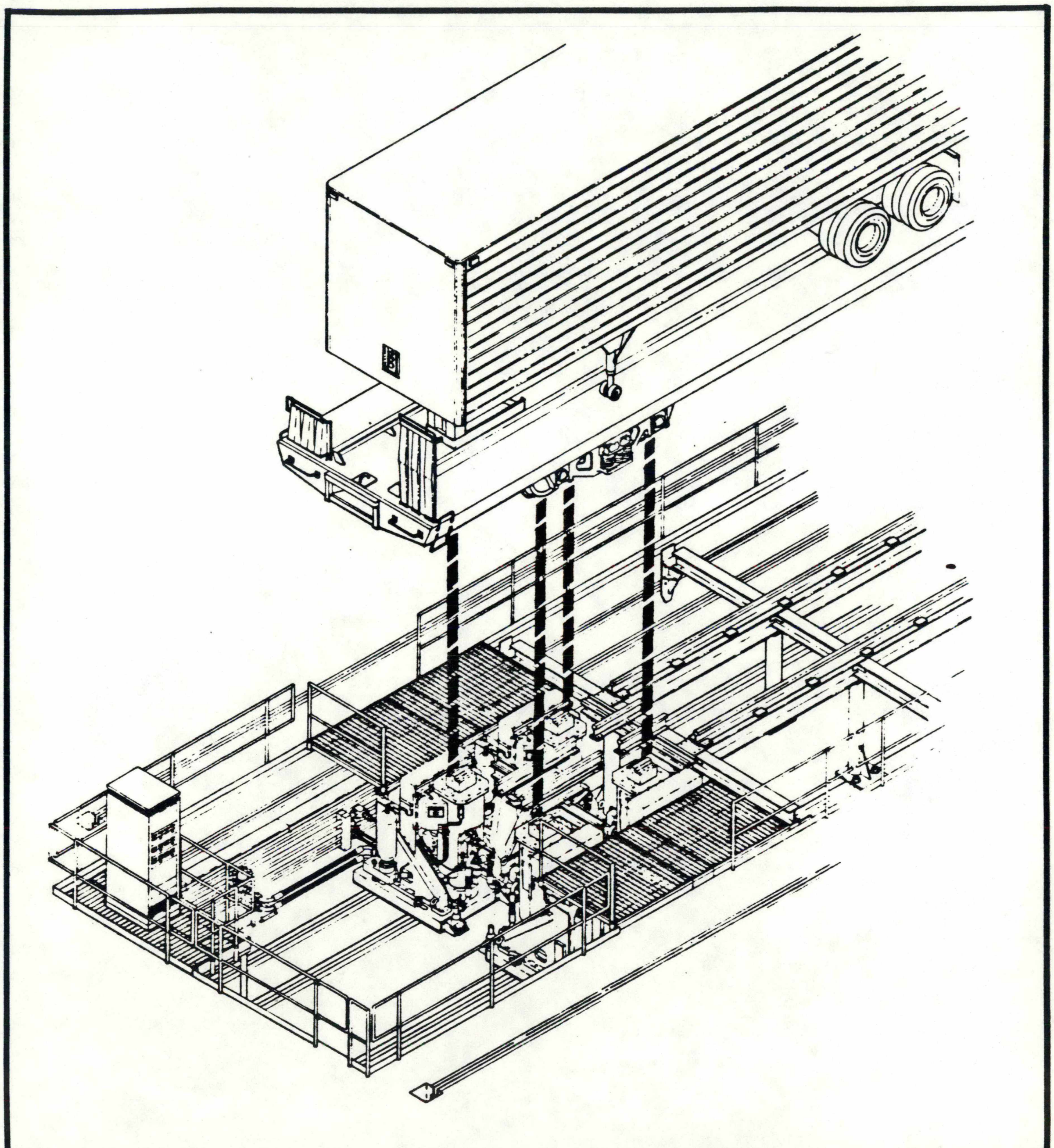

WYLE LABORATORIES

SCIENTIFIC SERVICES AND SYSTEM GROUP
COLORADO SPRINGS DIVISION

Technical Report Documentation Page

1. Report No.	2. Government Accession No.	3. Recipient's Catalog No.
FRA/ORD-78/43A		

4. Title and Subtitle
VSS Demonstration Program
Part 2 - Model Development and Analysis

5. Report Date
February 1979

6. Performing Organization Code

7. Author(s)
David Gibson, Michael Healy

8. Performing Organization Report No.

9. Performing Organization Name and Address
Wyle Laboratories
Scientific Services and Systems Group
4620A Edison Avenue
Colorado Springs, CO 80915

10. Work Unit No. (TRAIS)

11. Contract or Grant No.
DOT-FR-64200

12. Sponsoring Agency Name and Address
U.S. Department of Transportation
Federal Railroad Administration
Office of Research and Development
Washington, DC 20590

13. Type of Report and Period Covered
Final Report

14. Sponsoring Agency Code
FRA/RRD-11

15. Supplementary Notes
Part 1 of this document includes system performance evaluation information.
FRD Report #1

16. Abstract

The Vertical Shaker System (VSS) was the initial test program to be conducted at the Rail Dynamics Laboratory. The objectives of this program were to demonstrate the performance and capabilities of the VSS and to accumulate test data to be used in checking the validity of analytical models. The experiments were performed on three different load configurations of a trailer-on-flatcar. The test program was found to be successful. Pretest planning, to specify input levels and motion requirements, was essential to effective VSS operation. Log books, used to record program events as they occurred, were found to be invaluable in post test analyses.

Part 2 of the report includes a description of the analytical model development of the TOFC configurations, documentation of the associated time domain computer program, test data used to verify the analytical models of the TOFC configurations, and a description of the process of verification.

17. Key Words
Vertical Shaker System; Trailer-on-Flatcar; Wheel/Rail Interface; Vertical Input; Cross Level Input; Discrete Frequency Dwell and Decay; Cross-Coupling, Analytical Model Development

18. Distribution Statement
Document is available to the public through the National Technical Information Service, Springfield, VA 22161

19. Security Classif. (of this report)	20. Security Classif. (of this page)	21. No. of Pages	22. Price
Unclassified	Unclassified	262	

NOTICE

NOTICE

TABLE OF CONTENTS

Section
~~Paragraph~~ Page

TABLE OF CONTENTS (Cont'd)

SECTION 8 - CONCLUSIONS

APPENDICES

REFERENCES

LIST OF FIGURES

SECTION 6 - DATA ANALYSIS (Cont'd)

SECTION 7 - NONLINEAR PROGRAM DEVELOPMENT

SECTION 7 - NONLINEAR PROGRAM DEVELOPMENT (Cont'd)

APPENDIX D

LIST OF TABLES

SECTION 1 - INTRODUCTION

1.1 BACKGROUND

The Rail Dynamics Laboratory (RDL) at the Transportation Test Center (TTC) near Pueblo, Colorado has been designed and developed by the Federal Railroad Administration (FRA) to provide a laboratory in which basic studies in the areas of wheel/rail interaction, truck and suspension system design, vehicle body response and safety standards can be performed in a safe, controlled and economical environment.

The Vertical Shaker System (VSS) is the first phase in the development of the RDL. The primary purpose of the VSS is the study of sinusoidal excitation of rail vehicles to determine their structural dynamic characteristics. The VSS consists of four vertical hydraulic shakers capable of driving two axle sets of a rail vehicle to a sinusoidal environment at magnitudes representative of vertical track profiles. The rail vehicle can have wheel loads up to 40,000 pounds. Wyle Laboratories was responsible for the design, engineering, fabrication and system integration of the VSS and for the conduct of an acceptance and a performance demonstration test program.

1.2 SCOPE

The objectives of the VSS Demonstration Program were to demonstrate VSS performance and capabilities and to train the RDL operational personnel in its use. A test plan was developed that incorporated a trailer-on-flatcar (TOFC) as the test specimen designated for use during the test. Prior to testing, analytical models of the TOFC were developed to aid the structuring of definitive test procedures. Based on the results of response analyses performed using these analytical models, shaker force parameters, vehicle limit check requirements, and instrumentation types were identified.

A six week test and training program was performed using as the test specimens three configurations of the TOFC. During the conduct of the test program, data and information were obtained that allowed for the demonstration and evaluation of:

- a. Excitation system capabilities
- b. Range of allowable input regimes
- c. Control system performance
- d. Operating procedures
- e. Data acquisition system adequacies
- f. Data analysis capabilities
- g. Maintenance procedures.

Results of the VSS demonstration and evaluation were presented in this first part of the Demonstration Program report. This second part of the Demonstration Program Report will include a description of the analytical model developed for the TOFC configurations and an analysis of the test data acquired during the program.

The analytical model was developed to aid in test planning and data analysis. The model was based on finite element idealization as discussed in the following section.

SECTION 2 - FINITE ELEMENT MODELING

2.1 BACKGROUND

The practical application of the finite element modeling technique had its advent in the structural analysis of high performance aircraft and spacecraft structures. Most early aircraft could be approximated by a collection of beam-like one dimensional structures, but modern aircraft began to adapt theories to aircraft structure which viewed them as an assemblage of a finite number of elastic components. In all of these applications matrix formulations were developed as a means of organizing the bookkeeping. The numerical solutions were then reduced to a process of addition, subtraction, multiplication, inversion, and the determination of the characteristic eigenvectors of the matrices. However, the handling of the matrices for any problem of greater than few degrees of freedom by hand or desk calculator was a formidable exercise. Fortunately the development of the high speed digital computer occurred coincidentally with this requirement for handling a large volume of calculations. The combination of finite element modeling techniques and the high speed digital computer resulted in a fast and accurate way of analyzing complex structures.

The finite element modeling technique embodies a lumped element approach, wherein the distributed physical properties of a structure are represented by a model consisting of a finite number of idealized substructures or elements that are interconnected at a finite number of grid points, to which loads or constraints can be applied. The grid point definition forms the basic framework for the structural model between which structural elements may be placed.

Analysis of the trailer-on-flatcar (TOFC) configuration lends itself to the finite element technique. It is a complex system with many interconnected flexible components which requires a detailed model to adequately idealize the structure. The approach taken for the frequency domain model was to utilize one of the commercially available general purpose computer programs for the development and analysis of the finite element model.

relationship

to come ?

Analysis System (ANSYS) which was developed and is being maintained and advanced by the personnel of Swanson Analysis Systems, Inc. It utilizes the matrix displacement method of analysis based upon finite element idealizations.

2.2 APPLICATION TO TRAILER-ON-FLATCAR

The ANSYS program was used to obtain finite element models of the flatcar and the two trailers. These models were then combined with flatcar truck and trailer suspension models to develop complete models of the various test configurations. The models could then be analyzed to obtain static deflections, normal modes and frequencies, responses to sinusoidal inputs, and transient decay responses. The purpose in obtaining this data was for use in pretest planning, to aid in real time test control, and for use in posttest analysis of test data.

The input levels and preliminary limit check requirements for use in the VSS - Demonstration Test Procedure were developed using the finite element models of the various configurations. A discussion of the limit checks and input levels actually used are contained in Part 1 of this report. Utilizing these models, tables of pretest predicted responses at various locations on the test specimen were prepared for use in real time evaluation of test data. These tables were used to evaluate response data, to establish revised limit checks values and to revise input levels for follow on tests.

In the posttest analysis of the test data, the model parameters were varied as an aid in identifying test resonant frequencies. Upon establishing the major resonant frequencies of each configuration, the model parameters were varied to obtain the best agreement between model prediction and test data. The results of this posttest analysis of the data is contained in Section 5.

2.3 ANSYS COMPUTER PROGRAM

The ANSYS computer program is a large scale general purpose computer program for the solution of engineering analysis problems. The matrix displacement method of analysis based upon finite element idealization is employed throughout. This report will not detail the analysis methods or programming techniques used by the ANSYS program. Reference 2 contains a description of the analysis methods and details of the programming techniques required to run ANSYS. Reference 4 contains the theoretical development of structural dynamics methods used in supportive analyses. However, certain features of the ANSYS program are discussed in the following sections as an aid in understanding the TOFC model and analysis results. The various analyses performed on the TOFC configurations using ANSYS are discussed in detail in Section 3 along with selected results of these analyses.

2.3.1 Dynamic Matrix Reduction

Using the finite element technique for a complex structure such as the TOFC results in a structural model with a large number of degrees-of-freedom (dof). The flatcar model alone has 720 dof in its idealization. However, it is unnecessary to conduct the dynamic analyses with the total number of dof. Rotational dof and selected translational dof can be reduced from the dynamic model without affecting the dynamic characteristics of the lower frequency modes. ANSYS uses the Guyan reduction procedures for reducing the number of dof for dynamic analyses. This technique preserves the potential energy of the system but modifies, to some extent, the kinetic energy.

The dynamic matrix reduction is accomplished in ANSYS by selecting those dof which are determined by the user to be necessary to describe dynamics of the system. The flatcar structure was represented by 32 dof. The program then takes the complete mass and stiffness matrices and reduces the order of these matrices down to the specified number of dof using consistent matrix condensation.

Many sets of dynamic dof which will provide acceptable results from an analysis are possible. Experience has shown that for models such as the TOFC, neglecting stretching modes, selecting rotational inertia dof, and choosing dynamic dof at least equal to two or three times the number of modes of interest will result in reasonable lower modes and responses.

2.3.2 Damping

Damping may be included in structural response determination by several methods: uniform mass or structural damping, material dependent damping, and lumped damping elements. The damping in the trucks and trailer suspension systems was described by using the lumped damping elements. Uniform structural damping was used for the flatcar and trailer bodies. In this case the damping matrix is obtained by multiplying β times the stiffness matrix, where $\beta \equiv \xi / \pi f$ and ξ is a modal damping ratio and f is a frequency. Since only a single value of β is allowed, the user must select the most dominant natural frequency for the computation of β. For this case the higher frequencies will be damped more, and lower frequencies will be damped less.

SECTION 3 - FINITE ELEMENT MODELS

3.1 FLATCAR

3.1.1 Structure

The flatcar body structure was modeled using the ANSYS program. The flatcar drawings listed in Table 3-1 were used to determine the geometry of the flatcar. Based on that information the node point locations and structural model idealization shown in Figure 3-1 were defined. Each of the structural node points was assigned a number and structural members were identified and connected between the node points. Typical cross sections of the flatcar are shown in Figure 3-2. ANSYS three dimensional beam elements were used to model the flatcar structural members for connecting the grid points. The flatcar weight not taken into account by the beam elements was added as lumped mass at the appropriate node points. The total weight of the model was adjusted to agree with the actual flatcar weight. Section properties were calculated for each of the beam elements which make up the flatcar structure using the drawings in Table 3-1. The model includes a beam element model of the trailer hitches (as described in Section 3.1.3) and node point locations for the trailer tires as shown in Figure 3-1.

The resulting model for the flatcar structure has 80 node points with six dof at each node point for a total of 480 dof. The number of dof were then reduced using the dynamic matrix reduction technique of ANSYS. The flatcar body has eleven retained node points with 26 dof chosen as shown in Figure 3-3. The trailer hitches add two node points and eight dof. The resulting reduced mass, stiffness, and damping matrices were written on tape and stored to be recalled later for additional analyses.

3.1.2 Trucks

The model for the trucks consisted of two node points for each truck with 3 dof at each node point. Springs and dampers were used to connect the node points to account for the flexibility of the truck. Rigid beams with the mass lumped at their center were used to connect the spring/damper elements as shown in Figure 3-4. The truck model was tied into the flexible flatcar model at node points 28 and 140.

Table 3-1. Drawing List

A. FLATCAR BODY (PULLMAN - STANDARD DRAWINGS)

1. Dwg M-042-622-A, General Arrangement
2. Dwg 6-B-7814, General Arrangement Model No. 5 Rigid Hitch

B. PLATFORM TRAILER (TRAILMOBILE DRAWINGS)

1. Dwg 1-0-4029, Underframe Assy 2" bolster centers
2. Dwg 1-A1-426, Main Rail Assy.
3. Dwg 3-0-430, Suspension Assy Tandem Axle

C. VAN TRAILER (TRAILMOBILE DRAWINGS)

1. Dwg 1-0-4169, Underframe Assy.
2. Dwg 3-0-425 Suspension Ass'y Tandem Axle
3. Dwg 1002-0-49, Fifth Wheel Ass'y
4. Dwg 514-0-1002, Roof Assembly

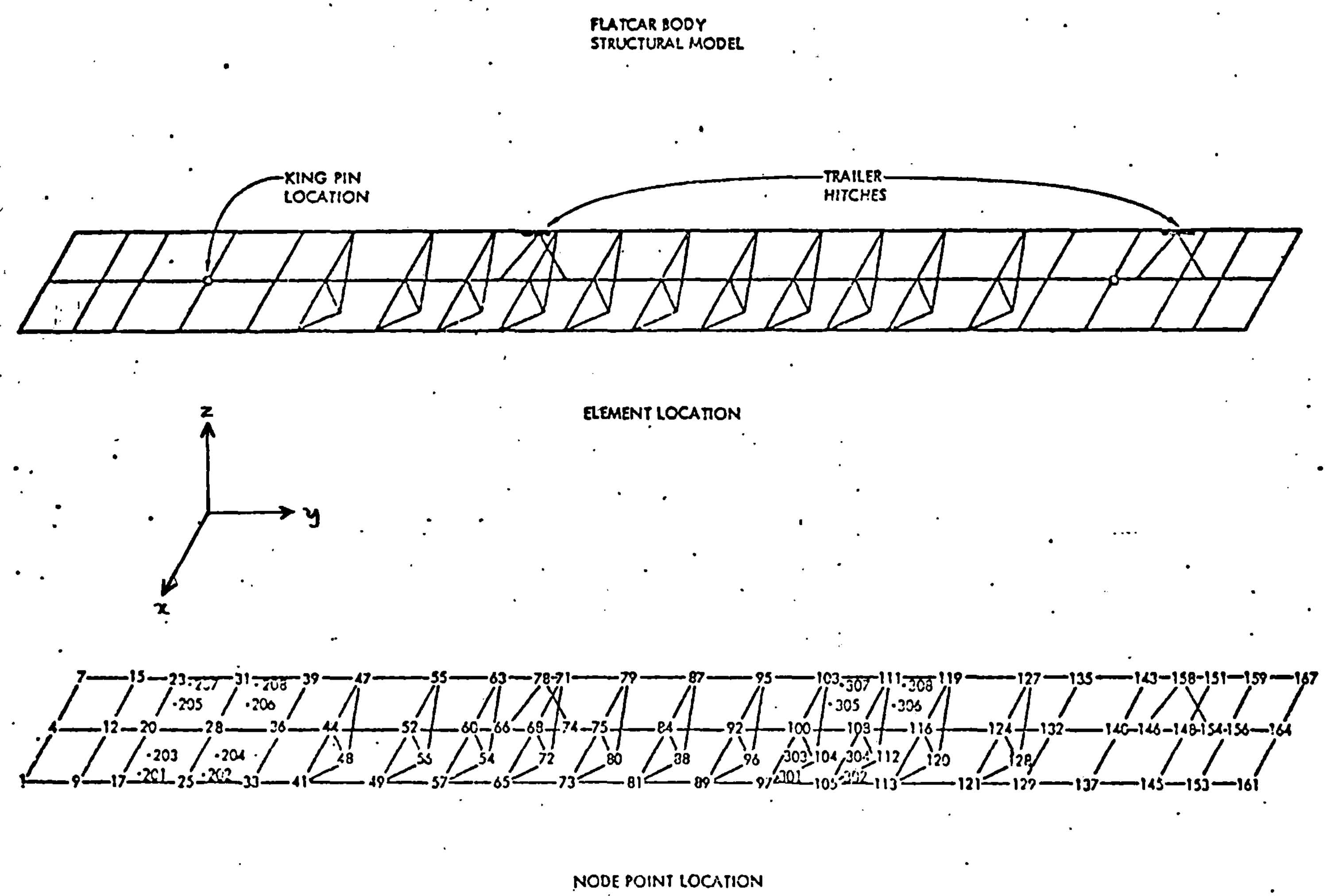

Figure 3-1. Flatcar Structural Model

FLATCAR CROSS SECTIONS

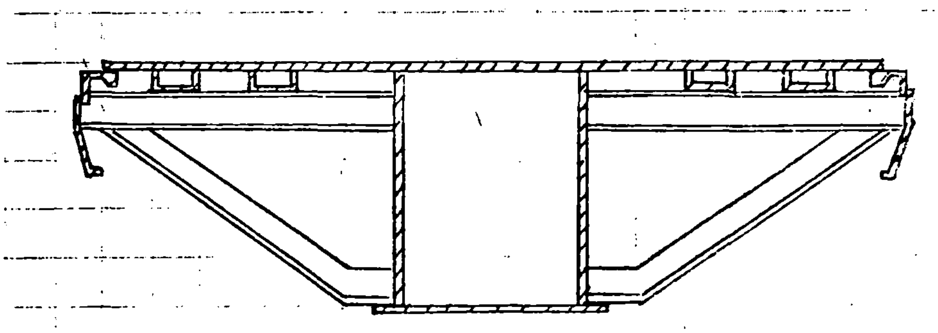

cross section at lateral support

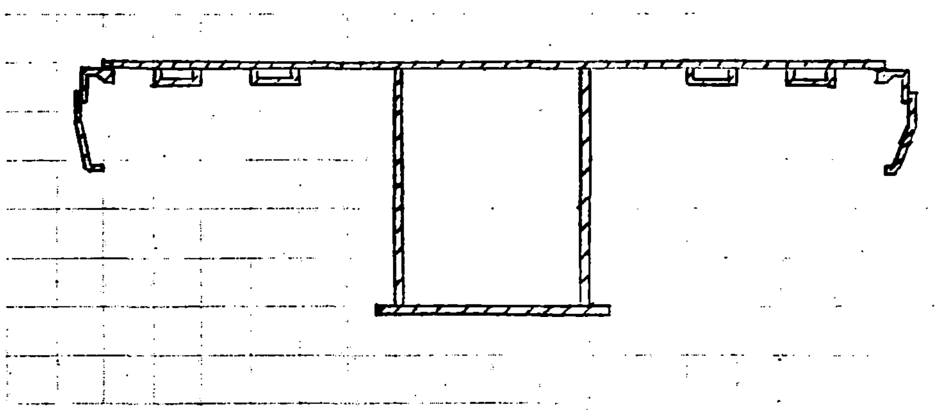

cross section between lateral supports

Figure 3-2. Typical Flatcar Cross Section

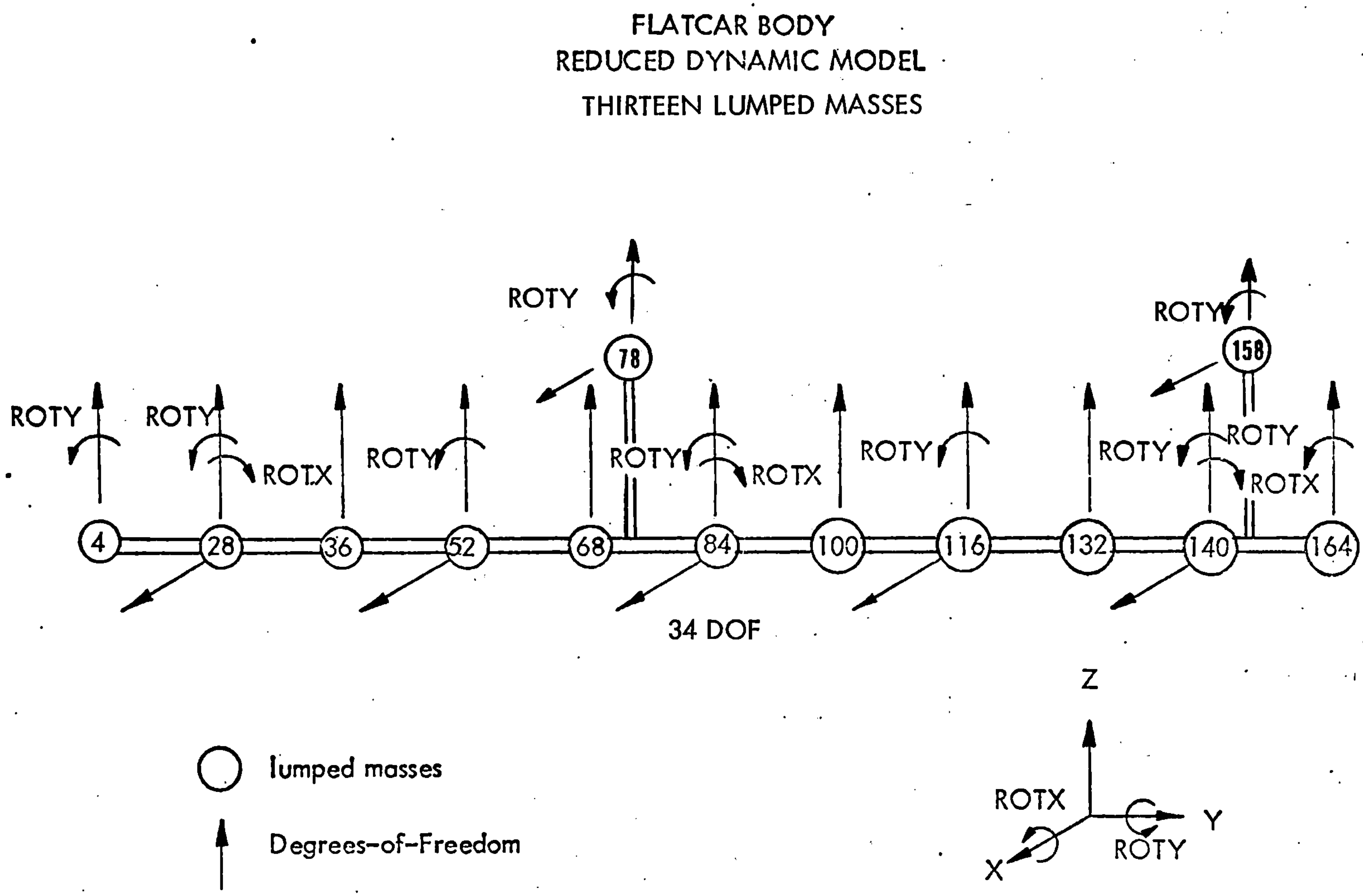

Figure 3-3. Simplified Flatcar Model

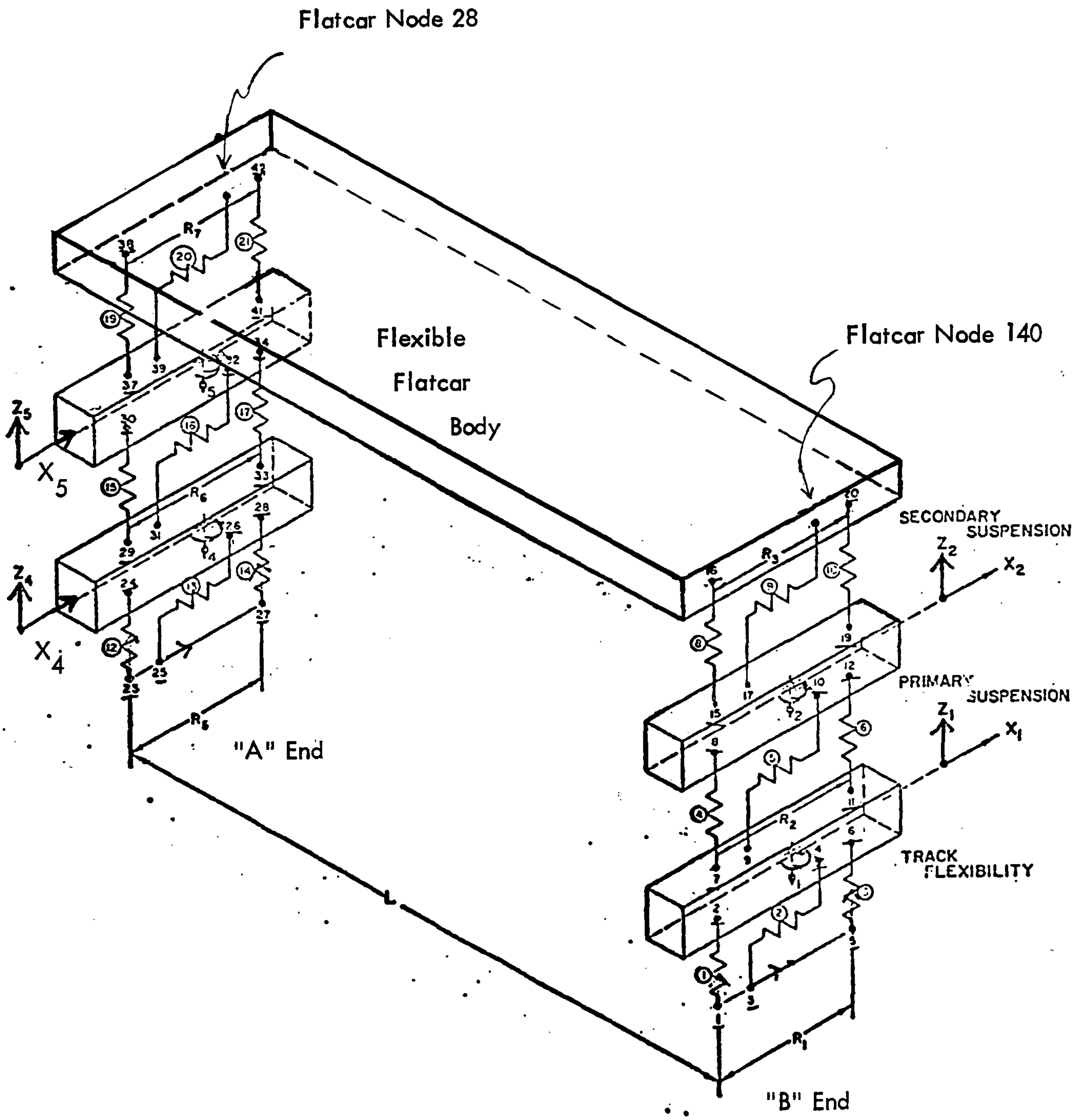

Figure 3-4. Flatcar Dynamic Model

3.1.3 Trailer Hitch

A model 5 trailer hitch was used on the TOFC to support each trailer at its forward end. The trailer hitch consists of three main members as shown in Figure 3-5. The model for the hitch consisted of two beam elements for the vertical and diagonal struts, with a node point at the top plate. The 1150 pound weight of the trailer hitch was lumped at the three node point locations comprising the three corners of the hitch. Trailer hitch spring constants were calculated for a load applied to the top of the hitch using the ANSYS model described above and are shown in Table 3-2. Their values were obtained by applying a unit load in each of the specified directions and calculating the resultant deflection.

3.1.4 Coordinate Reference System

In order to provide a common base to reference locations on the TOFC, the following coordinate system was established. The origin was placed at the "A" end of the flatcar on the center of the deck. All locations on the flatcar and both trailers were then defined in relation to this reference. The coordinates of primary locations on the TOFC are shown in Figure 3-6.

3.2 TRAILERS

3.2.1 Platform Trailer Structure

The platform trailer was modeled using the same approach as with the flatcar. Table 3-1 contains the drawing list used to model the platform trailer. The resulting structural model is shown in Figure 3-7 along with the node point numbering system. The platform trailer lading, as defined in Part 1 of this report, was modeled as lumped masses at the appropriate node points. The node points contain appropriate rotary inertia to account for the decrease in c.g. height. A dynamic matrix reduction was performed to reduce the model to 20 dof as shown in Figure 3-8. These matrices were then written on tape and stored for both the loaded and the unloaded configurations of the platform trailer.

3.2.2 Van Trailer Structure

The van trailer was initially modeled using the same approach as with the platform trailer and is shown in Figure 3-9. Early in the van trailer modeling task it was de-

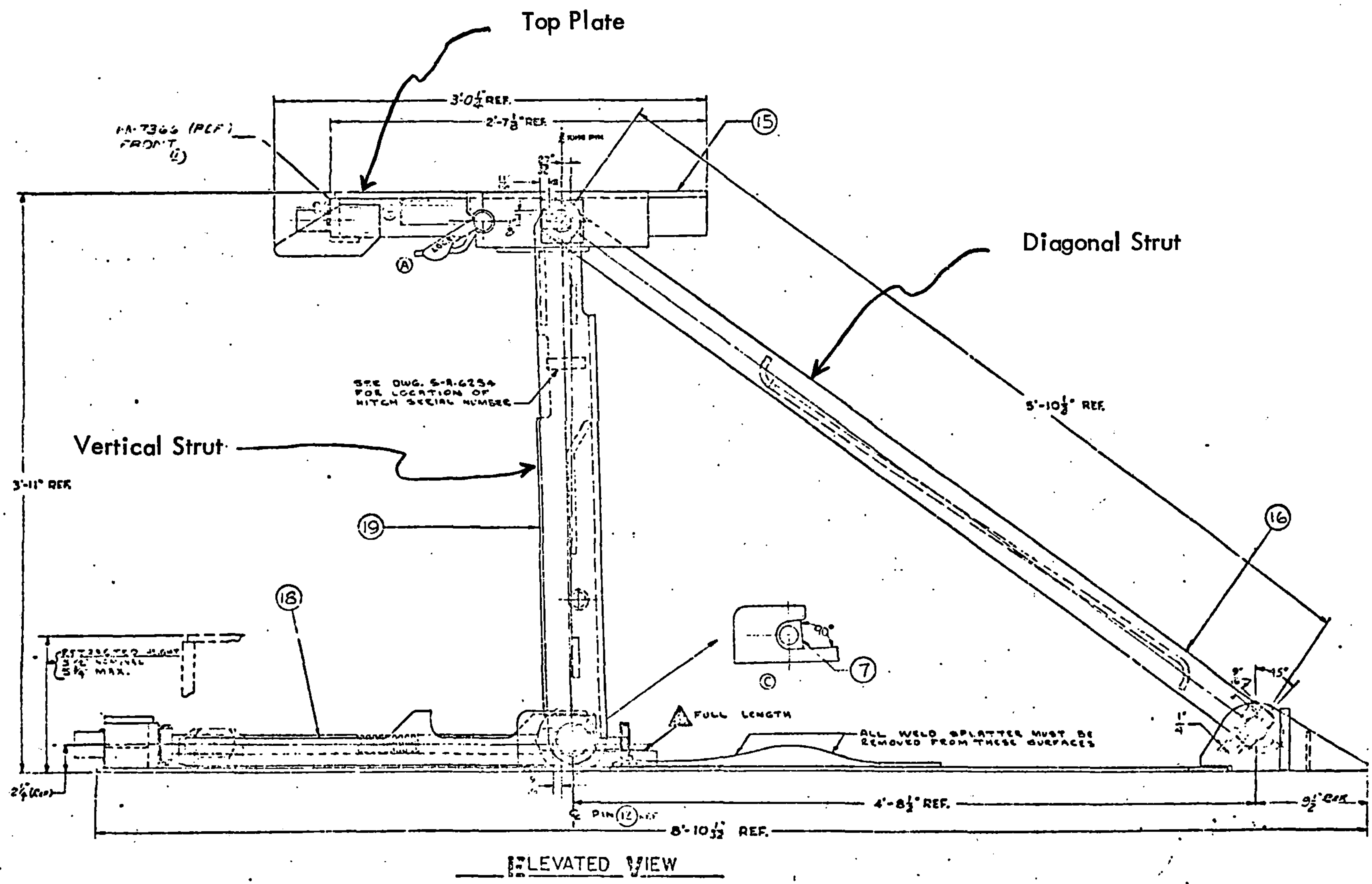

Figure 3-5. Trailer Hitch Structure

Table 3-2. Trailer Hitch Model Spring Constants

$h_x = 1.35 \times 10^5$ lbs/in

$h_y = 2.01 \times 10^6$ lbs/in

$h_z = 8.1 \times 10^6$ lbs/in

$h_{ROTX} = 1.25 \times 10^7$ in-lbs/rad

$h_{ROTY} = 1.13 \times 10^8$ in-lbs/rad

$h_{ROTZ} = 0.0$

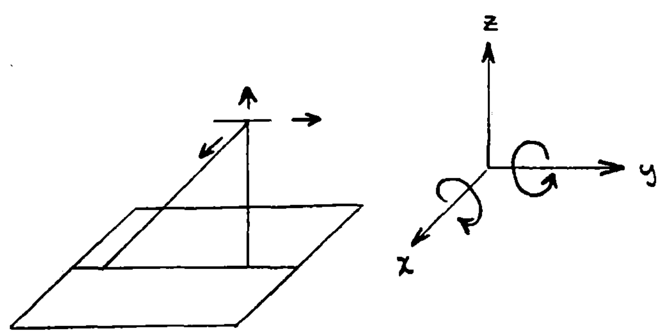

COMBINED MODEL

NODE NUMBER LOCATION

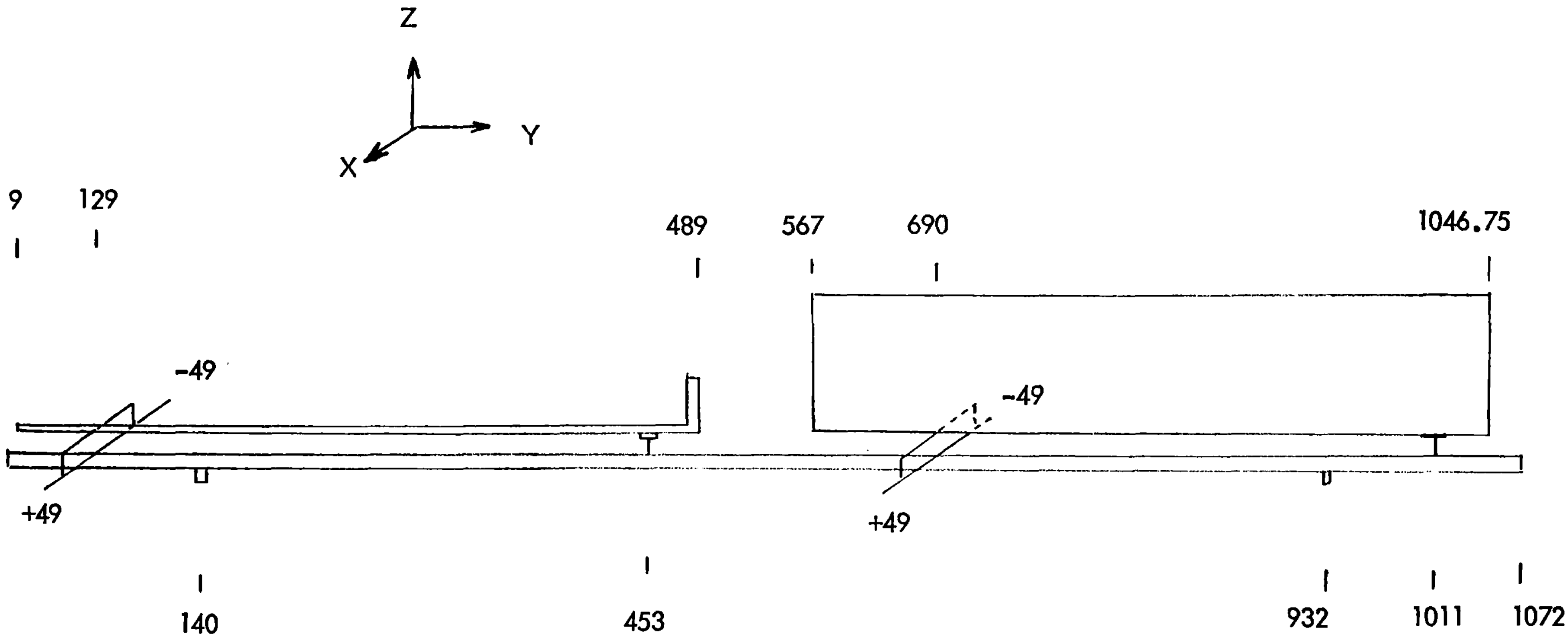

Figure 3-6. Coordinate Locations

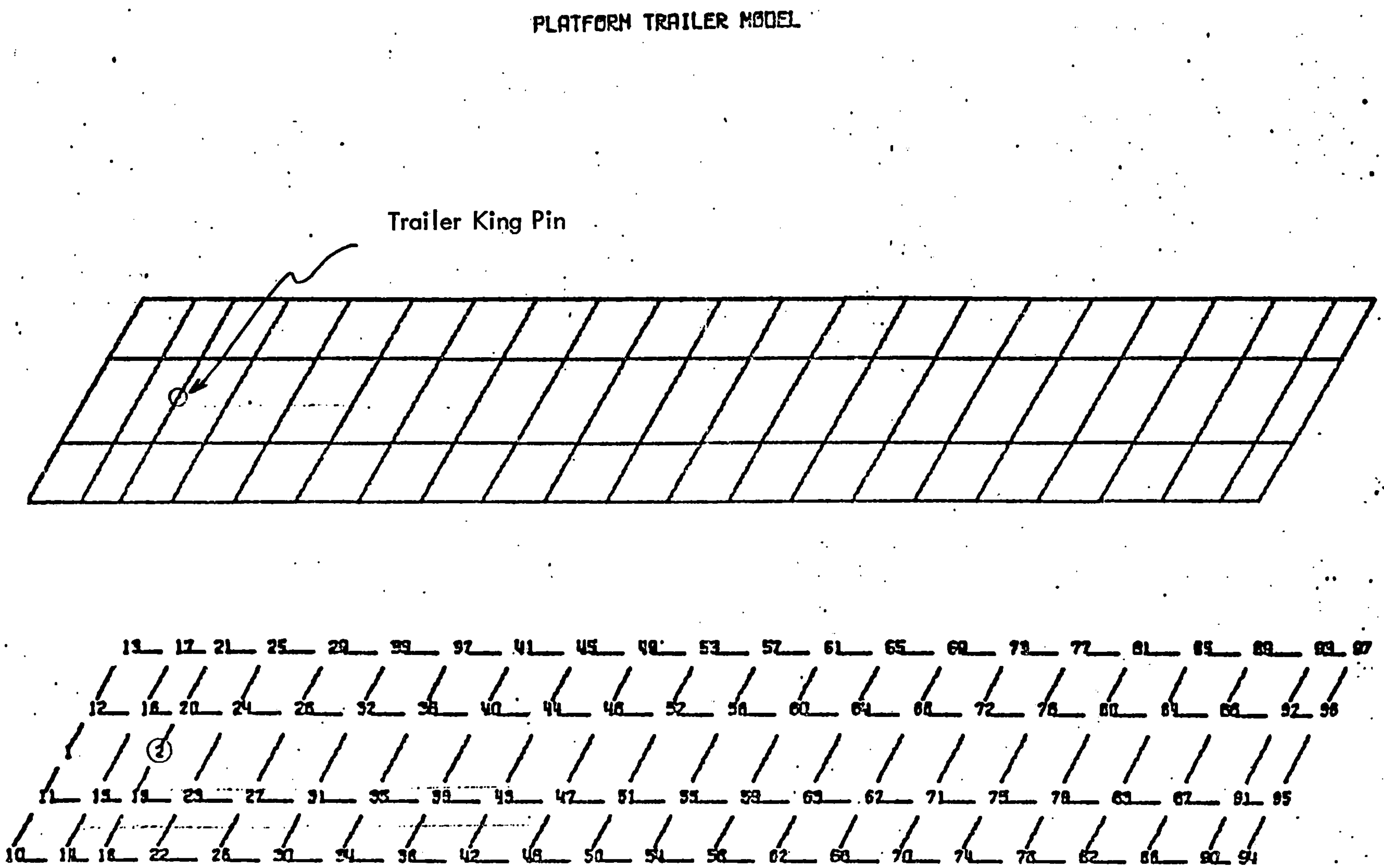

Figure 3-7. Platform Trailer Structural Model

SIMPLIFIED VAN TRAILER MODEL

Nine Node Points

20 dof

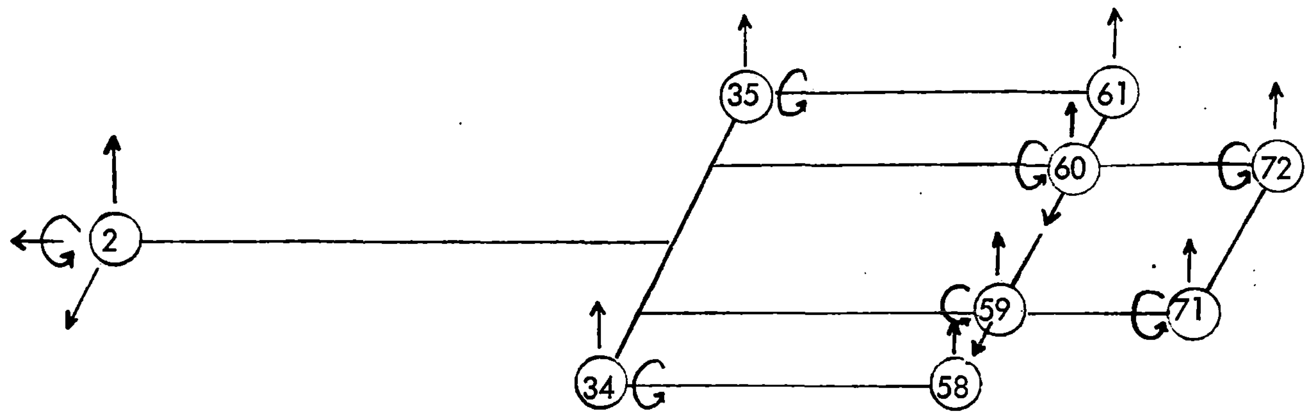

SIMPLIFIED PLATFORM TRAILER MODEL

Ten Node Points

21 dof

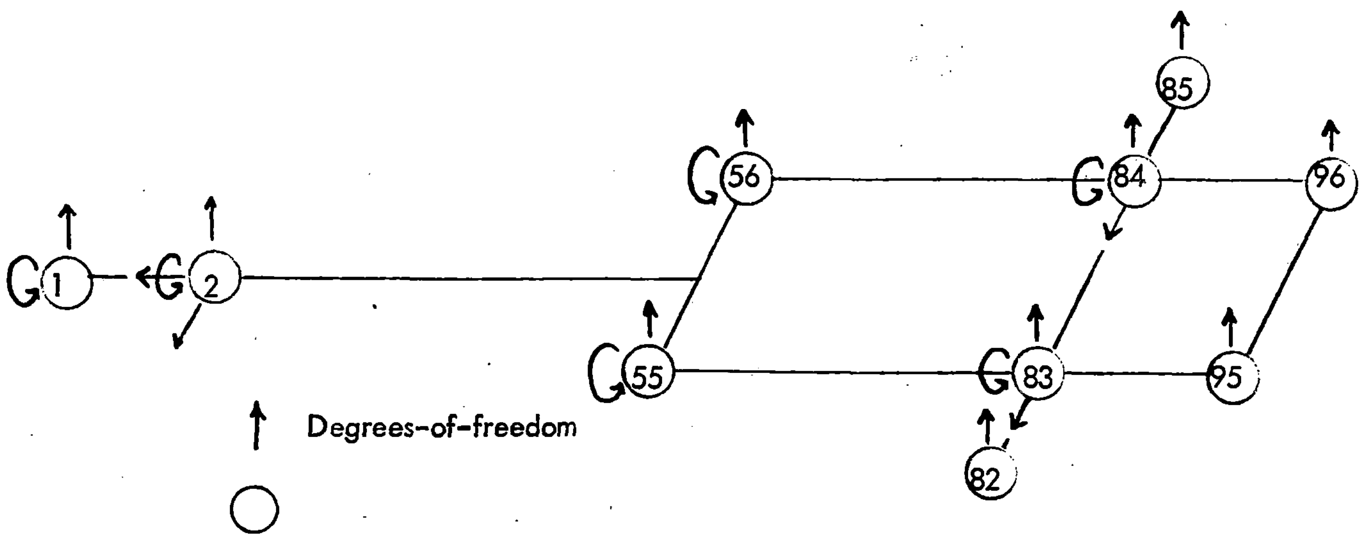

Figure 3-8. Simplified Trailer Models

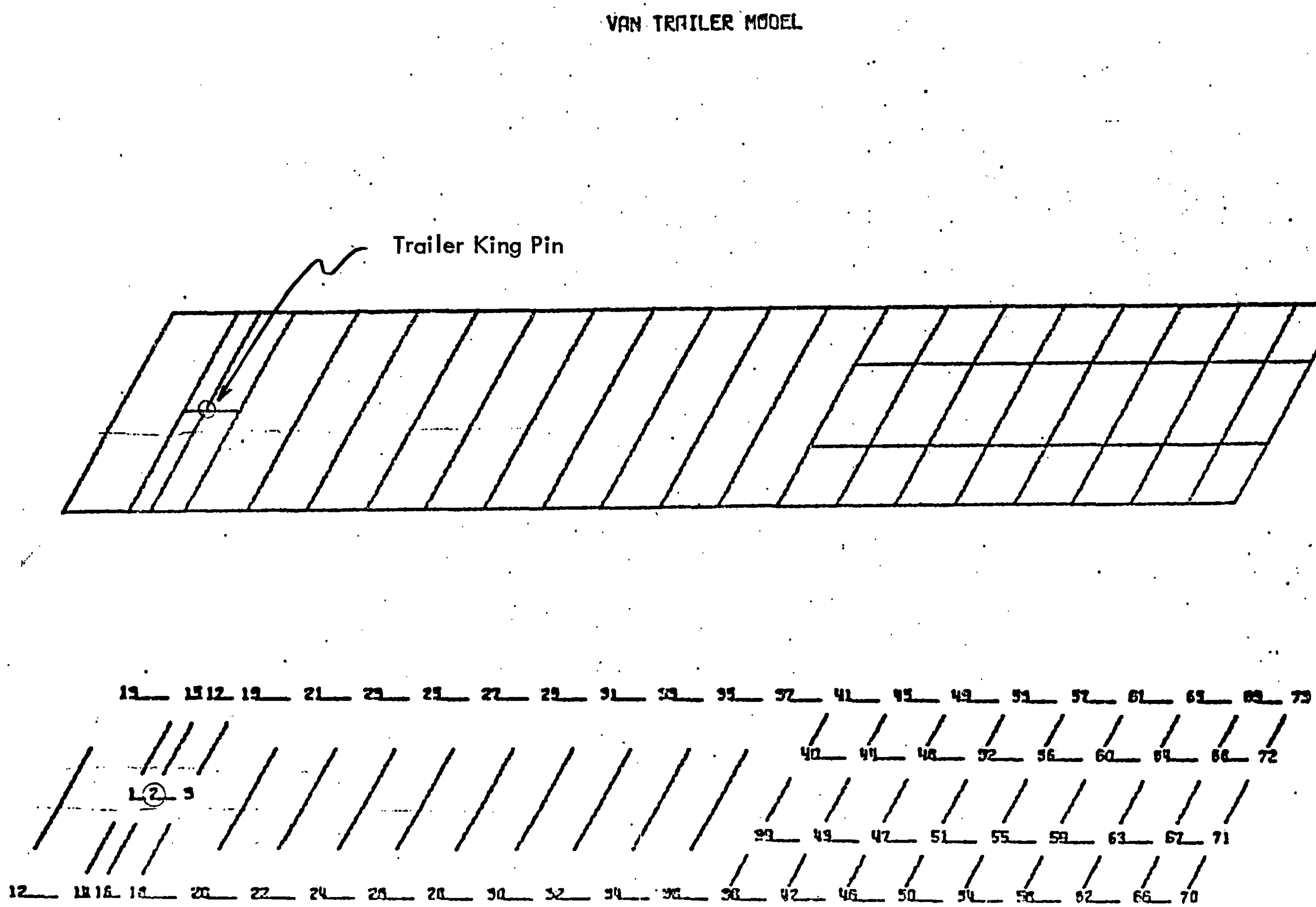

Figure 3-9. Van Trailer Structural Model

termined that much of the load is carried in the roof of the van and the attempts to model the structure as shown in Figure 3-9 required modification of the body stiffness to account for the added stiffness effect from the roof. Static measurements were then obtained on the trailers in the loaded and unloaded conditions to compare with the model predictions. These measurements are described and recorded in Part 1 of this report. The model of the platform trailer showed good agreement with the measured data; however, the van trailer model did not agree with the measured values. Additional efforts would be required in modeling the van roof structure to obtain a valid finite element model of the van trailer.

In lieu of the more detailed modeling approach, results of the van characterization test were used to obtain a simplified beam model for the van trailer structure.

Results of the van characterization showed the van to have a first body bending resonance of approximately 6.8 Hz. The model for the van structure was obtained by using a beam of appropriate cross section and stiffness to give the correct weight and section modulus. Comparison of data on the Demonstration Test and model predictions using the beam model shows this approach to be adequate.

3.2.3 Trailer Suspension System Model

One trailer suspension system model was made and used for both the van and platform trailers. The schematic for this model is shown in Figure 3-10(a) for the platform trailer and in Figure 3-11(a) for the van trailer. It consisted of a beam element for the axle and spring/damper elements connecting the axle to the trailer body and to the flatcar. The lower spring/damper elements are a model of the tires and were based on the tire force-deflection curves provided by Goodyear Tire Company shown in Figure 3-12. The tires actually used on the test trailers are not the same as those used to acquire the test in Figure 3-12. However, the manufacturer said the data in Figure 3-12 was the best available and would give a good approximation of the tires used on the test vehicles. From this figure it can be seen that the tire spring constants are nonlinear and dependent on tire pressure. Linear approximations can be made of the curves by drawing a straight line through them as shown in Figure 3-12. During the Demonstration Test a tire pressure of 80 psi to 85 psi (see Part 1, Appendix D) was maintained in each tire throughout the test program. For the tire model a stiffness

** zero g position subtract approx. 1/4" for unloaded trailer weight

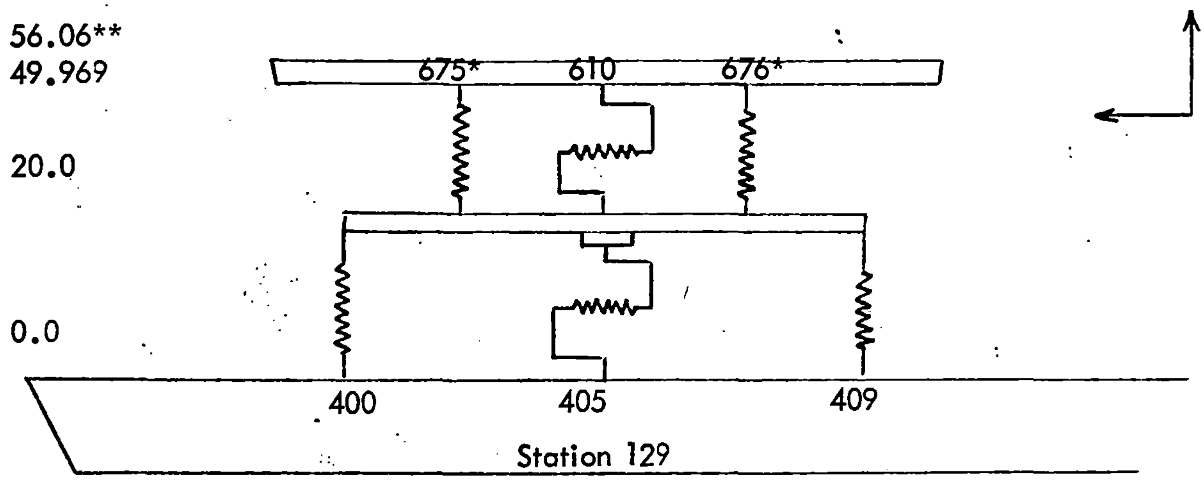

* tandems in forward position

(a) Suspension System

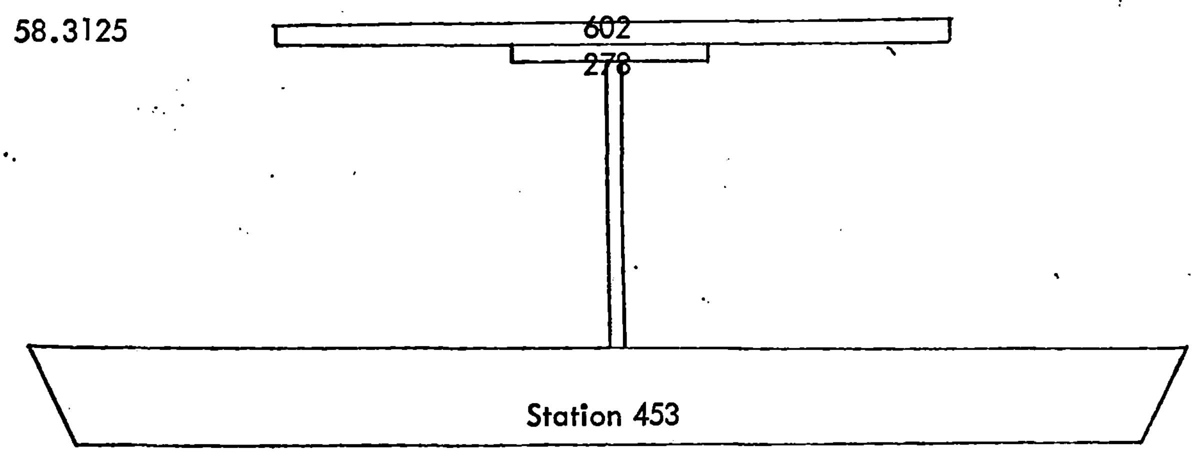

(b) Trailer Hitch

Figure 3-10. Platform Trailer Model

**Dimensions are for zero gravity, subtract 1/4" for 1 g with unloaded van

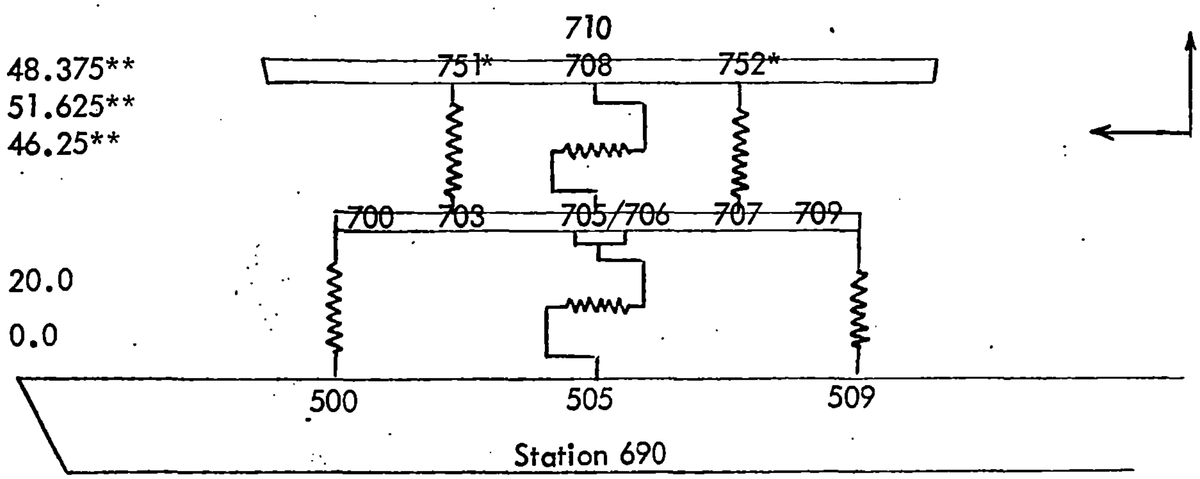

*Tandems in forward position

(a) Suspension System

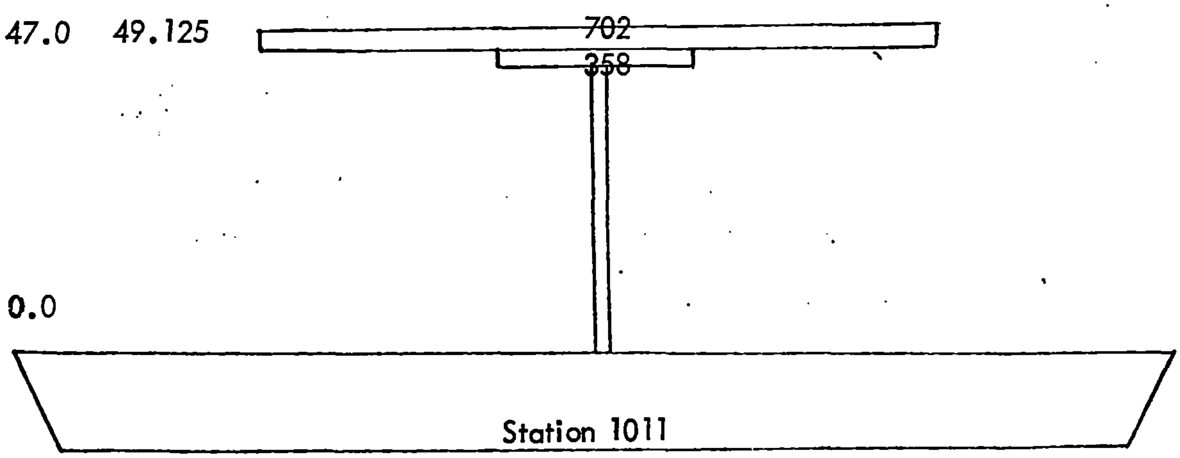

(b) Trailer Hitch

Figure 3-11. Van Trailer Model

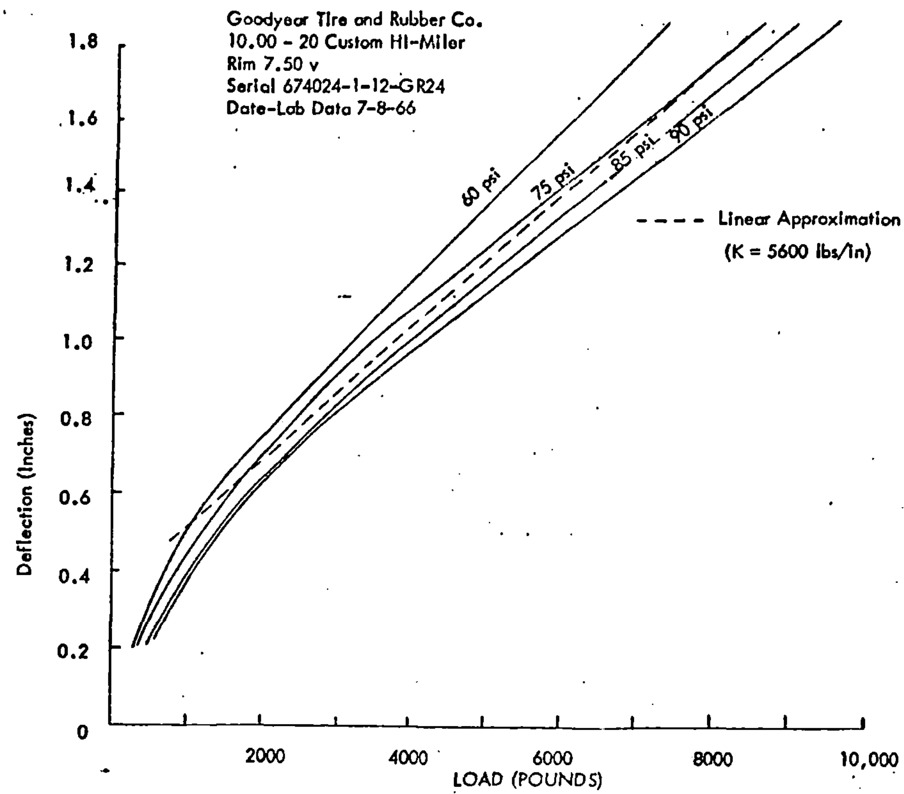

LOAD DEFLECTION CURVES

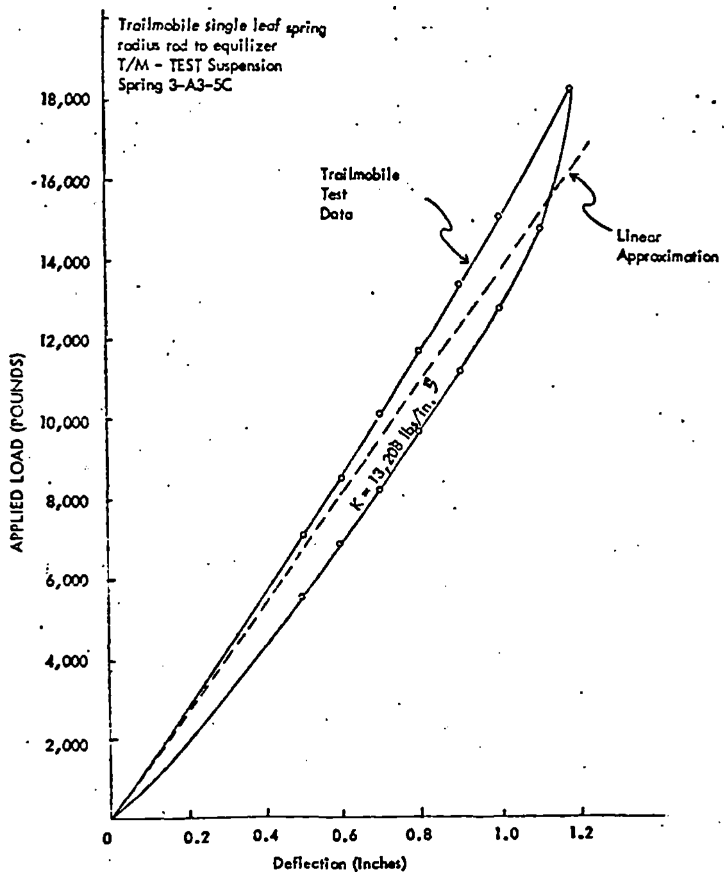

LEAF SPRING DEFLECTION

Figure 3-12. Trailer Suspension Data

value of 5600 pounds/inch (as shown in Figure 3-12) was used for each tire. The upper spring/damper element was a model of the trailer lead springs and was based on the leaf spring data provided by Trailmobile and shown in Figure 3-12. A linear approximation was developed and used for the leaf springs. Test data was not available to develop any approximate value for the lateral springs in the model; therefore, an arbitrary value of 10,000 pounds/inch was used.

During the Demonstration Test the trailer tandems were placed in the forward position for the entire test. However, provisions are made in the model for easily varying the tandem position if required.

3.3 COMBINED MODEL

The reduced matrices for the above models were all stored on tape. They can then be recalled in any combination to model various configurations. For the Demonstration Test three configurations were analyzed: (1) an empty flatcar, (2) a flatcar with two loaded trailers, and (3) a flatcar with an empty platform trailer. It is possible to analyze any combination of flatcar and loaded or unloaded trailers as required.

3.3.1 Node Numbering System

In order to facilitate analysis of the model data, a node numbering system was established as shown in Table 3-3 so that the area of a nodal location can be readily established. For example, when interested in the response of the van trailer, only node numbers beginning with seven hundred need be examined.

3.3.2 Connecting Springs

The attach points between the trailers and the flatcar consists of the locations where the hitch assembly attaches to the trailer king pin and where the tires rest on the floor of the flatcar. These attach points were modeled as shown in Figure 3-10 for the platform trailer and in Figure 3-11 for the van trailer. At the trailer hitch the appropriate node on the hitch was coupled to the appropriate node on the trailer. The only degree of freedom not coupled was the rotation about the x-axis. At the tire location, the spring model for the tires was connected directly to a node on the flatcar. The connecting points were set up in the program so it was easy to add or delete various trailer configurations from the model. Also, the connection point for the trailer tires on the flatcar were written so that they could be easily moved to account

Table 3-3. Node Numbering System

COMBINED MODEL

NODE NUMBERS	COMPONENT
1 - 99	Boundary Nodes
100 - 199	Truck Model
200 - 599	Flatcar Structure Model
600 - 699	Platform Trailer Model
700 - 799	Van Trailer Model

for changes in tandem location when required in Figure 3-7. These matrices were then written on tape and stored for both the loaded and unloaded configurations of the platform trailer.

SECTION 4 - MODAL ANALYSES

The reduced mass and stiffness matrices developed for the models described in Section 3 were utilized to perform various analyses to obtain information on static deflections, modes, damped frequency response, and transient responses. These analyses were used to support the pretest planning activity and posttest data analysis. The following sections describe these types of analyses performed with some of the results summarized. Where these analyses were used to aid in test data interpretation, the results are presented in Section 6.

4.1 WEIGHT AND INERTIA CALCULATIONS

The weights for the flatcar and trailers were based on a combination of measured data and analysis as summarized in Table 4-1. The fully loaded flatcar and each of the loaded trailers were weighed and recorded on commercial scales. The empty flatcar and each of the unloaded trailer weights were based on nominal values for the given type of vehicle. The weight for the trailer tandems represents that weight which moves with the tandems and was calculated from center of gravity data provided by Trailmobile for the tandems in the forward and rear position. The structural element weights were computed by the ANSYS program and then lumped weights were added to the models at the proper node points to bring the model weights into agreement with the data presented in Table 4-1. The modified mass matrices were then analyzed to determine c.g. locations and the associated moments of these inertia. Data for the flatcar, platform trailer, and van trailer are shown in Tables 4-2, 4-3, and 4-4, respectively.

4.2 MODAL ANALYSIS

Modal analyses of the models were used to calculate natural frequencies and mode shapes for the analytical model. A discrete system with n degrees of freedom will have n natural frequencies and mode shapes which characterize the behavior of the system. Assuming that the structure is undamped and that there are no external forces applied, the differential equations of motion can be written as follows:

$$(M)\{\ddot{x}\} \cancel{\equiv} + (K)\{x\} \equiv 0$$

The normal mode method is characterized by the fact that these differential equations of motion can be decoupled when the displacements are expressed in terms of the

Table 4-1. Weight Summary

FULLY LOADED FLATCAR

FLATCAR STRUCTURE	52,561 lb	
FLATCAR TRUCKS	17,239 lb	
INSTRUMENTATION	100 lb	69,900 lb (Configuration 1)
VAN STRUCTURE	9,098 lb	
VAN TANDEMS	3,157 lb	
LADING (SAND BAGS)	49,825 lb	
		62,080 lb*
PLATFORM STRUCTURE	10,293 lb	
PLATFORM TANDEMS	2,707 lb	
LADING (LEAD WEIGHTS)	48,980 lb	
		61,980 lb*
	TOTAL	193,960 lb* (Configuration 2)
		82,900 lb (Configuration 3)

*Actual Weighed Values

Table 4-2. Flatcar Mass and Moment of Inertia Data

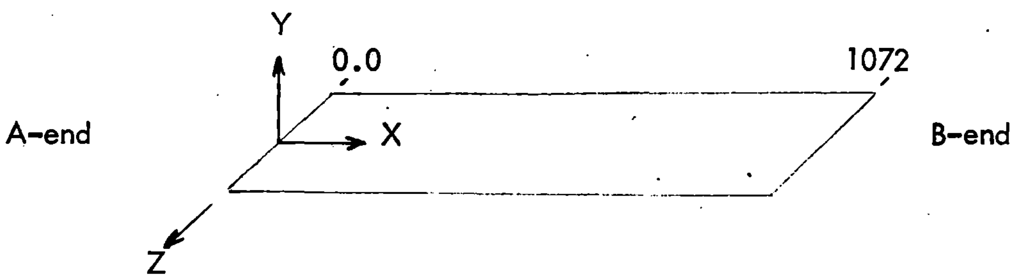

FLATCAR STRUCTURE* (TTAX 973295)

Weight	=	52.562 lb	
I_{xx}	=	1.147×10^7 slug-in^2.	About Centroid
I_{yy}	=	1.116×10^5 slug-in^2.	
I_{zz}	=	1.156×10^7 slug-in^2.	

Centroid

X_c	=	0.0 in.
Y_c	=	543.9 in.
Z_c	=	32.0 in. (above rail)

Table 4-3. Platform Trailer Mass and Moment of Inertia Data

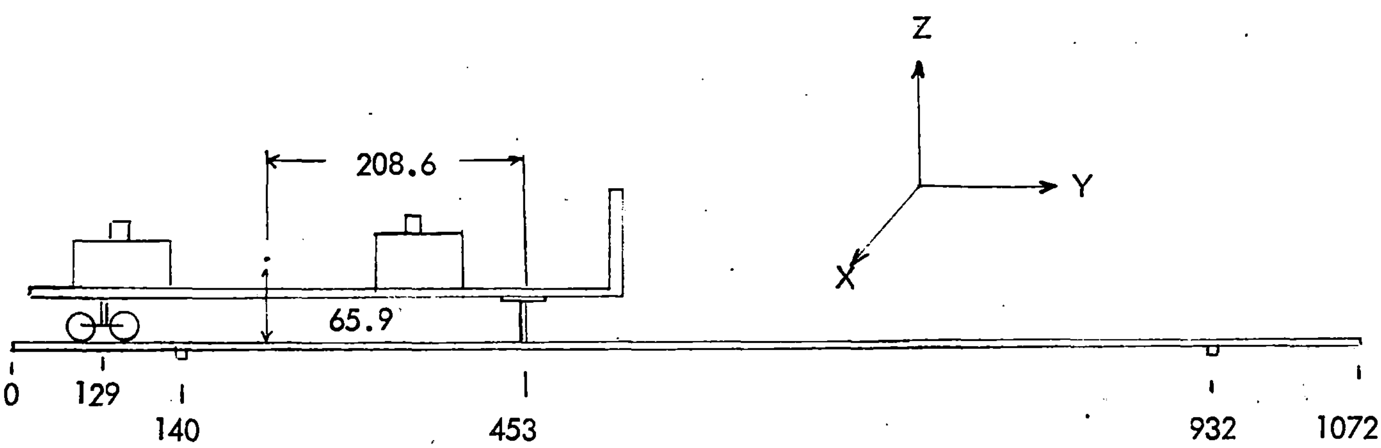

Trailer structural weight 10,293 lb

Trailer tandems weight 2,707 lb

Trailer lading weight 47,180 lb

Trailer structure & lading weight 57,473* lb

C.G.* x_c = 0.0 in.

y_c = 244.4 in.

z_c = 65.9 in.

I^*_{xx} = 1.31×10^6 slug-in.^{2}

I^*_{yy} = 1.02×10^5 slug-in.^{2}

I^*_{zz} = I_{xx}

*Does not include tandems

Table 4-4. Van Trailer Mass and Moment of Inertia Data

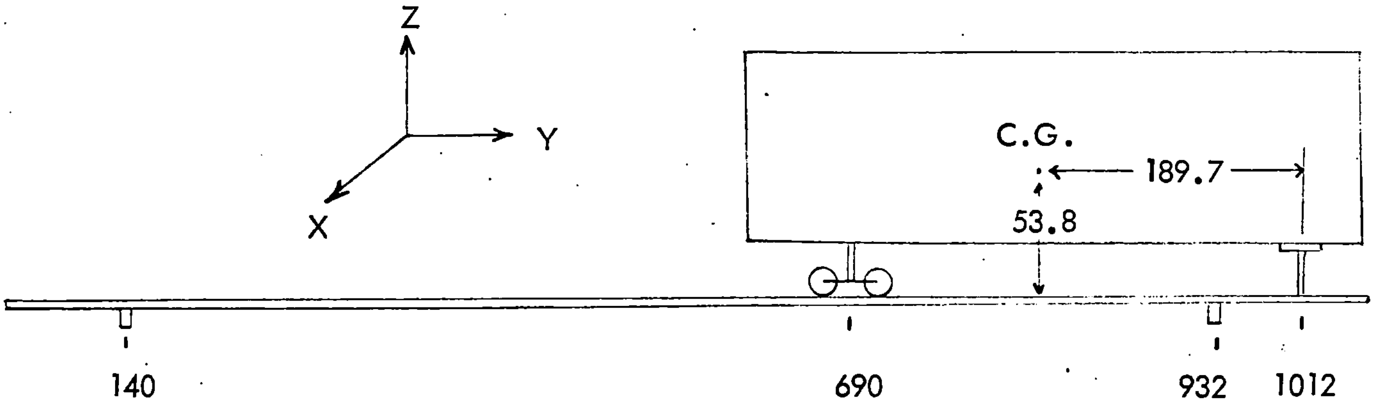

Trailer structure weight	9098 lb
Tandems weight	3157 lb
Lading weight	49,825 lb
Trailer body & lading weight	58,923* lb

C.G.* $x_c = 0.0$ in.

$y_c = 831.3$ in.

$z_c = 53.8$ in.

$$I^*_{xx} = 2.94 \times 10^6 \text{ slug-in.}^2$$

$$I^*_{yy} = 25.5 \times 10^4 \text{ slug-in.}^2$$

$$I^*_{zz} = 3.19 \times 10^6 \text{ slug-in.}^2$$

*Does not include tandems

normal modes. Thus the system is broken down into n independent differential equations rather than a system of n simultaneous differential equations. The eigenvectors of the matrix $\left((M)^{-1}(K) \right)$ uncouples the system of equations. Let (ϕ) be a matrix whose columns are the eigenvectors of $\left((M)^{-1}(K) \right)$ and define the vector η by

$$x = (\phi)\,\eta$$

then the uncoupled differential equation may be written:

$$(\grave{}MM)\,\ddot{\eta} + (\acute{}MK)\,\eta \equiv 0$$

This results in n uncoupled differential equation with natural frequencies:

$$\omega_i = \sqrt{\frac{K_i}{M_i}}$$

The ANSYS program uses a Jacobi interation to yield a complete set of the eigenvalues and eigenvectors described above.

As an example of this type of analysis the modes of a flatcar simply supported at the king pin were calculated using the ANSYS program. The resulting set of eigenvalues (natural frequencies) is shown in Table 4-5 and shows the first natural frequency of the flatcar structure to be 4.2 Hz.

This result agrees with the analysis of test data in Section 6.2.1 which indicates the first flatcar structural bending mode to be around 4.1 Hz. The first three eigenvectors for the simply supported flatcar are shown in Table 4-6 and show the first resonant frequency to be a vertical bending mode.

The ANSYS program has the capability to graphically display modal displacements; however, the approach used for the TOFC analyses (saving mass and stiffness matrices on tape) prevents mode shape plots of the TOFC model from being displayed.

Table 4-5. Simply Supported Flatcar Natural Frequencies

MODAL ANALYSIS - FLATCAR UNDERFRAME - SIMPLY SUPPORTED MODES

***** EIGENVALUE (NATURAL FREQUENCY) SOLUTION *****

MODE	FREQUENCY (CYCLES/TIME)
1	4.2092
2	4.5524
3	9.1395
4	12.757
5	14.719
6	17.094
7	22.508
8	23.002
9	25.399
10	31.339
11	37.613
12	38.464
13	50.746
14	57.234
15	57.896
16	58.917
17	79.867
18	98.058
19	98.812
20	101.97
21	117.42
22	136.59
23	156.37
24	237.95
25	273.05
26	408.34
27	432.84

Table 4-6. Simply Supported Flatcar Mode Shapes

***** EXPANDED MODE SHAPE FOR MODE 1 ***** FREQUENCY = 4.20922 (CYCLES/TIME)

NODE	UX	UY	UZ	ROTX	ROTY	ROTZ
104			-.825580E-01		-.323157E-10	
128	0.	0.	0.	.574353E-03	0.	
136			.317350E-01			
152	-.181289E-07		.812982E-01		-.396328E-09	
168			.113629			
178	-.396057E-07	-.574883E-02	.119730		-.400709E-09	
184	-.199532E-07		.126111	-.165837E-05	-.147361E-09	
200			.113340			
216	-.814916E-08		.810485E-01		.305399E-09	
232			.317009E-01			
240	0.	0.	0.	-.575538E-03	.474919E-09	
258	.257581E-07	.276720E-01	-.464927E-01		.560174E-09	
264			-.830927E-01		.541557E-09	
MAXIMUM VALUE						
NODES	178	258	184	240	258	0
DISPL	-.396057E-07	.276720E-01	.126111	-.575539E-03	.560174E-09	0.

***** EXPANDED MODE SHAPE FOR MODE 2 ***** FREQUENCY = 4.55240 (CYCLES/TIME)

NODE	UX	UY	UZ	ROTX	ROTY	ROTZ
104			-.210323E-07		.797539E-04	
128	0.	0.	0.	.142642E-09	0.	
136			.737194E-08			
152	-.133714E-02		.149597E-07		.113586E-02	
168			.132612E-07			
178	.633595E-01	.179790E-06	.108483E-07		.138488E-02	
184	-.210027E-02		.194743E-08	-.122445E-09	.166305E-02	
200			-.119091E-07			
216	-.150608E-02		-.190279E-07		.195462E-02	
232			-.146881E-07			
240	0.	0.	0.	.383161E-09	.201437E-02	
258	.967175E-01	.151462E-06	.402731E-07		.204230E-02	
264			.783930E-07		.203955E-02	
MAXIMUM VALUE						
NODES	258	178	264	240	258	0
DISPL	.967175E-01	.179790E-06	.783930E-07	.383161E-09	.204230E-02	0.

***** EXPANDED MODE SHAPE FOR MODE 3 ***** FREQUENCY = 9.13951 (CYCLES/TIME)

NODE	UX	UY	UZ	ROTX	ROTY	ROTZ
104			.748650E-06		.719969E-05	
128	0.	0.	0.	-.444665E-08	0.	
136			-.196162E-06			
152	.817230E-01		-.271550E-06		.870448E-04	
168			-.205443E-06			
178	.127466	.372462E-05	-.165951E-06		.230961E-03	
184	.123577		-.263053E-07	.197486E-08	.118093E-03	
200			.213306E-06			
216	.814775E-01		.343854E-06		.133290E-03	
232			.235330E-06			
240	0.	0.	0.	-.521093E-08	.126442E-03	
258	-.469541E-01	.406510E-05	-.471750E-06		.879499E-04	
264			-.867698E-06		.123138E-03	
MAXIMUM VALUE						
NODES	178	258	264	240	178	0
DISPL	.127466	.406510E-05	-.867698E-06	-.521093E-08	.230961E-03	0.

4.3 STATIC ANALYSES

The stiffness matrice for a finite element model provides the force displacement relationship for the entire structure. The general form of the equilibrium equation for the total structure is:

$$(K)\{U\} \equiv \{F\}$$

where, (K) is structure stiffness matrix

$\{U\}$ is a vector of the nodal displacements of the structure

$\{F\}$ is a vector of the corresponding forces.

If sufficient boundary conditions are imposed on (U) to guarantee a unique solution, the equilibrium equation can be solved to obtain the nodal point displacement at each node in the structure using standard matrix formulation. From these displacements the forces and stresses within each structural element can be calculated.

The ANSYS program can be used to assemble the stiffness matrices for any combination of the models developed in Section 3 and solve the equilibrium equation for a given set of boundary conditions. As an example of this analysis method, a static analysis was performed on a fully loaded flatcar (configuration 2) to determine the displacements and structural loads due to the effects of gravity. The combined model consisted of the flatcar and trucks, a loaded van trailer, and a loaded platform trailer. The boundary conditions were specified as fixed displacement at the support points (node point numbers 1, 3, 5, 23, 25, and 27 as shown in Figure 3-4) and a vertical load of one unit of acceleration (1 g). The resulting displacement solution is shown in Table 4-7 where the node numbers refer to those developed in Section 3.3.1 for the combined model and the displacements are inches for translation and radians for rotation. The node point number for the flatcar center is 84 from Figure 3-1. Adding 200 to this number from Table 3-4 for the flatcar results in a combined model node number of 284. From Table 4-7, the deflection at node 284 is 4.31 inches in the negative direction (refer to Figure 3-1 for coordinate system). This is the total deflection at the flatcar center due to gravity. From this displacement solution the load in each of the structural members was calculated and a partial listing is shown in Table 4-8. Based on these results, the load at node point 1 is 48,575 pounds, which is the static load that will be supported by the two right hand actuators.

Table 4-7. Static Analysis For Fully Loaded Flatcar

```
STATIC ANALYSIS OF FULLY LOADED FLATCAR


***** ELEMENT STRESSES *****

LINE ELEMENT STRESSES ASSUME WEIGHT IS CONCENTRATED AT NODAL POINTS
REACTION FORCES AND ELEMENT FORCES ASSUME DISTRIBUTED WEIGHTS

ELEM    1   NODES    1  102   FORCE=  -48575.3       STRETCH= -.00024   RATE=   .200000E+09
FORCES ON NODE    1  0.            0.            -.485753E+05
FORCES ON NODE  102  0.            0.             .485753E+05

ELEM    2   NODES    5  106   FORCE=  -48575.5       STRETCH= -.00024   RATE=   .200000E+09
FORCES ON NODE    5  0.            0.            -.485755E+05
FORCES ON NODE  106  0.            0.             .485755E+05
FORCES ON NODE    1  0.            0.            -.908991E+04
FORCES ON NODE    5  0.            0.            -.908991E+04

ELEM    5   NODES    3  109   FORCE=  -.243237E-07   STRETCH= -.00000   RATE=   100000.
FORCES ON NODE    3   .243237E-07  0.            0.
FORCES ON NODE  109  -.243237E-07  0.            0.

   SUPER ELEMENT      6 NODAL FORCES
     NODE  DIRECT         VALUE          NODE  DIRECT       VALUE          NODE  DIRECT        VALUE
      102   FZ        -48575.3            106   FZ       -48575.5           109   FZ       .155054E-08
      117   FZ        -.145686E-06        109   FX        .243237E-07       117   FX       .677626E-20
      109   MY         .101714E-07        117   MY       -.736384E-11       124   FZ      -48846.6
      128   FZ        -48846.8            131   FZ       -.866491E-08       139   FZ      -.205290E-06
      131   FX        -.605815E-07        139   FX       -.271051E-19       131   MY       .150413E-06
      139   MY        -.363277E-11        204   FZ        3199.54           228   FZ       37507.1
      236   FZ        -.385668E-06        252   FZ        .263957E-06       268   FZ      -.255957E-05
      284   FZ        -.152936E-05        300   FZ        25463.6           316   FZ       13104.1
      332   FZ        -.146982E-06        340   FZ        .380183E-06       364   FZ      -.670734E-07
      228   FX        -.392211E-07        252   FX       -.504342E-14       284   FX       .712494E-08
      316   FX         .141259E-07        340   FX       -.160536E-13       204   MY      -.814799E-12
      228   MY         6.04896            252   MY       -.369717E-11       284   MY       .670224
      316   MY         1.47447            340   MY        .195717E-10       364   MY       .349294E-12
      228   MX        -.866567E-07        284   MX        .257641E-04       340   MX      -.102902E-04
      278   FX         .393866E-07        278   FY       -.208762E-05       278   FZ       21273.1
      358   FX        -.200977E-07        358   FY        .599393E-06       358   FZ       24870.2

ELEM    7   NODES  400  600   FORCE=  -20353.2       STRETCH= -.90863   RATE=   22400.0
FORCES ON NODE  400  0.            0.            -.203532E+05
FORCES ON NODE  600  0.            0.             .203532E+05

ELEM    8   NODES  409  609   FORCE=  -20353.4       STRETCH= -.90863   RATE=   22400.0
FORCES ON NODE  409  0.            0.            -.203534E+05
FORCES ON NODE  609  0.            0.             .203534E+05


   SUPER ELEMENT     17 NODAL FORCES
     NODE  DIRECT         VALUE          NODE  DIRECT       VALUE          NODE  DIRECT        VALUE
      601   FZ        -.226532E-07        602   FZ       -21273.1           655   FZ      -.116015E-06
      656   FZ         .137516E-07        674   FZ       -.239323E-07       675   FZ      -18999.7
      676   FZ        -19000.0            677   FZ       -.594673E-08       683   FZ       .334921E-07
      684   FZ        -.579848E-07        695   FZ       -.218133E-07       696   FZ      -.304663E-07
      602   FX        -.393882E-07        675   FX        .196216E-07       676   FX       .196216E-07
      683   FX         .140187E-13        684   FX       -.909640E-14       602   FY       .223233E-05
      601   MY        -.144428E-08        602   MY        .334694E-08       655   MY      -.938599E-06
      656   MY        -.832166E-06        675   MY       -.101691E-05       676   MY      -.610729E-06
      683   MY        -.126700E-06        684   MY       -.191867E-06

ELEM   18   NODES  500  700   FORCE=  -18613.7       STRETCH= -.83097   RATE=   22400.0
FORCES ON NODE  500  0.            0.            -.186137E+05
FORCES ON NODE  700  0.            0.             .186137E+05

ELEM   19   NODES  509  709   FORCE=  -18613.8       STRETCH= -.83097   RATE=   22400.0
FORCES ON NODE  509  0.            0.            -.186138E+05
FORCES ON NODE  709  0.            0.             .186138E+05

   SUPER ELEMENT     28 NODAL FORCES
     NODE  DIRECT         VALUE          NODE  DIRECT       VALUE          NODE  DIRECT        VALUE
      702   FZ        -24870.2            734   FZ       -.102518E-07       735   FZ      -.901491E-08
      750   FZ        -.540222E-07        751   FZ       -17026.1           752   FZ      -17026.2
      753   FZ        -.974978E-09        771   FZ       -.212176E-07       772   FZ      -.123146E-08
      759   FZ         .582149E-07        760   FZ       -.536093E-07       702   FX       .204448E-07
      751   FX        -.108676E-07        752   FX       -.108676E-07       759   FX       .114448E-13
      760   FX        -.575561E-14        702   FY       -.755099E-06       702   MY       .232831E-09
      734   MY        -.124404E-06        735   MY       -.115542E-07       751   MY      -.155554E-05
      752   MY        -.131025E-05        759   MY       -.466767E-06       760   MY      -.373111E-06
      771   MY         .163327E-07        772   MY       -.519794E-07

ELEM   29   NODES   25  131   FORCE=   .605815E-07   STRETCH=  .00000   RATE=   100000.
FORCES ON NODE   25  -.605815E-07  0.            0.
FORCES ON NODE  131   .605815E-07  0.            0.

ELEM   30   NODES   23  124   FORCE=  -48846.6       STRETCH= -.00024   RATE=   .200000E+09
FORCES ON NODE   23  0.            0.            -.488466E+05
FORCES ON NODE  124  0.            0.             .488466E+05
```

Table 4-8. Partial Load Analysis For Fully Loaded Flatcar

STATIC ANALYSIS OF FULLY LOADED FLATCAR

***** DISPLACEMENT SOLUTION *****

NODE	UX	UY	UZ	ROTX	ROTY	ROTZ
1	.108700E-33	.108700E-33	0.			
3	0.					
5	.108700E-33	.108700E-33	0.			
23			0.			
25	0.					
27			0.			
102			-.242877E-03			
106			-.242877E-03			
109	.243237E-12		-.183022E-03		-.104015E-10	
117	.486475E-12		-2.01420		-.538598E-07	
124			-.244233E-03			
128			-.244234E-03			
131	-.605815E-12		-.183966E-03		-.121897E-10	
139	-.121163E-11		-2.02626		-.631192E-07	
204			-.866227		-.635240E-07	
228	-.124192E-11		-2.04936	-.903177E-02	-.635769E-07	
236			-2.57534			
252	-.570240E-09		-3.46207		-.617477E-07	
268			-4.06551			
278	-.286607E-05	.184118	-4.18515			
284	-.485655E-09		-4.31061	-.783846E-04	-.604636E-07	
300			-4.08153			
316	-.507564E-10		-3.46807		-.586159E-07	
332			-2.54705			
340	.498637E-12		-2.03716	.812731E-02	-.542481E-07	
358	-.254228E-05	-.321771	-1.47976			
364			-1.08066		-.543508E-07	
400			-1.95636			
405	-.124192E-11					
409			-1.95637			
500			-4.01253			
505	-.186662E-09					
509			-4.01253			
600	-.849489E-12	0.	-2.86499	0.	-.100095E-01	0.
601			-3.97748		-.498022E-06	
602	-.286607E-05	.184118	-4.18515		-.498048E-06	
603	-.849489E-12	0.	-3.01560	0.	-.696471E-02	0.
605	-.849489E-12	0.	-3.08199	0.	-.182584E-06	0.
606	-.124192E-11					
607	-.849489E-12	0.	-3.01561	0.	.696438E-02	0.
608	-.849489E-12					
609	-.849489E-12	0.	-2.86500	0.	.100092E-01	0.
610	-.457057E-12					
655			-4.39017		.101265E-02	
656			-4.39019		-.101365E-02	
674			-3.77556			
675	-.457070E-12		-3.73488		.886532E-03	
676	-.457044E-12		-3.73490		-.887538E-03	
677			-3.77560			
683	.413362E-06		-3.44033		.698129E-03	
684	.413362E-06		-3.44035		-.699149E-03	
695			-3.05568			
696			-3.05570			
700	-.186880E-09	0.	-4.84349	0.	-.914165E-02	0.
702	-.254228E-05	-.321771	-1.47976		-.396697E-06	
703	-.186880E-09	0.	-4.98106	0.	-.636538E-02	0.
705	-.186880E-09	0.	-5.04180	0.	-.101388E-06	0.
706	-.186662E-09					
707	-.186880E-09	0.	-4.98107	0.	.636519E-02	0.
708	-.186880E-09					
709	-.186880E-09	0.	-4.84350	0.	.914146E-02	0.
710	-.187097E-09					
734			-6.57399		.133843E-02	
735			-6.57402		-.133897E-02	
750			-5.73010			
751	-.187098E-09		-5.62563		.243063E-02	
752	-.187096E-09		-5.62563		-.243107E-02	
753			-5.73012			
759	.371529E-06		-5.19266		.193732E-02	
760	.371529E-06		-5.19267		-.193774E-02	
771			-4.62831		.116678E-02	
772			-4.62832		-.116720E-02	
MAXIMUM VALUE						
NODES	278	358	735	228	600	0
DISPL	-.286607E-05	-.321771	-6.57402	-.903177E-02	-.100095E-01	0.

This type of analysis provided valuable information in the pretest planning where deflections at various points on the TOFC were required and to determine what the resulting loads on the actuator would be.

4.4 DECAY ANALYSIS

The equations of motion for a finite element structural system can be written in matrix form:

$$(M)\{U\} + (C)\{U\} + (K)\{U\} \cancel{+} = \{f(t)\}$$

The above equation is solved in the time domain by straight-forward numerical integration, starting from some known initial state of the system at time zero. For the linear case where the M, C, and K matrices are constant and the time interval is constant throughout, the matrices can be inverted once and the transient analysis is reduced to a series of matrix multiplications.

The transient analysis capability was used in the evaluation of the data taken during the decay test. An example of the results of a transient response analysis is shown in Figure 4-1. In this example the configuration 1 (empty flatcar) was given an input sinusoidal excitation of ± 1 inch. After one cycle the excitation was stopped at zero and the resultant analytical decay traces on the flatcar plotted. This is shown in Figure 4-1 where responses are plotted for the center and end of the flatcar. From this plot resonant frequencies and damping values were obtained in Section 6 for comparison with measured test data.

4.5 FREQUENCY RESPONSE ANALYSIS

The equations of motion for a structural system being forced by a function which is harmonic at some frequency is:

$$\left[-w^2(M) + j\,W(C) + (K) \right] \{U\} = \{F_o \sin wt\}$$

Using the mass, stiffness, and damping matrices which have previously been saved on tape, ANSYS solves the above equation for values of $\{U_o\}$ versus frequency. The

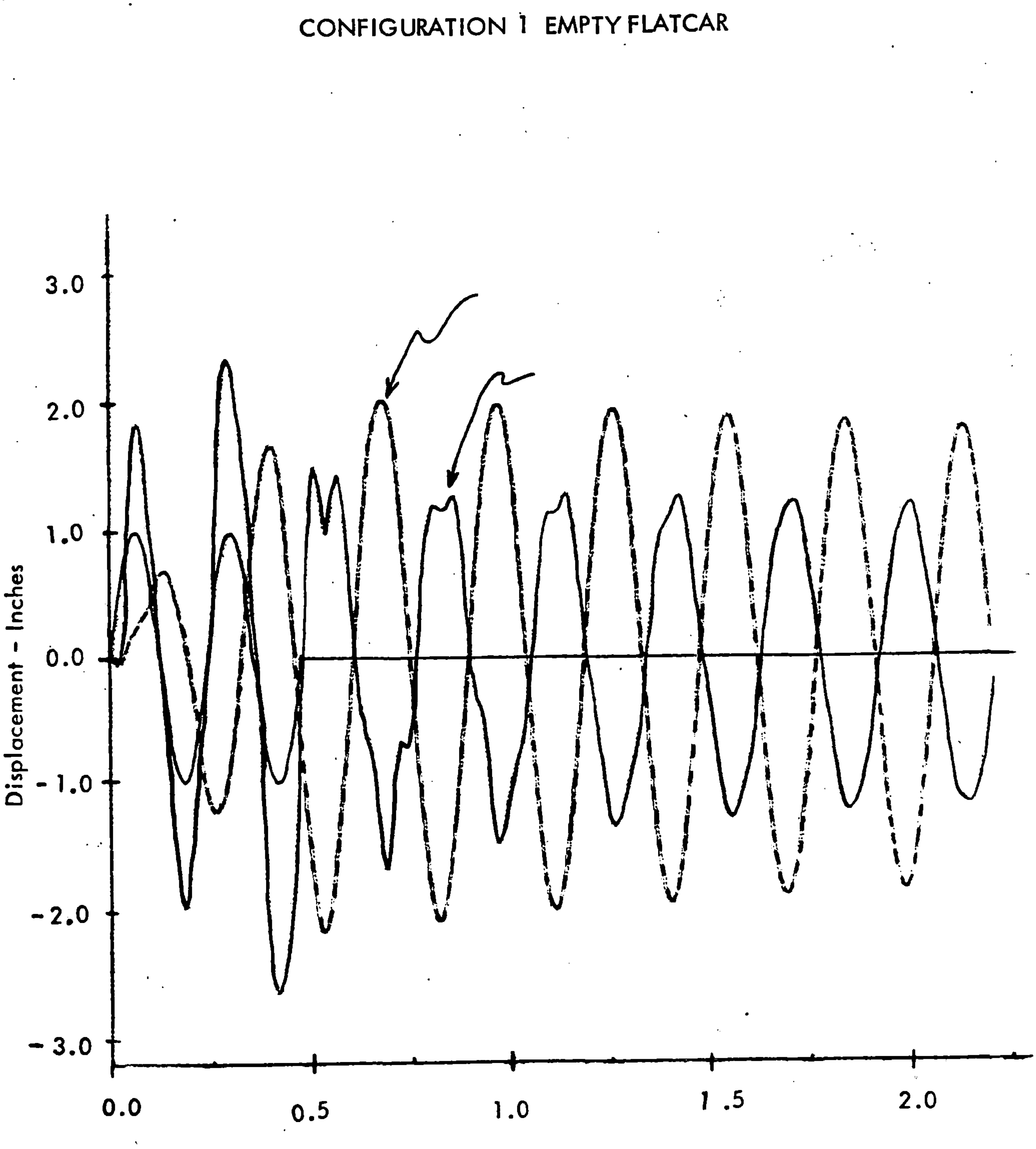

Figure 4-1. Decay Analysis Example

solution will be of the form $U_o \cos (wt)$ and the printout consists of amplitude V_o and phase angle, ϕ, of the response relative to the forcing function. Detail of the theoretical aspects are covered in Reference 1.

ANSYS is used to solve for the response to constant 1 inch displacement at various frequencies from 0.1 Hz to 30 Hz. These values are then saved on tape and can be used to obtain any desired shape response or converted to velocity and accelerations using:

$$V = (2\pi f) D$$

$$A = \frac{(2\pi f)^2 D}{g}$$

Examples of frequency domain calculations using the above techniques for data analysis are shown in Section 6.

The frequency domain calculation capability was used in the pretest planning to establish actuator capability. The controls program Act Cap calculates actuator capability as a function of frequency for a given load. The load must be expressed in terms of a dynamic stiffness at the actuator heads. ANSYS was used to calculate the dynamic stiffness of the various configurations for input to the actuator capability program. For configuration 1 (empty flatcar) the dynamic stiffness information is shown in Table 4-9 and the resultant actuator capability in Figure 4-2.

4.6 PLOT PROGRAM

An in-house plot program was written to enable frequency domain plots to be made of both predictions and test results. The test results are input to the program from punch cards obtained from the TFA program. Analytical data is obtained from tape where it was written during the frequency response analysis program. Thus the program can be used to plot overlays from multiple test runs to compare repeatibility, to plot predictions in which some coefficient has been varied to see the effects of that coefficient, and to plot overlay comparisons between prediction and tests. In addition to overlays, the program can be used to plot data on log or linear scales. This can be a valuable aid in interpreting data, as can be seen from Figure 4-3 where the same

Table 4-9. Dynamic Stiffness, Empty Flatcar

-DYNAMIC STIFFNESS AT ACTUATOR (IN/LBS)
DRIVE POINT

-POINT NO-	-FRQ (HZ)-	-MAGNITUDE -	-PHASE(DEG)-
1	.1000	.822000E-01	-180.000
2	.4000	.510000E-02	-180.000
3	1.000	.790000E-03	-179.500
4	1.600	.289000E-03	-177.900
5	2.000	.172200E-03	-175.100
6	2.400	.108000E-03	-168.800
7	2.800	.724000E-04	-151.900
8	3.000	.694000E-04	-136.300
9	3.200	.856000E-04	-125.700
10	3.400	.110700E-03	-133.900
11	3.600	.110300E-03	-150.800
12	3.800	.931000E-04	-161.600
13	4.000	.773000E-04	-166.400
14	4.200	.655000E-04	-168.300
15	4.400	.567000E-04	-168.800
16	4.800	.447000E-04	-167.900
17	5.200	.369000E-04	-166.100
18	5.600	.315000E-04	-164.000
19	6.000	.276000E-04	-162.000
20	6.600	.234000E-04	-159.500
21	7.000	.212000E-04	-158.100
22	7.600	.188200E-04	-156.600
23	8.200	.168800E-04	-155.700
24	9.000	.148600E-04	-155.200
25	9.400	.140200E-04	-155.200
26	10.00	.129400E-04	-155.700
27	12.00	.979000E-05	-158.100
28	14.00	.780000E-05	-161.500
29	16.00	.612000E-05	-166.600
30	18.00	.472000E-05	-168.600
31	20.00	.384000E-05	-169.200
32	22.00	.320000E-05	-170.300
33	24.00	.269000E-05	-171.500
34	26.00	.228000E-05	-172.200
35	28.00	.196000E-05	-172.200
36	30.00	.171000E-05	-172.700

MAXIMUM ACTUATOR CAPABILITY FOR CONFIGURATION 1

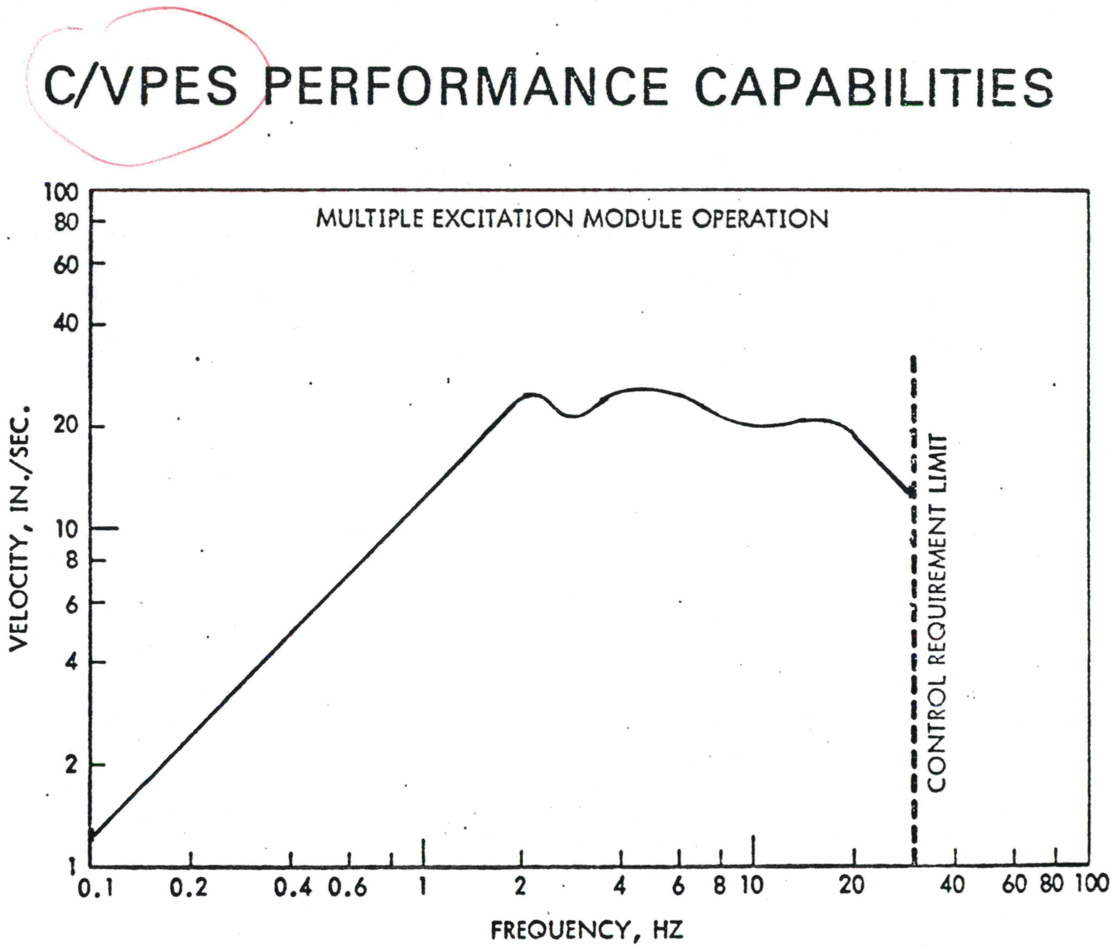

Figure 4-2. Actuator Capability, Empty Flatcar

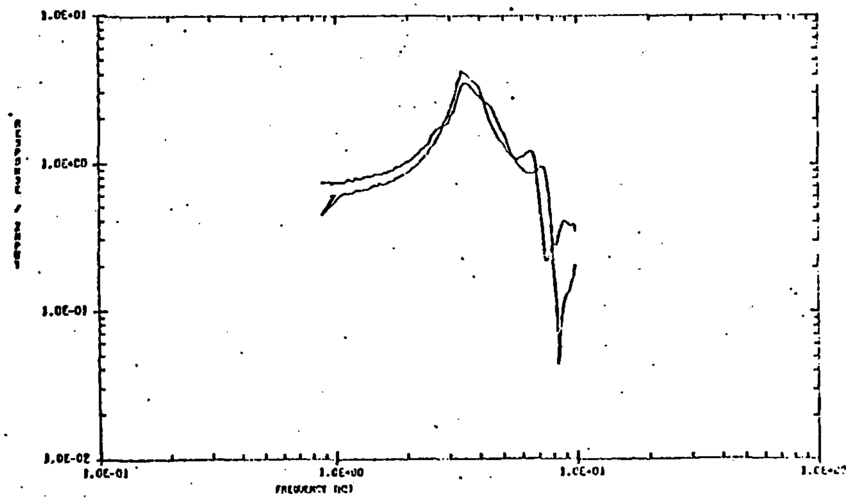

Log-Log Plot

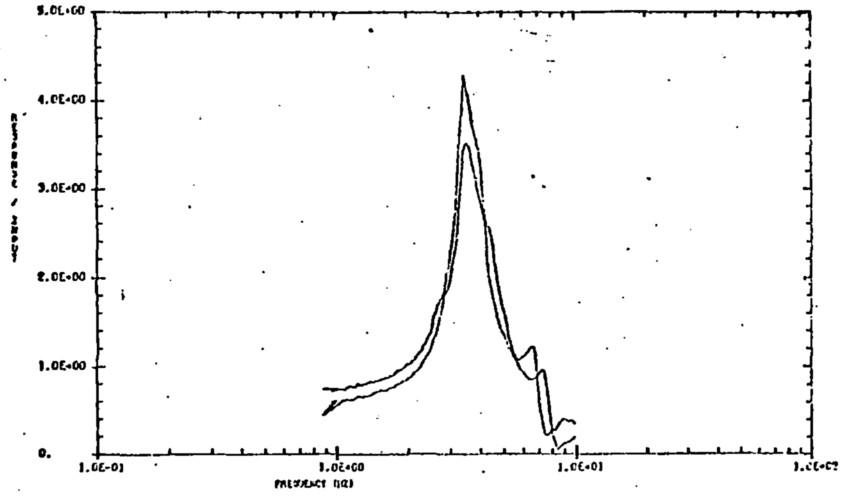

Linear-Log Plot

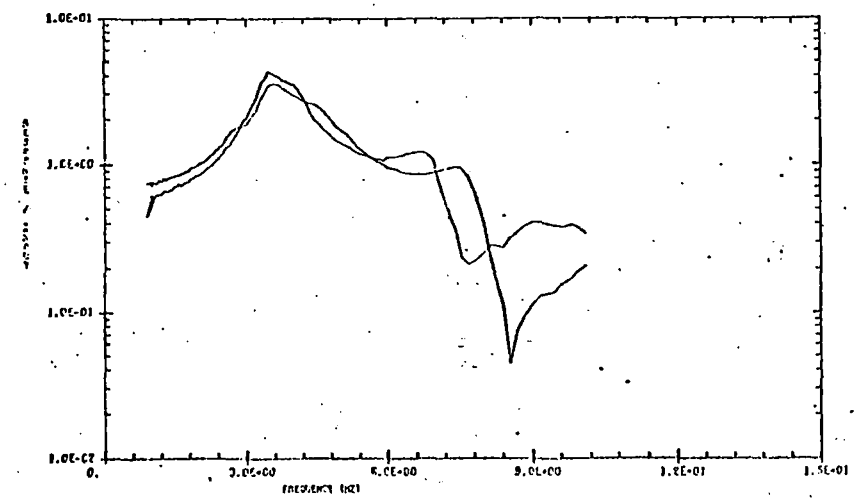

Log-Linear Plot

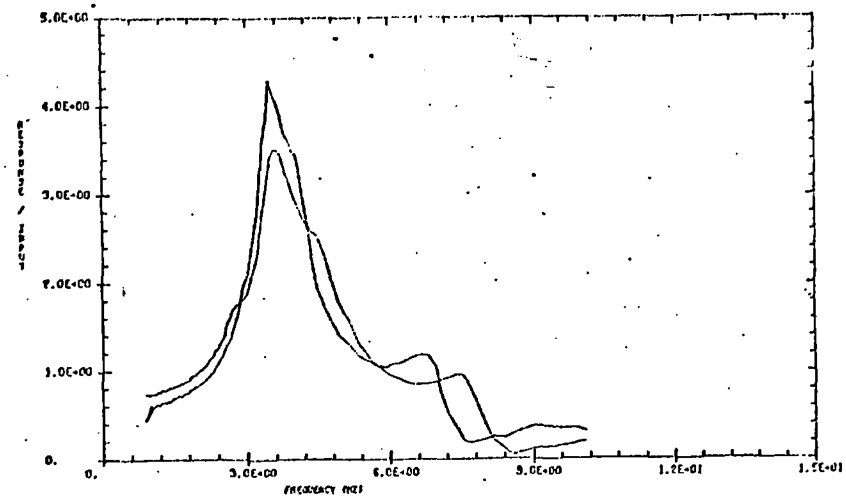

Linear-Linear Plot

Figure 4-3. Data Plotting Capability

overlay was plotted on log and linear scales. As can be seen the visual interpretation is significantly different depending on the scales chosen. In this report the data is plotted using the scales which best show the interpretation of the data being discussed. In addition the plot program will prepare tables of pretest predictions as shown in Tables 4-10 and 4-11. These tables can then be used as an aid in running the test.

Table 4-10. Example of Pretest Computer Simulation

COMPUTER SIMULATION FOR RESPONSES

CONFIGURATION 2, FULLY LOADED FLATCAR

HIGH LEVEL SINUSOIDAL SWEEP
SHAKERS IN PHASE

ACTUATOR INPUT TO SPECIMEN

FREQUENCY (HZ)	INPUT DISPLACEMENT (INCHES)	INPUT VELOCITY (IN/SECOND)	INPUT ACCELERATION (G)
.20	2.00000	2.51327	.00818
.30	2.00000	3.76991	.01841
.40	2.00000	5.02655	.03273
.50	2.00000	6.28319	.05114
.60	2.00000	7.53982	.07364
.70	2.00000	8.79646	.10023
.80	2.00000	10.05310	.13091
.90	2.00000	11.30973	.16569
1.00	2.00000	12.56637	.20455
1.20	2.00000	15.07964	.29455
1.40	2.00000	17.59292	.40092
1.60	2.00000	20.10619	.52365
1.80	2.00000	22.61947	.66275
2.00	1.75070	22.00000	.71622
2.20	1.59155	22.00000	.78784
2.40	1.45892	22.00000	.85946
2.60	1.34670	22.00000	.93108
2.80	1.25050	22.00000	1.00271
3.00	1.16714	22.00000	1.07433
3.20	1.09419	22.00000	1.14595
3.40	1.02983	22.00000	1.21757
3.60	.97261	22.00000	1.28919
3.80	.92142	22.00000	1.36081
4.00	.87535	22.00000	1.43244
4.50	.77809	22.00000	1.61149
5.00	.70028	22.00000	1.79055
5.50	.63662	22.00000	1.96960
6.00	.58357	22.00000	2.14865
6.50	.53868	22.00000	2.32771
7.00	.50020	22.00000	2.50676
7.50	.46685	22.00000	2.68582
8.00	.43768	22.00000	2.86487
8.50	.41193	22.00000	3.04393
9.00	.38905	22.00000	3.22298
9.50	.36857	22.00000	3.40204
10.00	.35014	22.00000	3.58109
12.50	.28011	22.00000	4.47636
15.00	.23343	22.00000	5.37164
17.50	.20008	22.00000	6.26691
20.00	.15400	19.35165	6.30000
22.50	.12168	17.20147	6.30000
25.00	.09856	15.48132	6.30000
27.50	.08145	14.07393	6.30000
30.00	.06844	12.90110	6.30000

Table 4-11. Example of Pretest Computer Simulation

COMPUTER SIMULATION FOR RESPONSES

CONFIGURATION 2, FULLY LOADED FLATCAR

HIGH LEVEL SINUSOIDAL SWEEP
SHAKERS IN PHASE

RESPONSE ACCELEROMETER CHANNEL NUMBER 89

FREQUENCY (HZ)	INPUT ACCELERATION (G)	RESPONSE ACCELERATION (UZ 284)	TRANSFER FUNCTION (UZ 284)/(INPUT)
.20	.00818	.00416	.50862
.30	.01841	.00957	.51986
.40	.03273	.01756	.53654
.50	.05114	.02863	.55978
.60	.07364	.04355	.59135
.70	.10023	.06356	.63412
.80	.13091	.09070	.69282
.90	.16569	.12841	.77505
1.00	.20455	.18289	.89409
1.20	.29455	.39958	1.35657
1.40	.40092	.79279	1.97742
1.60	.52365	.23797	.45445
1.80	.66275	.71741	1.08249
2.00	.71622	.39465	.55102
2.20	.78784	.32034	.40661
2.40	.85946	.28852	.33569
2.60	.93108	.26659	.28633
2.80	1.00271	.24594	.24527
3.00	1.07433	.21125	.19663
3.20	1.14595	.15004	.13093
3.40	1.21757	.14722	.12091
3.60	1.28919	.28704	.22265
3.80	1.36081	.42844	.31484
4.00	1.43244	.51790	.36155
4.50	1.61149	.52084	.32320
5.00	1.79055	.35171	.19643
5.50	1.96960	.73748	.37443
6.00	2.14865	1.36503	.63530
6.50	2.32771	1.73775	.74655
7.00	2.50676	1.78188	.71083
7.50	2.68582	1.51532	.56419
8.00	2.86487	1.14921	.40114
8.50	3.04393	.82355	.27055
9.00	3.22298	.54914	.17038
9.50	3.40204	.31616	.09293
10.00	3.58109	.16157	.04512
12.50	4.47636	1.27358	.28451
15.00	5.37164	.89779	.16714
17.50	6.26691	.74049	.11816
20.00	6.30000	.49891	.07919
22.50	6.30000	.57235	.09085
25.00	6.30000	.22987	.03649
27.50	6.30000	.09052	.01437
30.00	6.30000	.07219	.01146

SECTION 5 - EVALUATION OF TEST DATA

During the course of the Demonstration Test Program, a total of 107 test runs were made on three flatcar configurations. An average of 140 frequency points were sampled for each of 110 channels on every run for a total of approximately 1.5 million data points. Any attempt to completely analyze and catalogue this much data was well beyond the scope of this effort. So the approach taken was to analyze only select runs from the test program and then to present only select data channels from this analysis in this report. Thus, when data comparisons are present, they represent only a sample of the total data obtained during the test program. However, in each case an attempt was made to select the most representative data to present in this report.

5.1 REPEATABILITY

To assess the degree of repeatability obtainable during the Demonstration Test, tables were prepared which compare the input and responses measured during two identical runs. Runs 72 and 73 were the two identical runs chosen for this comparison. The average of the four inputs are shown in Table 5-1 and show an average difference of about ± 1%. There is no discernable pattern to the differences. A response on the flatcar and each of the vans are shown in Tables 5-2 through 5-4. Here the average percentage difference is around ±10% and again there is no discernable pattern to the difference. It should be noted that while some of the variations approach 70% at some frequencies, these large variations seem to occur at the off resonant frequencies. At resonant peaks the variation seems to be around 10%. Comparisons made of other response channels show the same magnitude of variation. It appears from this data that the actuators are ample to provide repeatable inputs but that the responses on the specimen can vary somewhat from run to run for the same input.

Comparisons of the repeatability of dwell are shown in Tables 5-5 and 5-6. The first table compares dwells that were run sequentially without shutting the system down. Table 5-6 compares dwells that were run on different days. The tables show a larger variation between nonsequential dwells, but the data scatter is still about the same as shown for sweep.

Table 5-1. Sweep Data Repeatability

DEMONSTRATION TEST CONFIGURATION 2

AVERAGE INPUT

FREQUENCY (HZ)	RESPONSE RUN 72	RESPONSE RUN 73	PERCENTAGE DIFFERENCE
1.10	.2962	.3013	1.7
1.18	.2975	.2939	-1.2
1.27	.2993	.2902	-3.1
1.36	.2949	.2972	.8
1.46	.2964	.2969	.1
1.58	.2978	.3008	1.0
1.70	.2941	.2939	-.1
1.84	.2993	.2953	-1.3
1.99	.2932	.2941	.3
2.15	.2938	.2945	.3
2.32	.2983	.2979	-.1
2.50	.2971	.2975	.2
2.71	.2989	.2962	-.9
2.93	.2960	.2957	-.1
3.16	.2779	.2818	1.4
3.44	.2601	.2582	-.7
3.72	.2420	.2410	-.4
4.02	.2276	.2246	-1.3
4.36	.2086	.2089	.1
4.73	.1901	.1939	2.0
5.11	.1779	.1807	1.6
5.55	.1668	.1674	.4
6.04	.1573	.1549	-1.5
6.54	.1446	.1449	.2
7.10	.1348	.1339	-.7
7.69	.1252	.1252	-.0
8.36	.1171	.1190	1.6
9.05	.1092	.1098	.6
9.83	.1011	.1016	.4
10.71	.0964	.0967	.3
11.57	.0884	.0899	1.6
12.52	.0835	.0863	3.3
13.68	.0799	.0785	-1.7
14.83	.0745	.0753	1.0
16.07	.0658	.0669	1.7
17.47	.0569	.0570	.2
18.96	.0494	.0491	-.7
20.63	.0422	.0430	2.0
22.40	.0366	.0357	-2.6
24.26	.0312	.0308	-1.3
26.44	.0272	.0266	-2.0
28.65	.0216	.0219	1.5
31.09	.0184	.0182	-1.3

AVERAGE PERCENTAGE DIFFERENCE = .8

MAXIMUM PERCENTAGE DIFFERENCE = 3.3 AT 12.52 HZ

MINIMUM PERCENTAGE DIFFERENCE = -.0 AT 2.76 HZ

Table 5-2. Sweep Data Repeatability

DEMONSTRATION TEST CONFIGURATION 2

MEASUREMENT NUMBER 89

FREQUENCY (HZ)	RESPONSE RUN 72	RESPONSE RUN 73	PERCENTAGE DIFFERENCE
1.10	.0258	.0236	-8.7
1.18	.0346	.0332	-4.1
1.27	.0361	.0421	15.5
1.36	.0478	.0501	4.5
1.46	.0729	.0619	-16.3
1.58	.1100	.1101	.1
1.70	.2473	.2517	1.8
1.84	.3791	.3916	3.2
1.99	.3590	.3446	-4.1
2.15	.2878	.2907	1.0
2.32	.1931	.1908	-1.2
2.50	.2074	.2149	3.5
2.71	.0989	.1016	2.7
2.93	.0851	.0571	-39.3
3.16	.0281	.0413	37.9
3.44	.0503	.0657	26.6
3.72	.0491	.0597	19.5
4.02	.0957	.1058	10.0
4.36	.0633	.1092	53.1
4.73	.2033	.1620	-22.6
5.11	.1520	.1561	2.7
5.55	.2710	.2754	1.6
6.04	.2328	.2453	5.2
6.54	.1187	.1330	11.4
7.10	.2356	.2636	11.2
7.69	.5591	.5974	6.6
8.36	.3416	.3856	12.1
9.05	.2676	.2861	6.7
9.83	.3697	.3654	-1.2
10.71	.3960	.3791	-4.4
11.57	.3889	.4037	3.7
12.52	.3465	.3480	.4
13.68	.2135	.2547	17.6
14.83	.1286	.1068	-18.5
16.07	.1799	.1758	-2.3
17.47	.2850	.2818	-1.1
18.96	.6755	.6532	-3.3
20.63	.7952	.8767	9.7
22.40	1.0275	.9994	-2.8
24.26	.8013	.7856	-2.0
26.44	.6973	.6177	-12.1
28.65	.6024	.6453	6.9
31.09	.3370	.3148	-6.8

AVERAGE PERCENTAGE DIFFERENCE = 9.2

MAXIMUM PERCENTAGE DIFFERENCE = -69.7 AT 4.45 HZ

MINIMUM PERCENTAGE DIFFERENCE = .0 AT 5.90 HZ

Table 5-3. Sweep Data Repeatability Comparison, Measurement

DEMONSTRATION TEST CONFIGURATION 2

MEASUREMENT NUMBER 123

FREQUENCY (HZ)	RESPONSE RUN 72	RESPONSE RUN 73	PERCENTAGE DIFFERENCE
1.10	.0490	.0396	-21.3
1.18	.0486	.0564	14.8
1.27	.0646	.0612	-5.4
1.36	.0699	.0713	1.9
1.46	.0627	.0559	-11.4
1.58	.1348	.1020	-27.7
1.70	.1840	.1749	-5.0
1.84	.1940	.2154	10.4
1.99	.2491	.2599	4.2
2.15	.3971	.3879	-2.3
2.32	.4295	.4553	5.8
2.50	1.0485	1.1329	7.7
2.71	.8785	.7585	-14.7
2.93	.5386	.4897	-9.5
3.16	.3880	.4756	20.3
3.44	.3020	.3238	7.0
3.72	.2622	.3523	29.3
4.02	.5668	.4537	-22.2
4.36	.6146	.5876	-4.5
4.73	.5941	.6739	12.6
5.11	.4160	.4491	7.6
5.55	.3541	.3831	7.8
6.04	.3797	.3515	-7.7
6.54	.2825	.2539	-10.7
7.10	.5016	.4614	-8.4
7.69	.4503	.4744	5.2
8.36	.5886	.6392	8.2
9.05	.6914	.7227	4.4
9.83	.7484	.8298	10.3
10.71	1.1481	1.1702	1.9
11.57	1.3164	1.4313	8.4
12.52	1.4131	1.3376	-5.5
13.68	.8124	1.2895	45.4
14.83	.5694	1.2166	72.5
16.07	.3478	.4543	26.6
17.47	.1852	.1004	-59.4
18.96	.8673	.9379	7.8
20.63	1.3238	1.2407	-6.5
22.40	1.5081	1.4151	-6.4
24.26	1.6070	1.5262	-5.2
26.44	2.3343	1.3335	-54.6
28.65	.8109	.8685	6.9
31.09	.7248	.8223	12.6

AVERAGE PERCENTAGE DIFFERENCE = 13.6

MAXIMUM PERCENTAGE DIFFERENCE = 80.3 AT 14.15 HZ

MINIMUM PERCENTAGE DIFFERENCE = -.0 AT 10.04 HZ

Table 5-4. Sweep Data Repeatability Comparison

DEMONSTRATION TEST CONFIGURATION 2

MEASUREMENT NUMBER 81

FREQUENCY (HZ)	RESPONSE RUN 72	RESPONSE RUN 73	PERCENTAGE DIFFERENCE
1.10	.0362	.0348	-3.9
1.18	.0461	.0462	.3
1.27	.0562	.0561	-.0
1.36	.0683	.0657	-4.0
1.46	.0854	.0850	-.5
1.58	.1541	.1527	-.9
1.70	.3127	.3086	-1.3
1.84	.4496	.4528	.7
1.99	.3224	.3324	3.1
2.15	.1813	.1973	8.5
2.32	.0937	.0845	-10.4
2.50	.3531	.3564	.9
2.71	.3589	.3591	.0
2.93	.3611	.3620	.3
3.16	.3230	.3276	1.4
3.44	.3078	.3425	10.7
3.72	.2983	.2688	-10.4
4.02	.2379	.2318	-2.6
4.36	.1438	.1658	14.2
4.73	.2210	.2006	-9.7
5.11	.2131	.2235	4.8
5.55	.2672	.2764	3.4
6.04	.2327	.2643	12.7
6.54	.3972	.3842	-3.3
7.10	.6292	.6620	5.1
7.69	.6282	.6223	-.9
8.36	.4536	.4644	2.4
9.05	.3029	.2918	-3.7
9.83	.1751	.1720	-1.8
10.71	.1706	.1605	-6.1
11.57	.1665	.1671	.4
12.52	.1744	.1569	-10.6
13.68	.0978	.0790	-21.3
14.83	.0493	.0534	7.9
16.07	.0912	.0739	-20.9
17.47	.0624	.0622	-.2
18.96	.0618	.0720	15.1
20.63	.0728	.0816	11.4
22.40	.0758	.0739	-2.6
24.26	.0784	.0787	.4
26.44	.0617	.0561	-9.5
28.65	.0277	.0267	-3.9
31.09	.0745	.0403	-59.6

AVERAGE PERCENTAGE DIFFERENCE = 7.0

MAXIMUM PERCENTAGE DIFFERENCE = 69.3 AT 30.43 HZ

MINIMUM PERCENTAGE DIFFERENCE = .0 AT 2.71 HZ

Table 5-5. Dwell Data Comparison (Sequential Runs)

CONFIGURATION 2

SHAKERS IN-PHASE

Meas. No.	Amplitude Run 1	Amplitude Run 2	Percentage Difference	Phase Run 1	Phase Run 2
f_{input}	2.00	2.00	0		
Input	.148	.147	-0.7		
A_{89}	.241	.251	+4.1	87	87
S_{51}	3448	3488	+1.2	-92	-94
A_{127}	.189	.187	-1.1	-78	-78
A_{66}	.088	.083	-5.8	-147	-154
A_{96}	.142	.124	-13.5	79	80
D_{104}	.178	.181	1.7	71	69
A_{65}	.128	.095	-29.6	101	138
A_{128}	.439	.432	-1.6	-88	-88
A_{72}	.076	.076	0	-172	-128

Average 7.3

Table 5-6. Dwell Data Comparison (Non-Sequential Runs)

CONFIGURATION 2

SHAKERS IN-PHASE

Meas. No.	Amplitude Run 1	Amplitude Run 2	Percentage Difference	Phase Run 1	Phase Run 2
f_{input}	2.00 Hz	2.00	0		
Input	.280 in	.263 in	-6.2		
A_{89}	.365 g	.354 g	-3.1	53	50
S_{51}	5494 psi	5792 psi	5.3	-128	-133
A_{127}	.272 g	.207 g	-27.1	-102	-112
A_{66}	.245 g	.304 g	21.5	-179	-151
A_{96}	.179 g	.170 g	-5.1	46	41
D_{104}	.295 in	.217 in	-30.5	55	41
A_{65}	.149 g	.092 g	-47.3	93	99
A_{128}	.732 g	.739 g	2.4	-128	-133
A_{72}	.223 g	.252 g	12.2	162	-152
A_{124}	.292 g	.281 g	-3.8	-124	-131

Average 15.8

5.2 COMPARISON OF SWEEP AND DWELL

The sweep program consists of a series of dwells at discrete frequencies between a specified starting and stopping frequency. The discrete frequencies are logarithmically calculated by the program based on an input parameter Q. The amount of time spent at each frequency and the sampling rate are also specified by the program. This means the user has no choice in the amount of time which is allowed for the specimen to come to equilibrium. Dwell, on the other hand, allows the operator to specify the frequency, and he can wait as long as desired before taking data samples. Table 5-7 was prepared to compare measured response between sweep and dwell. The percentage difference between sweep and dwell is slightly larger than that experienced between sweep runs and seems to indicate that dwell will reach higher levels than dwell. A more detailed comparison between sweep and dwell in sections shows very good agreement between sweep and dwell.

5.3 FORWARD AND REVERSE SWEEP

The VSS has the capability to perform sweeps in the forward (increasing frequency) or in the reverse (decreasing frequency) direction. The purpose of this capability was to be able to identify any nonlinear behavior which might result from the direction in which the sweep is performed. Sweep runs 56 and 72 on configuration 2 were identical runs in level and shaker phase. The difference in the two runs was that 56 was started at 1 Hz and swept to 30 Hz while 72 was started at 30 Hz and swept to 1 Hz.

Comparative plots of measurements on the flatcar are shown in Figure 5-1 for these two runs. The top graphs shows the amplification factor for the flatcar center and the bottom graph shows the displacement across the spring group. Both graphs show little change in resonant frequencies, but there are differences in the response amplitudes. Table 5-8 lists the variation between runs 56 and 72 for the flatcar center amplification. It shows percentage difference greater than that which was obtained between identical sweep runs (Table 5-2). Comparative plots for the van and platform trailers amplification factors are shown in Figure 5-2. Measurement 81 is tabulated in Table 5-9. Again, the curves show good agreement between resonant frequencies, but considerable differences in the amplitudes.

Table 5-7. Data Comparison (Sweep and Dwell)

CONFIGURATION 2

SHAKERS IN-PHASE

Meas. No.	Amplitude Sweep	Amplitude Dwell	Percentage Difference	Phase Sweep	Phase Dwell
f_{input}	2.023 Hz	2.046 Hz	+ 1%		
Input	.297 in	.300 in	+ 1%		
A_{89}	.315 g	.343 g	+ 8.5	50°	56^{9}
S_{51}	4321 psi	5609 psi	+ 25.9	-134	-134
A_{127}	.232 g	.266 g	+ 13.7	-88	-86
A_{66}	.305 g	.295 g	- 3.3	161	175
A_{96}	.179 g	.208 g	+ 15.0	22	39
D_{104}	.238 in	.278 in	+ 15.5	60	14
A_{65}	.141 g	.175 g	+ 21.5	118	119
A_{128}	.559 g	.750 g	+ 29.2	- 129	-134
A_{72}	.267 g	.270 g	1.1	-178	171
A_{124}	.282 g	.321 g	12.9	-140	-127

Average 14.7

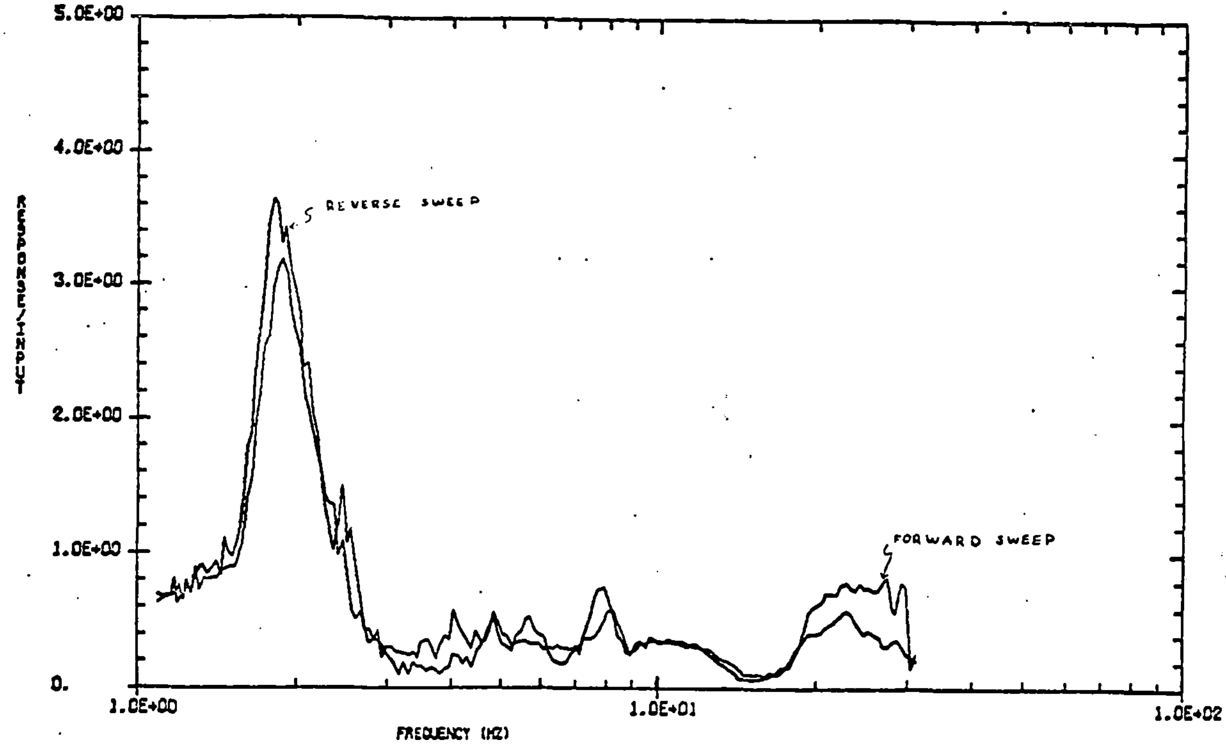

FORWARD AND REVERSE SWEEP COMPARISON, CONFIG 2, MEAS 89

(a)

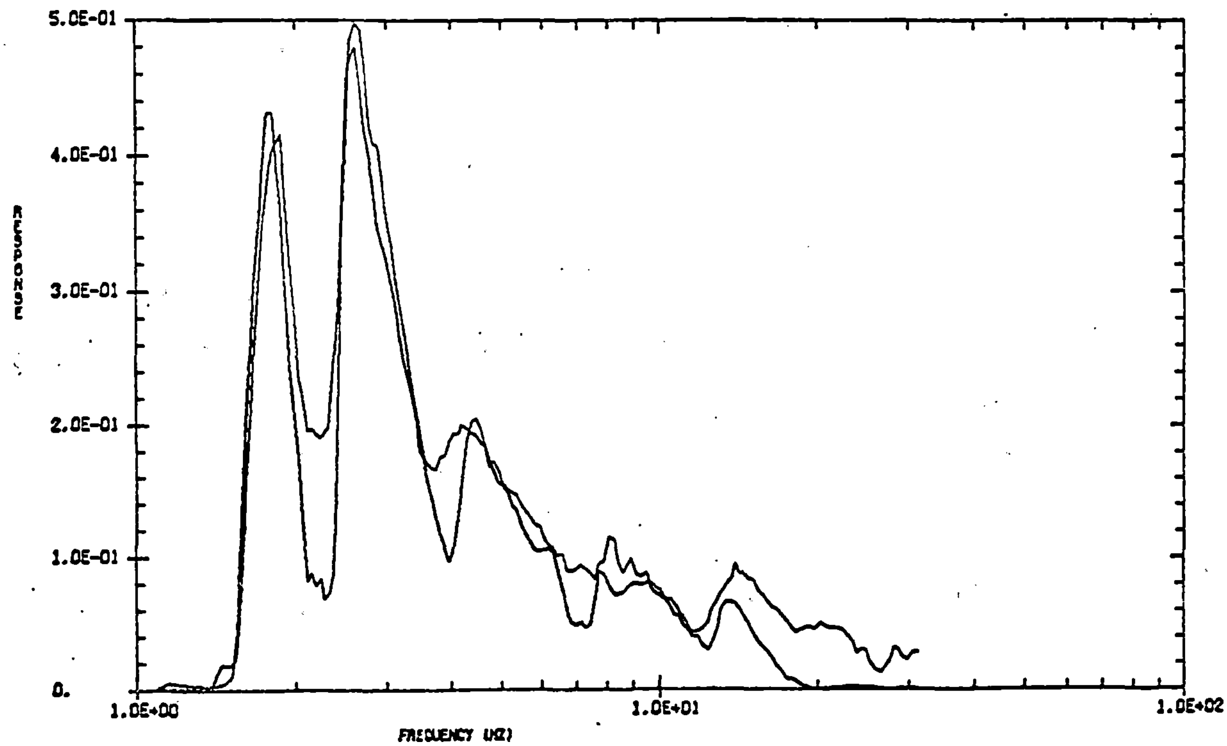

FORWARD AND REVERSE SWEEP COMPARISON, CONFIG 2, MEAS 104

(b)

Figure 5-1. Comparison of Forward and Reverse Sweep, Flatcar

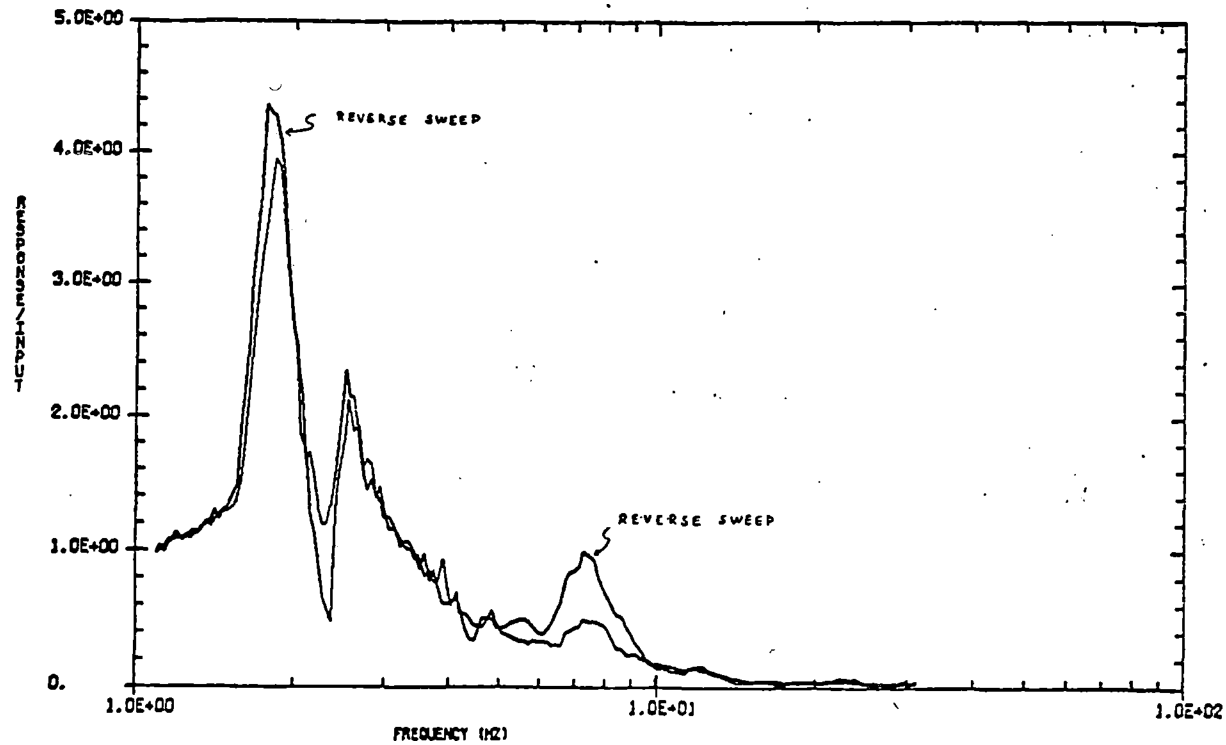

FORWARD AND REVERSE SWEEP COMPARISON, CONFIG 2, MEAS 81

(a)

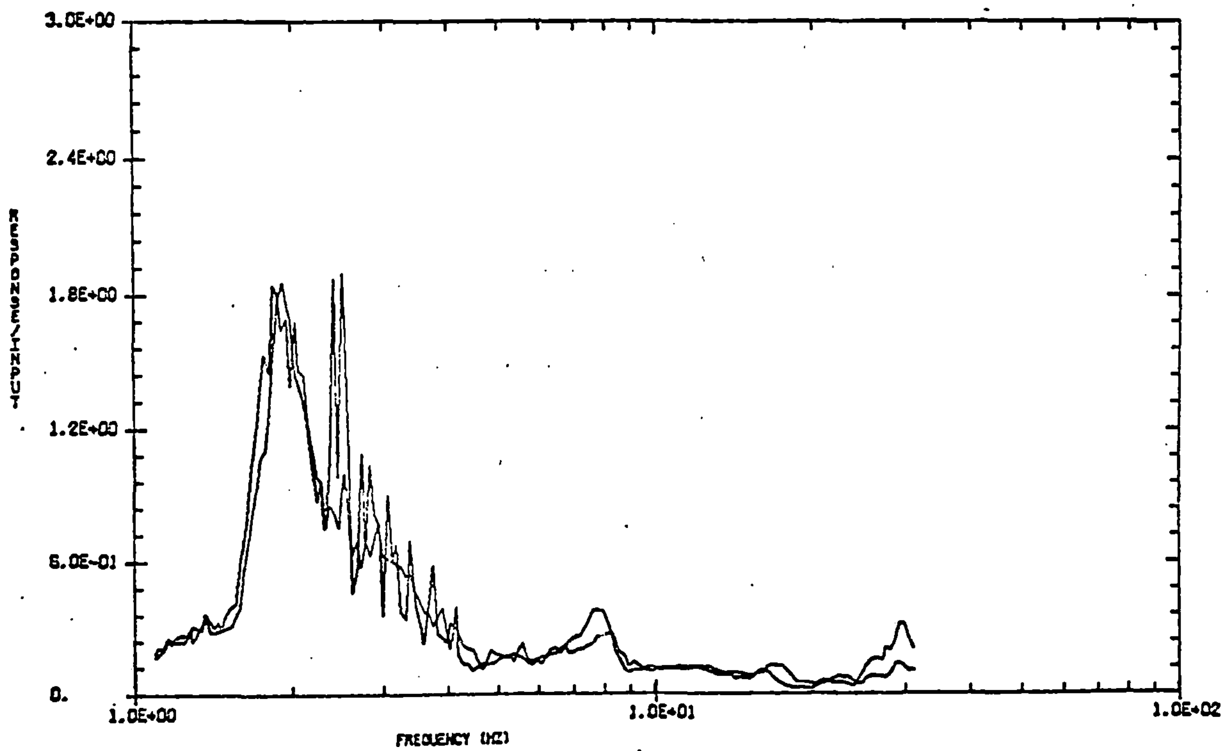

FORWARD AND REVERSE SWEEP COMPARISON, CONFIG 2, MEAS 96

(b)

Figure 5-2. Comparison of Forward and Reverse Sweep, Trailers

Table 5-8. Meas 89 Forward and Reverse Sweep Comparison

COMPARISON OF FORWARD AND REVERSE SWEEP

DEMONSTRATION TEST CONFIGURATION 2

MEASUREMENT NUMBER 89/INPUT

FREQUENCY (HZ)	RESPONSE RUN 56	RESPONSE RUN 72	PERCENTAGE DIFFERENCE
1.10	.6383	.6963	8.7
1.20	.7625	.6325	-18.6
1.31	.7255	.8954	21.0
1.44	.8682	.8357	-3.8
1.58	1.0699	1.4128	27.6
1.73	2.5282	3.0520	18.8
1.91	3.0686	3.4318	11.2
2.11	2.0775	2.4098	14.8
2.31	1.3623	1.1625	-15.8
2.55	.5815	1.1797	67.9
2.82	.3740	.3813	1.9
3.11	.2687	.1706	-44.7
3.44	.2157	.1565	-31.8
3.79	.3248	.1053	-102.1
4.18	.4313	.1816	-81.5
4.63	.3569	.3712	3.9
5.12	.3892	.3135	-21.6
5.67	.3297	.5289	46.4
6.28	.2906	.2151	-29.8
6.95	.3177	.2929	-8.1
7.67	.4269	.7285	52.2
8.54	.4265	.3557	-18.1
9.49	.3072	.3364	9.1
10.45	.3656	.3480	-5.0
11.53	.3227	.3166	-1.9
12.85	.2407	.2187	-9.6
14.21	.1451	.0749	-63.8
15.72	.1078	.0688	-44.1
17.46	.1592	.1582	-.6
19.33	.5641	.4032	-33.3
21.51	.7001	.4873	-35.8
23.82	.7331	.4952	-38.7
26.43	.7322	.3805	-63.2
29.12	.7856	.3229	-83.5

AVERAGE PERCENTAGE DIFFERENCE = 28.0

MAXIMUM PERCENTAGE DIFFERENCE = -102.1 AT 3.79 HZ

MINIMUM PERCENTAGE DIFFERENCE = -.1 AT 10.25 HZ

Table 5-9. Meas 81 Forward and Reverse Sweep Comparison

COMPARISON OF FORWARD AND REVERSE SWEEP

DEMONSTRATION TEST CONFIGURATION 2

MEASUREMENT NUMBER 81/INPUT

FREQUENCY (HZ)	RESPONSE RUN 56	RESPONSE RUN 72	PERCENTAGE DIFFERENCE
1.10	.9882	.9782	-1.0
1.20	1.0953	1.1303	3.2
1.31	1.1253	1.1330	.7
1.44	1.2693	1.2326	-2.9
1.58	1.5306	1.9788	25.5
1.73	3.2034	3.9616	21.2
1.91	3.4380	3.8533	11.4
2.11	1.6746	1.7639	5.2
2.31	1.1930	.5643	-71.6
2.55	2.1548	2.1234	-1.5
2.82	1.6311	1.5157	-7.3
3.11	1.1718	1.2017	2.5
3.44	.9319	.9583	2.8
3.79	.7663	.7295	-4.9
4.18	.5439	.5549	2.0
4.63	.4476	.5127	13.5
5.12	.3792	.4395	14.7
5.67	.3151	.4725	40.0
6.28	.3034	.4727	43.6
6.95	.4348	.8478	64.4
7.67	.4681	.8185	54.5
8.54	.2790	.5109	58.7
9.49	.1933	.2121	9.3
10.45	.1296	.1533	16.8
11.53	.1357	.1355	-.2
12.85	.0904	.1110	20.4
14.21	.0616	.0354	-54.0
15.72	.0400	.0511	24.6
17.46	.0242	.0346	35.6
19.33	.0424	.0320	-28.0
21.51	.0463	.0454	-1.9
23.82	.0705	.0406	-53.9
26.43	.0181	.0337	60.2
29.12	.0294	.0371	23.2

AVERAGE PERCENTAGE DIFFERENCE = 23.0

MAXIMUM PERCENTAGE DIFFERENCE = -95.5 AT 2.36 HZ

MINIMUM PERCENTAGE DIFFERENCE = -.0 AT 1.24 HZ

5.4 LINEARITY OF RESPONSES

For a linear system, the amplification factors measured on the test specimen should be independent of the input amplitude. Thus, plots of amplification factors for a given configuration should be the same regardless of input. When these plots were prepared for the various configurations, they showed a considerable difference in amplification factors, depending on input amplitudes. Plots of this data and a discussion of the changes are contained in Section 6 as a function of the configuration being tested.

SECTION 6 - DATA ANALYSIS

6.1 ACQUISITION AND ANALYSIS OF DATA

The data acquired during the DTP consisted of response measurements made on accelerometers, strain gages, and displacement transducers mounted on the test specimen. The instrumentation description and mounting locations are contained in Part I of this report. The measurement reference numbers used in this report are the same as in Part I. The excitation system consisted of four actuators forcing the test specimen with a sinusoidal excitation through the "A" end truck. The details of the actuator system and specimen mounting on the test fixture is discussed in Part I. Data was acquired during the demonstration test using the sweep, dwell, and high sample rate recording capability of the VSS. The VSS data acquisition and reduction capability are discussed in detail in Part I along with samples of the various types of reduced data. Also contained in Part I is the detailed run logs with a complete description of all runs made during the DTP. As discussed previously, because of the large volume of data acquired, this report will present only a very small portion of the data actually acquired. However, the data presented is representative of the total data acquired.

The primary tool for analysis of the test data was the frequency domain plots obtained from sweep analysis. These plots were examined to obtain resonant peak and resultant amplitude. In particular the plots of response/input (transfer function or amplification factor) were valuable in determining specimen responses. The usual input reference for the response accelerometers was the four shaker head accelerometers. However, in the low frequencies the shaker head accelerometers were so noisy that better transfer functions could be obtained by using the input displacement times $(2\pi f l^2/g)$ to obtain - an input acceleration for the transfer function calculation. This approach was used interchangeably during the data analysis, and a reference to input may refer to either.

Each of the three configurations tested (as discussed in Part I) during the DTP was subjected to shaker in-phase and shaker out-of-phase test excitation. The in-phase consisted of all four actuators moving up and down together and would tend to excite a bounce or vertical bend mode. The out-of-phase consisted of the two actuators on the right side of the vehicle moving 180 degrees out-of-phase with the two actuators on the left side of the vehicle and would tend to excite rocking or torsional modes. In the remainder of the text this is referred to as in-phase or out-of-phase testing.

The prime purpose of the DTP was to demonstrate the operation of the VSS on a test specimen and to verify the operation of the total system. The schedule constraints of the program were such that time was not allocated for a detailed evaluation of the data during testing, so it was not possible to plan testing to provide an in depth characterization of the test specimen. This can be seen many places in the analysis of the data which follows where conclusions have to be drawn from incomplete data. Conclusions are drawn in an attempt to provide some insight into the characteristics of the TOFC in order that future programs may be able to structure tests that will provide more detail and insight into the characteristics of the specimen. When additional test data becomes available, the conclusions drawn in this report are subject to revision.

6.2 CONFIGURATION 2

6.2.1 Response Frequencies

The frequency domain plots of the configuration 1 test data were examined to establish the significant resonant frequency. Examples of this data are shown in Figures 6-1 to 6-5, and the resultant test frequencies are summarized in Table 6-1. The transfer function to the center of the flatcar for in-phase excitation is shown in Figure 6-1 and its principal resonance is a double peak at 3.6 to 4.2 Hz. This phenomenon is discussed in more detail in Section 6.2.3. The flatcar body structural amplification is shown in Figure 6-2 (a) and clearly indicates the first bending mode of the flatcar at 4.2 Hz. Also shown in Figure 6-2 is the displacement measured across the flatcar truck spring group and it shows two resonances with significant motion in the springs. These two resonances correspond to the rigid body bounce and pitch modes of the flatcar.

The transfer functions for the out-of-phase excitation in Figure 6-3 (a) shows predominant resonance at 2.4 and 10.2 Hz. The phase plot in 6-3 (b) of accelerometers at the A and B end of the flatcar shows the 2.4 Hz resonance to be in-phase or a flatcar body torsional mode. Figure 6-3 (b) also shows the B end (meas 65) to have an amplification over the A end (meas 85) at 11 Hz indicating a torsional mode in which one end is rocking with much larger amplitudes than the other end.

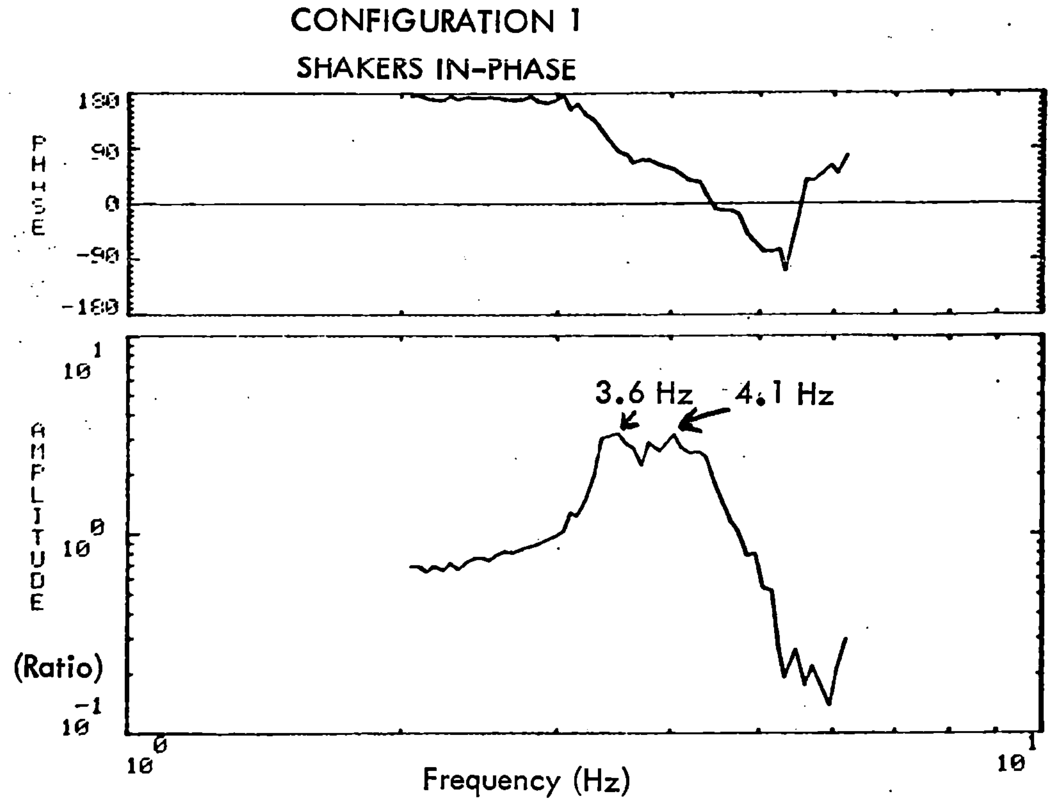

CONFIGURATION 1, EMPTY FLATCAR, 0.3 FULL LEVEL SINE SWEEP, RUN 22

89/Input, Flatcar Center Transfer Function

(a)

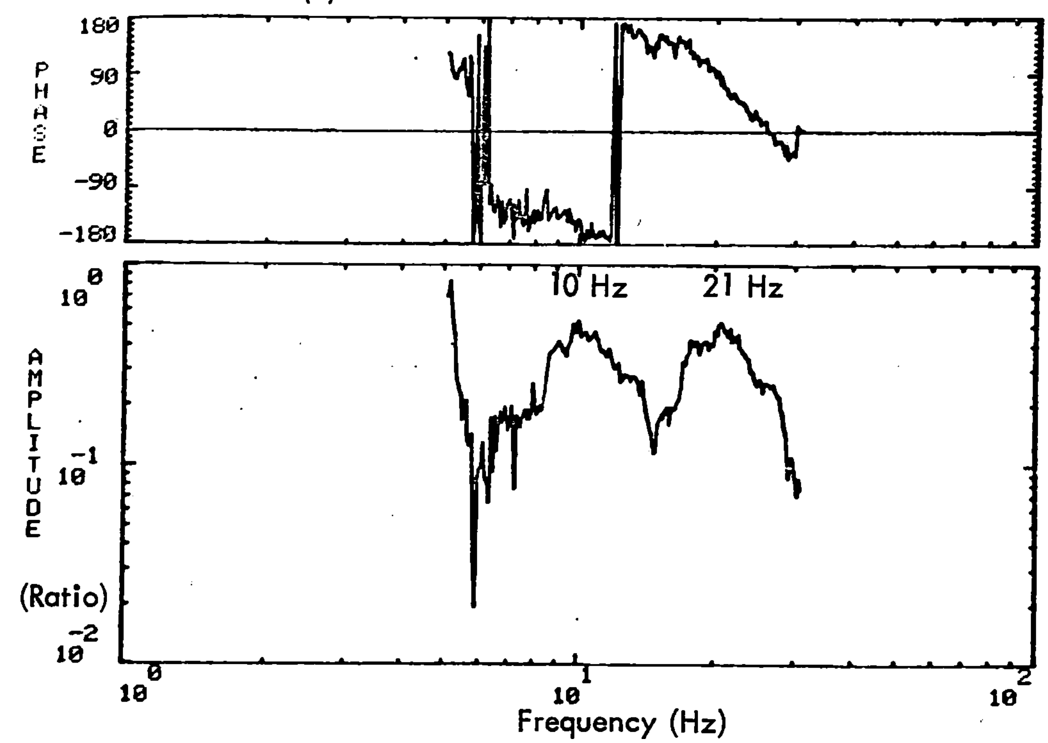

CONFIGURATION 1, EMPTY FLATCAR, 0.5 FULL LEVEL SINE SWEEP, RUN 21

89/Input, Flatcar Center Transfer Function

(b)

Figure 6-1. Response At Flatcar Center, Configuration 1

CONFIGURATION 1

SHAKERS IN-PHASE

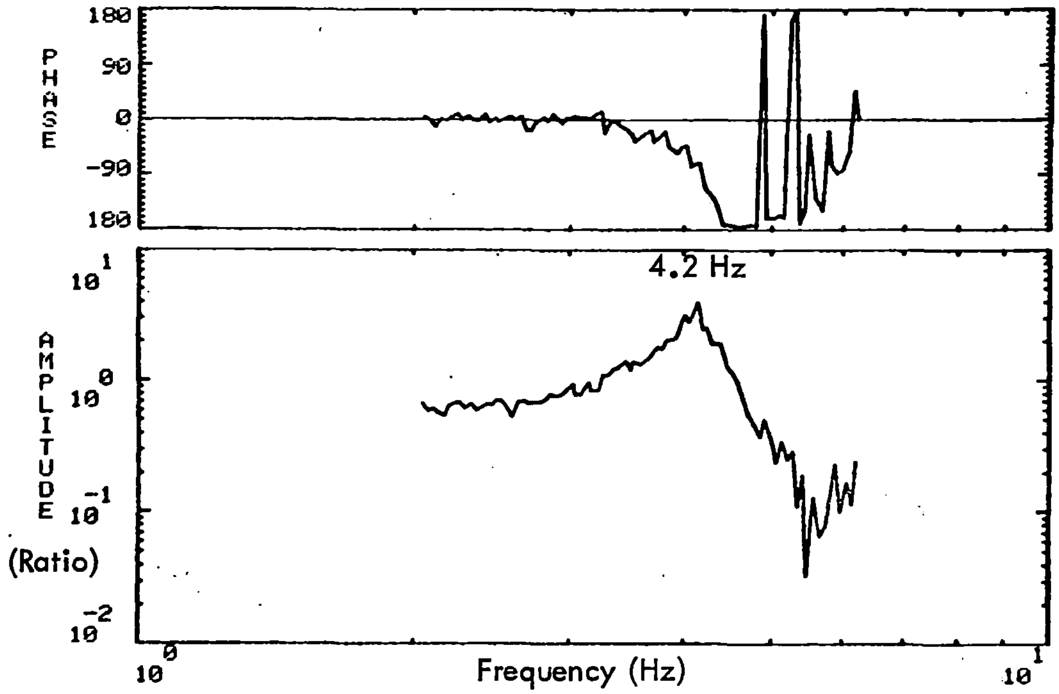

CONFIGURATION 1, EMPTY FLATCAR, 0.3 FULL LEVEL SINE SWEEP, RUN 20

89/65, Flatcar Structural Amplification

(a)

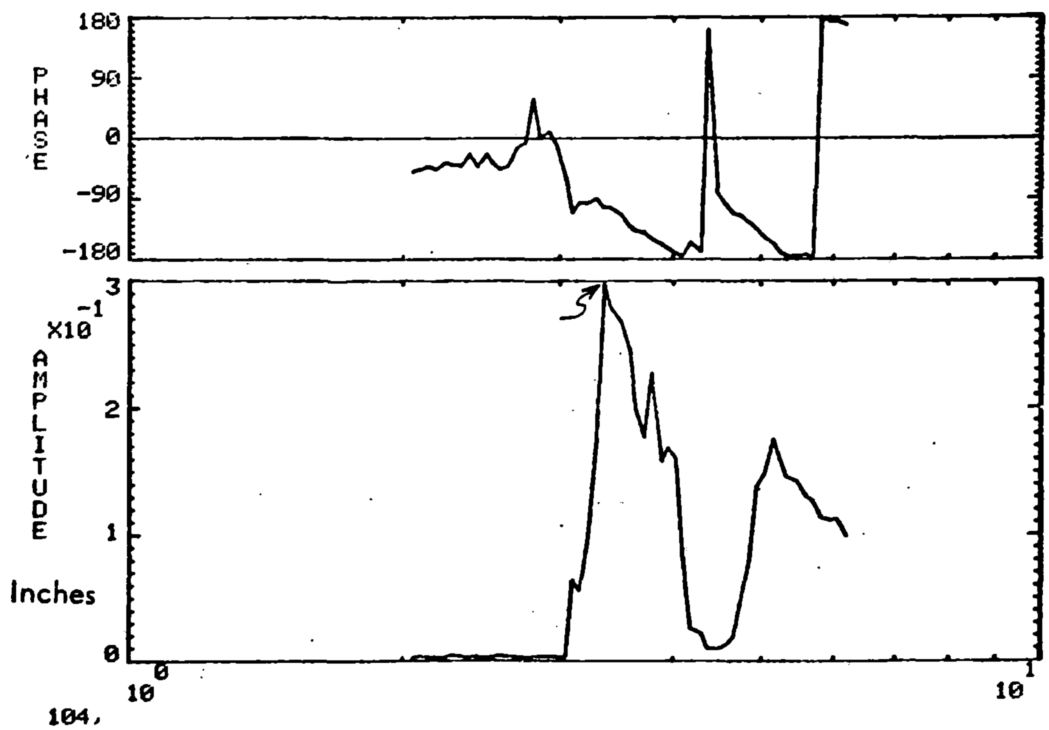

CONFIGURATION 1, EMPTY FLATCAR, 0.3 FULL LEVEL SINE SWEEP, RUN 22

104, Displacement across Spring nest

(b)

Figure 6-2. Flatcar Responses

CONFIGURATION 1

SHAKERS OUT-OF-PHASE

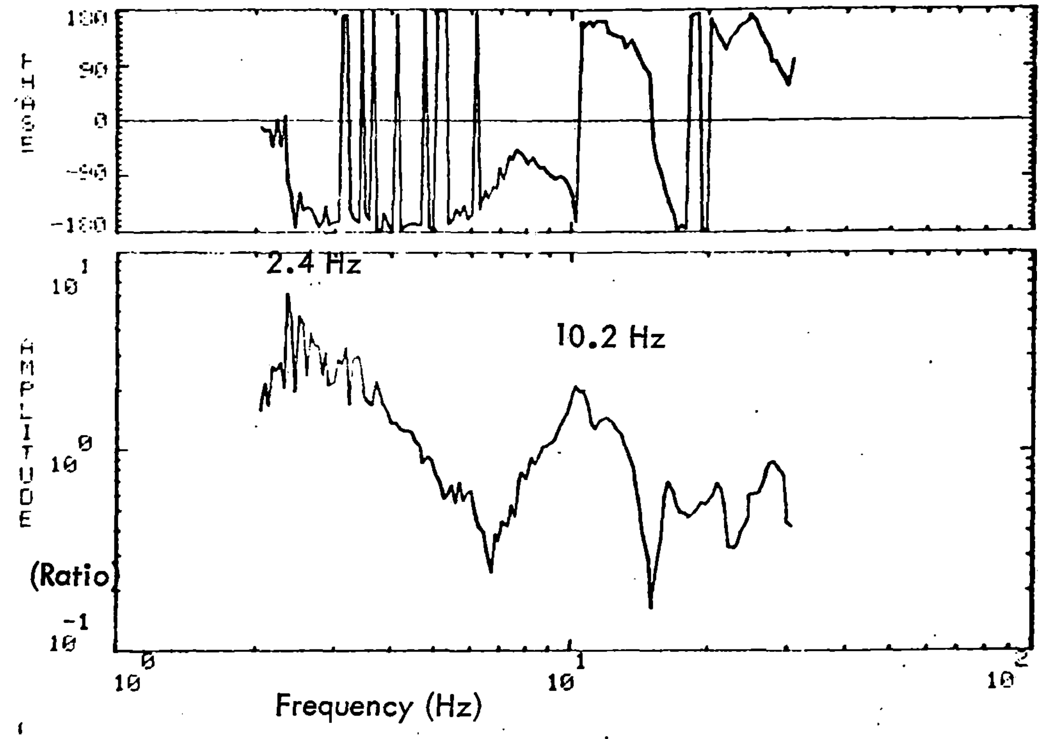

CONFIGURATION 1, FULL LEVEL SINE SWEEP, OUT-OF-PHASE, RUN 92

65/Input, Amplification factor

(a)

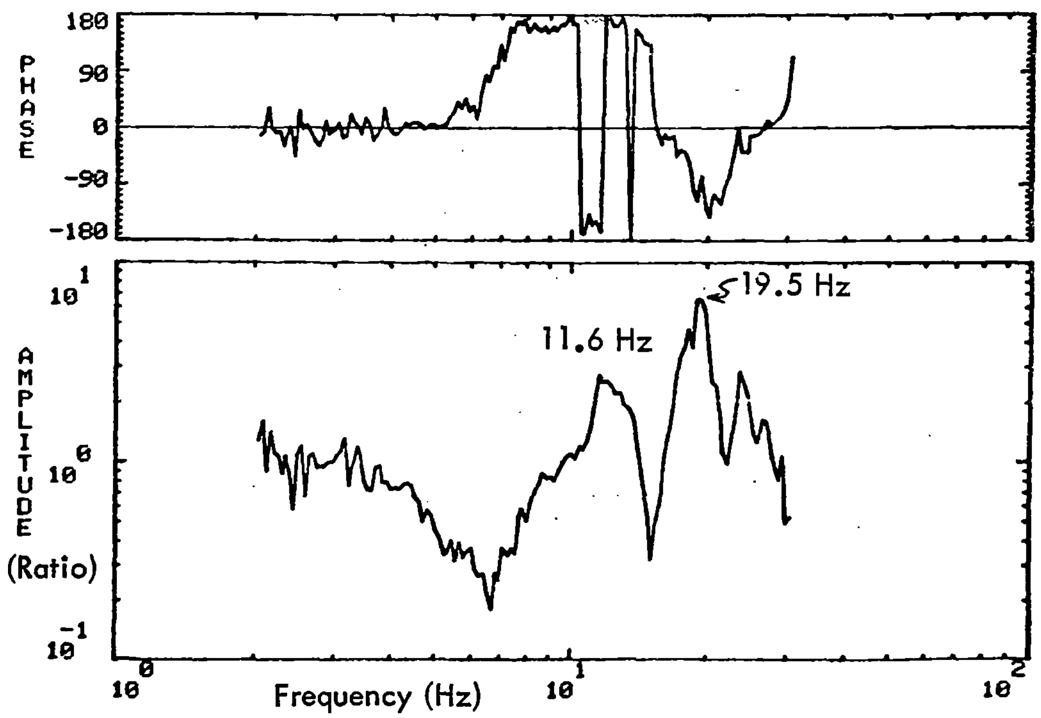

CONFIGURATION 1, FULL LEVEL SINE SWEEP, OUT-OF-PHASE, RUN 92

65/85 Torsional Response

(b)

Figure 6-3. Flatcar Torsional Responses

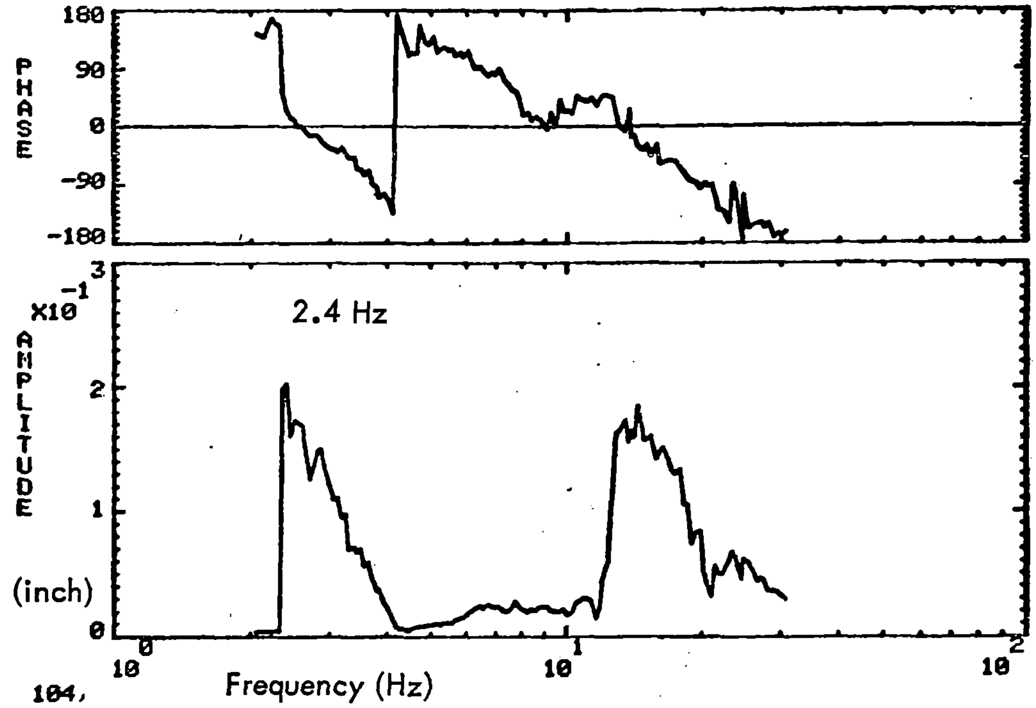

CONFIGURATION 1, FULL LEVEL SINE SWEEP, OUT-OF-PHASE, RUN 92

106, Motion across Spring group

(a)

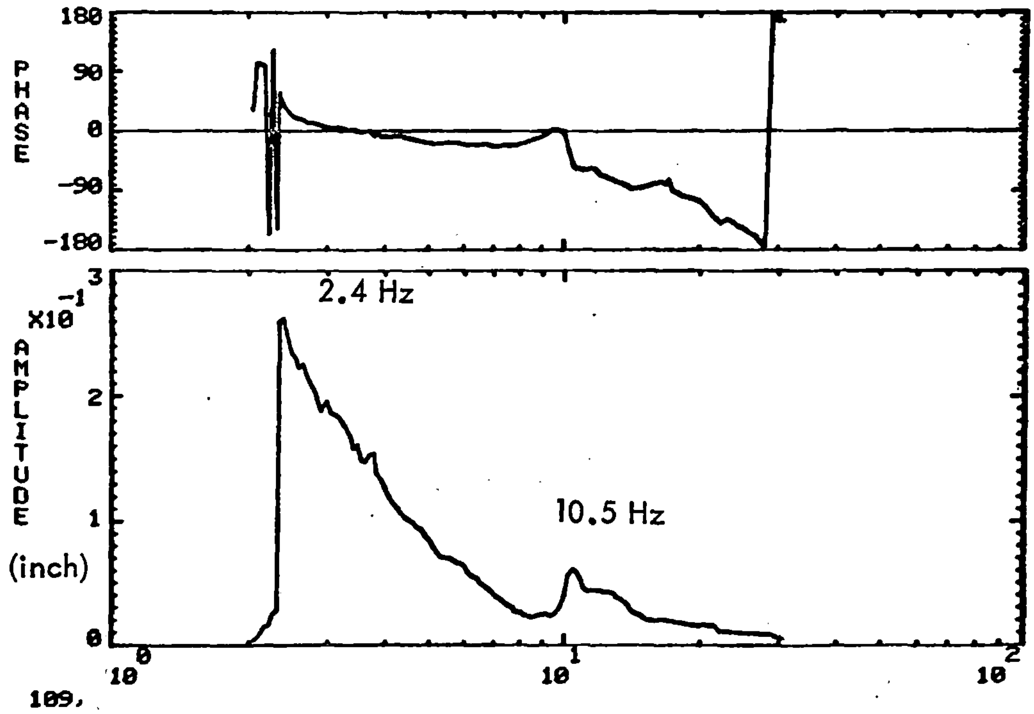

CONFIGURATION 1, FULL LEVEL SINE SWEEP, OUT-OF-PHASE, RUN 92

109, Flatcar Centerplate Rocking

(b)

Figure 6-4. Flatcar Displacement Measurements

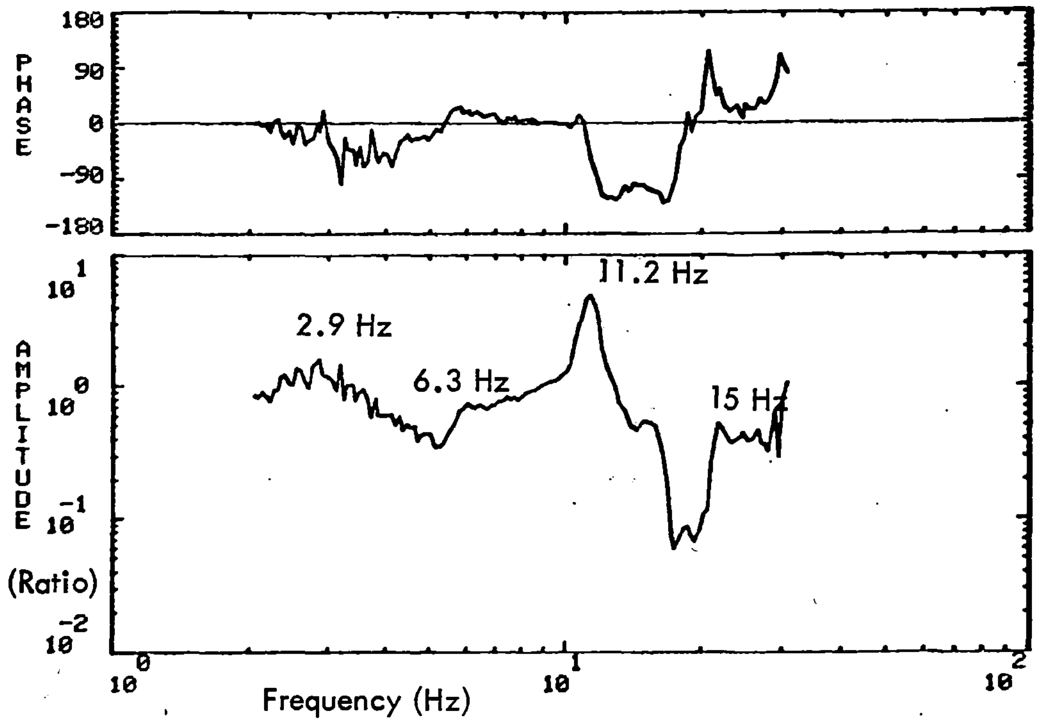

CONFIGURATION 1, FULL LEVEL SINE SWEEP, OUT-OF-PHASE, RUN 92

116/69 Flatcar Lateral Structural Amplification

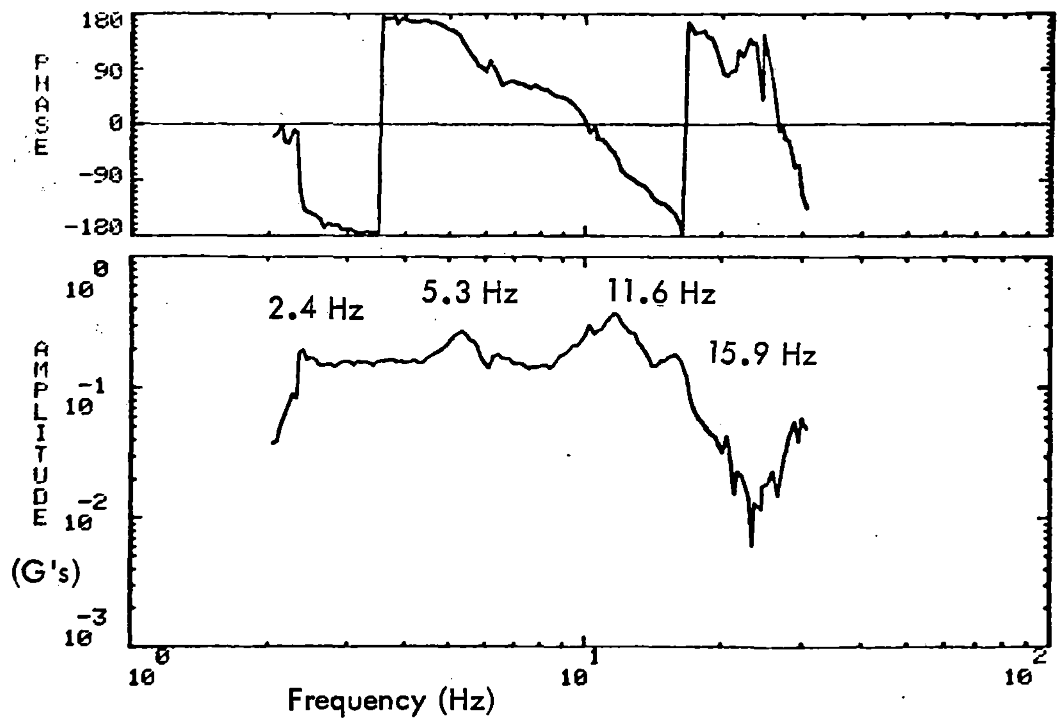

CONFIGURATION 1, FULL LEVEL SINE SWEEP, OUT-OF-PHASE, RUN 92

86, Flatcar Lateral Response

(b)

Figure 6-5. Flatcar Lateral Responses

Table 6-1. Response Frequencies, Configuration 1

Mode	Test	Revised Model
Rocking	2.6 Hz	2.7 Hz
Sway	**	3.4 Hz
Rigid Body Bounce	3.6 Hz	3.6 Hz
1st Vertical Body Bending	4.2 Hz	4.2 Hz
Rigid Body Pitch	5.3	5.1
2nd Vertical Body Bending	10	11
1st Lateral Body Bending	11.2	11.2
1st Torsional	11	12
3rd Vertical Body Bending	16.3	20.5
2nd Lateral Body Bending	**	23
4th Vertical Body Bending	26	28

**Not Identifiable

The displacement measurement made on the spring nest and the truck to flatcar bolster are shown in Figure 6-4. The most significant thing to note in the figures is the rocking of the flatcar on the center plate at the lower resonance. Because the truck to flatcar bolster measure was made much closer to the center of the flatcar, the rocking angle on the center plate is much greater for the truck to flatcar bolster than for the same deflection at the spring group. The rocking on the center plate becomes much less as the frequency increases. The flatcar lateral responses are shown in Figure 6-5. The most significant resonance occurs at 11.5 Hz and the plot (Figure 6-5 (a)) of flatcar lateral structural amplification indicates this to be a lateral bending mode.

The resonant frequencies measured during the test are summarized in Table 6-1 for configuration 1. As can be seen from the data in Figures 6-1 to 6-5 the frequency can vary depending on which accelerometer or transfer function is being used. The frequencies in Table 6-1 are the best estimate for the actual frequency based on all the data and may vary somewhat from those frequencies noted in the plot figures.

Another technique which proved useful in picking out resonant frequencies was to analyze the decay-time history in the form of PSD's. This is shown in Figure 6-6, a time history of accelerometer 118 and PSD's of this time history at three successive time slices. In the first PSD (6-6 (b)) the drive signal of 1.5 Hz is still apparent, as is a lot of energy resulting from many frequencies being excited by the transient caused by shutdown. The drive frequency refers to the sinusoidal frequency at which the specimen was being driven prior to being shut down and the start of decay. By the third time slice all the energy that is left has been transferred into the first three bending modes as shown in Figure 6-6 (d). The energy spike at 60 Hz is noise. The resulting frequency information from the PSD analysis is summarized in Table 6-2, along with a comparison of the frequencies as established using the sweep plot data.

6.2.2 Flatcar Model Modifications

The measured resonant frequencies from the test data were used to modify the finite element model to bring test and measured results into agreement. The predominant response frequency was the first flatcar bending mode response at 4.2 Hz. Thus the flatcar structural model (described in 2.1.1) was modified to obtain a first bending frequency of 4.2 Hz and damping of .54%. The bending frequency and damping were

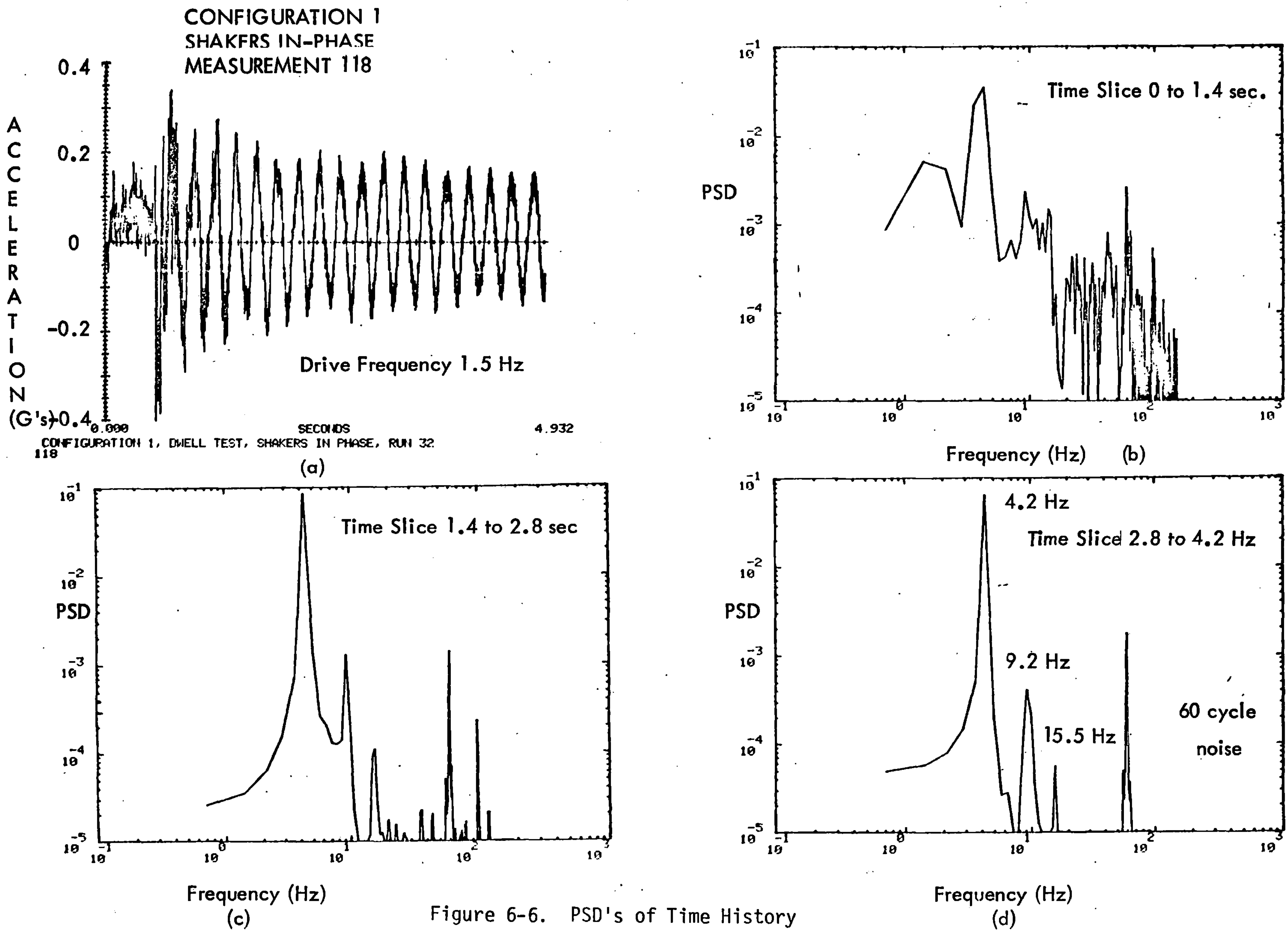

Figure 6-6. PSD's of Time History

CONFIGURATION 1

SHAKERS IN-PHASE

MEASUREMENT 89

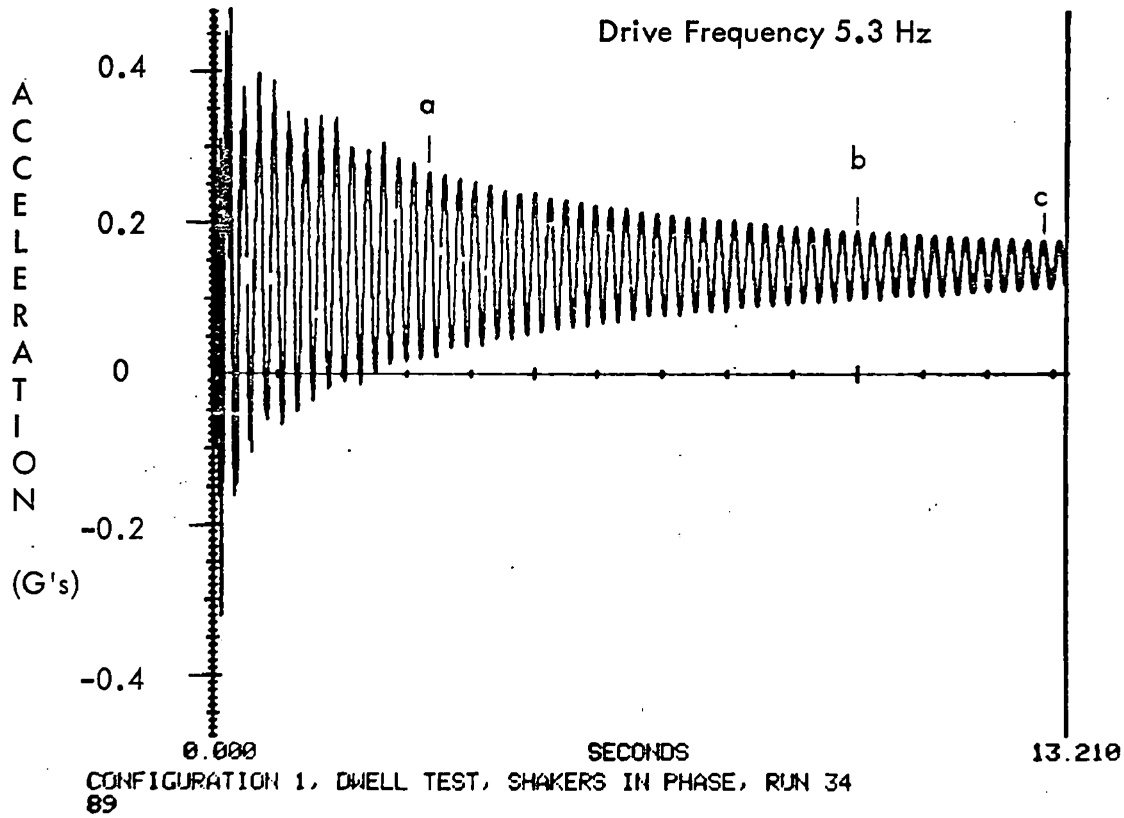

t_a = 3.32 sec. t_b = 9.94 sec t_c = 12.81 sec.

x_a = .24 p-p x_b = .09 pp x_c = .06g p-p

$$f_n = \frac{\text{number cycles}}{\Delta t} \qquad \zeta = \frac{1}{2\pi(\text{no. cycles})} \ln \frac{x_1}{x_2}$$

$$f_{ab} = \frac{28 \text{ cycles}}{6.62 \text{ sec}} = 4.22 \text{ Hz} \qquad \zeta_{a-b} = \frac{1}{2\pi(28)} \ln\left(\frac{.24}{.09}\right) = 0.55\%$$

$$f_{bc} = \frac{12 \text{ cycles}}{2.87 \text{ sec}} = 4.18 \text{ Hz} \qquad \zeta_{b-c} = \frac{1}{2\pi(12)} \ln\left(\frac{.09}{.06}\right) = 0.54\%$$

$$f_{ac} = \frac{40 \text{ cycles}}{9.49 \text{ sec}} = 4.21 \text{ Hz} \qquad \zeta_{ac} = \frac{1}{2\pi(40)} \ln\left(\frac{.24}{.06}\right) = 0.55\%$$

Figure 6-7. Flatcar Decay Trace

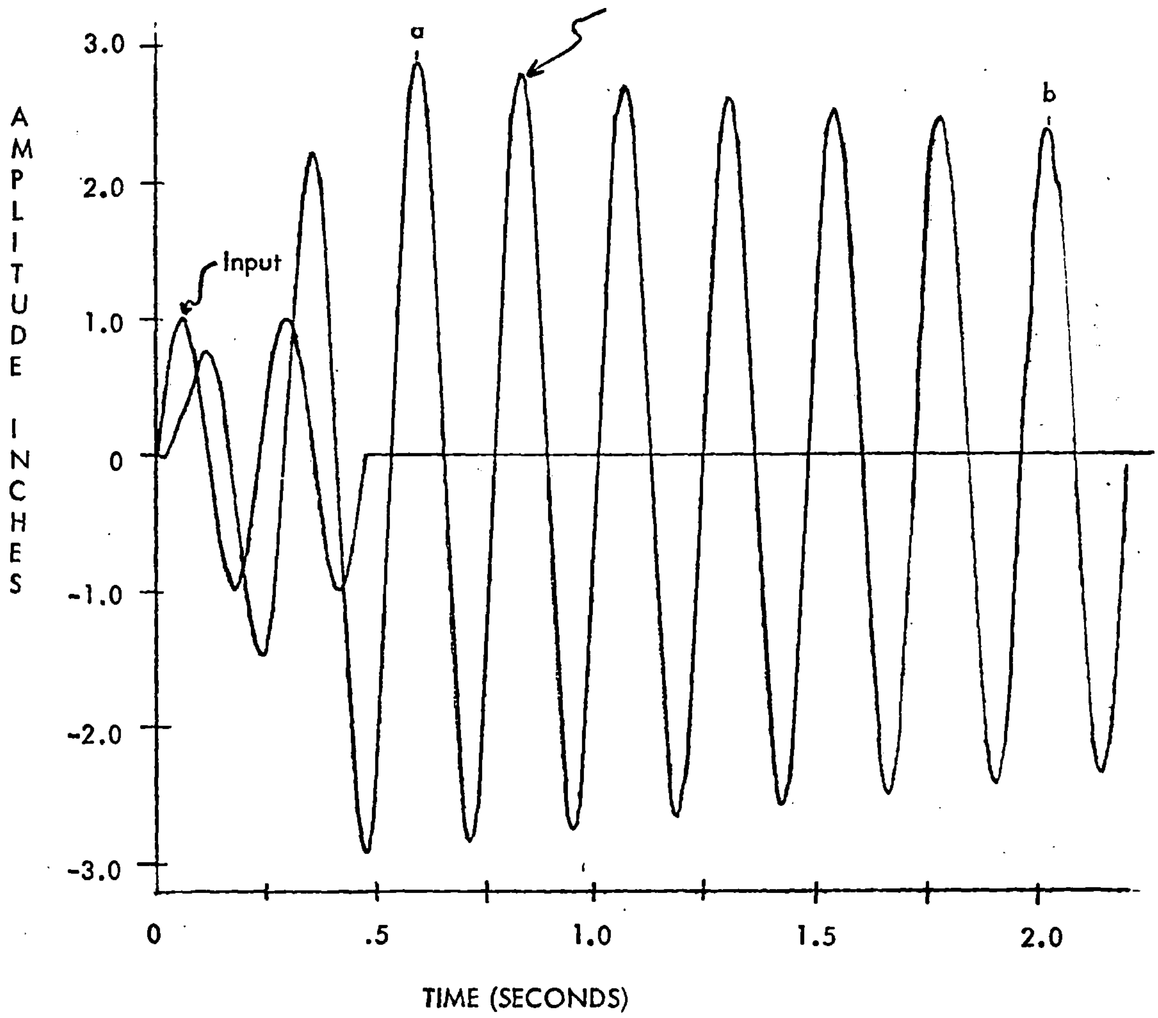

$t_a = 0.594$ sec $\quad t_b = 2.018$ sec.

$x_a = 2.8825 \quad x_b = 2.3810$

$$f_{ab} = \frac{\text{No. Cycles}}{\Delta t} = \frac{6 \text{ cycles}}{1.424 \text{ sec}} = 4.2 \text{ Hz}$$

$$\zeta = \frac{1}{2\pi n} \ln \frac{x_a}{x_b} = \frac{1}{2\pi 6} \ln \frac{2.8825}{2.3810} = 0.51\%$$

Figure 6-8. Analytical Decay Time History

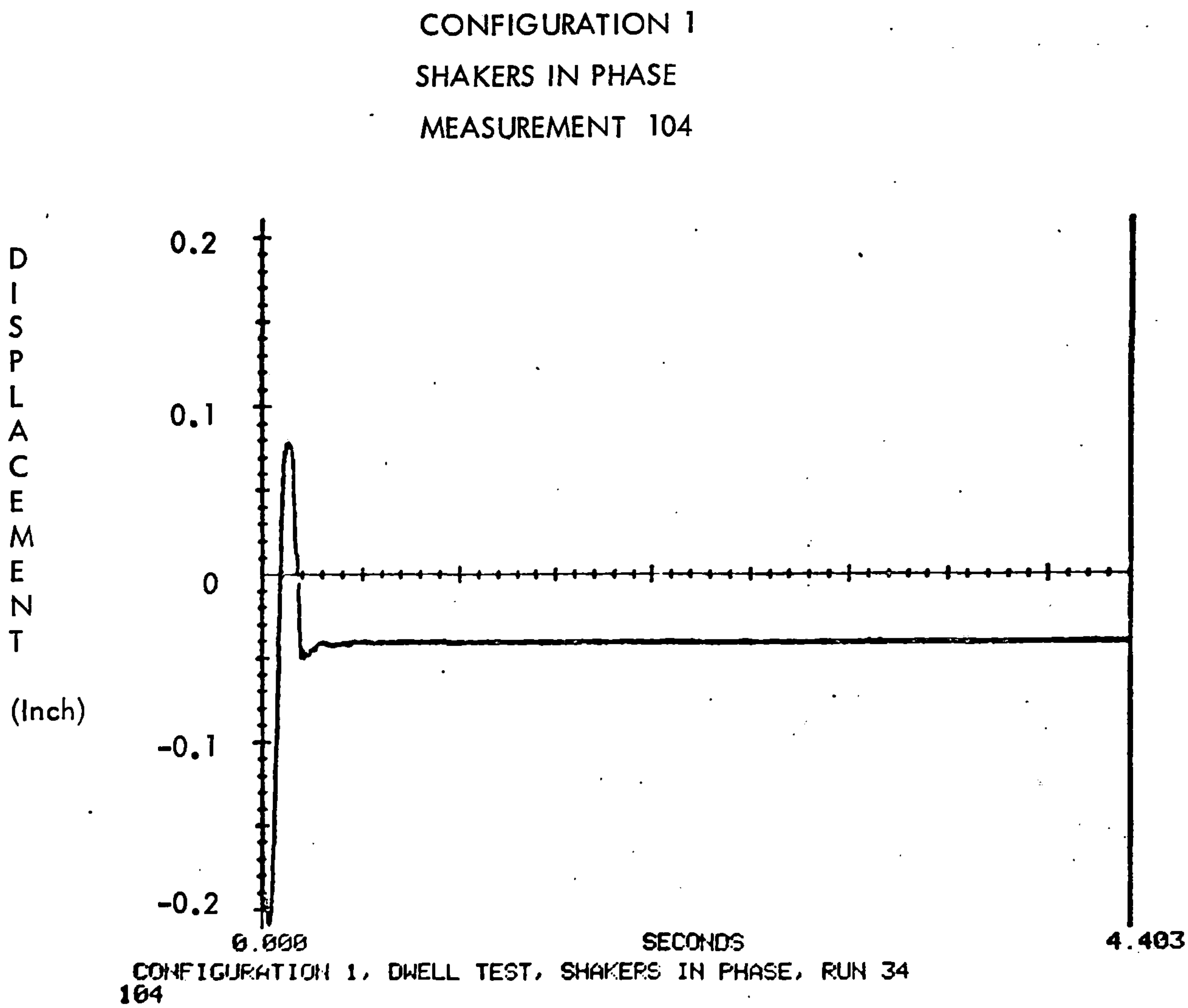

Figure 6-9. Displacement Across Spring Group

obtained from decay traces such as those shown in Figure 6-7 for the accelerometer at the center of the flatcar. The damping value was calculated using the log decrement measured from the decay trace shown in Figure 6-7. Examination of the truck spring displacement measurement during the configuration 1 decay tests (Figure 6-9) shows that the friction snubbers lock the truck springs out immediately after the forced excitation is stopped. Thus for this configuration, the flatcar will act as a flexible beam on two rigid supports, and the decay frequency will be essentially the same as the first car body mode. Therefore, the approach taken was to adjust the structural mode of the flatcar body mode alone until it agreed with test data.

Using the transient response capability of ANSYS, time histories were obtained for the node at the center of the flatcar mode. The flatcar flexibility was adjusted until the analytical decay plot shown in Figure 6-8 was obtained. The finite element model was given an input excitation of ± 1 inch at the B end as shown by the input in Figure 6-8. The excitation was then stopped as done during the decay tests and the response as calculated for the center of the flatcar plotted. The resulting decay trace shown in Figure 6-8 could then be evaluated for resonant frequency and log decrement damping. The analytical curve agrees with the decay trace (Figure 6-7) measured during the test.

The stiffness of the flatcar structure was modified to obtain a first lateral bending frequency of 11.2 Hz to agree with test data. The torsional stiffness of the flatcar structure was modified to obtain a torsional mode of 11 Hz. Since the rigid body modes of the flatcar agreed with test results, no modifications had to be made to the truck spring constants.

This was then the analytical model of the flatcar which was used in the model analyses presented in this report. The resultant resonant frequencies (as determined in Section 6.3.4) are summarized in Table 6-1 as the modified model frequencies for comparison with the test data.

6.2.3 Linearity

6.2.3.1 In-Phase Excitation

To establish the linearity and repeatability of data from configuration 1, four runs at different amplitudes were chosen for comparison. The input amplitudes are plotted in

Figure 6-10. In-phase excitation runs 6, 16, and 20 were run at different amplitudes and runs 20 and 22 at the same amplitude. The basis for comparison was the transfer function (amplification factor) at the center of the flatcar (measurement 89/input). These are plotted in Figure 6-11 (a) for the runs at different amplitudes. For a linear system, the amplification factors should be independent of input amplitude. Up to 3 Hz and from 5 Hz to the end of the data the flatcar seems to be relatively linear; however, in the range of the first resonance frequency the flatcar response is very dependent on the input amplitude.

For low levels of input (run 6) the flatcar amplification is quite high and decreases as the input levels increase. Also, there is a change in the frequency at which the peak amplification factor occurs. This can be explained by the following: at the low input amplitudes the friction snubbers lock out the truck springs and the flatcar responds at the body bending frequency (4.2 Hz). The displacement across the truck springs is shown in Figure 6-11 (b) where there is practically no displacement for run 6. For the intermediate run (16) the motion across the truck springs (Figure 6-11 (b)) shows the amplitude beginning to increase. For the highest level run (2) the resonant peak has shifted down to 3.65 Hz, which is the response frequency of the combined truck/flexible flatcar. From Figure 6-11 (b) the spring group has started to move at 3.6 Hz, which is why the flatcar begins to respond at this frequency, but the friction snubber still causes some energy to be transferred to the 4.1 Hz mode, which is why the resonant frequency is double peaked. If a run could be made without the friction snubber, the flatcar should respond with a single peak at 3.6 Hz rather than the double peak which now occurs with the friction snubbers.

The above theory agrees with the decay test data that says the empty flatcar decays at 4.1 Hz, and the motion across the spring group goes to zero. It would also tend to explain the high amplification factors measured during the decay tests. The 1/2 percent damping measured corresponds to an amplification factor of 100. This compares to a maximum amplification factor of 8 (Figure 6-10 (b)) measured during sweep. The difference can be explained by the spring group which has a small amplitude (Figure 6-10 (b)) during run 16, which results in a much lower amplification factor; therefore, during the decay test, the spring group has no displacement, resulting in much larger amplitudes.

LINEARITY COMPARISON
CONFIGURATION 1
SHAKER INPUT

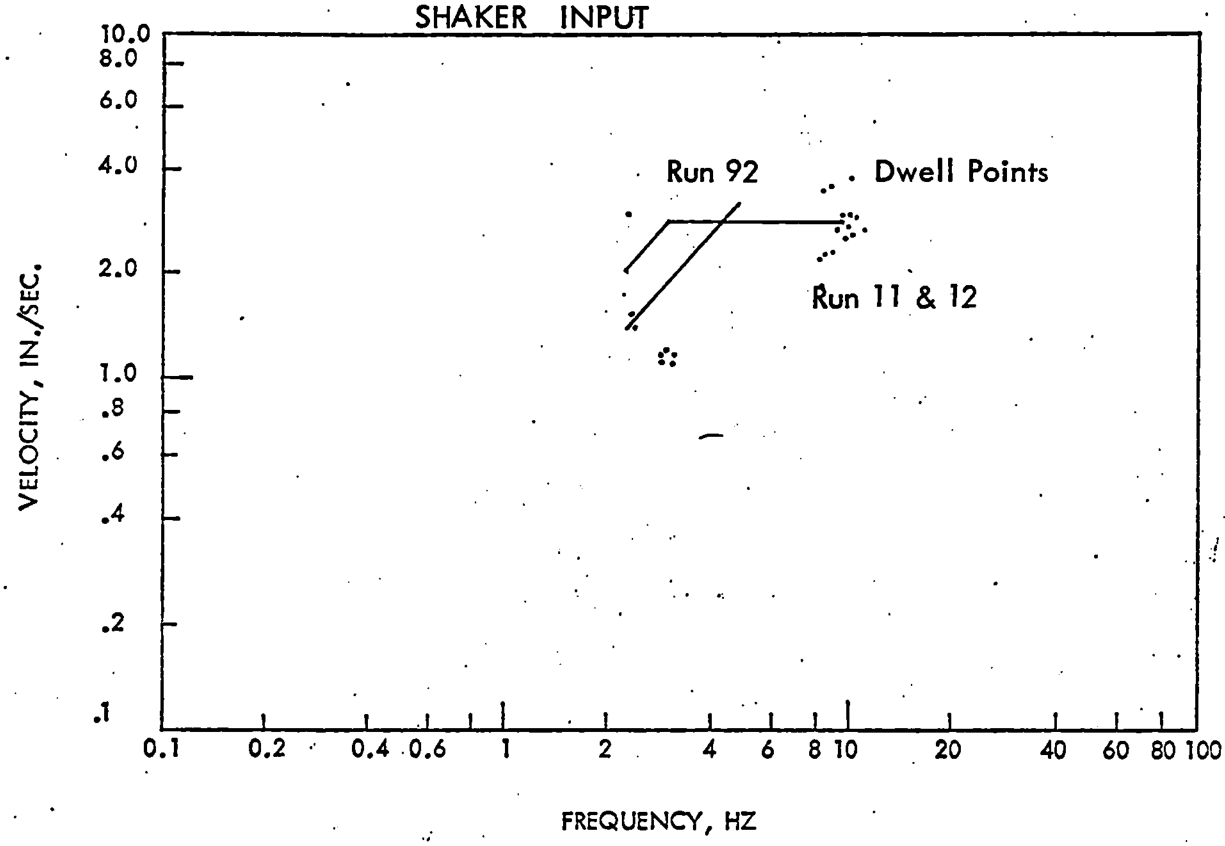

SHAKERS OUT-OF-PHASE

(b)

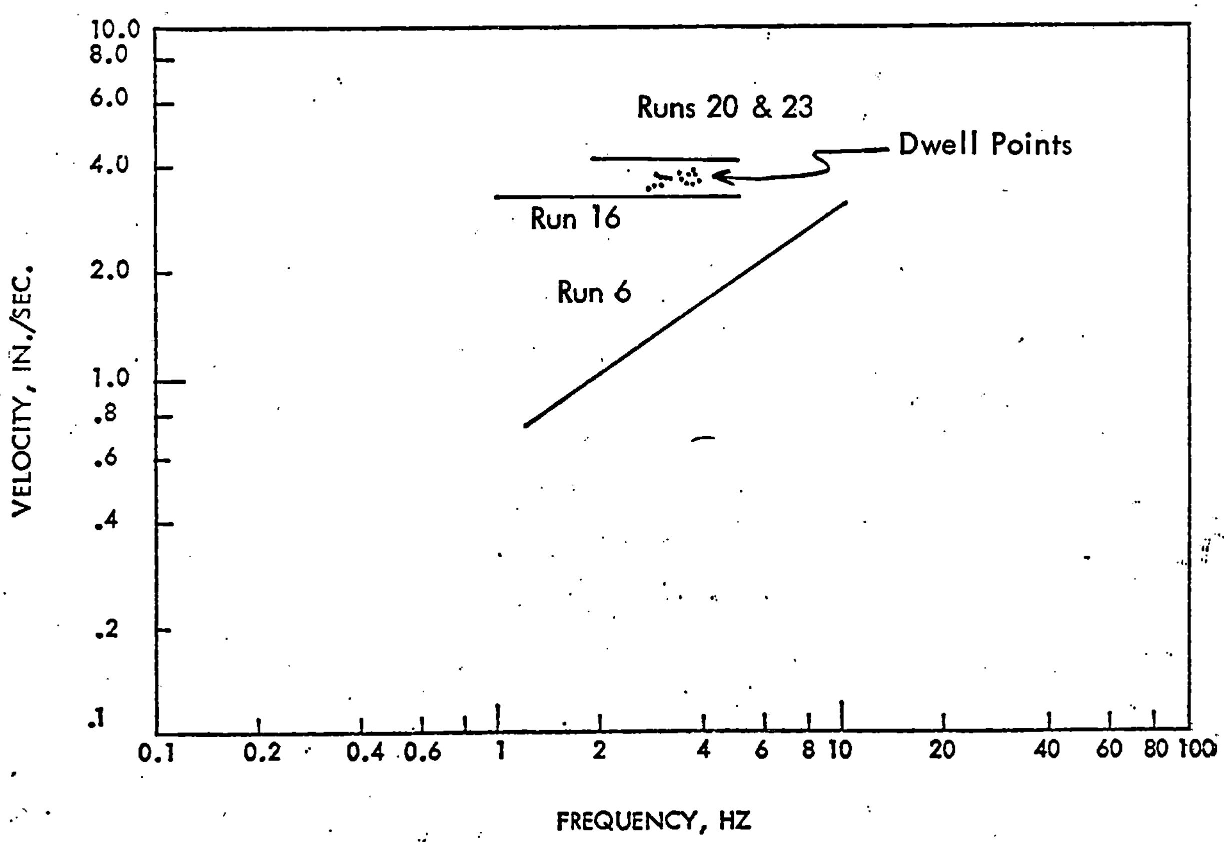

SHAKERS IN PHASE

Figure 6-10. Linearity Comparison Input Amplitudes

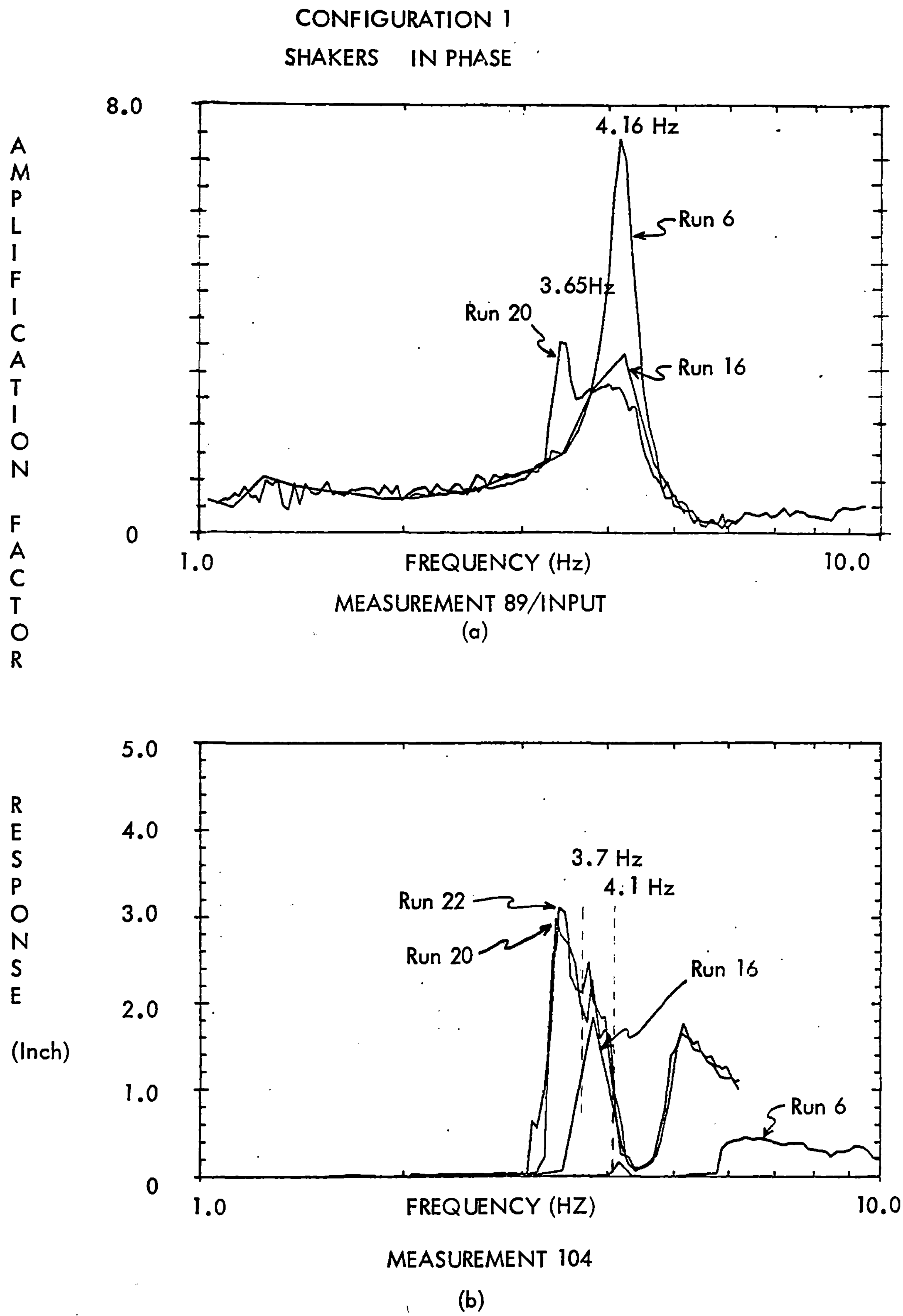

Figure 6-11. Configuration 1 Linearity Comparison

The two identical runs (20 and 22) are compared in Figure 6-12 and show excellent agreement except in the resonant frequency range, where the two runs show considerable variation between some frequency points. However, the shape of both curves show the same double-peaked resonance.

The Q value noted in Figure 6-12 is the Q at which each sweep was run. The higher the Q the greater the number of frequencies dwelled at for the sweep.

Various dwell tests were run at frequencies around the resonant frequency shown in Figure 6-10. The measured transfer function at the center of the flatcar for the dwell runs are plotted in Figure 6-12 and show excellent agreement with the sweep runs at the same amplitude.

The scatter which may seem to exist in the dwell data is most likely caused by the extreme sensitivity of the test to the input amplitude and not by the inability of the test setup to produce repeatable results.

It would seem from the excellent agreement between sweep and dwell that the sweep procedure provides a much better method of obtaining data. First, it provides many more data points with much easier handling of the data. It also would enable running several sweeps at various input amplitudes to provide a family of curves which would more clearly describe the variation in transfer function with input amplitude.

6.2.3.2 Out-of-Phase Excitation - For out-of-phase excitation the input levels for sweep and dwell are plotted in Figure 6-10 (b). The transfer functions to the flatcar are plotted in Figure 6-14 for the B end edge of the flatcar (Measurement 123) for the A end truck (Measurement 65). The frequencies up to 4 Hz show very large spikes and valleys in the data which are believed to be caused by aliasing of high frequency excitation resulting from the flatcar rocking on the center plate.

Aliasing, or frequency folding, occurs when a signal is sampled with fewer than two points per wavelength. This phenomenon is discussed in Section 3.2.3.2 of Part 1.

CONFIGURATION 1

SHAKERS IN PHASE

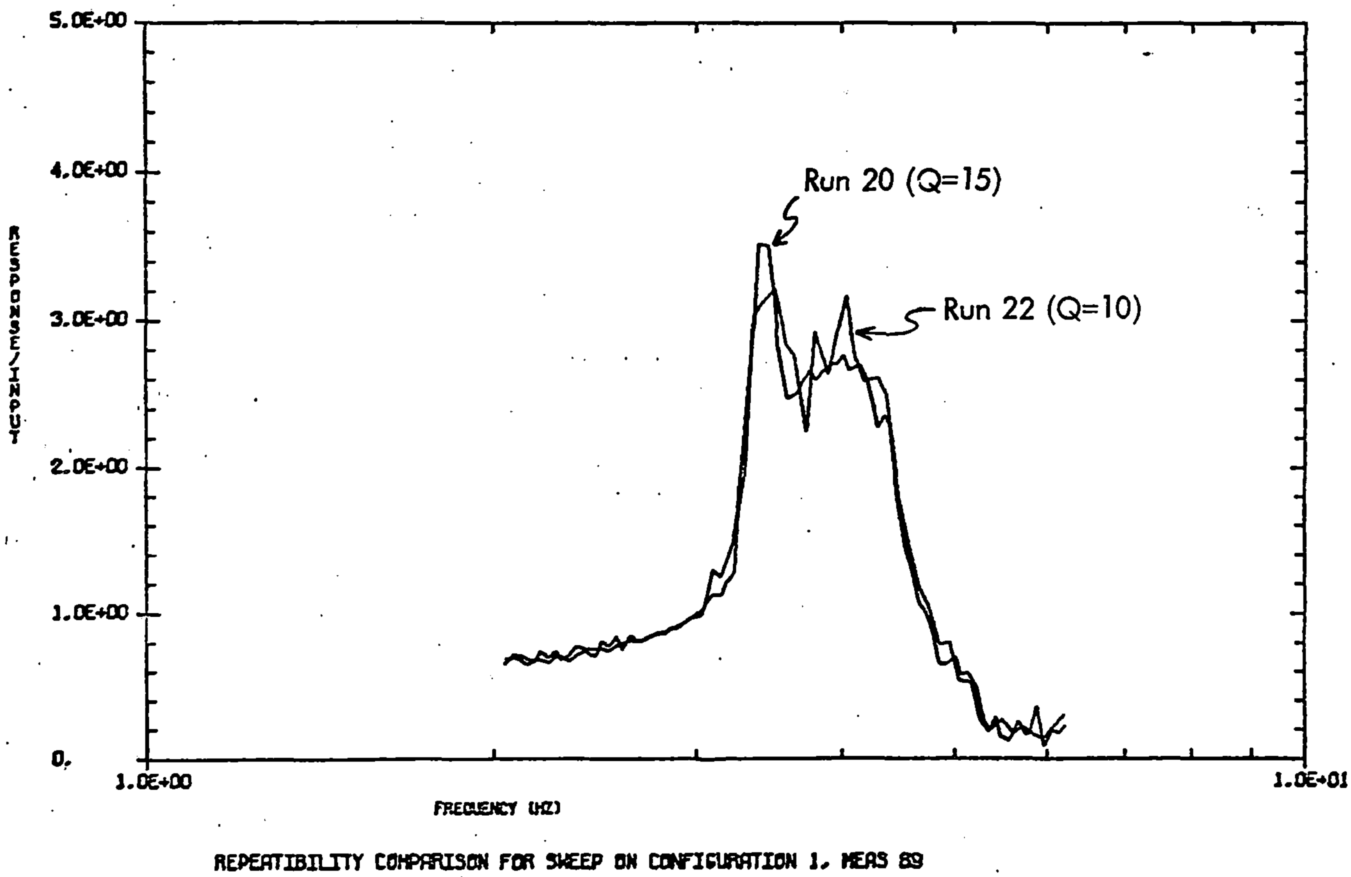

89/INPUT, Flatcar Body Transfer Function

Figure 6-12. Sweep Data Repeatability

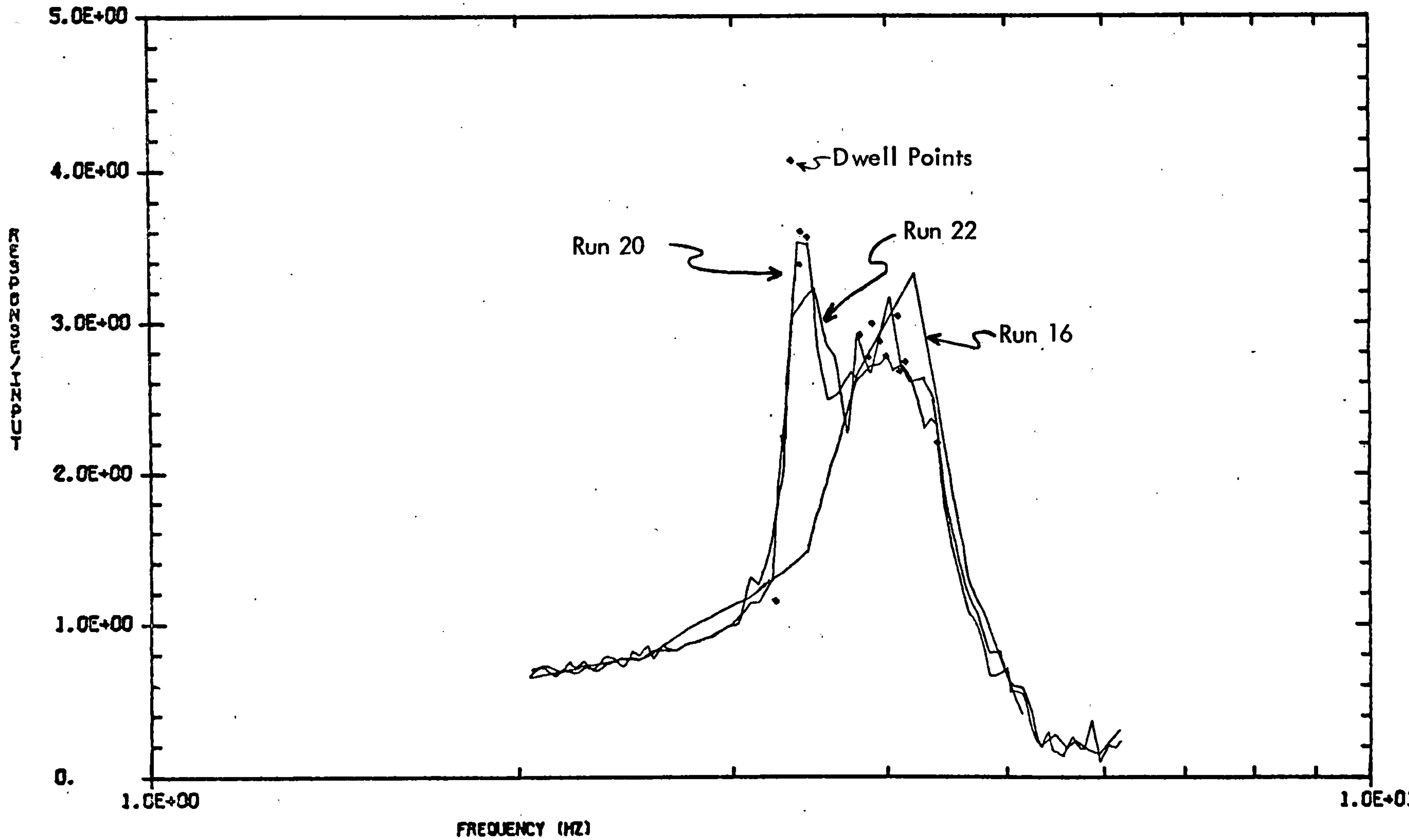

DWELL AND SWEEP COMPARISON FOR CONFIGURATION 1, MEAS. 89/INPUT

Figure 6-13. Dwell and Sweep Comparison

CONFIGURATION 1

SHAKERS OUT OF PHASE

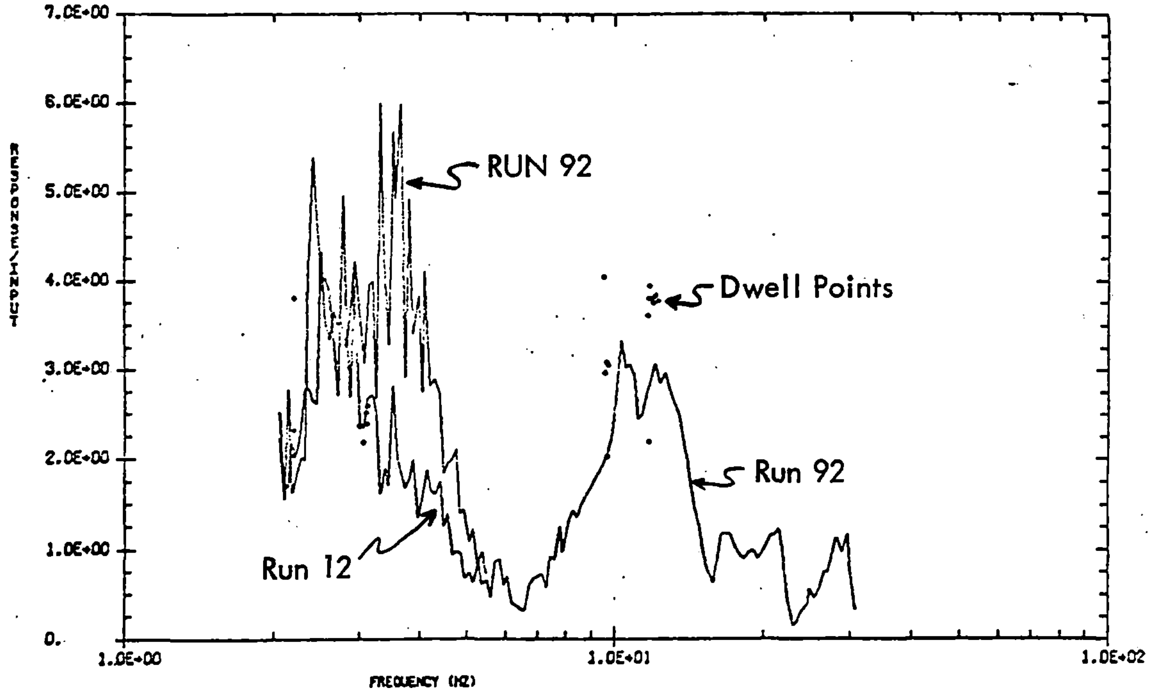

SWEEP AND DWELL COMPARISON FOR CONFIG 1, OUT OF PHASE, MEAS 123

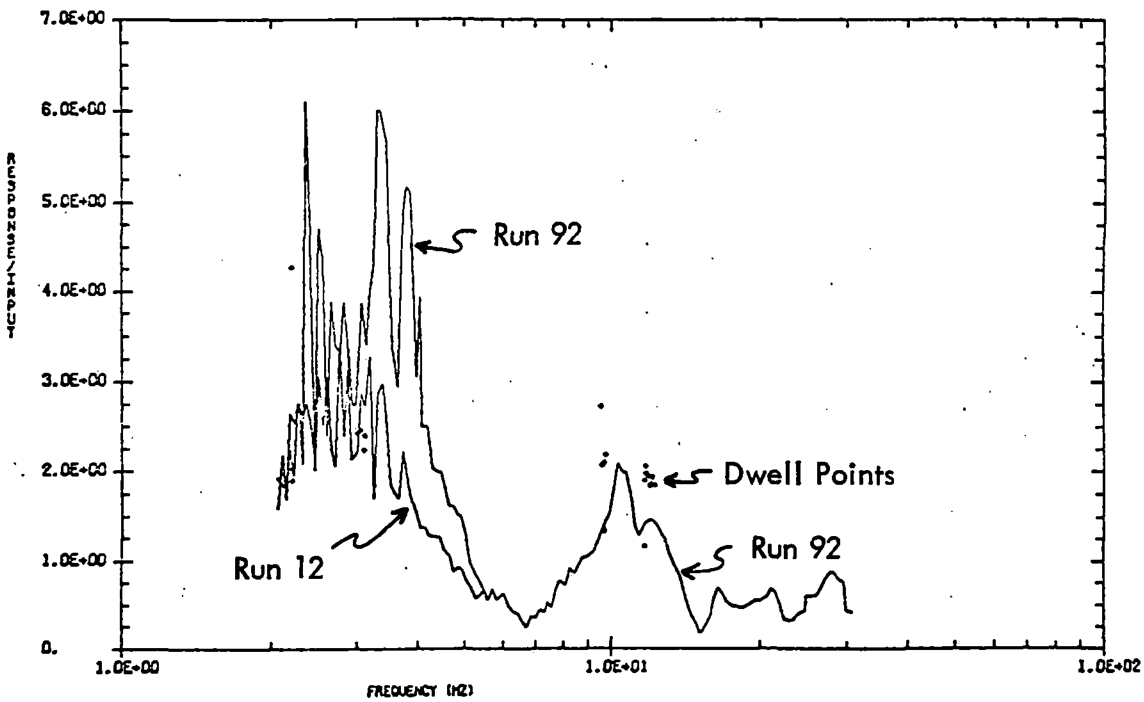

SWEEP AND DWELL COMPARISON FOR CONFIG 1, OUT OF PHASE, MEAS 65

Figure 6-14. Linearity Comparison

The truck to flatcar bolster measurements are shown in Figure 6-15 (a) and indicate large displacement in the low frequency but rapid tapering off by 5 Hz. The in-phase excitation had no center plate rocking, and the responses were also much smoother in the low frequencies (see Figure 6-1). The displacement across the spring group was about the same in both cases (Figures 6-12 (b) and 6-15 (a)).

The linearity comparison for the out-of-phase is a case where the schedule constraints precluded getting sufficient data to completely characterize the specimen. The two sweep runs plotted in Figure 6-14 show the transfer function in the low frequency range to be dependent on input amplitude.

The higher input level runs show greater amplification on the flatcar. Insufficient sweep data was made to draw conclusions in the higher frequencies.

Comparisons of dwell and sweep data in Figure 6-14 and 6-15 (a) show poor agreement. However, a more detailed comparison of the 6 to 12 Hz frequency range of Figure 6-14 (a) and Figure 6-16 shows that the variation between sweep and dwell may be a function of input amplitude. The transfer function seems to be inversely related to input amplitude. In all cases as the input amplitude increases the transfer function goes down. As in the case of in-phase excitation, the best approach would be to run a series of sweeps at various inputs to establish the actual dependence on amplitude.

Out-of-phase runs 11 and 12 were identical sweep. The transfer function at measurement 123 is compared in Table 6-3 for these runs and shows more data scatter than for in-phase. This would be expected from looking at the responses in the low frequency range (Figure 6-14 (a)).

6.2.4 Frequency Domain Responses

Using the modified flatcar model described in Section 6.2.2 and the ANSYS frequency domain calculation capability described in Paragraph 4.5, analytical calculations were made for the response of the flatcar at various measurement locations. Using the plot program capability described in Section 4.6, overlays were made to compare the analytical prediction with the data measured on the test program. The in-phase comparisons are made in Figures 6-17 through 6-19. The transfer functions to the deck

CONFIGURATION 1

SHAKERS OUT-OF-PHASE

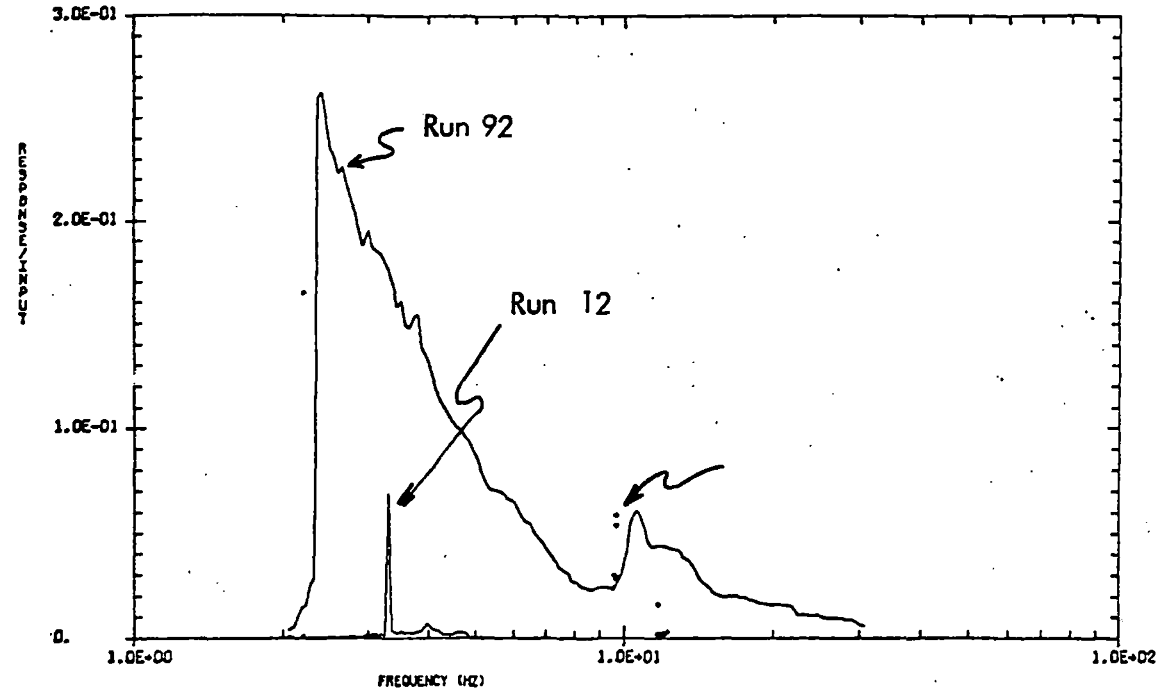

DWELL AND SWEEP COMPARISON FOR CONFIG 1, OUT OF PHASE, MEAS 104

109, Truck to Flatcar Bolster
(a)

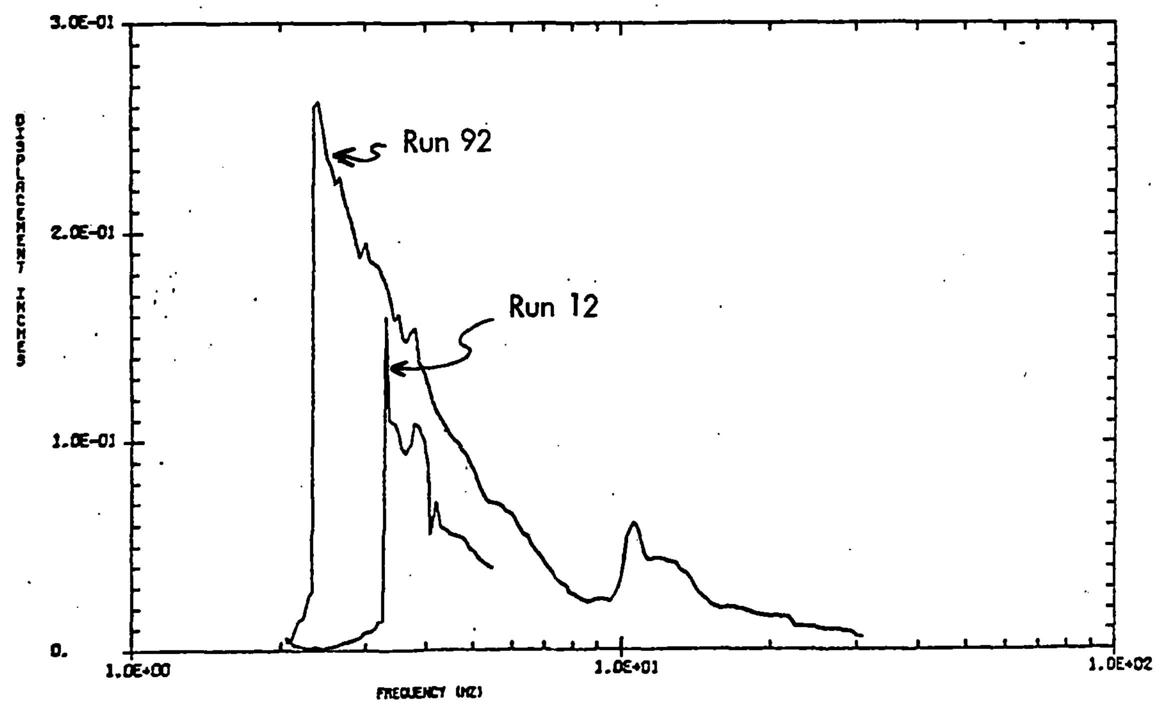

DISPLACEMENT MEASUREMENT ACROSS CENTER PLATE

Figure 6-15. Dwell and Sweep Comparison

CONFIGURATION 2, SHAKERS IN PHASE

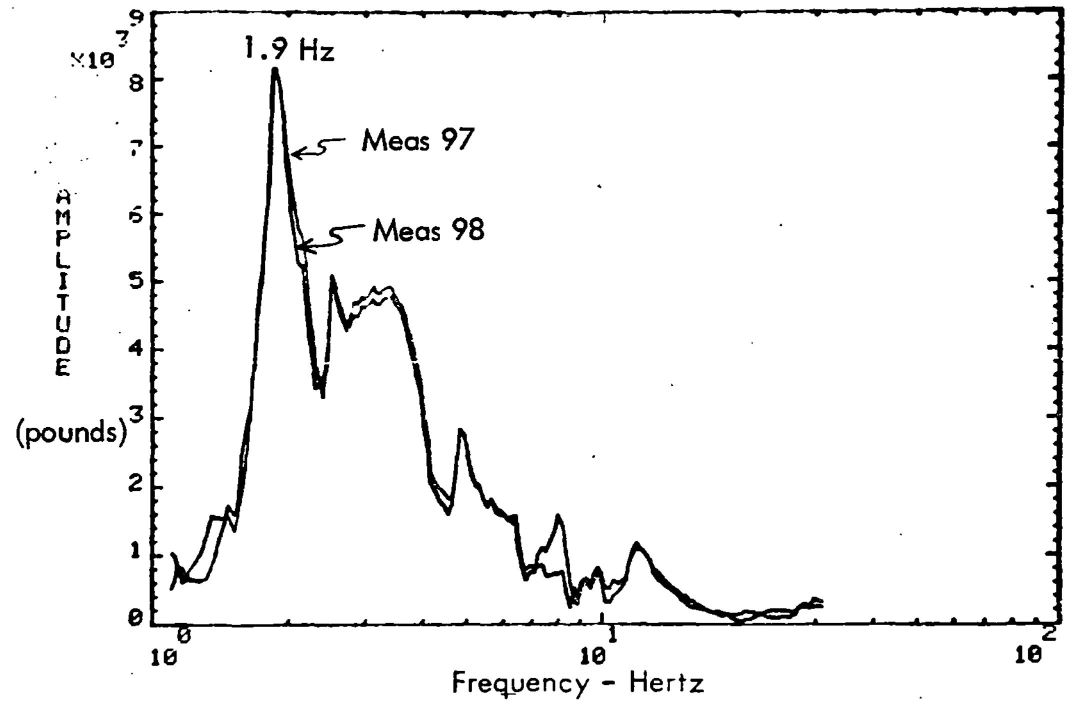

CONFIGURATION 2, HIGH LEVEL SINE SWEEP, SHAKERS IN PHASE, RUN 56

(a) Van Trailer Tire Force

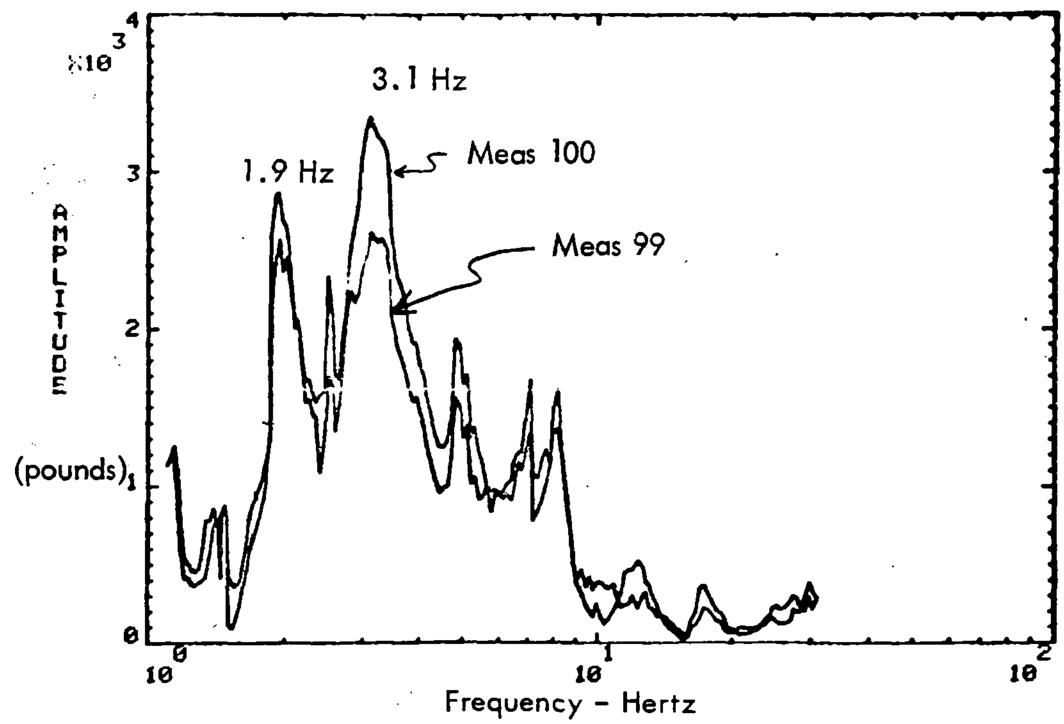

CONFIGURATION 2, HIGH LEVEL SINE SWEEP, SHAKERS IN PHASE, RUN 56

(b) Platform Trailer Tire Force

Figure 6-16. Trailer Tire Force Measurement

CONFIGURATION 1
SHAKERS IN PHASE

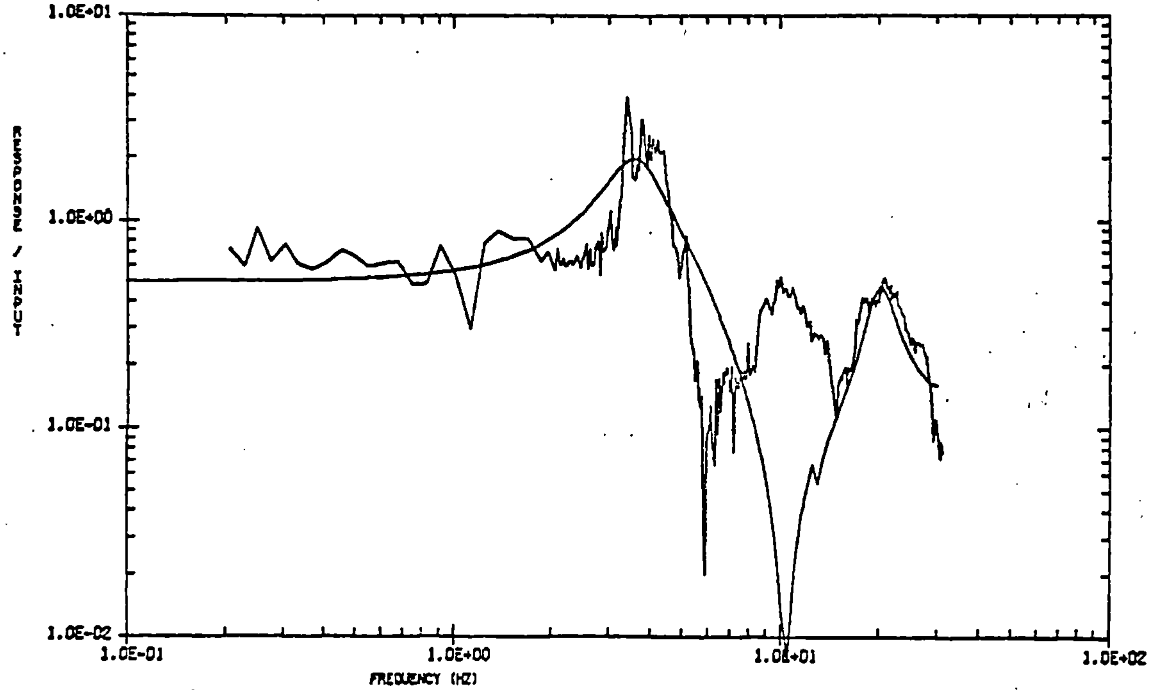

CONFIGURATION 1, SHAKERS IN PHASE, MEASUREMENT 89, REVISED TRANSFER FUNCTION

89/INPUT, Flatcar Center
(a)

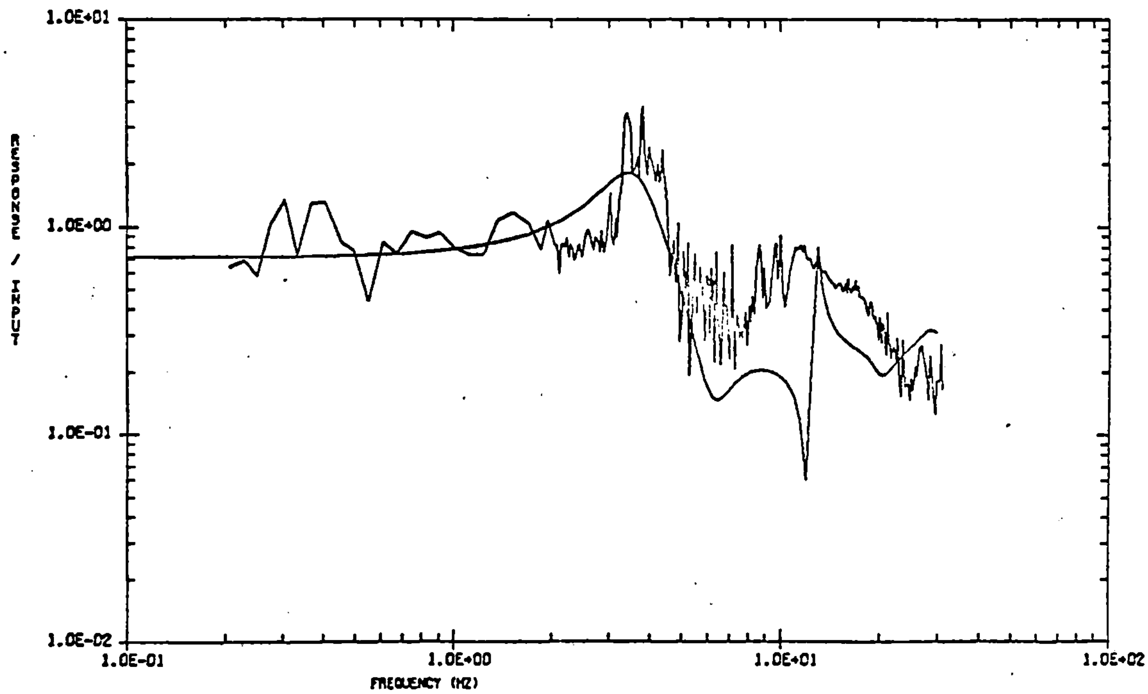

CONFIGURATION 1, SHAKERS IN PHASE, MEASUREMENT 117, REVISED TRANSFER FUNCTION

117/INPUT, Flatcar Deck
(b)

Figure 6-17. Model vs. Test Comparison Flatcar

CONFIGURATION 1
SHAKERS IN PHASE

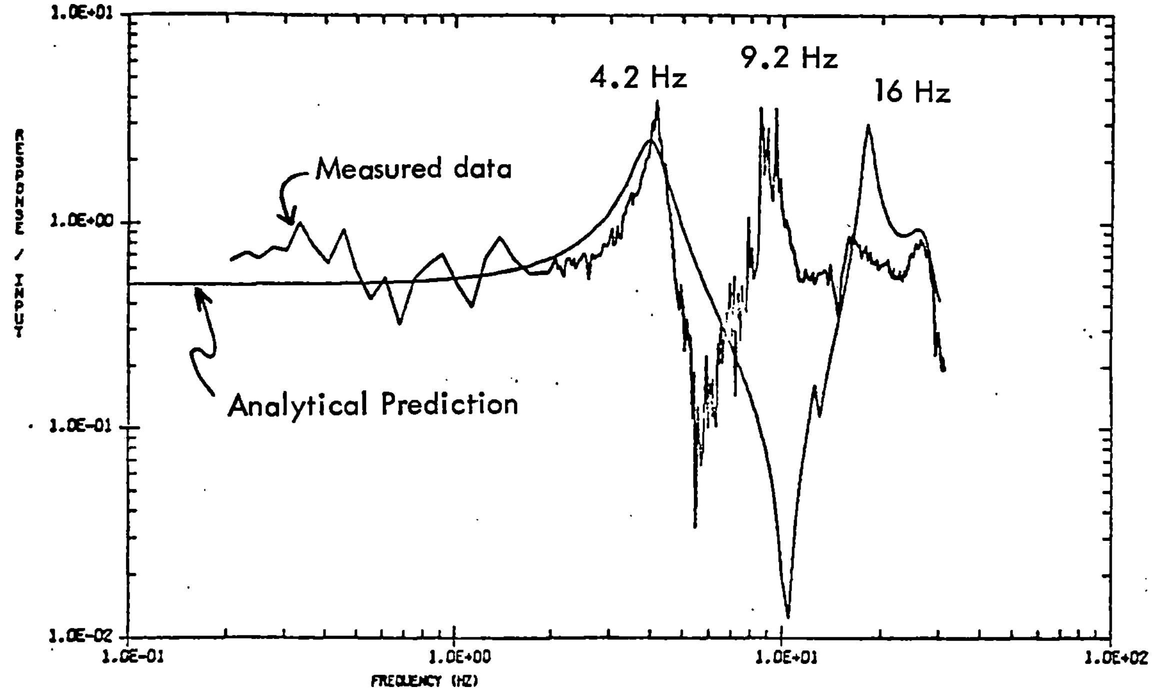

CONFIGURATION 1. IN-PHASE. MEAS 118/MEAS 65. REVISED TRANSFER FUNCTION

Meas 118/65, Flatcar Structural Amplification
(a)

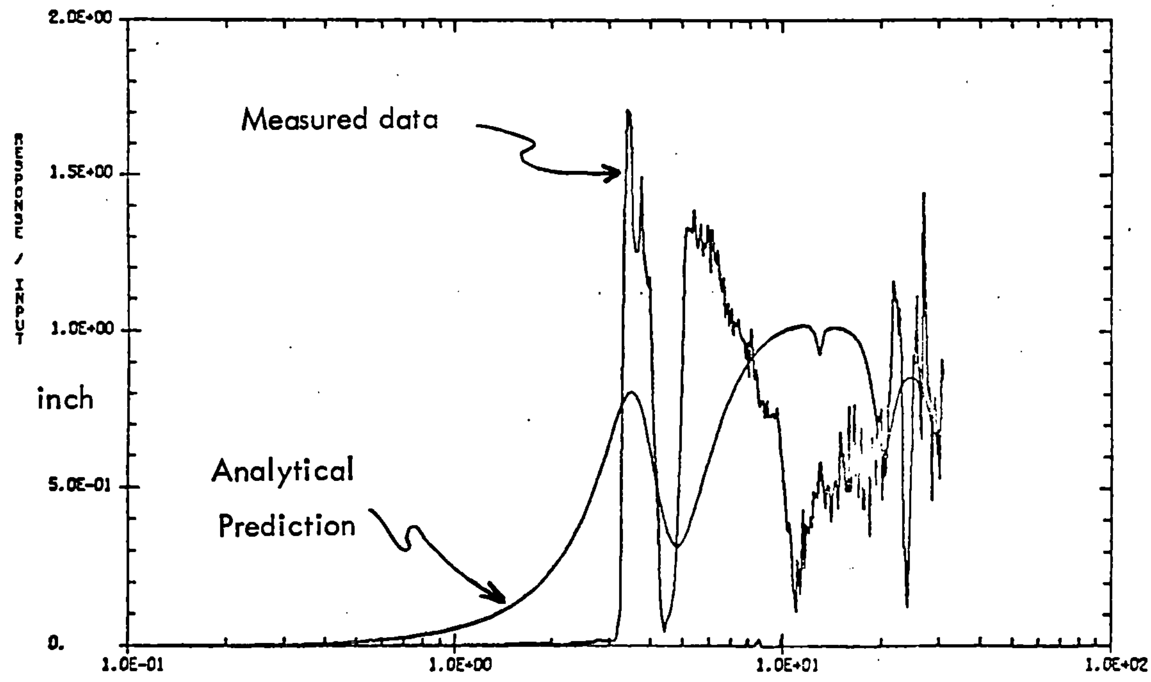

CONFIGURATION 1, SHAKERS IN PHASE, MEASUREMENT 104, REVISED TRANSFER FUNCTION

104, Spring Group Displacement
(b)

Figure 6-18. Model vs. Test Comparison

CONFIGURATION 1

SHAKERS IN PHASE

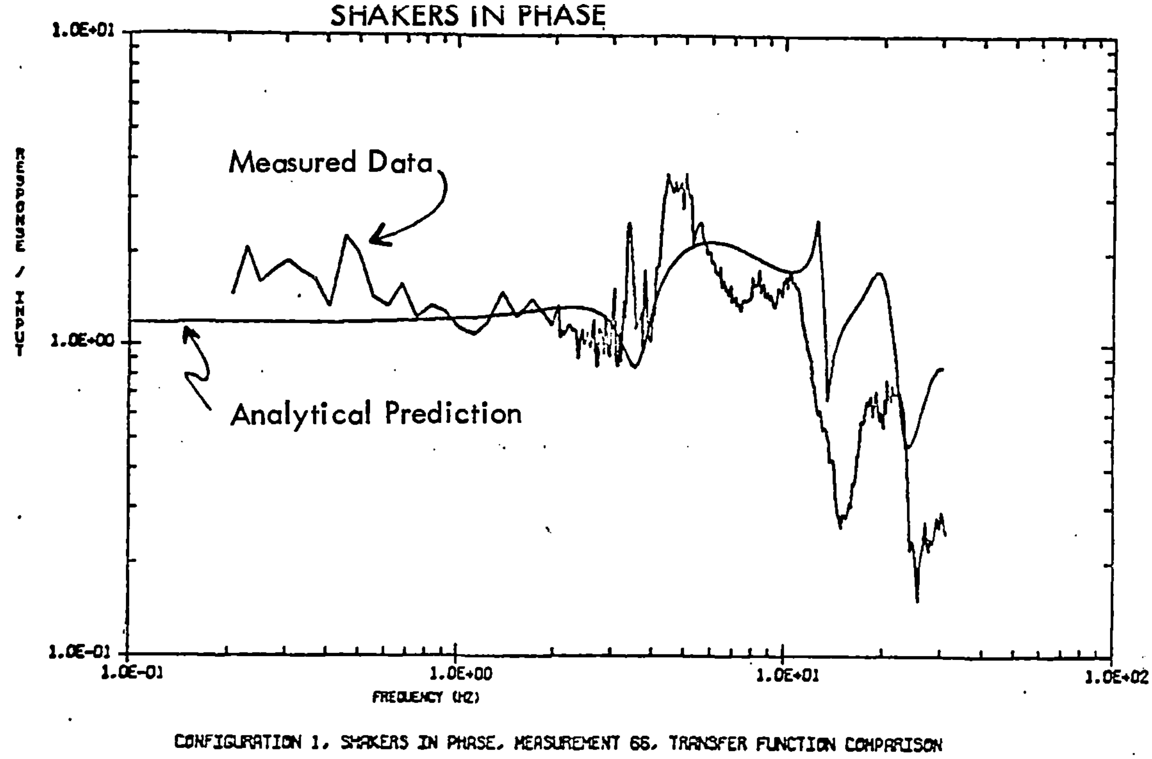

66/INPUT, Flatcar Deck at B End

(a)

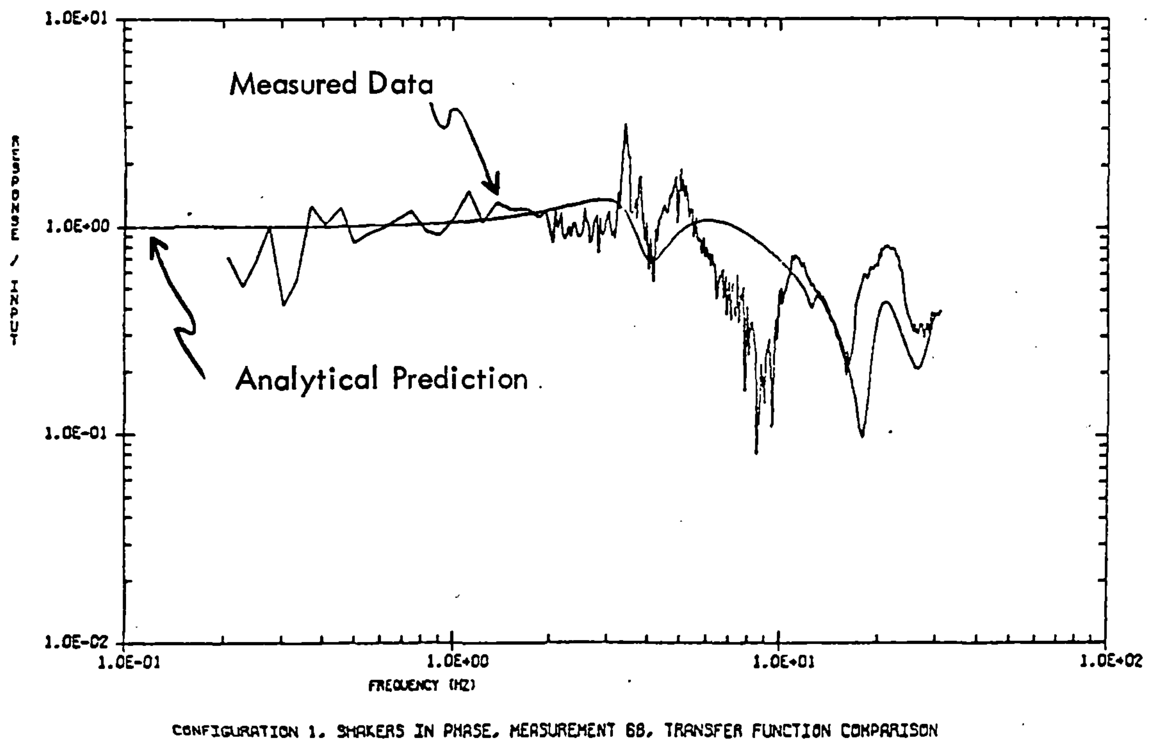

68/INPUT, Flatcar at B-end Truck

Figure 6-19. Model vs. Test Comparison

Table 6-2. Flatcar Resonance Frequencies, Configuration 1

MODE	SWEEP	DECAY (PSD)
1st VERTICAL BENDING	4.2 Hz	4.2 Hz
2nd VERTICAL BENDING	10	9.2 Hz
3rd VERTICAL BENDING	16.3	15.5 Hz
4th VERTICAL BENDING	26	25 Hz

Table 6-3. Sweep Data Repeatability

DEMONSTRATION TEST

CONFIGURATION 1, OUT OF PHASE

MEASUREMENT NUMBER 123

FREQUENCY (HZ)	RESPONSE RUN 11	RESPONSE RUN 12	PERCENTAGE DIFFERENCE
2.05	1.9436	2.2215	14.
2.10	1.7247	1.6976	-1.6
2.13	2.0182	1.6855	-16.5
2.18	2.2417	2.1755	-3.0
2.22	2.341	[illegible]	-13.3
2.27	2.099[illegible]	2.2157	5.[illegible]
2.32	3.3477	2.781	-1[illegible].5
2.35	2.4[illegible]2[illegible]	2.7[illegible]	11.[illegible]
2.40	3.[illegible]	2.[illegible]4[illegible]	-21.7
2.45	2.77[illegible]	2.61[illegible]	-5.[illegible]
2.49	2.[illegible]	4.33[illegible]	42.[illegible]
2.55	2.5[illegible]	3.[illegible]241	31.[illegible]
2.5[illegible]	2.2[illegible]4[illegible]	3.33[illegible]	4[illegible].7
2.65	3.3[illegible]27	3.5547	[illegible].
2.71	3.[illegible]79[illegible]	3.[illegible]1	-2.[illegible]
2.76	3.[illegible]54[illegible]	3.[illegible]3[illegible]	-12.[illegible]
2.81	1.[illegible]77[illegible]	3.24[illegible]	[illegible].[illegible]
2.88	3.72[illegible]	3.7[illegible]	.[illegible]
2.92	3.43[illegible]	4.22[illegible]1	2[illegible].[illegible]
2.99	3.555[illegible]	3.[illegible]3[illegible]	6.[illegible]
3.03	2.423[illegible]	3.[illegible]541	23.2
3.11	2.5714	3.[illegible]633	42.5
3.17	3.21[illegible]	3.9954	21.
3.22	2.1[illegible]7[illegible]	2.5[illegible]	21.2
3.2[illegible]	3.51[illegible]	6.0[illegible]	[illegible]2.1
3.34	[illegible].[illegible]52[illegible]	4.4133	-2[illegible].[illegible]

AVERAGE PERCENTAGE DIFFERENCE = [illegible].3

MAXIMUM PERCENTAGE DIFFERENCE = [illegible] AT 2.[illegible]1 HZ

MINIMUM PERCENTAGE DIFFERENCE = .[illegible] AT 2.88 HZ of the flatcar are shown in Figure 6-17. The most interesting thing to note is the high measured response at the center of the flatcar 6-17 (a) in the second bending mode frequency (9.2 Hz) where the analytical model predicts no response. Also, the model fails to predict the double peak in the first resonant peak caused by the nonlinear interaction of the friction snubbers. The flatcar structural amplification in Figure 6-18 (a) shows good agreement in the first mode (4.2 Hz). However, the third mode (16 Hz) fails to agree in amplitude because of the structural damping requirement in ANSYS (as discussed in Section 2.3.2) that it be based on the predominant mode. Thus using the ANSYS program, it was not possible to adjust the higher order modal damping to agree with test. Responses at the flatcar end and over the B-end truck are shown in Figure 6-19 along with the analytical prediction.

The out-of-phase analytical and test comparisons are shown in Figures 6-20 to 6-22. The transfer functions to the flatcar deck are shown in Figures 6-20 and 6-21. They show good agreement between frequencies, but the amplitudes vary somewhat from test because of the inability to adjust the structural damping in each mode. The flatcar lateral structural amplification in Figure 6-22 (a) shows the very predominant first lateral mode at 11 Hz. An attempt to predict the response of the truck bolster in Figure 6-22 did not prove too successful.

6.3 CONFIGURATION 2

6.3.1 Response

The frequency domain plots of the configuration 2 test data were examined to establish the significant resonant frequencies. Examples of this data are shown in Figures 6-23 to 6-26 for the in-phase excitation and in Figures 6-27 to 6-32 for the out-of-phase excitation. The resultant test frequencies are summarized in Table 6-4. The transfer function to the center of the flatcar and the flatcar structural amplification factor are shown in Figure 6-23 and show the first resonant frequency of the flatcar to be 1.9 to 2.0 Hz. The double peaked transfer function seen on Configuration 1 is not apparent in the Configuration 2 data. The displacement measurement across the spring group in Figure 6-24 (a) shows two very pronounced peaks corresponding to the bounce/bending and pitch frequencies of the flatcar. The resonant frequency at 1.9 Hz

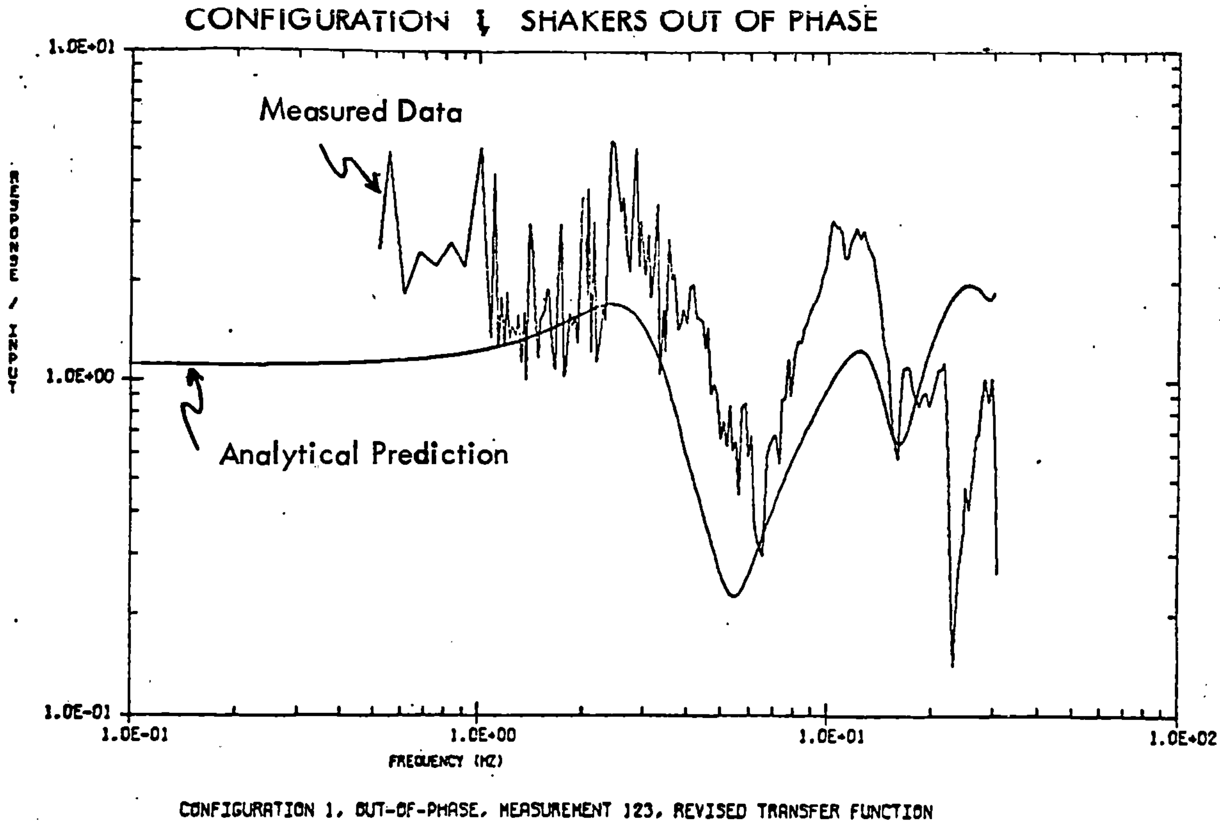

123/INPUT, Flatcar B-end Edge

(a)

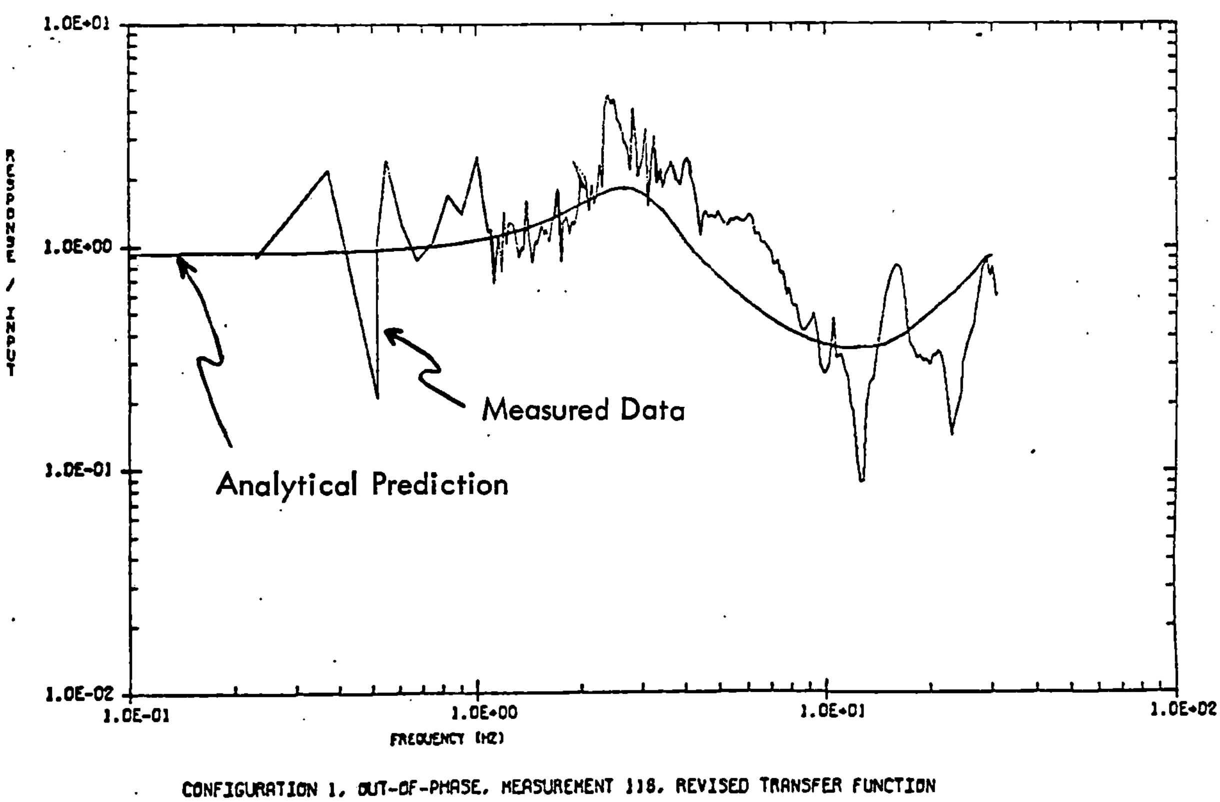

118/INPUT, Flatcar Deck Center

(b)

Figure 6-20. Model vs. Test Comparison

CONFIGURATION 1, SHAKERS OUT OF PHASE

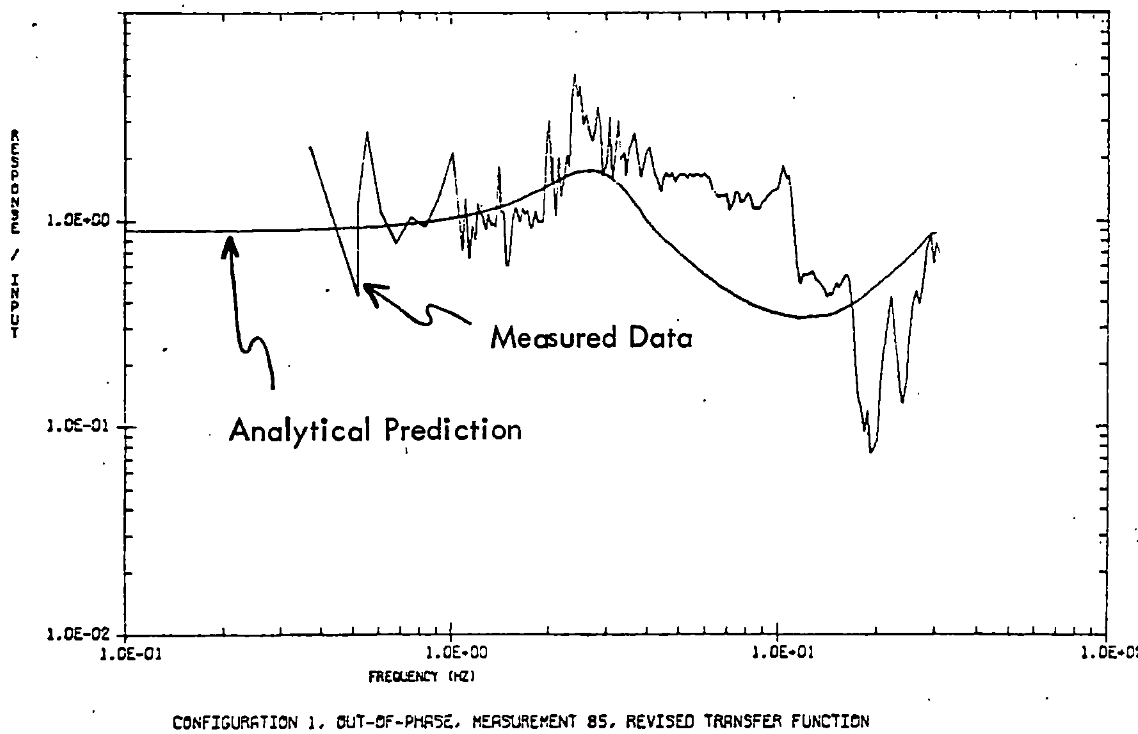

85/INPUT, Flatcar Over A-end Truck
(a)

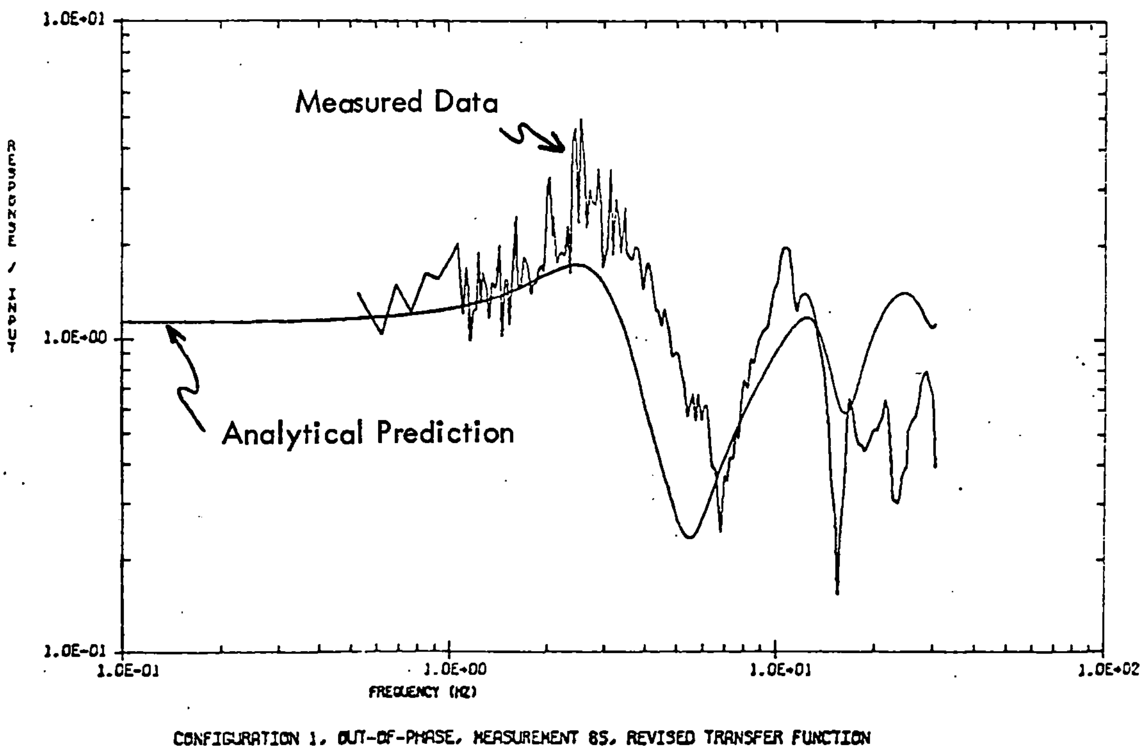

65/INPUT, Flatcar Over B-end Truck
(b)

Figure 6-21. Model vs. Test Comparison

CONFIGURATION 1 SHAKERS OUT-OF-PHASE

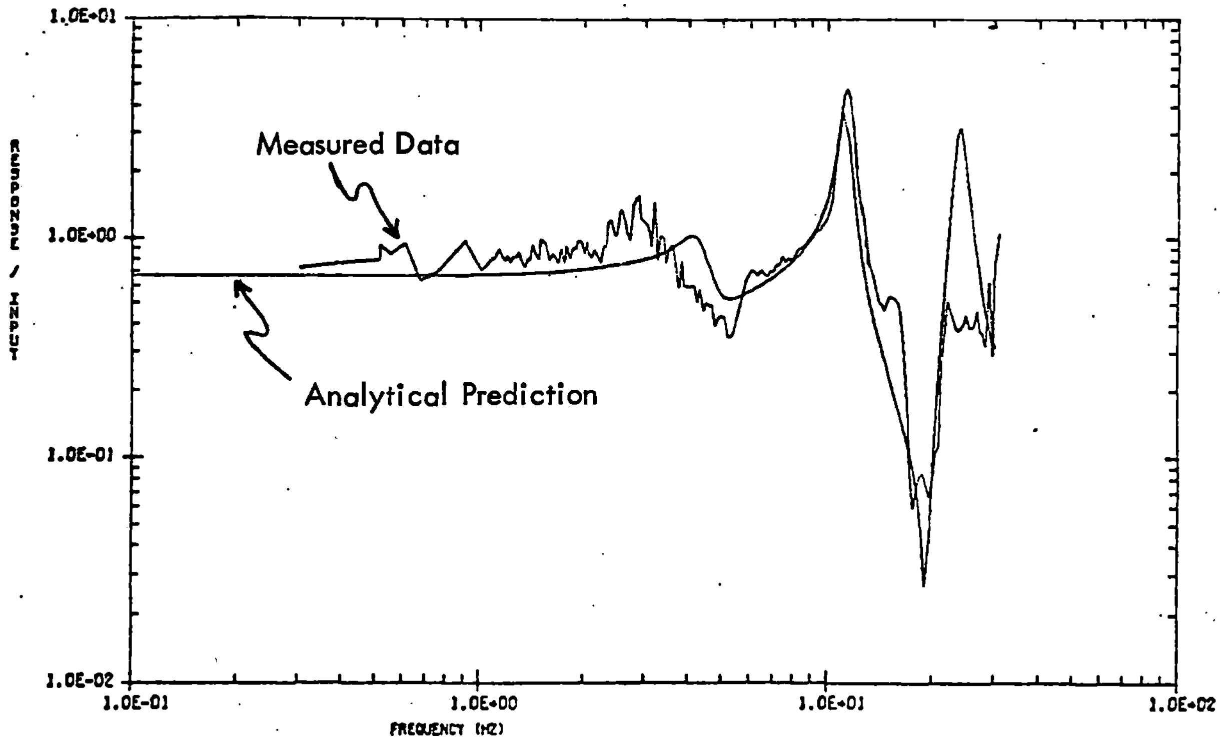

CONFIGURATION 1, OUT-OF-PHASE, MEAS 116/ MEAS 69, REVISED TRANSFER FUNCTION

MEAS 116/69, Flatcar Lateral Structural Amplification

(a)

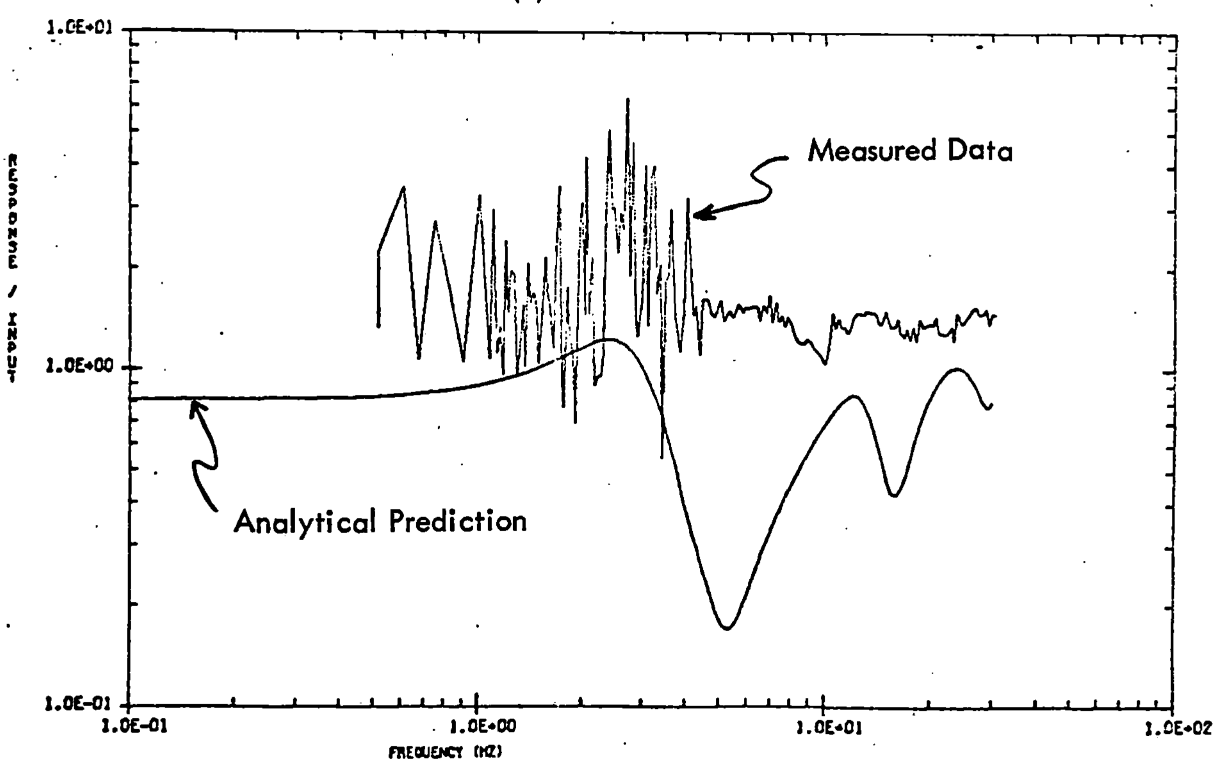

CONFIGURATION 1, OUT-OF-PHASE, MEASUREMENT 59, REVISED TRANSFER FUNCTION

MEAS 59, Truck Bolster

(b)

Figure 6-22. Model vs. Test Comparison

CONFIGURATION 2

SHAKERS IN PHASE

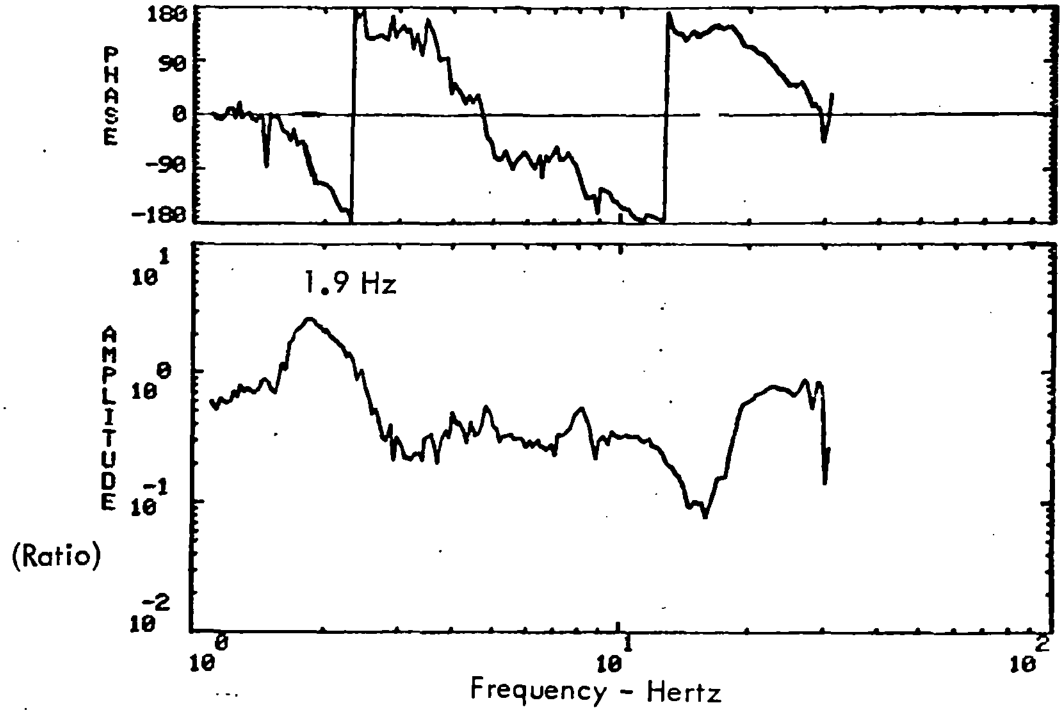

CONFIGURATION 2, HIGH LEVEL SINE SWEEP, SHAKERS IN PHASE, RUN 56

(a) 39/Input, Flatcar Transfer Function

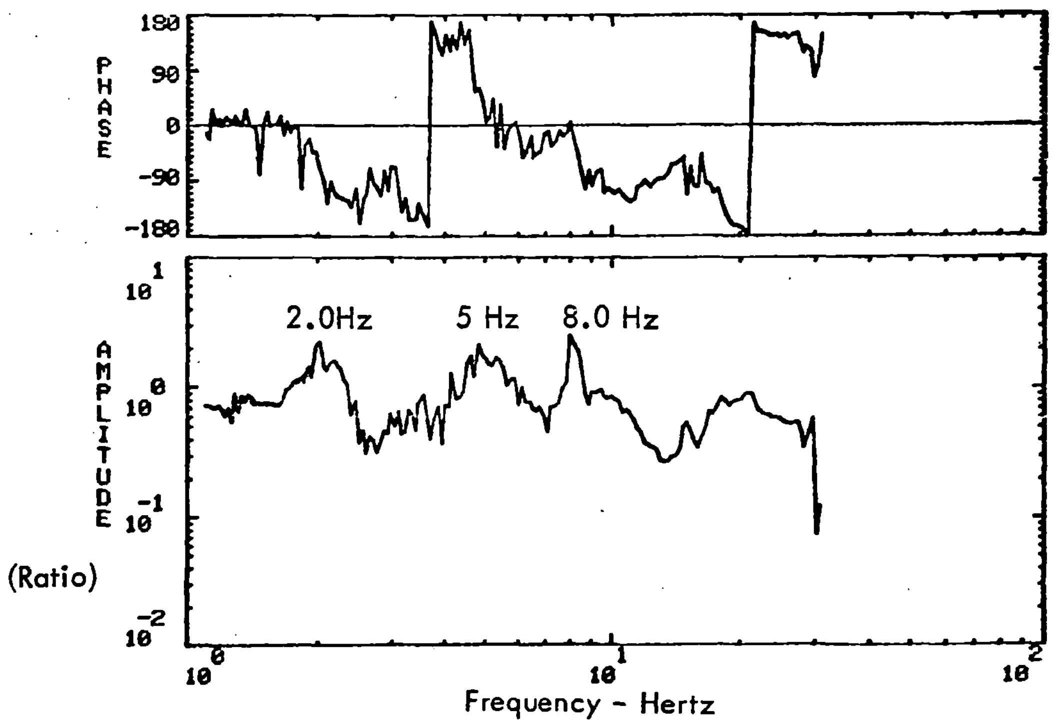

CONFIGURATION 2, HIGH LEVEL SINE SWEEP, SHAKERS IN PHASE, RUN 56

(b) 89/65, Flatcar Body Structural Amplification

Figure 6-23. Flatcar Body Transfer Functions, Configuration 2

CONFIGURATION 2

SHAKERS IN PHASF

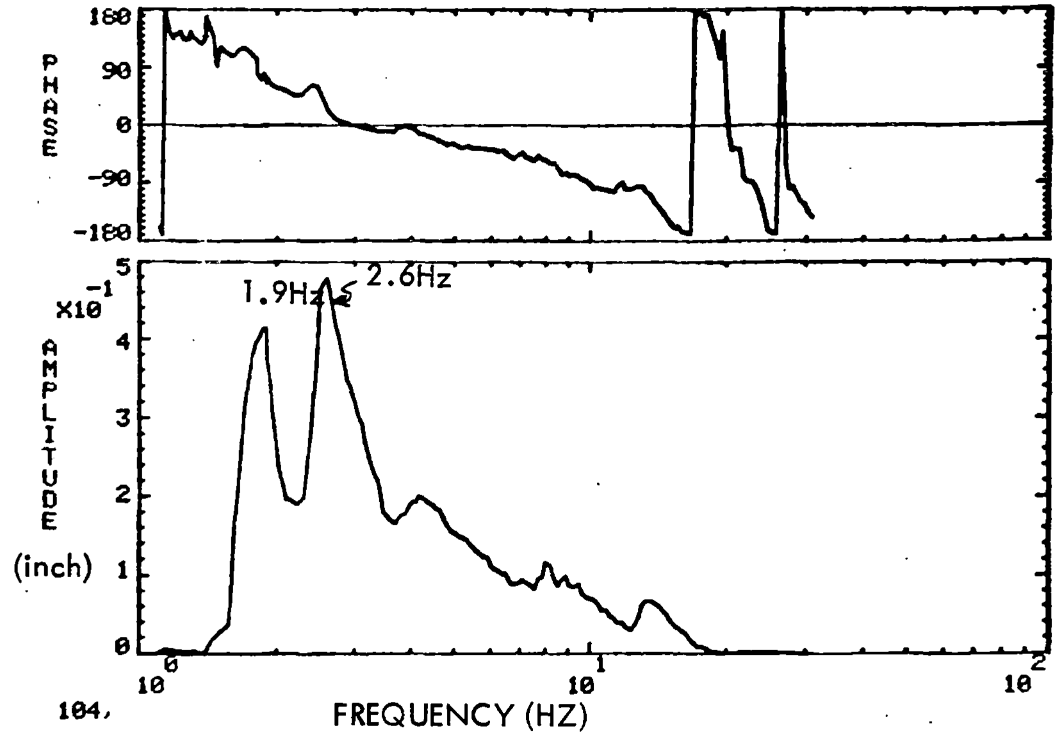

CONFIGURATION 2, HIGH LEVEL SINE SWEEP, SHAKERS IN PHASE, RUN 56

(a) 104, Displacement Across Spring Group

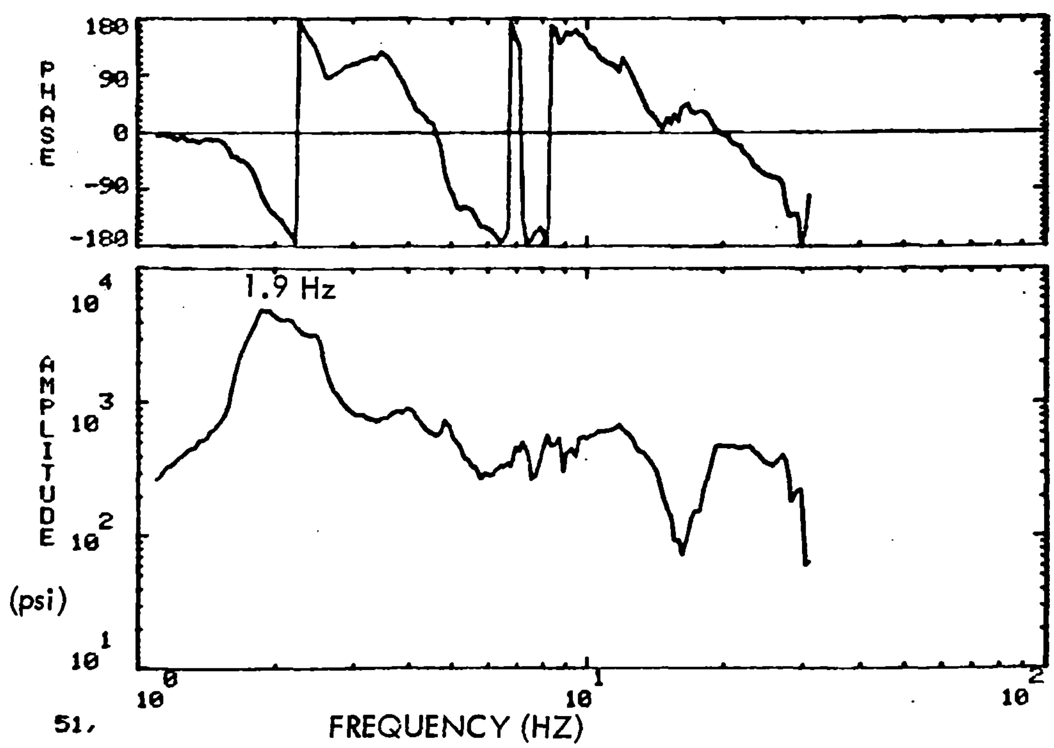

CONFIGURATION 2, HIGH LEVEL SINE SWEEP, SHAKERS IN PHASE, RUN 56

(b) 51, Main Sill Stress Level

Figure 6-24. Configuration 2 Measurements

CONFIGURATION 2

SHAKERS IN PHASE

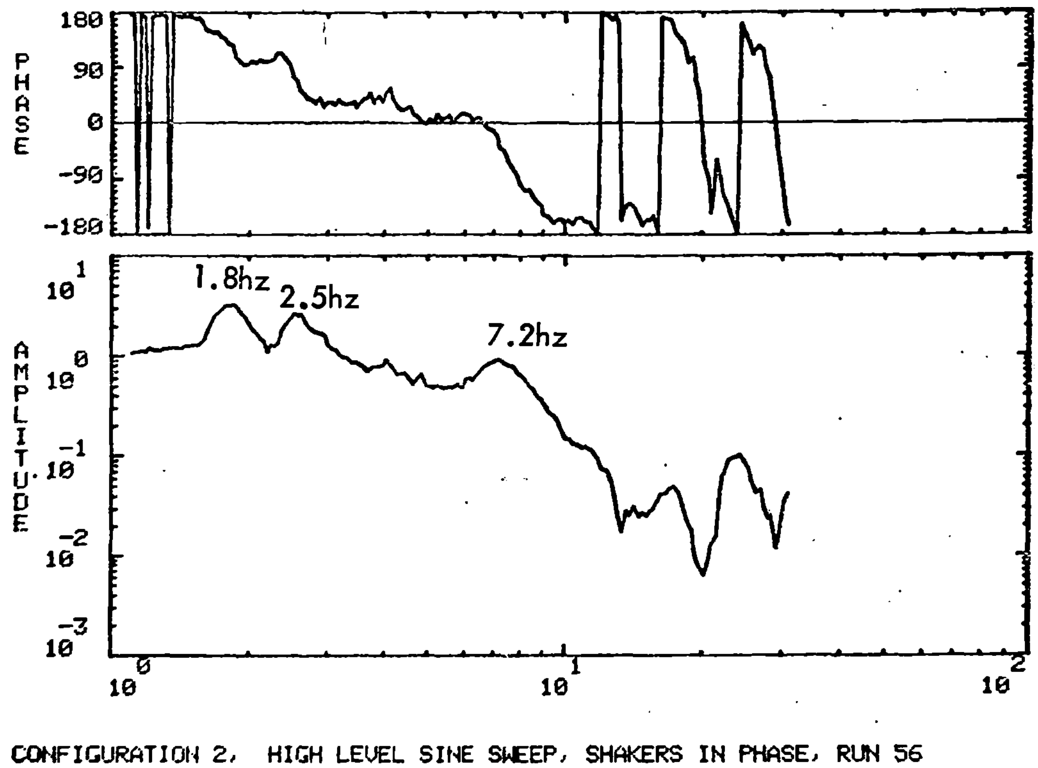

(a) 127/Input, Van Trailer Transfer Function

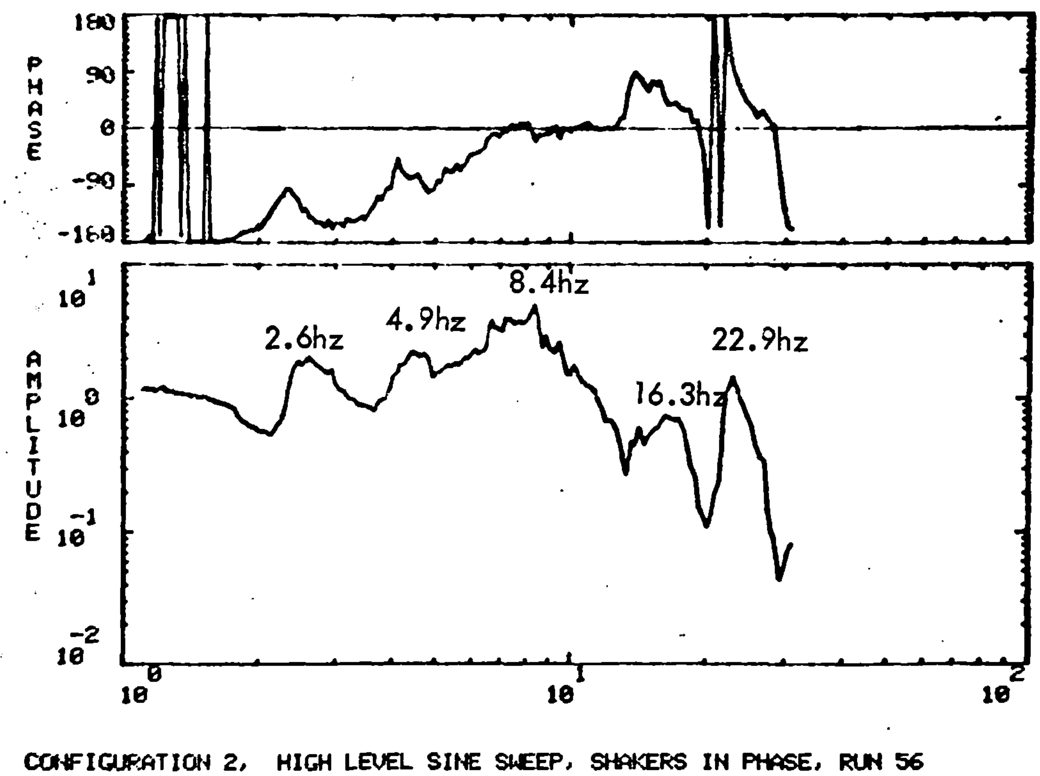

(b) 127/70, Van Trailer Structural Amplification

Figure 6-25. Van Trailer Transfer Functions

CONFIGURATION 2

SHAKERS IN PHASE

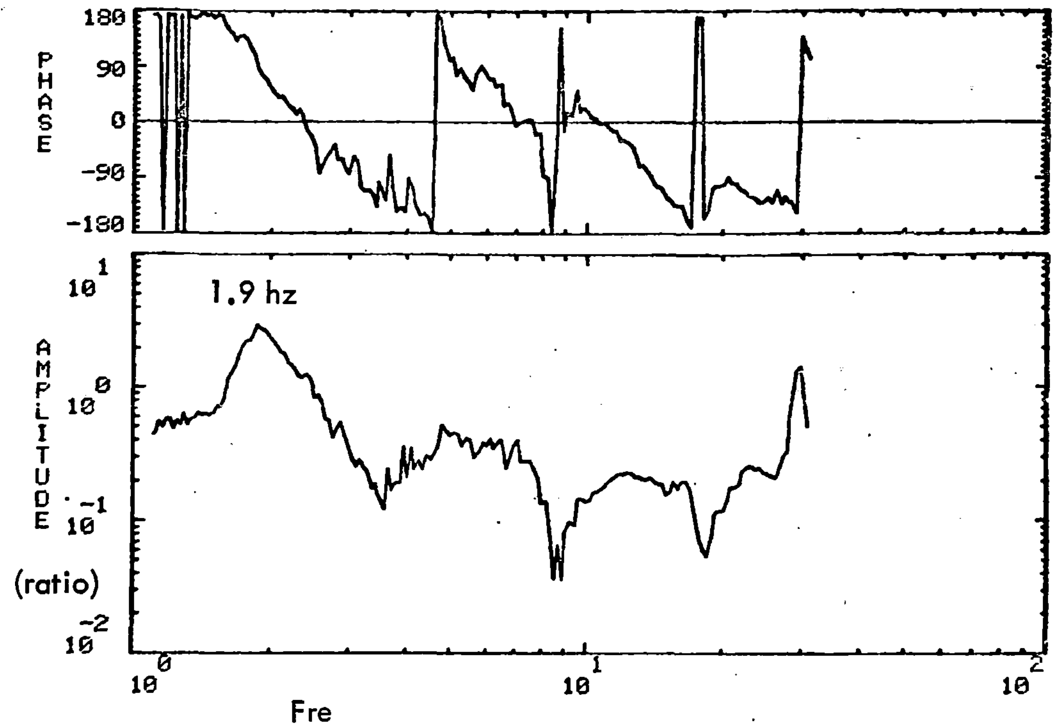

CONFIGURATION 2, HIGH LEVEL SINE SWEEP, SHAKERS IN PHASE, RUN 56

(a) 124/Input, Platform Trailer Transfer Function

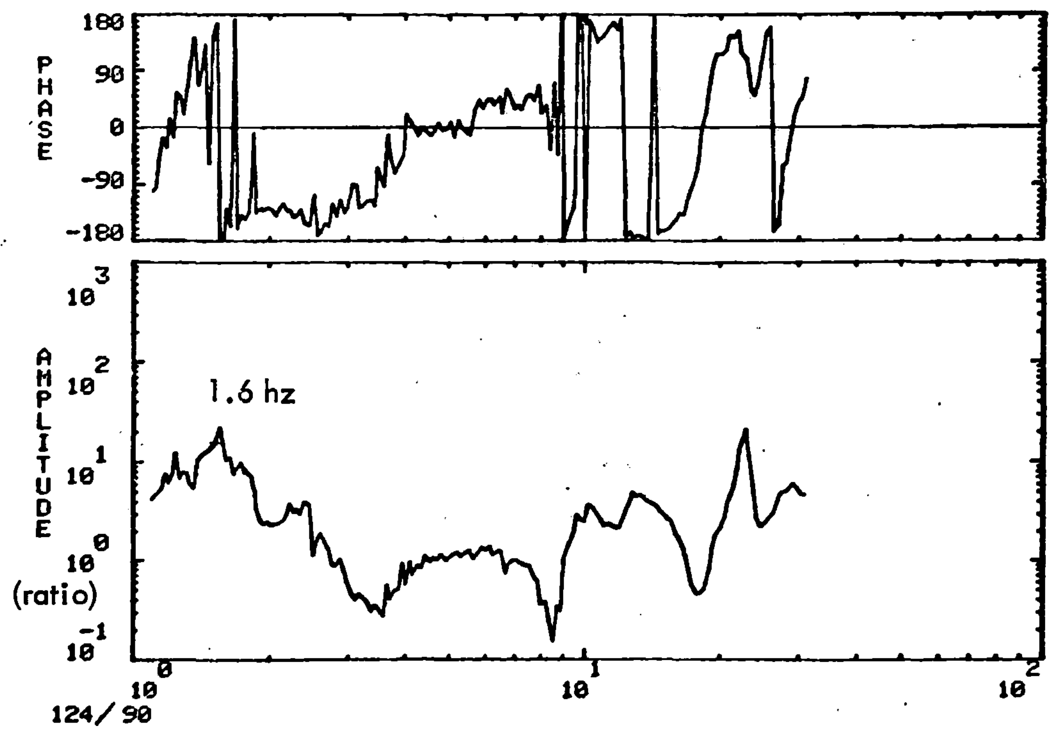

CONFIGURATION 2, HIGH LEVEL SINE SWEEP, SHAKERS IN PHASE, RUN 56

(b) 124/90 Platform Trailer Structural Amplification

Figure 6-26. Platform Trailer Responses

CONFIGURATION 2

SHAKERS OUT-OF-PHASE

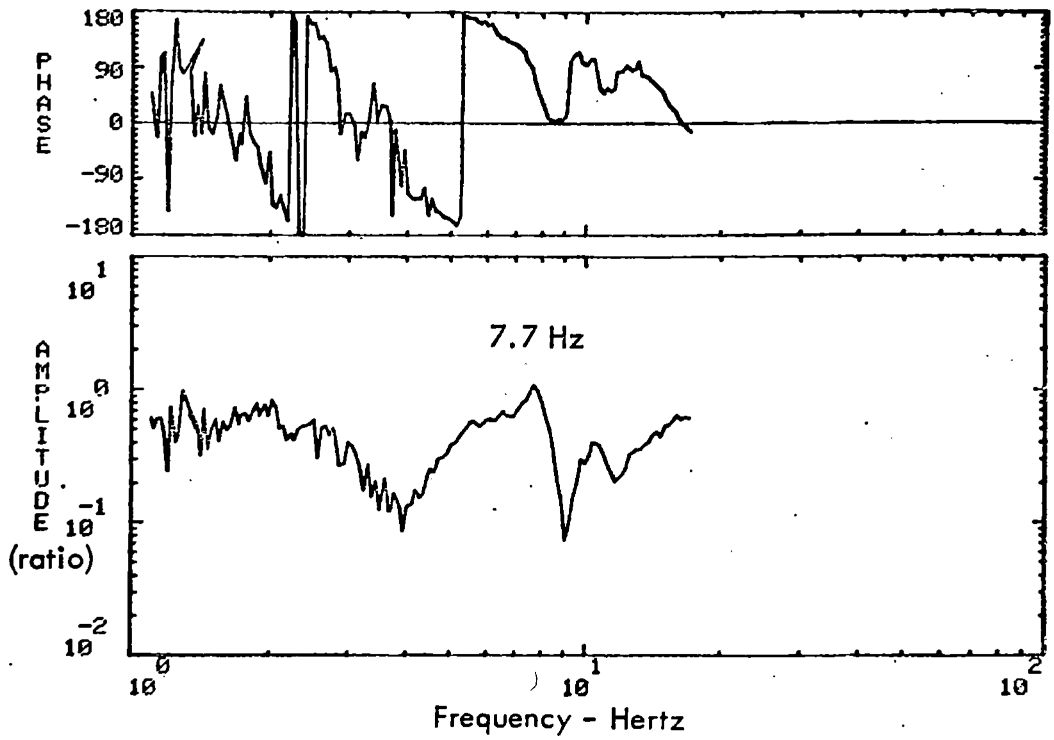

CONFIGURATION 2, HIGH LEVEL SINE SWEEP, SHAKERS OUT-OF-PHASE, RUN 84

(a) 118/Input, Flatcar Center Transfer Function

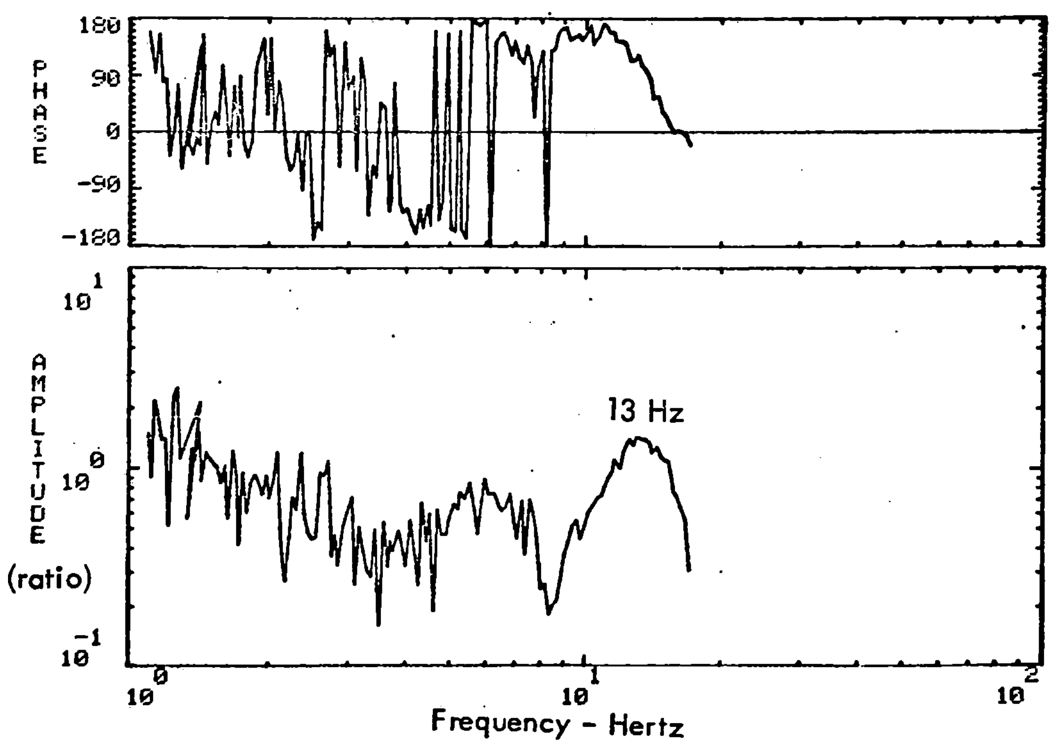

CONFIGURATION 2, HIGH LEVEL SINE SWEEP, SHAKERS OUT-OF-PHASE, RUN 84

(b) 123/Input, Flatcar End Transfer Function

Figure 6-27. Flatcar Transfer Functions

CONFIGURATION 2

SHAKERS IN PHASE

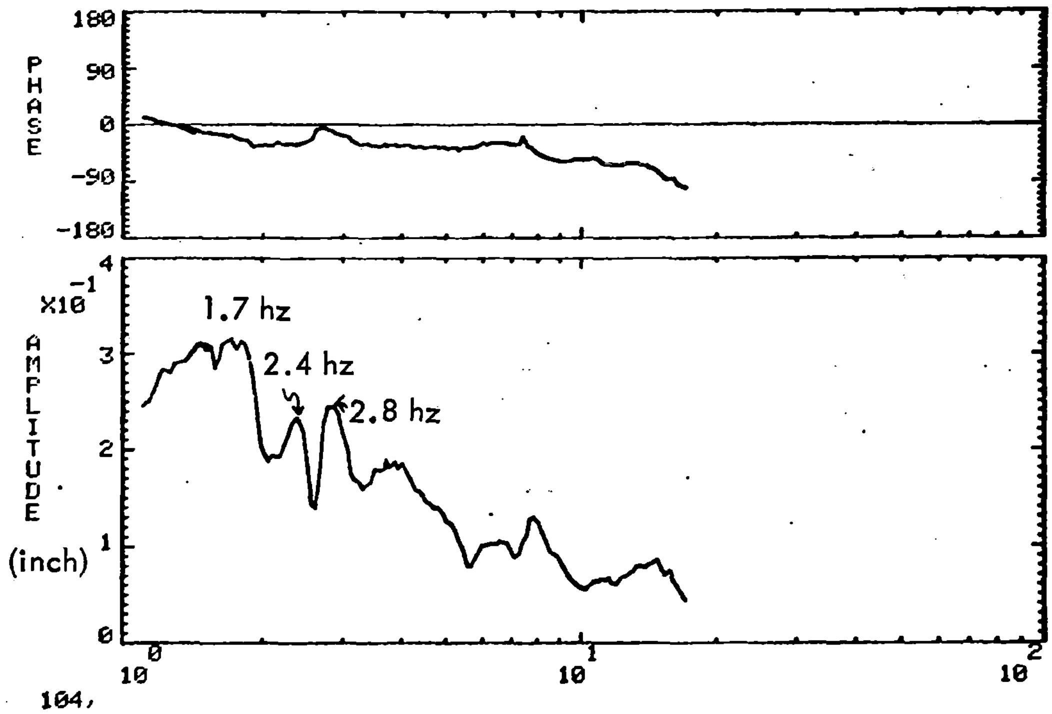

CONFIGURATION 2, HIGH LEVEL SINE SWEEP, SHAKERS OUT-OF-PHASE, RUN 84

(a) 104, Displacement Across Spring Group

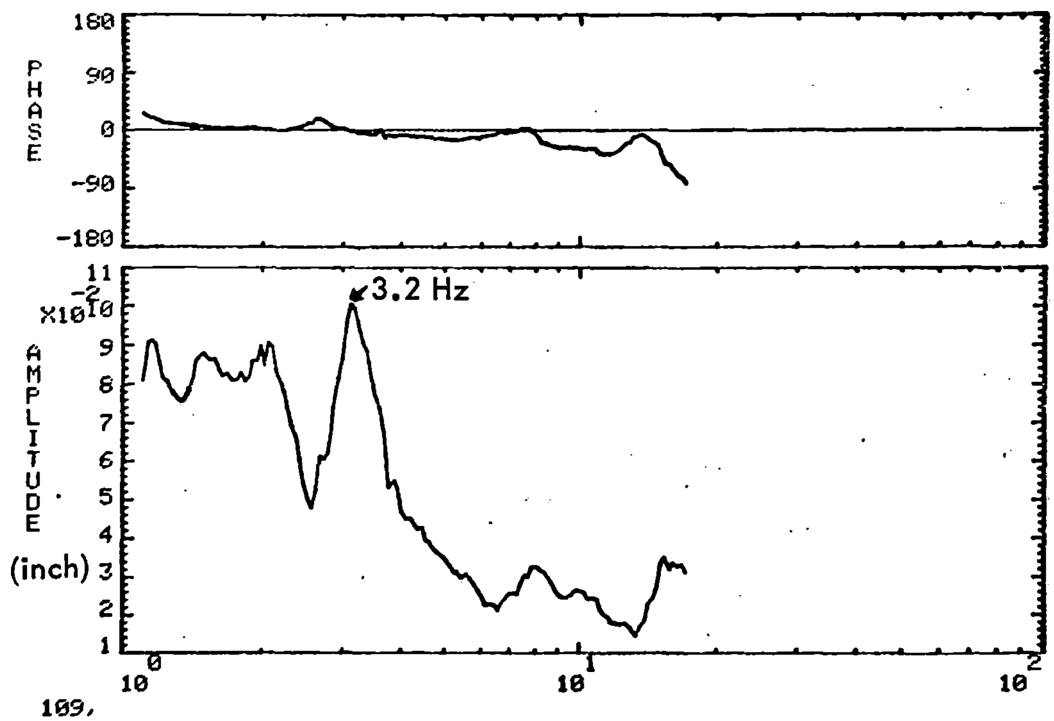

CONFIGURATION 2, HIGH LEVEL SINE SWEEP, SHAKERS OUT-OF-PHASE, RUN 84

(b) 109, Flatcar Rocking on Centerplate

Figure 6-28. Flatcar Displacement Measurements

CONFIGURATION 2
SHAKERS OUT OF PHASE

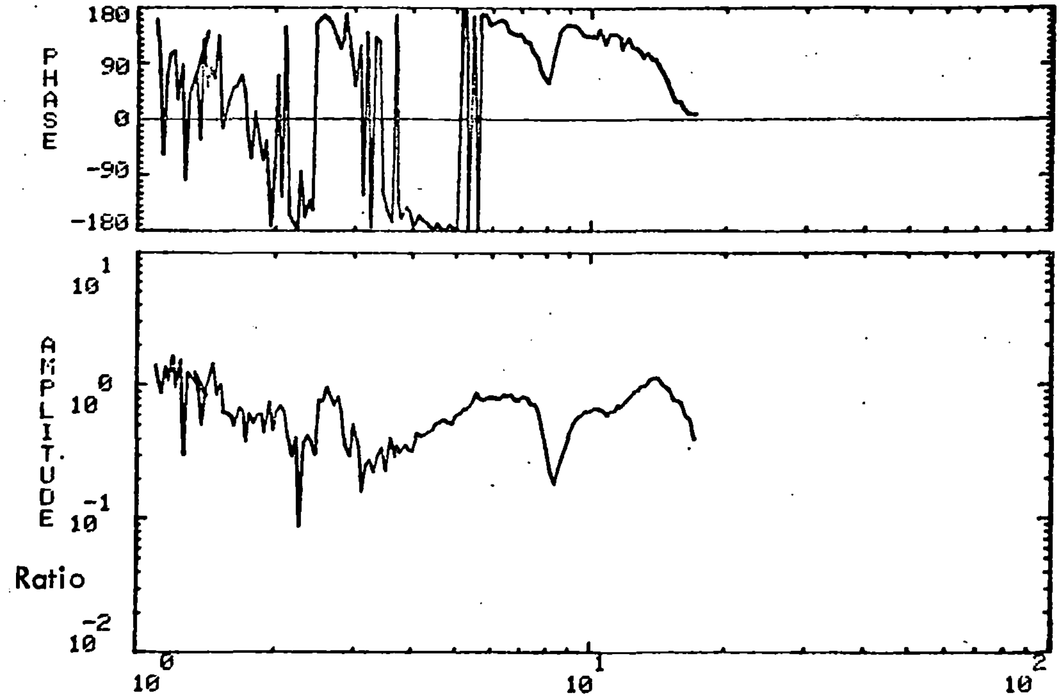

CONFIGURATION 2, HIGH LEVEL SINE SWEEP, SHAKERS OUT-OF-PHASE, RUN 84

(a) 65/Input, Flatcar Transfer Function

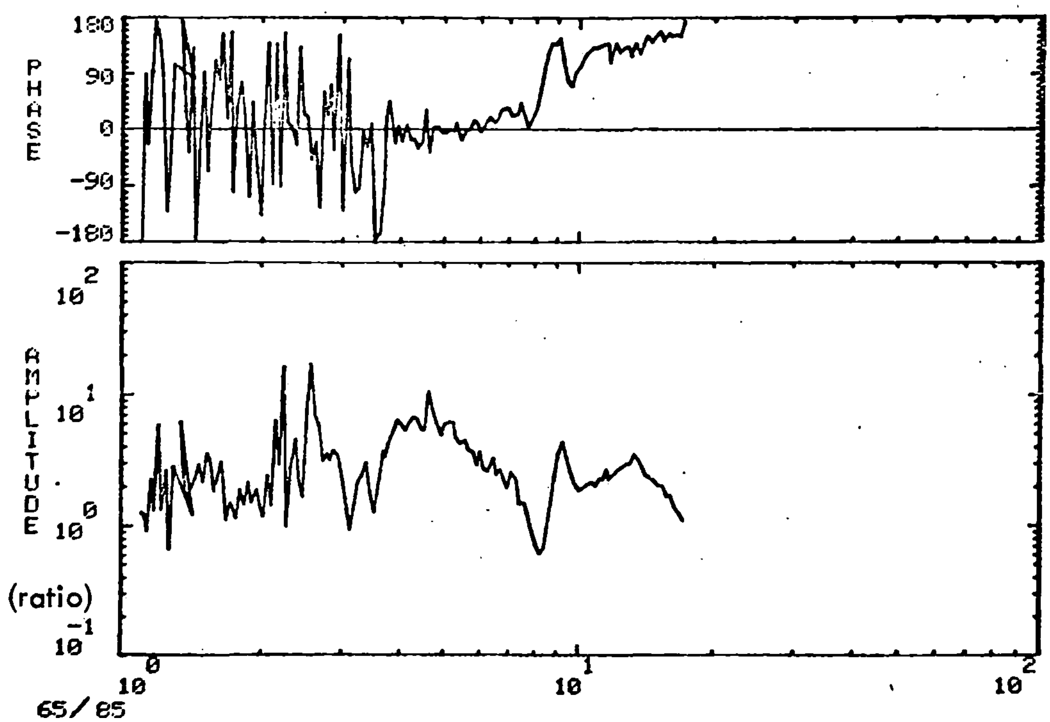

CONFIGURATION 2, HIGH LEVEL SINE SWEEP, SHAKERS OUT-OF-PHASE, RUN 84

(b) 65/85, Flatcar Torsional Transfer Function

Figure 6-29. Flatcar Vertical Transfer Function

CONFIGURATION 2

SHAKERS OUT OF PHASE

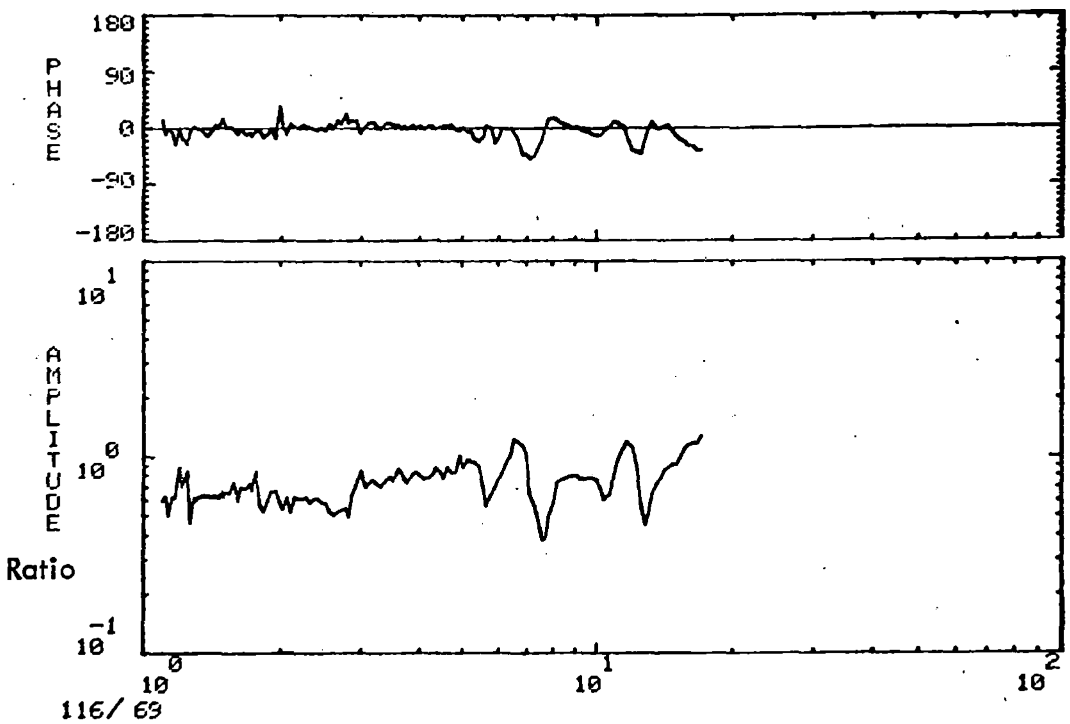

116/69, Flatcar Lateral Structural Amplification

Figure 6-30. Flatcar Lateral Transfer Functions

CONFIGURATION 2, SHAKERS OUT OF PHASE

Platform Trailer

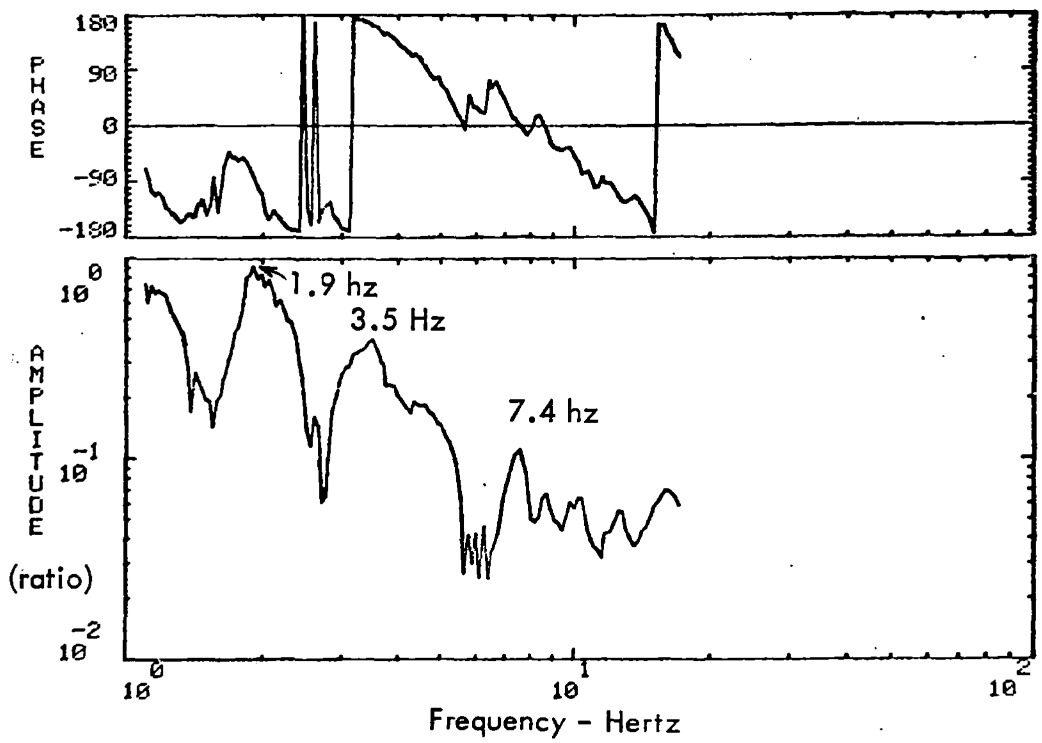

CONFIGURATION 2, HIGH LEVEL SINE SWEEP, SHAKERS OUT-OF-PHASE, RUN 84

(a) 75/Input Van Trailer Vertical Transfer Function

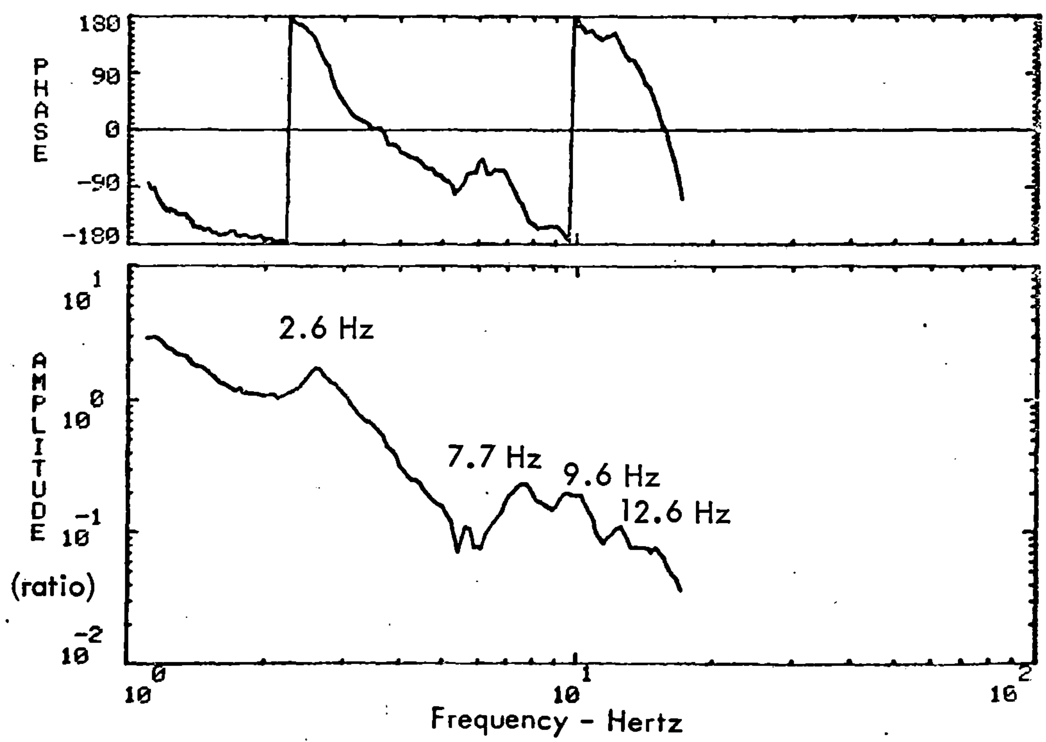

CONFIGURATION 2, HIGH LEVEL SINE SWEEP, SHAKERS OUT-OF-PHASE, RUN 84

(b) 71/Input, Van Trailer Lateral Transfer Function

Figure 6-31. Van Trailer Transfer Functions

CONFIGURATION 2, SHAKERS OUT OF PHASE
PLATFORM TRAILER

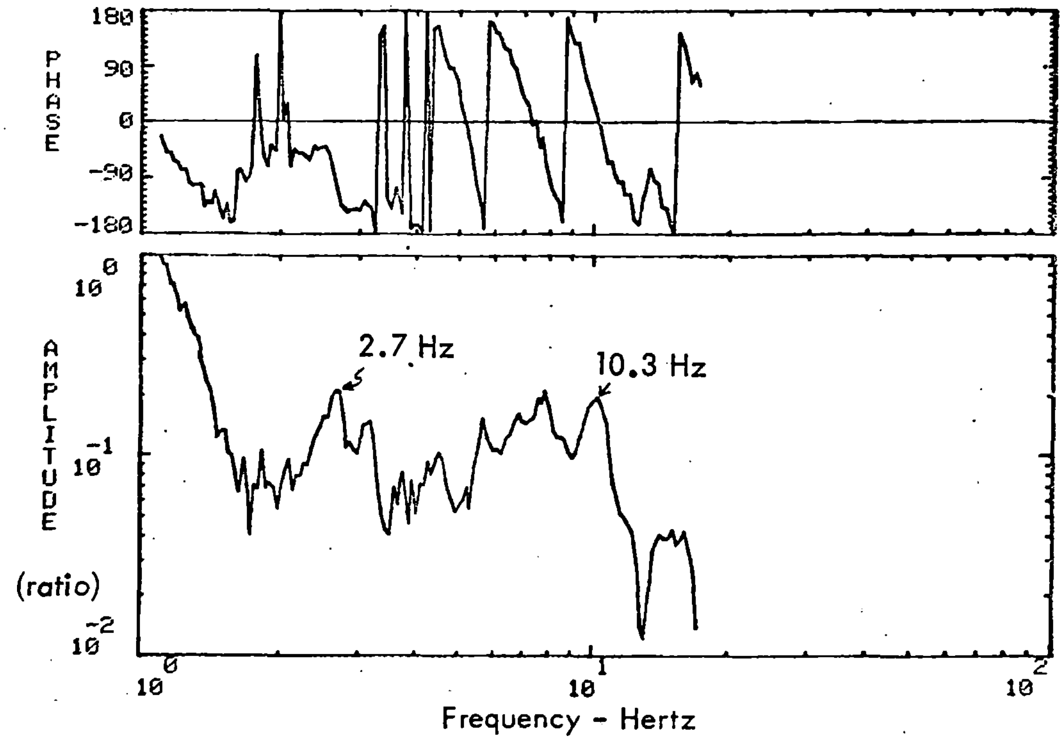

CONFIGURATION 2, HIGH LEVEL SINE SWEEP, SHAKERS OUT-OF-PHASE, RUN 84

(a) 95/Input, Platform Trailer Vertical Transfer Function

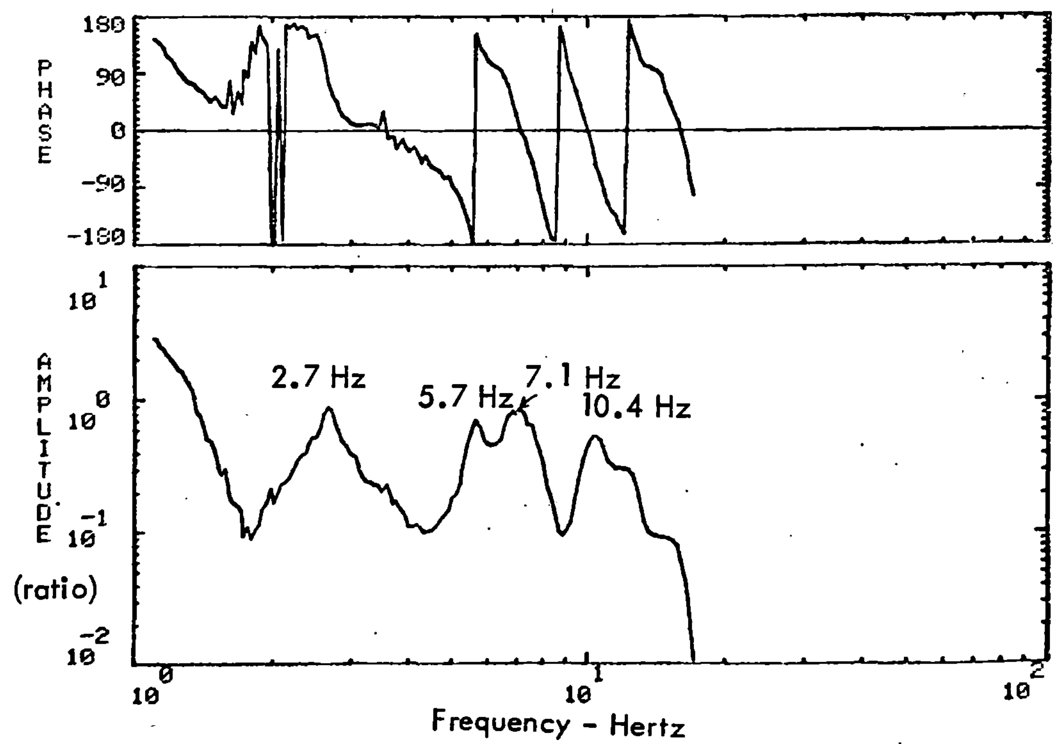

CONFIGURATION 2, HIGH LEVEL SINE SWEEP, SHAKERS OUT-OF-PHASE, RUN 84

(b) 91/Input, Platform Trailer Lateral Transfer Function

Figure 6-32. Platform Trailer Transfer Functions

Table 6-4. Response Frequencies, Configuration 2

Mode	Test Frequency	Analytical Model
Rocking	**	2.93 Hz
Sway	**	1.8
Bounce	1.9 Hz	1.4
Pitch	2.6	3.7
1st Bending	2.1	
2nd Bending	5.0	
1st Lateral bending	**	
1st Torsional	13	12
3rd Vertical bending	8.0 Hz	
Van Trailer Bounce	3.2 Hz	
Van trailer bending	6.7 Hz	
Platform trailer bounce	3.1 Hz	
Platform trailer bending	7.8 Hz	

is a combined rigid body bounce and flatcar first bending mode resulting from a coupling of the individual modes into a response at one frequency. The stress level in Figure 6-24 (b) shows the peak stress to occur in the first vehicle bending mode as would be expected. The van trailer transfer function and structural amplification factor are shown in Figure 6-25. The maximum response on the van occurs at the flatcar bending frequency. The structural amplification factor has its peak resonance at 8.4 Hz, indicating the van trailer's first flexible mode. The platform trailer response in Figure 6-26 again shows the predominant response in the first flatcar mode. The platform trailer structural amplification in Figure 6-26 (b) is difficult to establish a platform body resonant frequency from the data.

The transfer functions for the out-of-phase excitation are shown in Figures 6-27 through 6-31. The transfer functions for the flatcar are shown in Figure 6-27. The two predominant resonances are at 7.7 and 13 Hz, however the low frequencies are noisy and it is difficult to distinguish resonances below 4 Hz. This is again believed to be caused by aliasing (as discussed for configuration 1) of high frequency excitation resulting from the flatcar rocking. Examination of the displacement measurements between the truck and flatcar in Figure 6-28 (b) show some rocking on the center plate but considerably less than for configuration 1 (0.3 inches for configuration 1 versus 0.1 inches for configuration 3) and, consequently, the low frequency data is not as bad on configuration 2. Examination of the data measured on the two trailers (Figures 6-31 and 6-32) shows no high frequency aliasing, because the truck suspension system has damped out all the high frequency excitation before it reaches the trailer bodies. The displacement measurement across the spring group (Figure 6-28 (a)) shows three resonances at 1.7, 2.4 and 2.8 Hz. The phase relationship in Figure 6-29 (b) between the two ends of the flatcar show it to be moving in-phase until above 9 Hz, when the two ends begin moving out-of-phase with the two ends of the flatcar. The lateral structural amplification in Figure 6-30 shows no predominant peaks as did the configuration 1 measurement (Figure 6-1), indicating less tendency to respond laterally when carrying a full load.

The transfer functions measured on the van and platform trailers are shown in Figures 6-31 and 6-32 respectively.

Decay traces measured during configuration 2 testing were analyzed using the PSD technique as was done for configuration 1. This is shown in Figures 6-33 to 6-35. It is a little more difficult to identify the frequencies than for configuration 1 because of the greater complexity of configuration 2. The PSD analysis of the flatcar in Figure 6-33 and the trailers in Figures 6-34 and 6-37 all show the same predominant resonance peak at 2.1 to 2.2 Hz. The two trailers both show their bounce mode at 3.1 to 3.2 Hz.

Decay traces of the accelerometer at the flatcar center (89) are shown in Figures 6-36 and 6-37 for two different levels of input (but the same frequency). The response for the higher input amplitude shows a much higher decay rate. Also, the spring groups show some motion after the decay has started as opposed to configuration 1, where the spring group motions stopped immediately upon terminating the input. The input drive signal is also shown on both figures to aid in establishing the exact moment of decay initiation.

6.3.2 Tire Force Measurements

Pressure plates were placed under the trailer tires to measure the force exerted by the trailer tires on the flatcar deck. One plate was placed under the right wheel set and one plate under the left wheel set for each trailer. Prior to starting the configuration 2 testing the static weight exerted on each plate was recorded.

	Weight (Pounds)			
	Left Wheel	Right Wheel	Total	Analytical
Van Trailer	16452 (98)	17,268 (97)	33720	37,228
Platform Trailer	19464 (100)	17,816 (99)	37280	40,706

The analytical value was that obtained from Table 4-7 for a static analysis of the fully loaded flatcar. In Table 4-7 elements 7 and 8 are the platform trailer tires, and elements 18 and 19 are for the van trailer.

CONFIGURATION 2, SHAKERS IN PHASE

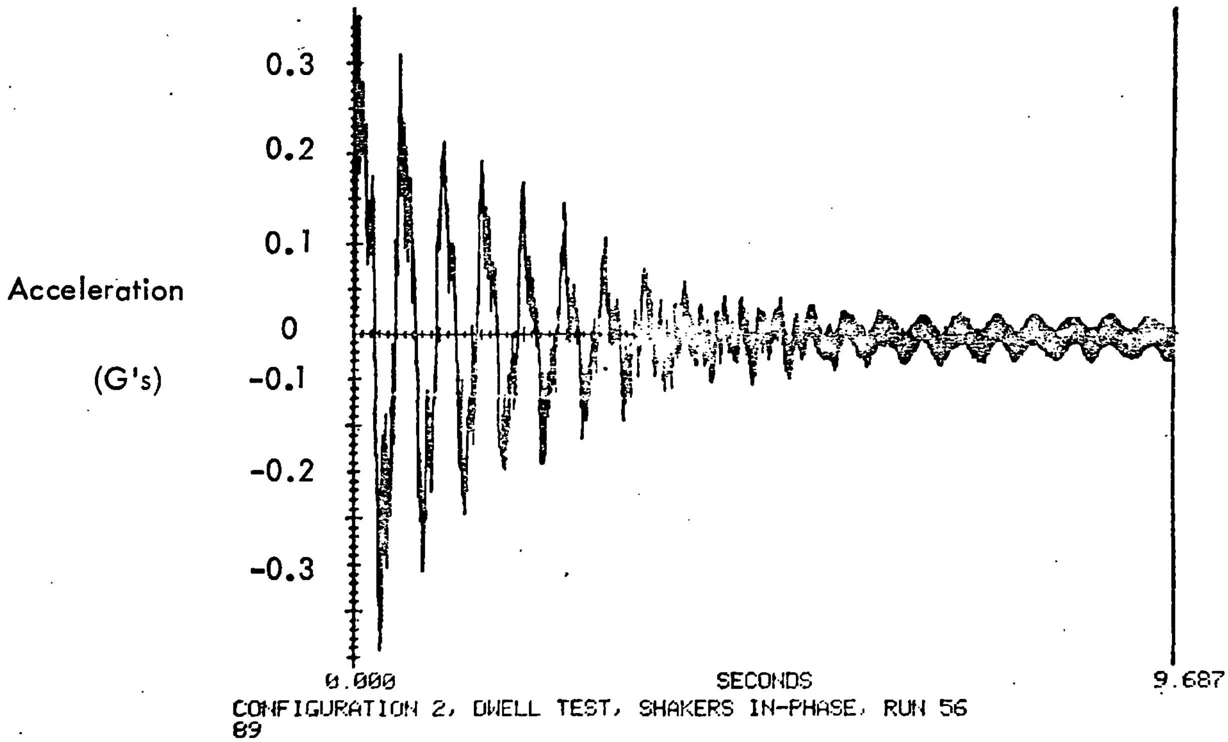

(a) Flatcar Decay Time History

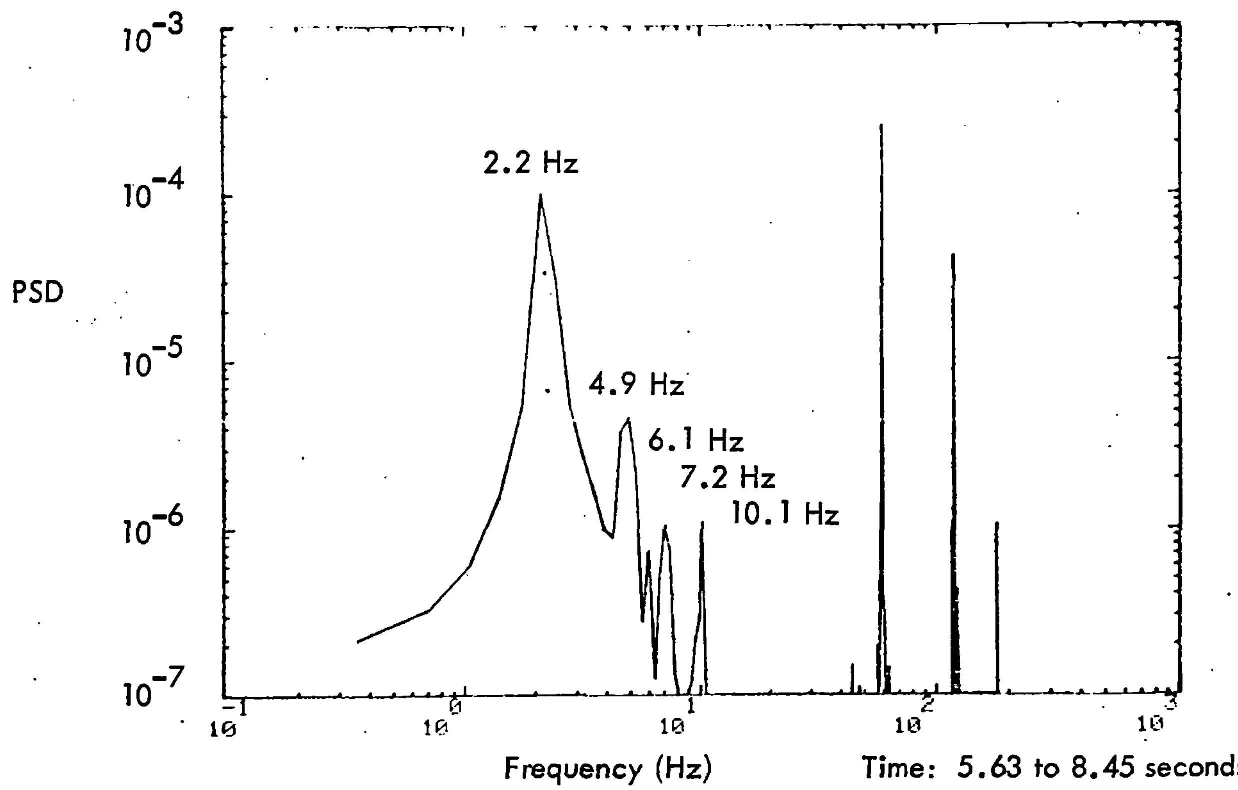

(b) Flatcar PSD

Figure 6-33. Flatcar Decay Time History and PSD

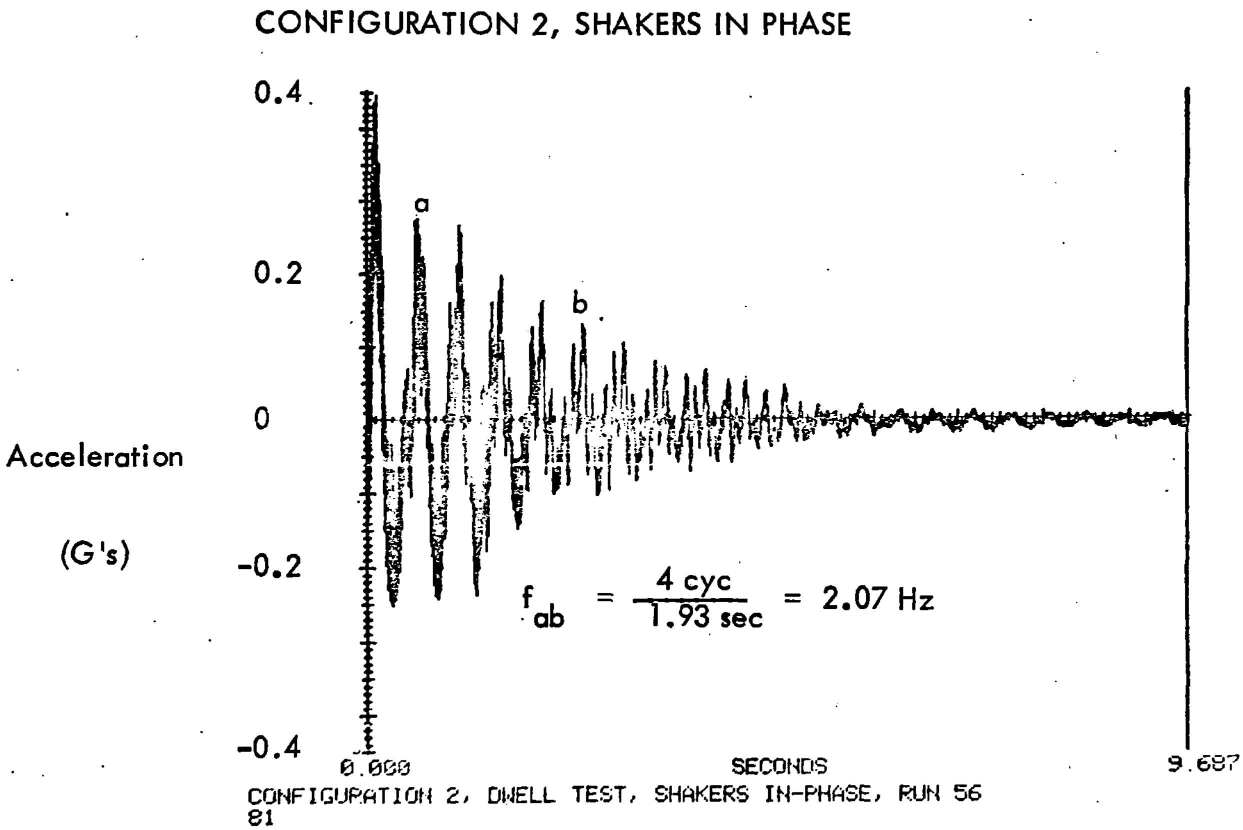

(a) Van Trailer Decay Time History

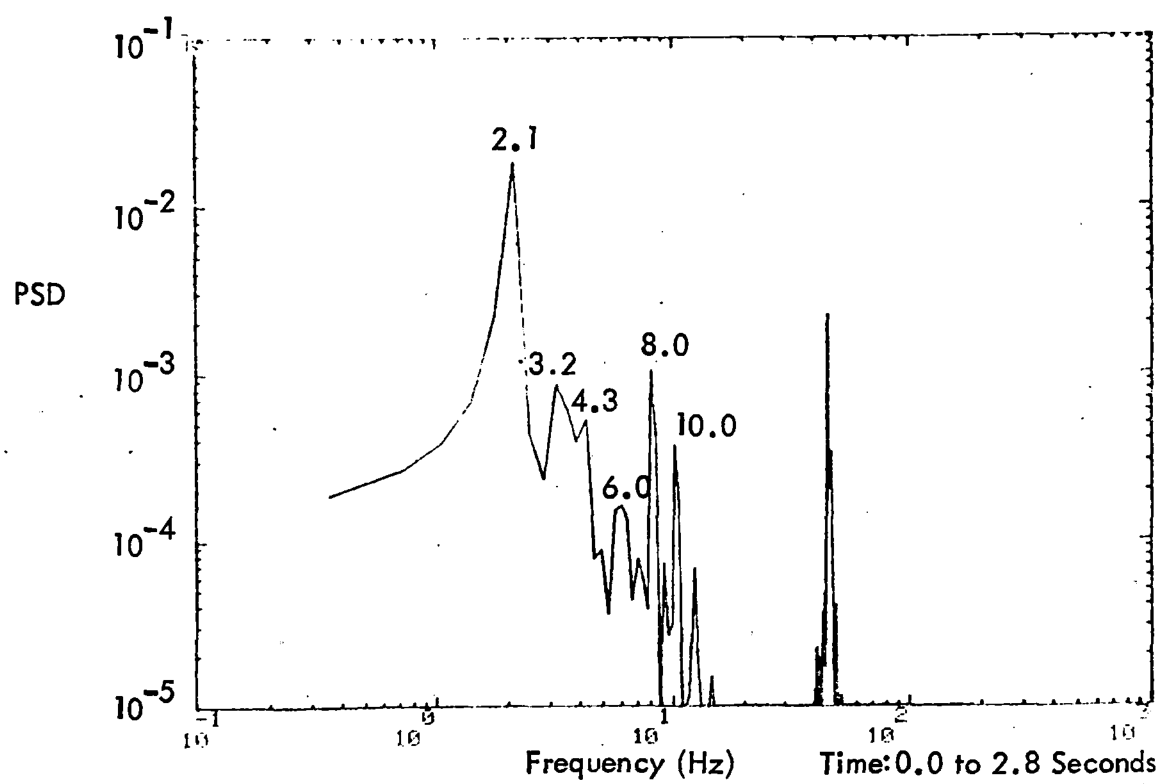

(b) Van Trailer PSD

Figure 6-34. Van Trailer Decay Time History and PSD

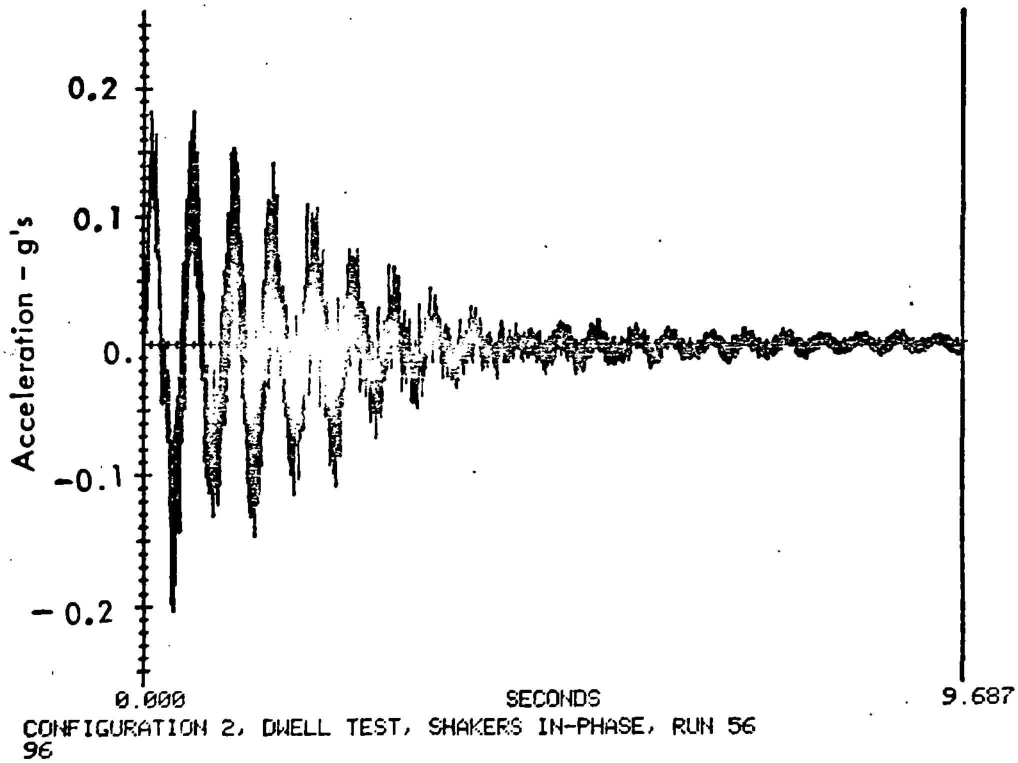

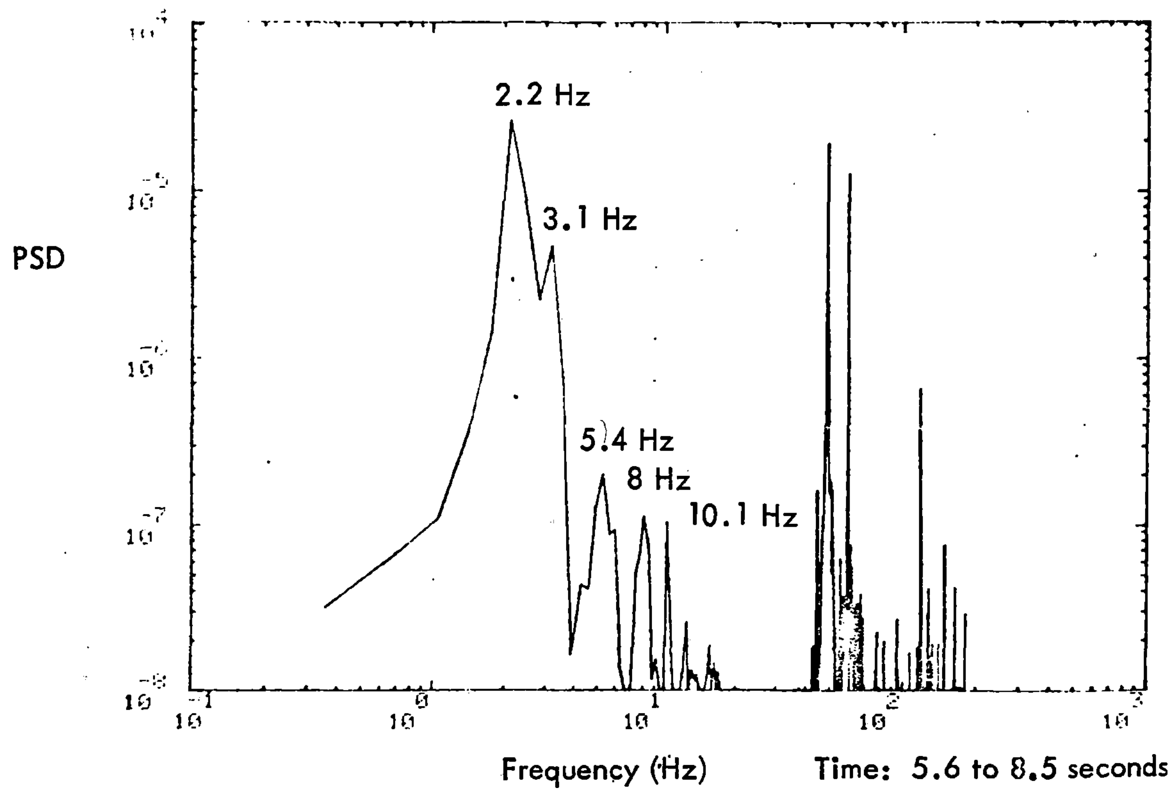

Figure 6-35. Platform Trailer Decay Time History and PSD

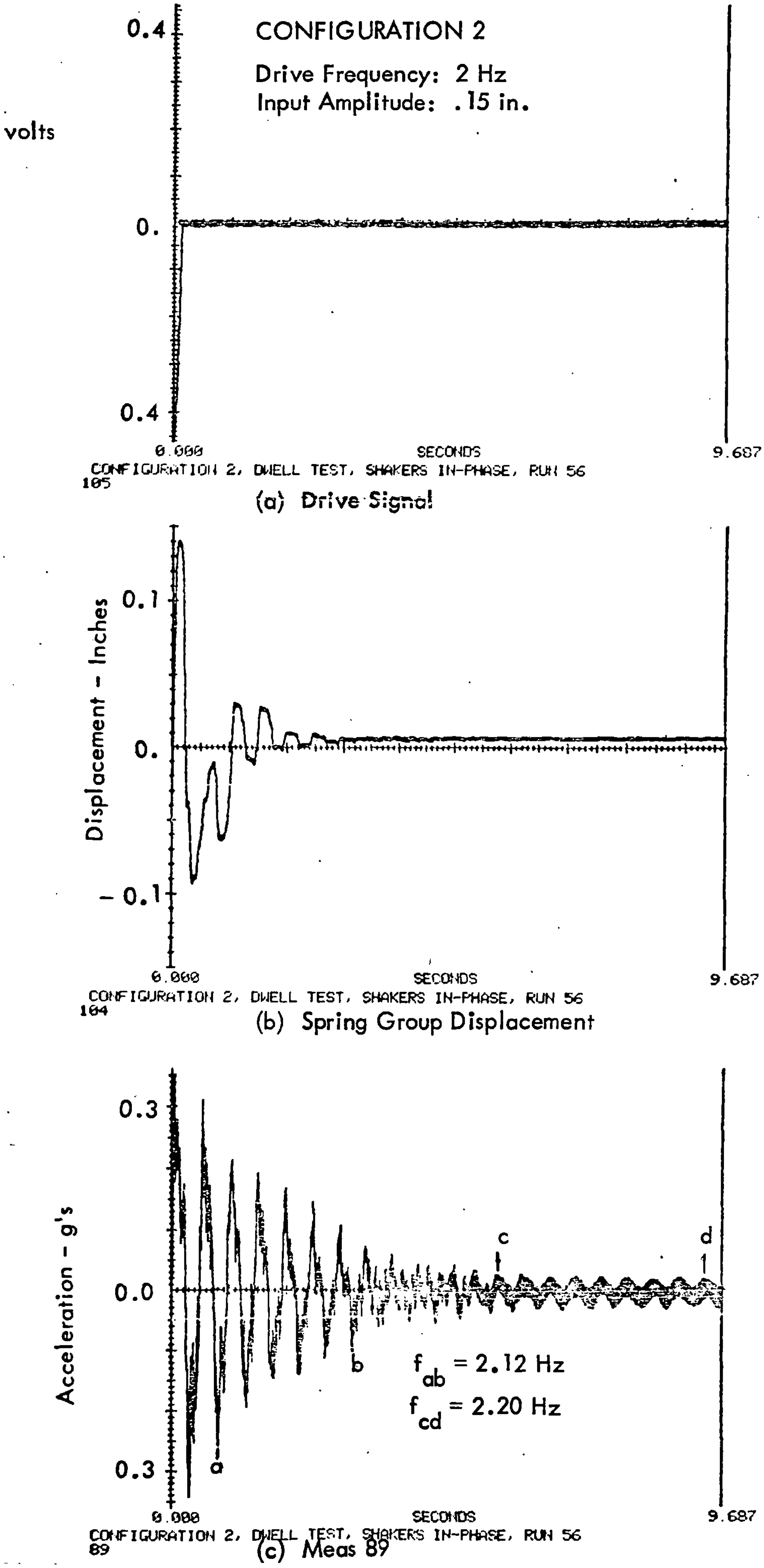

Figure 6-36. Configuration 2 Decay Traces

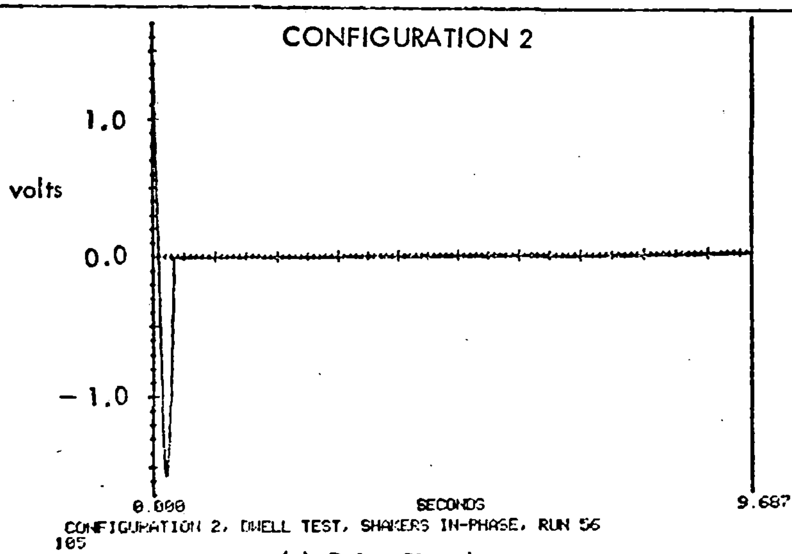

(a) Drive Signal

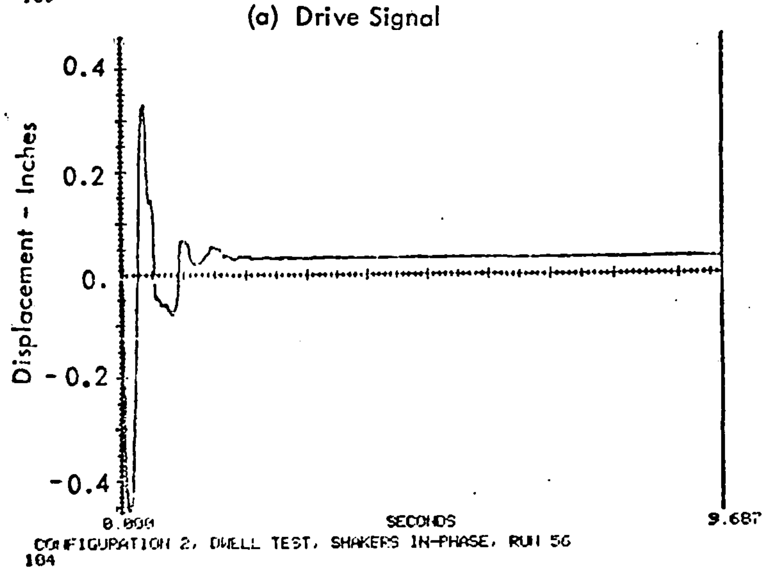

(b) Spring Group Displacement

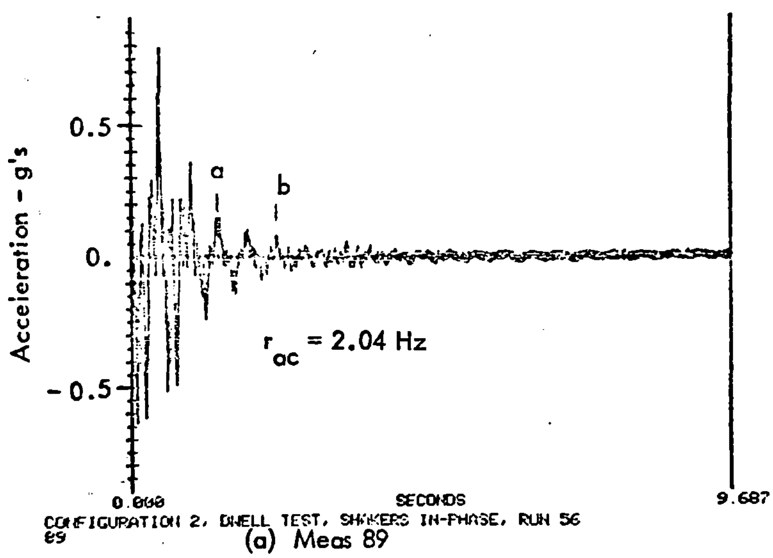

(a) Meas 89

Figure 6-37. Configuration 2 Decay Traces

After the static measurements were made, the force measurements were set at null so that measurements recorded during the test would include only the dynamic portion of the force exerted by the trailers. The dynamic forces measured during the sweep program are plotted in Figure 6-38. The van trailer measurement in Figure 6-16 (a) shows it's peak response at the first flatcar resonance while the platform trailer shows its peak response at the trailer bounce frequency of 3.1 Hz. This can be seen by noting that the van trailer tandem sits at the center of the flatcar where the flatcar has its maximum motion in the first mode while the platform trailer has its tandems near the A-end truck where a node point occurs for the first flatcar bending frequency. The large difference in the measured force level also shows the van trailer tandem to experience a much greater response level.

6.3.3 Strain Gage Measurements

Strain gages were placed on the bottom of the main sill of the flatcar to measure the stress levels induced in the flatcar during the test program. The exact location of these strain gages is defined in Part I. The strain gages were installed on the unloaded flatcar and calibrated to measure zero stress. After the two trailers were loaded, readings were made to record the stress induced in the flatcar due to the static loading. The measured values were as follows:

Strain Gage Number	Static Stress (psi)
50	6430
51	7439
52	6777

After recording the static stress due to the flatcars, the strain gages were set to zero for the configuration 2 testing. Thus the data recording during the vibration testing was the dynamic component of the stress. This can be seen in Figure 6-40 (b) where the time history for the strain gage is sinusoidal about zero. The frequency domain plots for the stress measurements are shown in Figure 6-39 and show a peak stress level of nearly 5000 psi at the first bending frequency. Above that frequency the levels fall off rapidly.

Analysis of the strain gage data shows these channels to be a good method of limiting the center deflection of the flatcar. On the demonstration test the deflection was

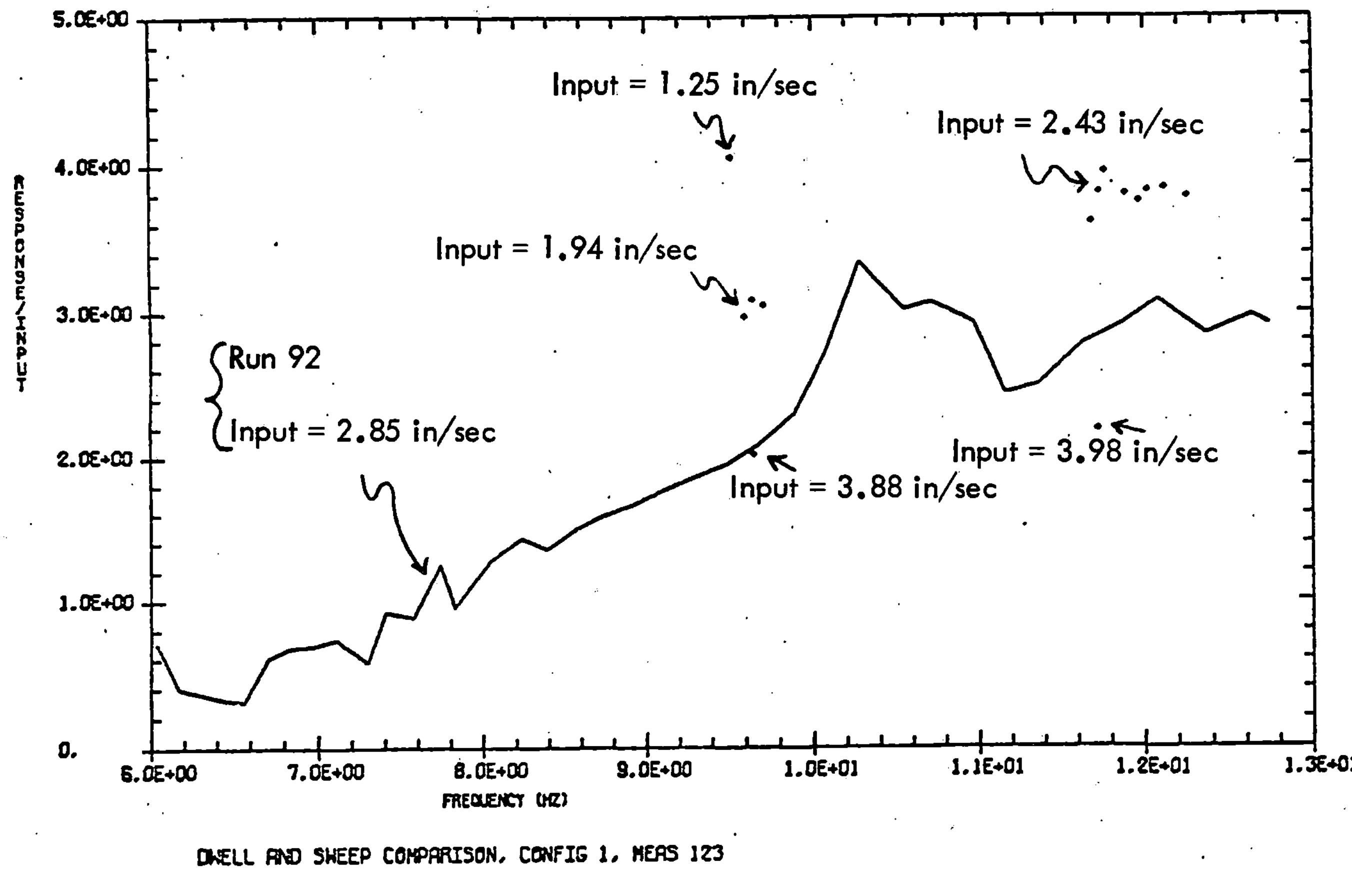

Figure 6-38. Dwell and Sweep Comparison

CONFIGURATION 2 SHAKERS IN PHASE

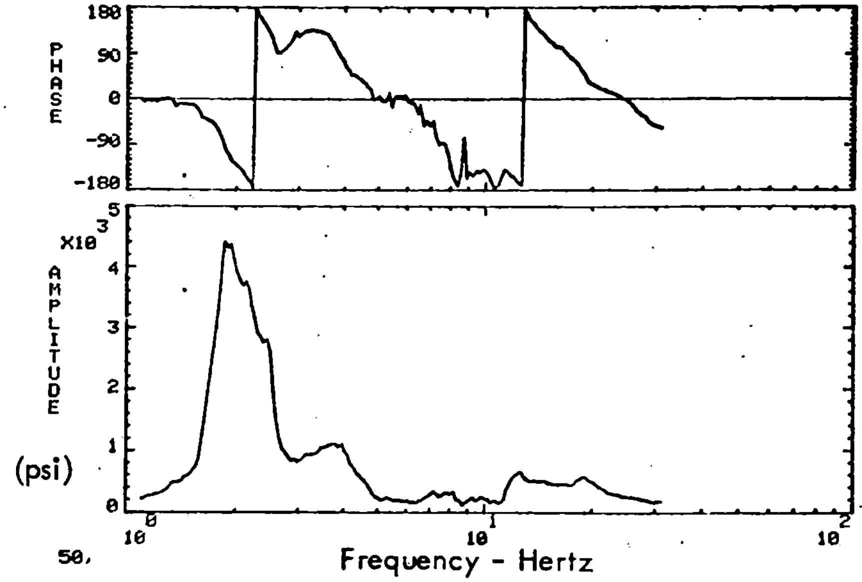

CONFIGURATION 2, HIGH LEVEL SINE SWEEP, SHAKERS IN PHASE, RUN 56

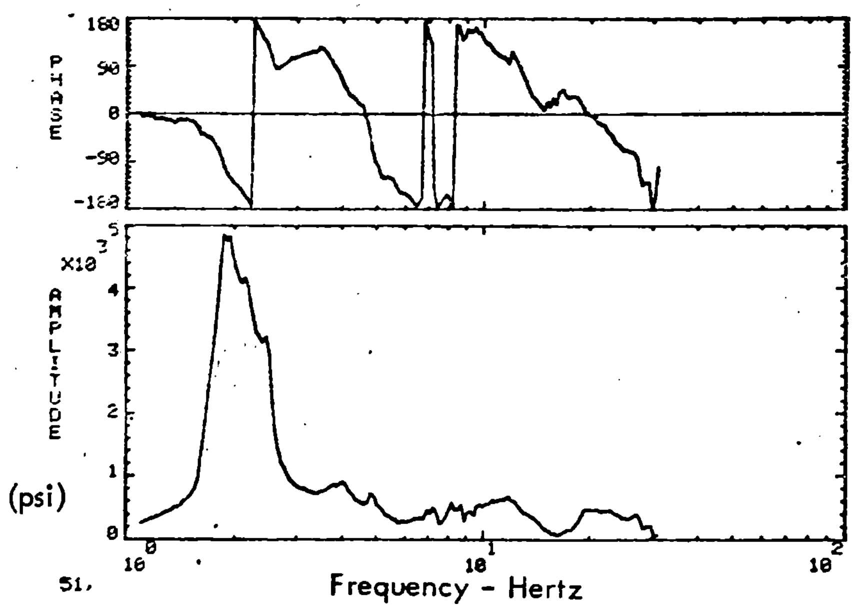

CONFIGURATION 2, HIGH LEVEL SINE SWEEP, SHAKERS IN PHASE, RUN 56

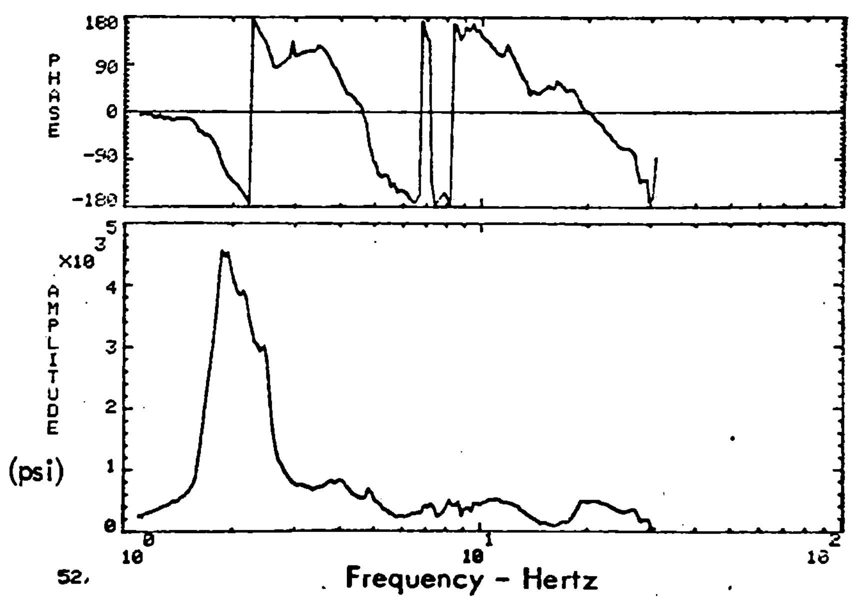

CONFIGURATION 2, HIGH LEVEL SINE SWEEP, SHAKERS IN PHASE, RUN 56

Figure 6-39. Strain Gage Measurements

limited by using the accelerometers. This can be seen in Figure 6-40 which shows time histories and PSD's of the input wave signal, the strain gage channel, and the accelerometer channel. The input signal in Figure 6-40 (a) is a clean sinusoid and the peak time history is equal to the peak sinusoidal value. In Figure 6-40 (b) the strain gage signal is a fairly clean sinusoid and the peak sinusoidal value is only slightly less than the peak time history. In 6-40 (c) the accelerometer time history has a lot of high frequency content, and the peak sinusoidal value is much less than the peak time history. The limit checking capability of the Vertical Shaker System (VSS) operates on peak time history values, while the quantity desired to be limited is the peak sinusoidal value. Thus, limiting the strain gage signal would come closer to actually limiting to a desired peak sinusoidal value.

Another advantage of the strain gage data is that it is a direct function of center deflection, while the acceleration limit was based on calculations and is valid at only the first bending frequency. This causes problems at frequencies above the first bending frequency where higher accelerations may occur (Figure 6-41 (a)) but where the corresponding displacement is less than the desired limit.

In order to establish a relationship between the measured strain and the center deflection a uniformly loaded beam model of the flatcar was chosen. For a uniformly loaded beam an analytical relationship between center deflection and strain can be developed as follows:

For uniformly loaded beam, center deflection is:

$$w_{center} = \frac{5wl^4}{384EI} \qquad (1)$$

The stress at the middle of the beam is:

$$s = \frac{Mc}{I} \quad \text{and } M = \frac{wl^2}{8I} \qquad (2)$$

$$s = \frac{wl^2c}{8I}$$

combining equations (1) and (2);

$$w = \frac{5I^4}{384EI} \left(\frac{8Is}{I^2c} \right)$$

$$w = \left(\frac{40I^2}{384Ec} \right) s$$

CONFIGURATION 2

SHAKERS IN PHASE

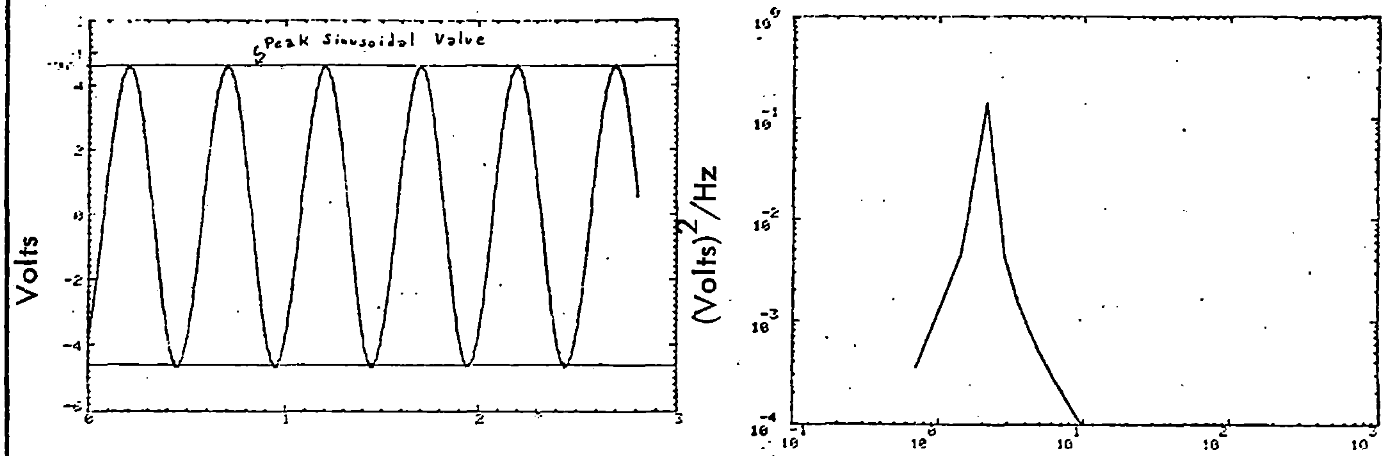

(a) Input Signal From Waveform Generator

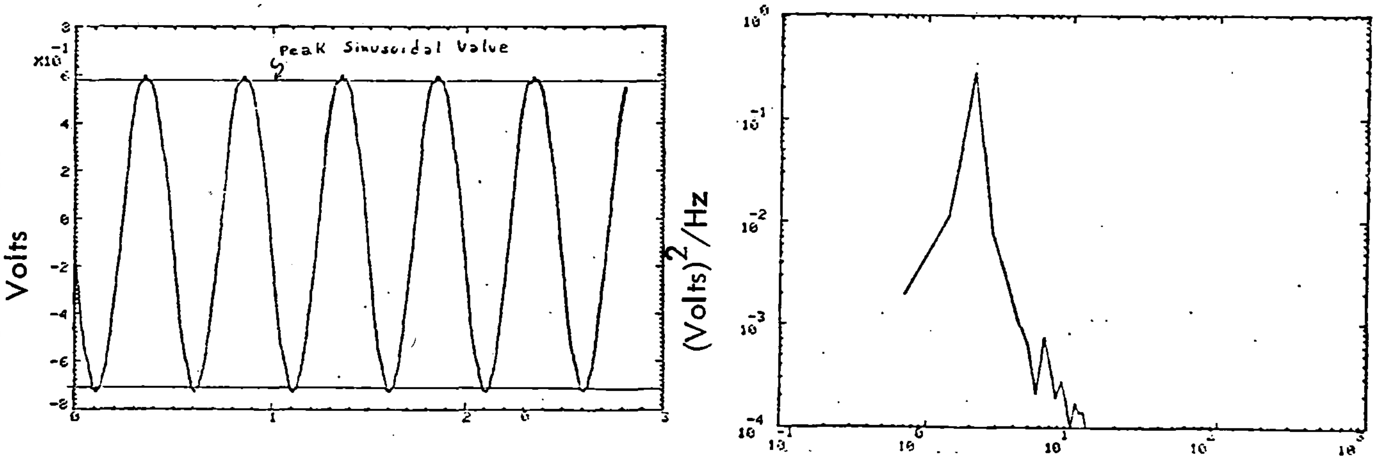

(b) Strain Gage Signal (conversion factor 1 volt = 5510 psi)

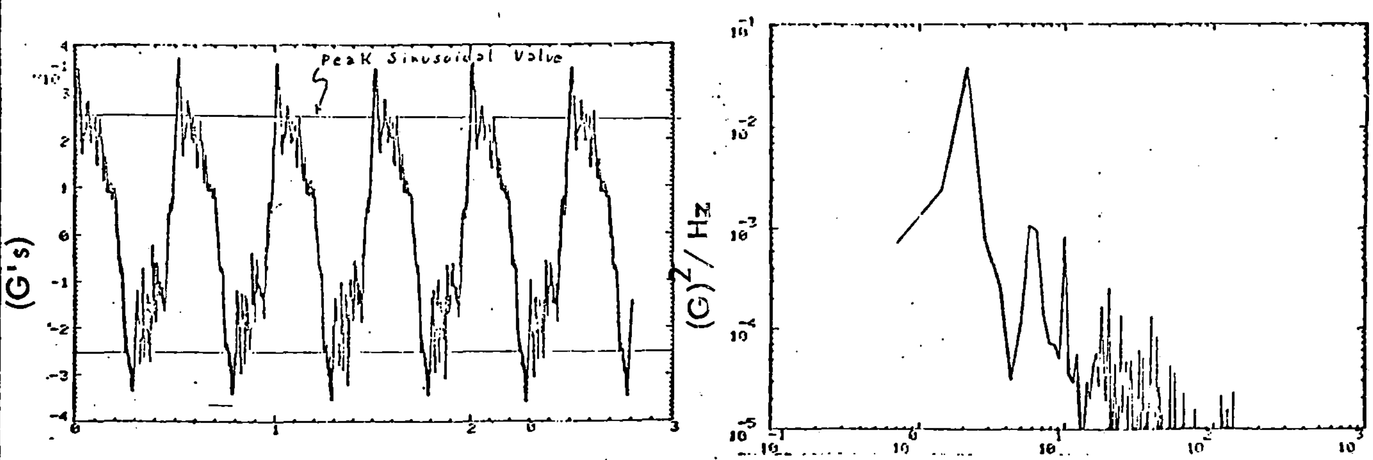

(c) 89, Flatcar Center Response

Figure 6-40. Time Histories and PSD's

CONFIGURATION 2

SHAKERS IN PHASE

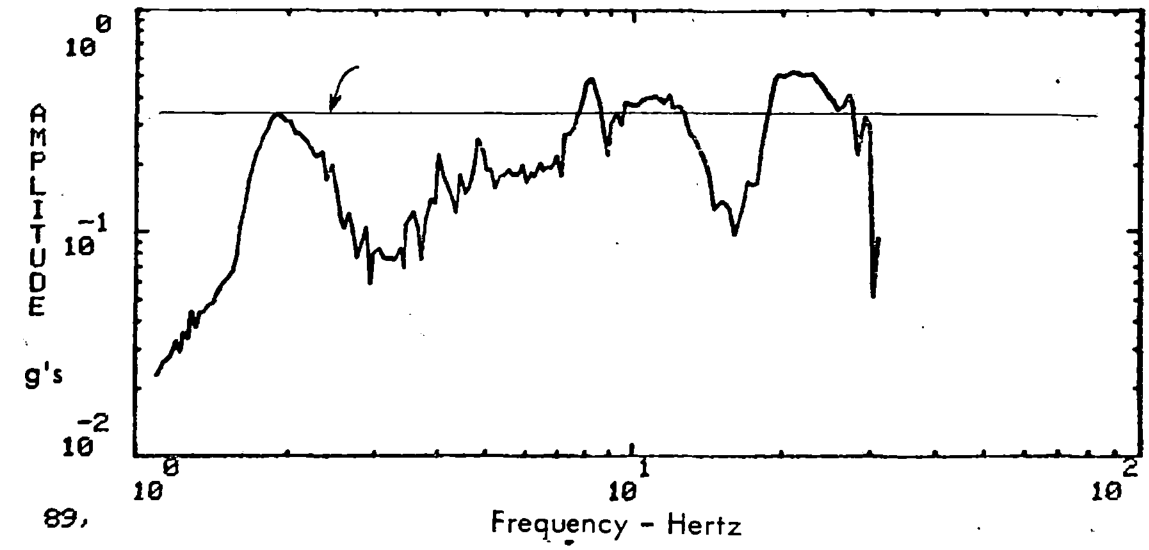

CONFIGURATION 2, HIGH LEVEL SINE SWEEP, SHAKERS IN PHASE, RUN 56

(a) Acceleration at Flatcar Center

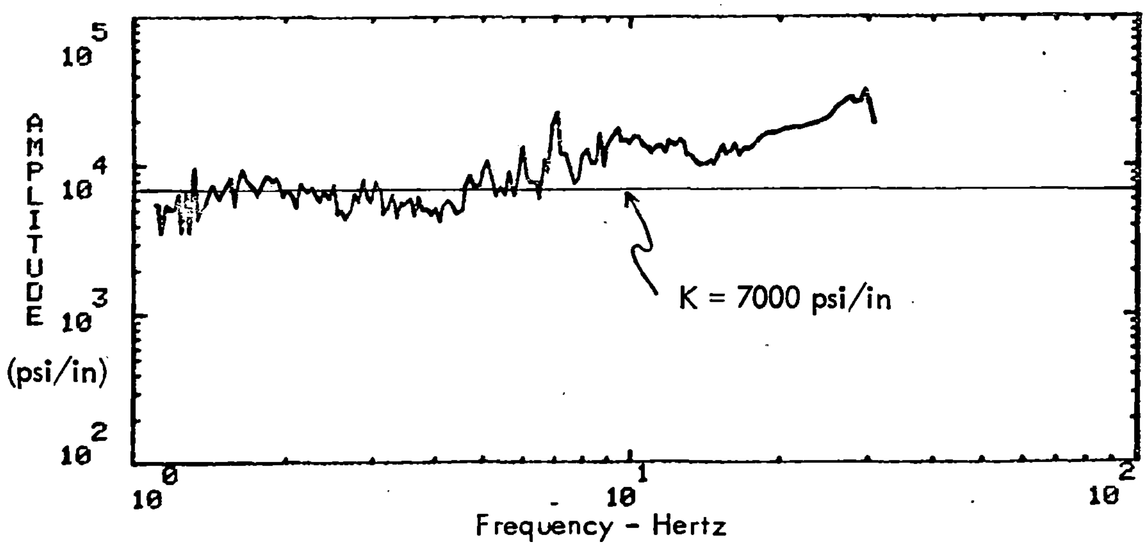

CONFIGURATION 2, HIGH LEVEL SINE SWEEP, SHAKERS IN PHASE, RUN 56

(b) Stress/Deflection Calculation

Figure 6-41. Flatcar Stress/Deflection Constant of

$$w = {}_{K}\,{}^{s}$$

This shows center deflection to be proportional to strain.

For uniaxial strain

$$s = E\,e$$

and

$$w = \frac{E}{K}\,e$$

A value for K can be derived from the test data as shown in Figure 6-41 (b). It was obtained by calculating the bending deflection at the center of the flatcar and dividing that into the measured stress. The calculated center deflection is shown in Figure 6-42 (a). A straight line approximation for the curve in Figure 6-42 (a) is K = 7000 psi/in. The calculated center deflection compared with the stress level divided by 7000 psi/in in Figure 6-42 (b) shows good agreement.

In considering the stress in the main sill, three components must be considered: (1) the dynamic stress induced in the sill due to the sinusoidal excitation of the flatcar, (2) the static stress induced by the lading on the flatcar, and (3) the static stress induced by the weight of the flatcar itself. The strain gages were set to the null position prior to each test, so the actual quantity measured was the dynamic stress. During configuration 2 testing, the maximum dynamic stress levels and deflection were:

Maximum dynamic deflection = 1.12 in
Maximum dynamic stress = 6668 psi

After loading the flatcar for configuration 2 but prior to zeroing the strain gages, the static stress due to the trailer weight was recorded.

CONFIGURATION 2

SHAKERS IN PHASE

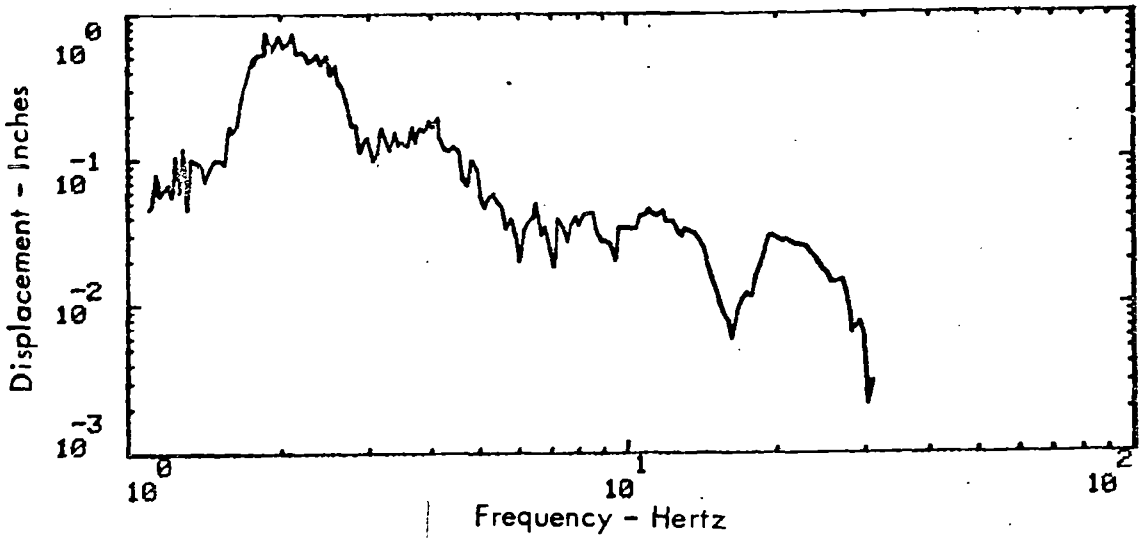

CONFIGURATION 2, HIGH LEVEL SINE SWEEP, SHAKERS IN PHASE, RUN 56

(a) Calculated Displacement Flatcar Center

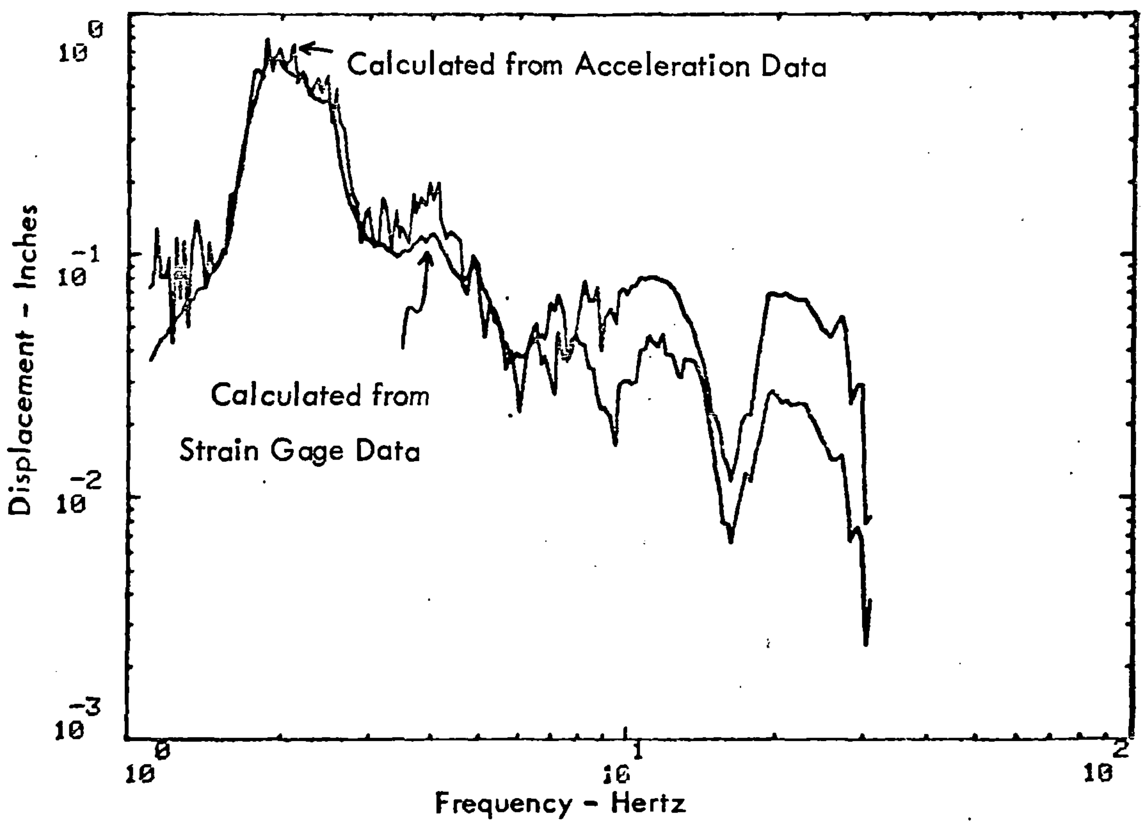

CONFIGURATION 2, HIGH LEVEL SINE SWEEP, SHAKERS IN PHASE, RUN 56

(b) Flatcar Center Deflection

Figure 6-42. Flatcar Center Deflection

Static stress = 7108 psi

$$\text{Deflection} = \frac{7108 \text{ psi}}{7000 \text{ psi/in}} = 1 \text{ in}$$

The stress and deflection due to the weight of the flatcar was obtained from the finite element model by applying a 1 g load to the empty flatcar model. The resulting deflection and bending stress is:

w = .56 in

Stress = .558 in x 7000 psi/in = 3903 psi

To summarize, the maximum stresses in the center sill during the DTP were as follows:

Loading	Stress (psi)	Deflection (inch)
Flatcar weight	3903	.56
Trailer loading	7108	1 in
Dynamic	6668	1.12 in

6.3.4 Linearity Comparison

The linearity of the responses was examined by plotting transfer functions for inputs at various levels. For a linear system the measured transfer function should be independent of amplitude. The input levels for the configuration 2 in-phase excitation are shown in Figure 6-43. The transfer function to the center of the flatcar (89/Input) are plotted in Figure 6-44 (a) for the three in-phase runs. The two runs at the same level (37 and 40) show very good agreement, while the run at the higher level shows a shift in peak for the resonance frequency and a decrease in the amplification factor. A comparison of dwell and sweep in Figure 6-44 (b) shows a difference between sweep and dwell results which is partially due to the difference in the input levels between sweep and dwell. However, the limited amount of dwell data makes it difficult to adequately compare sweep and dwell.

A more detailed plot of the linearity of the transfer function at the flatcar center in Figure 6-45 shows the resonant peak to shift down as the spring group opens up. In

LINEARITY COMPARISON, CONFIGURATION 2

SHAKER INPUT

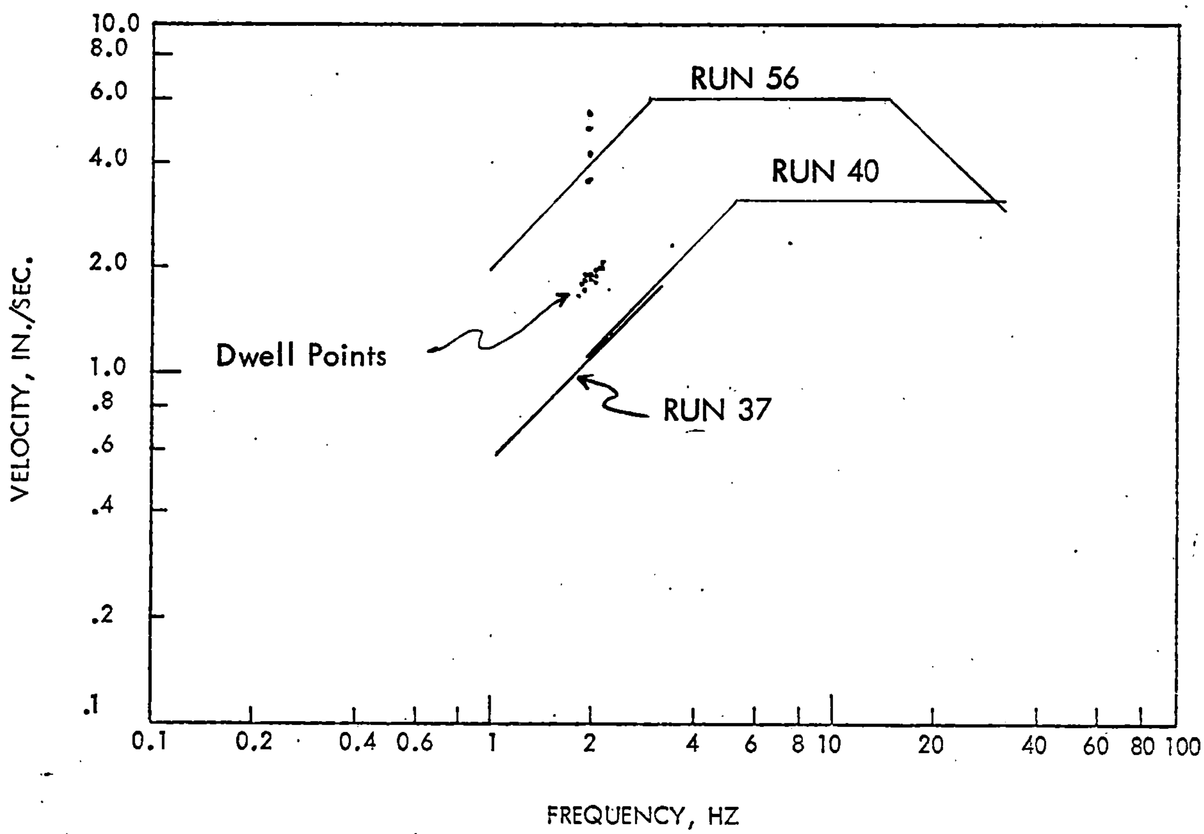

(a) Shakers In Phase

Figure 6-43. Linearity Comparison Input Amplitudes

CONFIGURATION 2

SHAKERS IN PHASE

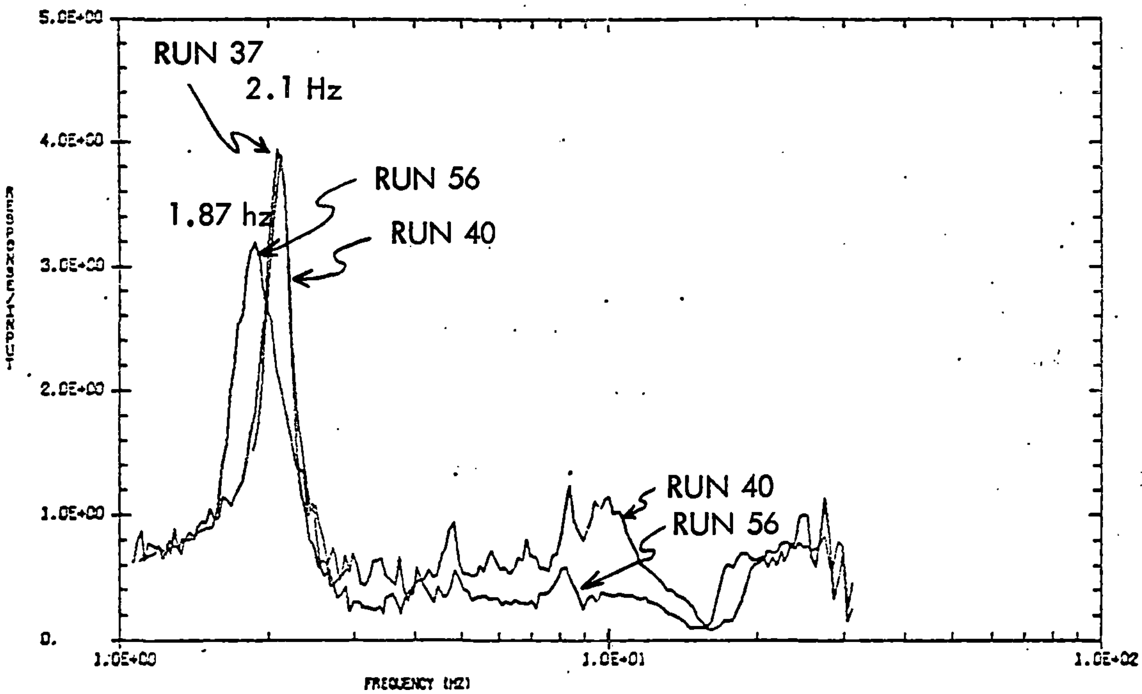

(a) 89/Input, Flatcar Center Transfer Function

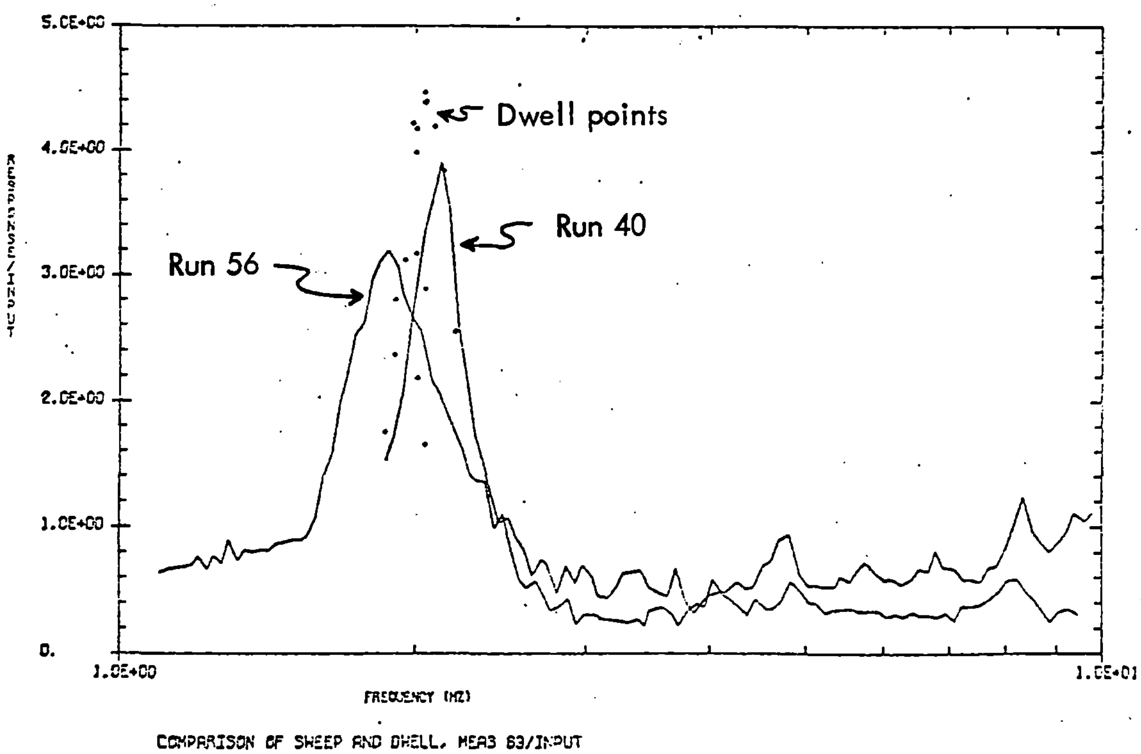

(b) 89/Input, Sweep and Dwell Comparison

Figure 6-44. Linearity and Sweep Comparison

CONFIGURATION 2
SHAKERS IN PHASE

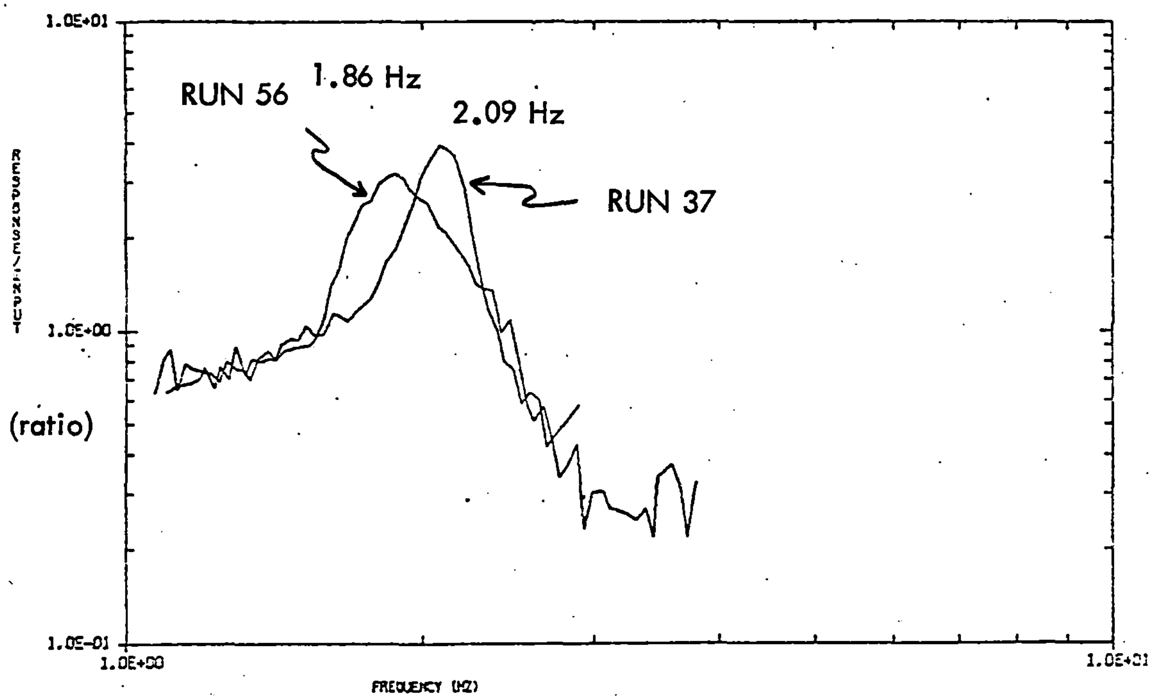

(a) 89/Input, Flatcar Transfer Function

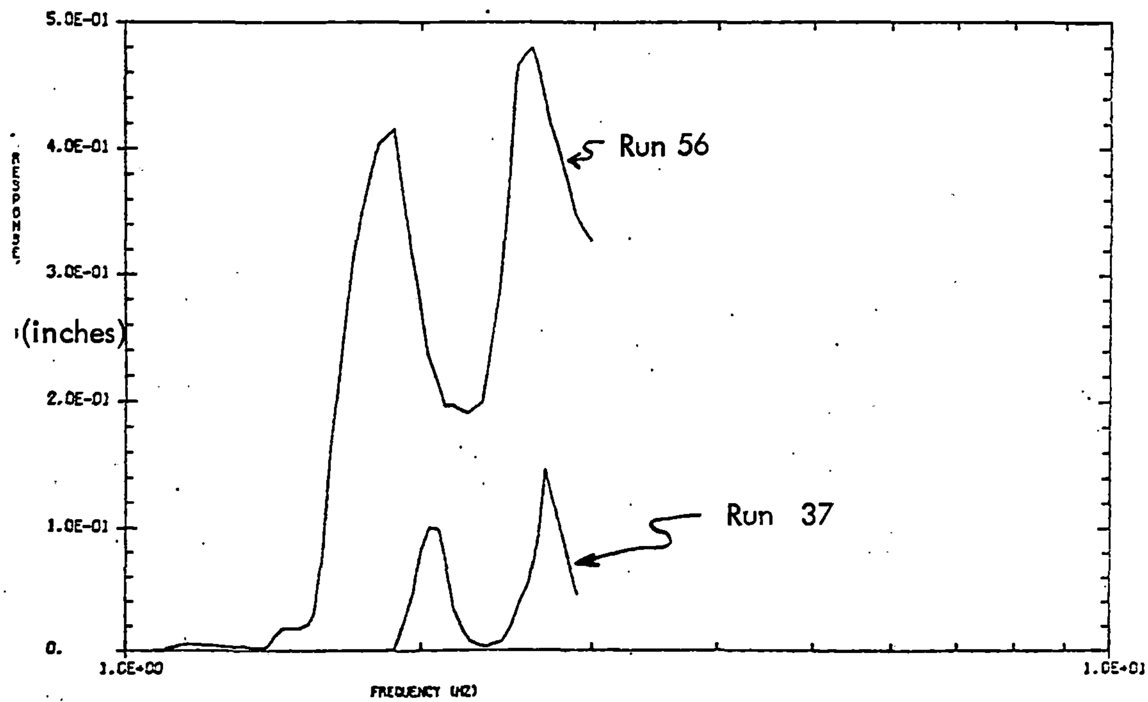

(b) 104, Spring Group Displacement

Figure 6-45. Flatcar Linearity Comparison

Figure 6-45 (b) the spring group is locked up until nearly 2 Hz for run 37 and the resonance peak is at 2.09 Hz. For run 56 the spring group starts movement well below 2 Hz, and the resonance peak shifts down to 1.86 Hz.

Measurements made on the van and platform trailers in Figure 6-46 show the same decrease in resonance frequency as the flatcar. However, the amplitudes on the van do not show a corresponding decrease in amplitude.

6.3.5 Frequency Domain Responses

The frequency domain analysis capability was used to make analytical predictions for the flatcar transfer functions. These are compared with the measured test data in Figures 6-47 and 6-48 for the in-phase excitation and in Figures 6-49 and 6-50 for the out-of-phase excitation. No attempt was made to adjust the model based on the configuration 2 data, so there is some discrepancy in the measured and analytical frequencies. Also the much greater complexity of the configuration 2 vehicle makes it more difficult to accurately model than the configuration 1 vehicle.

The frequency domain response calculation capability was also used to prepare analytical comparisons of the changes in responses due to variations in model parameters. This is shown in Figure 6-51 where the trailer lateral responses are plotted as a function of lateral spring constant. As discussed in section 3.2.3, no lateral spring constant data was available for the trailer tandems so an arbitrary value of 10^4 lbs/in was chosen for initial use in the model. Frequency domain plots in Figure 6-51 show the trailer's lateral responses when the lateral spring constant was increased to 10^5 lbs/in and 10^6 lbs/in. The results in Figure 6-51 show the responses to be relatively insensitive to the lateral spring constant for the trailer tandems. Thus it was felt that using 10^4 lbs/in was adequate until more detailed test data on the trailer tandems was available to provide a better spring constant.

Analytical transient decay plots are shown in Figure 6-52 for the flatcar and trailers. Analytical transient decay plots are shown in Figure 6-52 for the flatcar and trailers. In each case the input excitation was a sinusoid of ± 1 inch for one cycle. Figure 6-52 (a) shows the analytical decay responses at the flatcar center and flatcar end. Figure 6-52 (b) shows analytical decay responses at the center of the van and platform trailers.

CONFIGURATION 2
SHAKERS IN PHASE

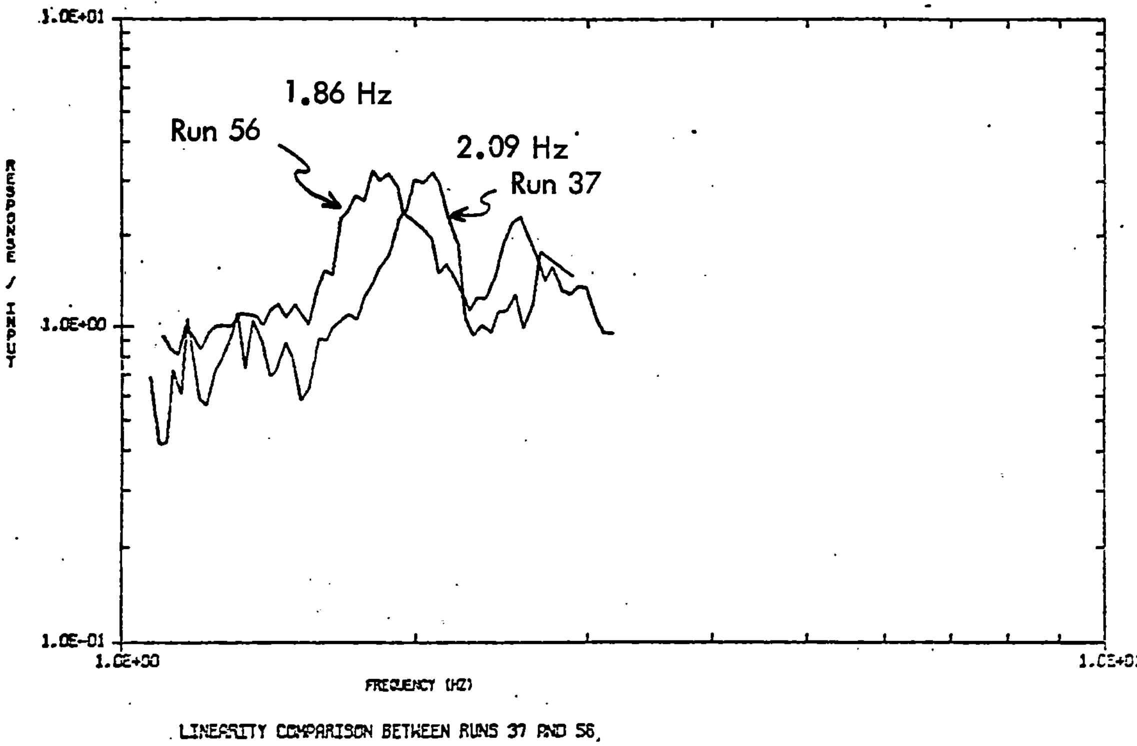

(a) 81/Input, Van Trailer Transfer Function

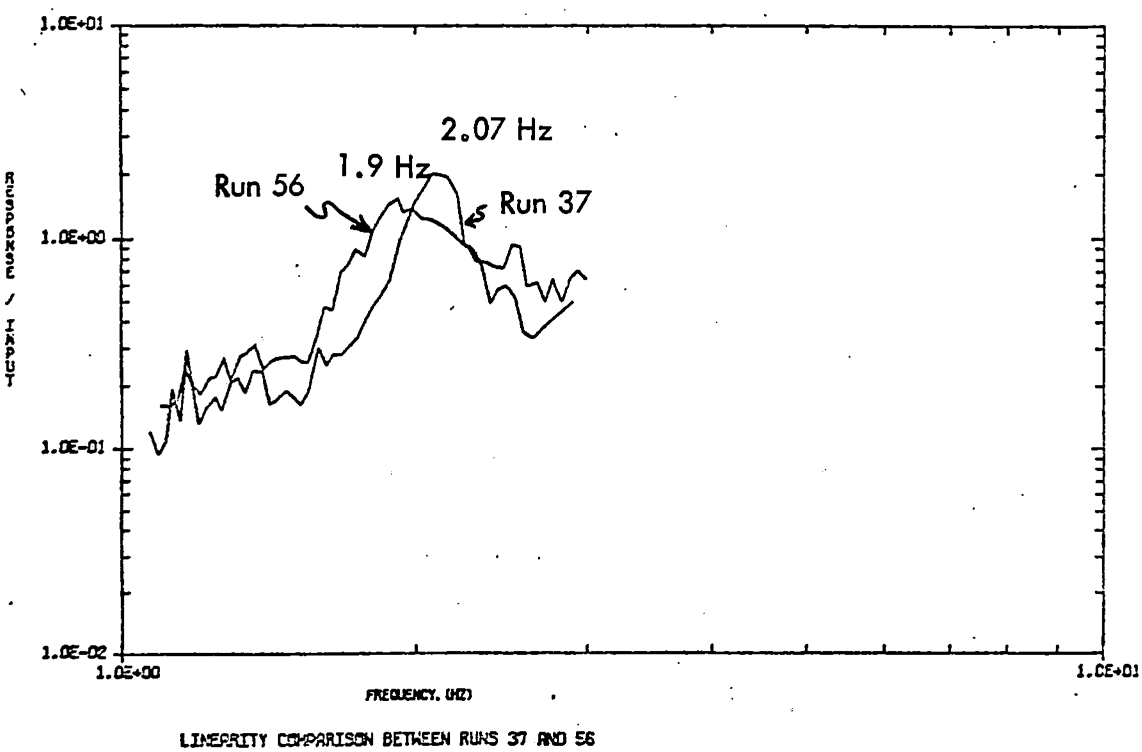

(b) 96/Input, Platform Trailer Transfer Function

Figure 6-46. Trailer Linearity Comparison

CONFIGURATION 2

SHAKERS IN PHASE

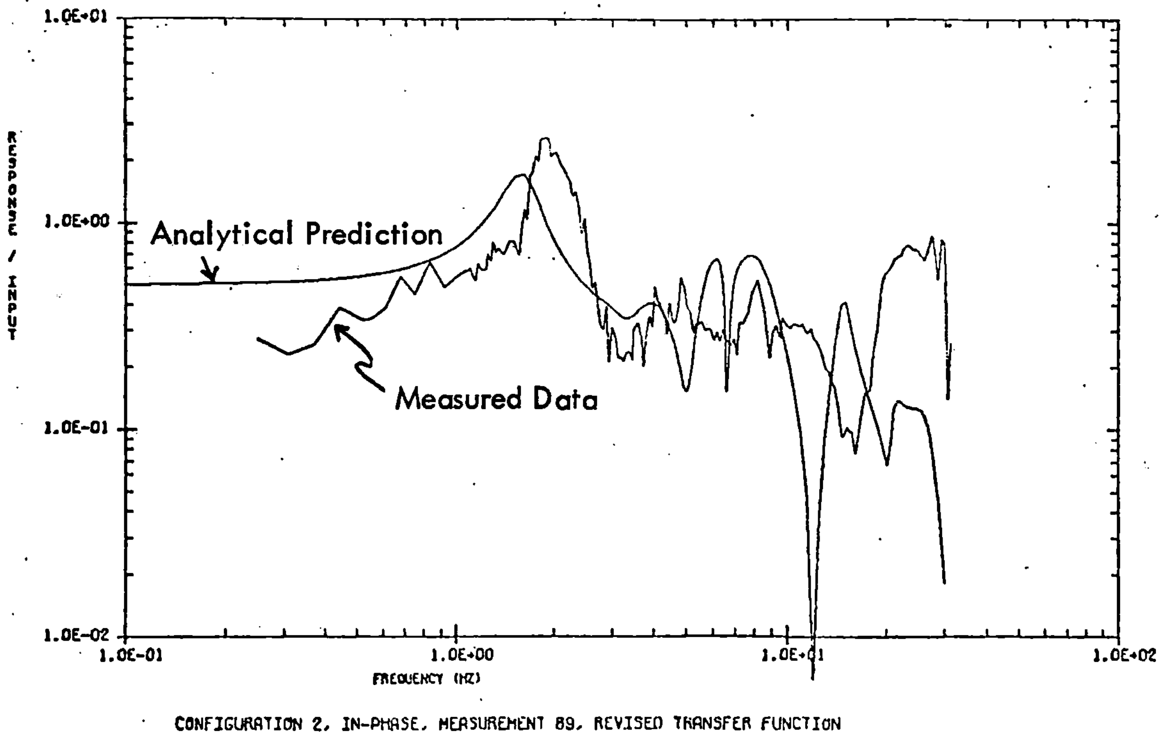

(a) 89/Input, Flatcar Center Transfer Function

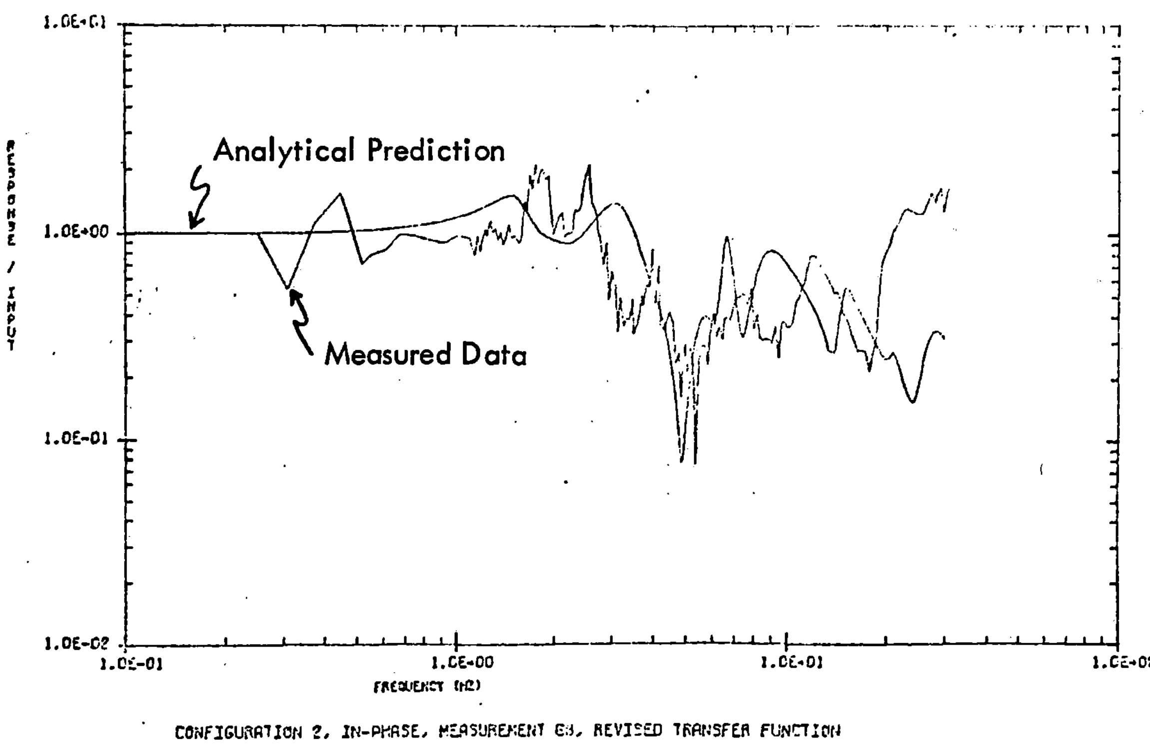

(b) 68/Input, Flatcar Transfer Function

Figure 6-47. Measured and Analytical Transfer Functions

CONFIGURATION 2

SHAKERS IN PHASE

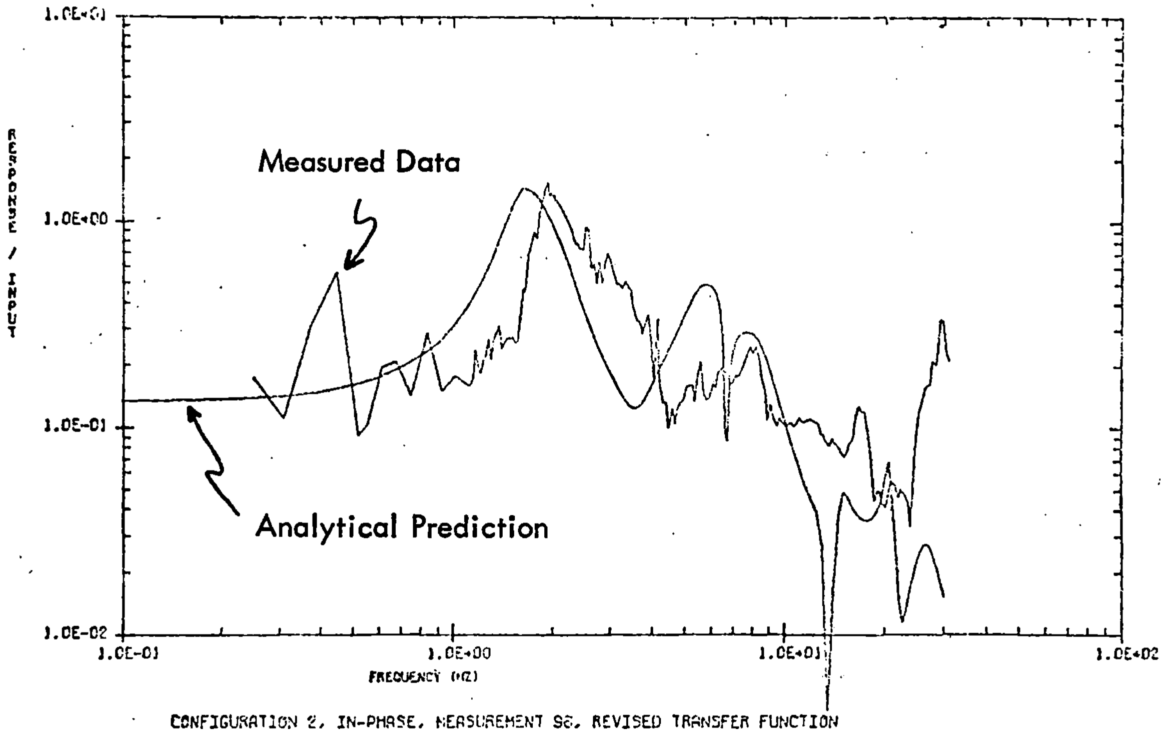

(a) 96/Input, Platform Trailer Transfer Function

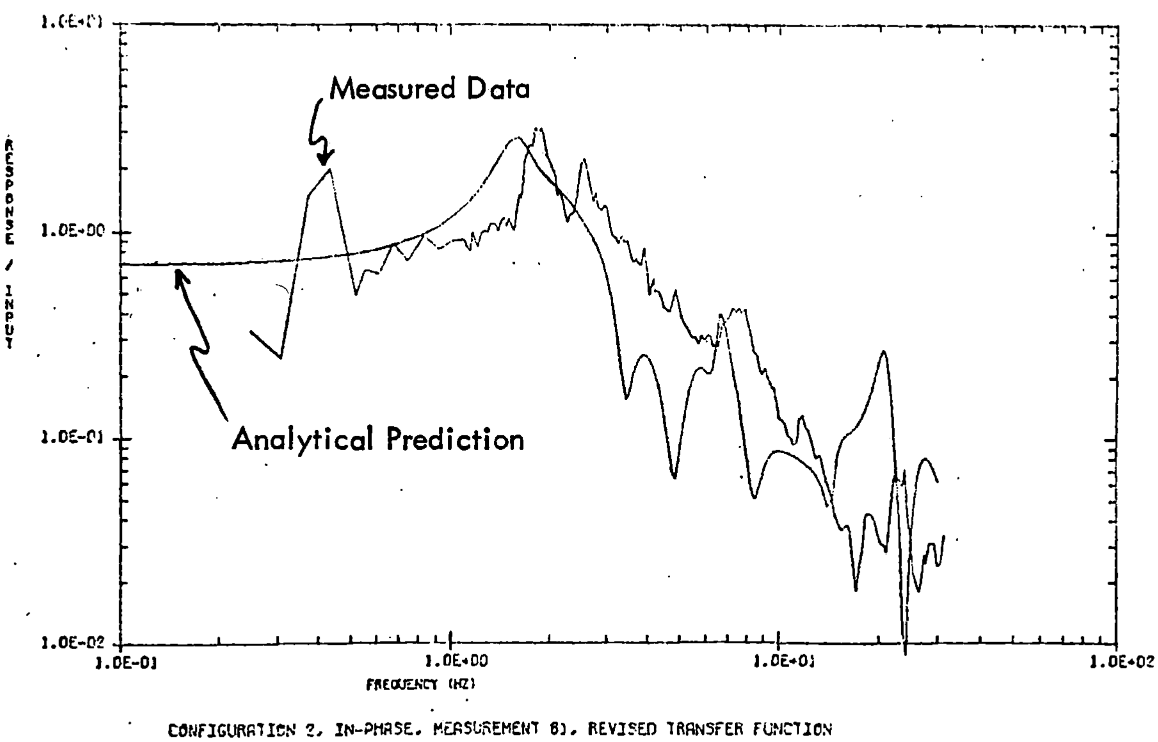

(b) 81/Input Van Trailer Transfer Function

Figure 6-48. Measured and Analytical Transfer Functions

CONFIGURATION 2

SHAKERS OUT OF PHASE

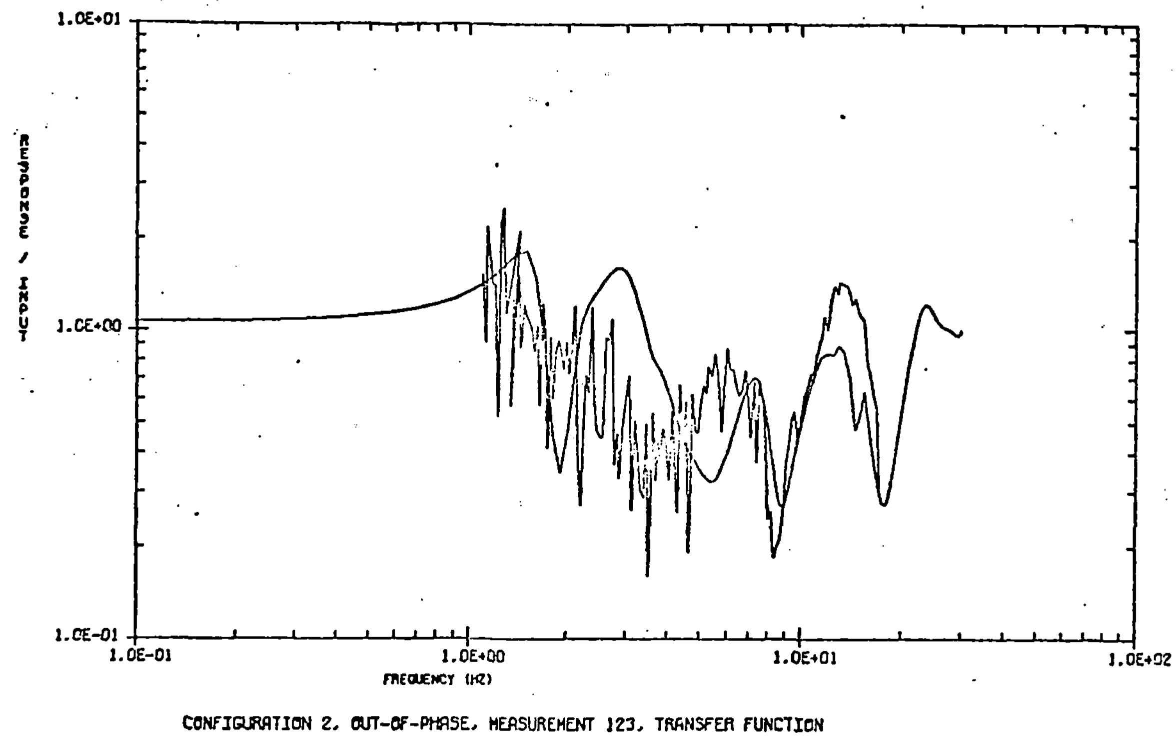

(a) 123/Input, Flatcar Transfer Function

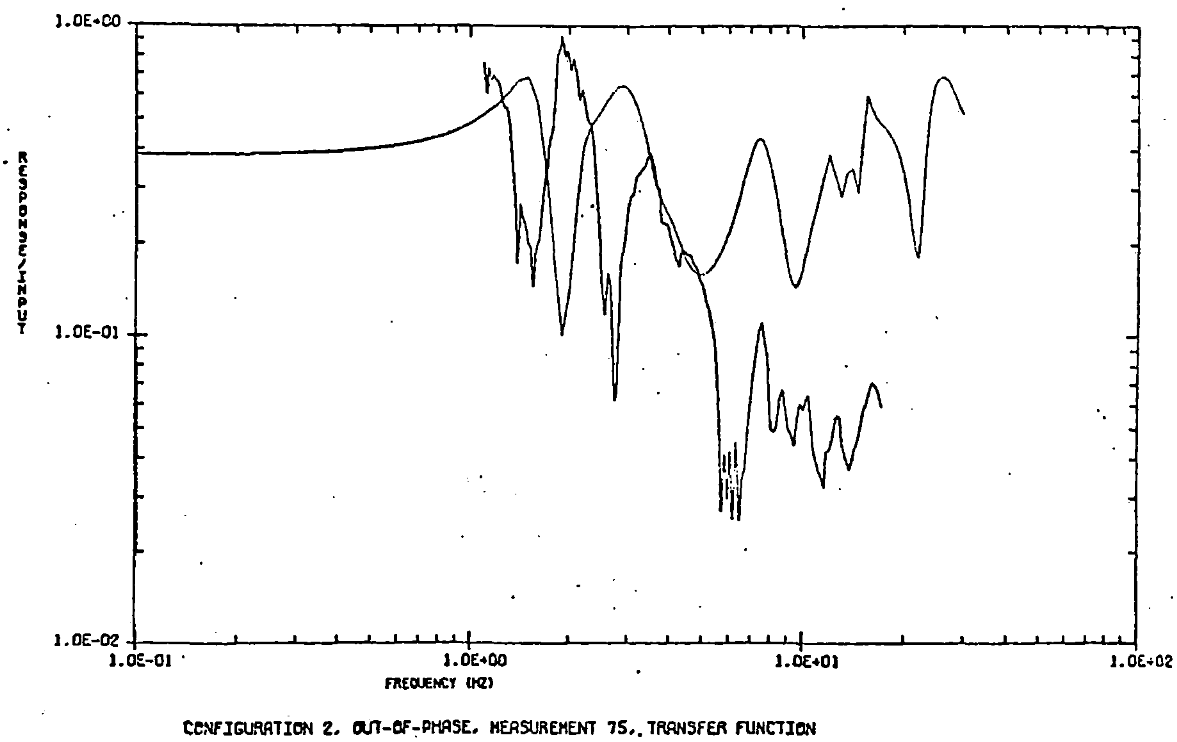

(b) 75/Input, Van Trailer Transfer Function

Figure 6-49. Measured and Analytical Transfer Functions

CONFIGURATION 2

SHAKERS OUT OF PHASE

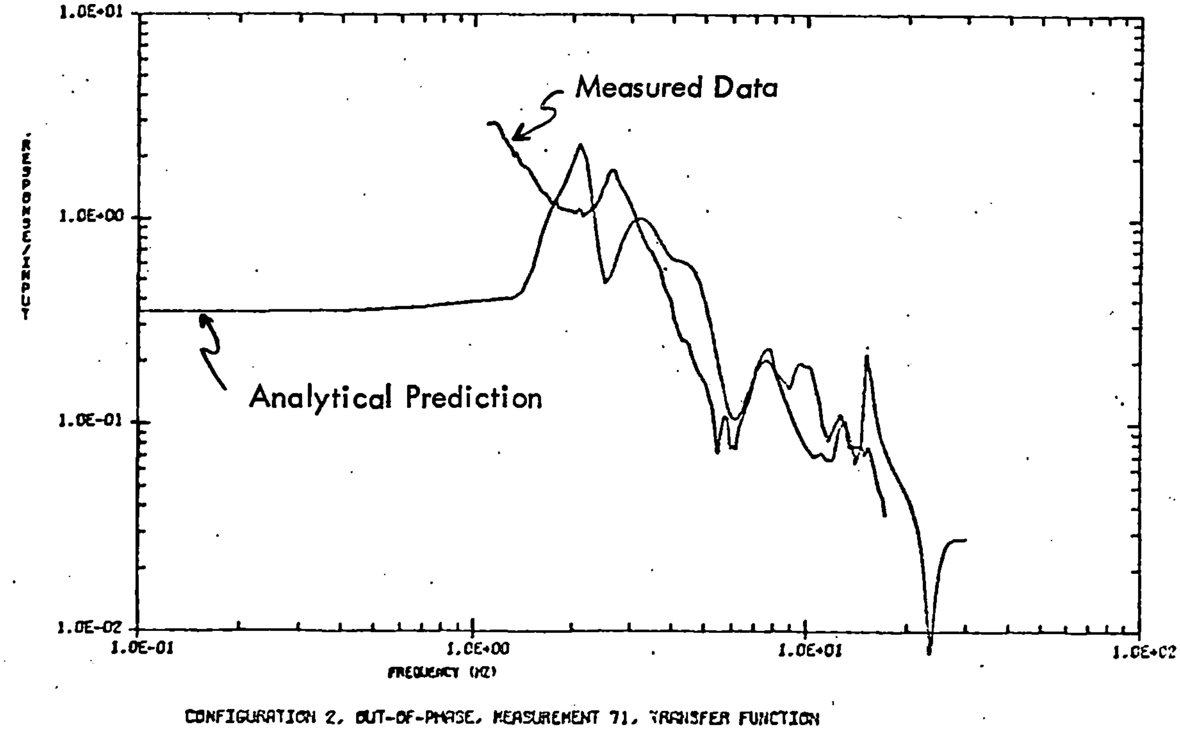

(a) 71/Input, Van Trailer Lateral Transfer Function

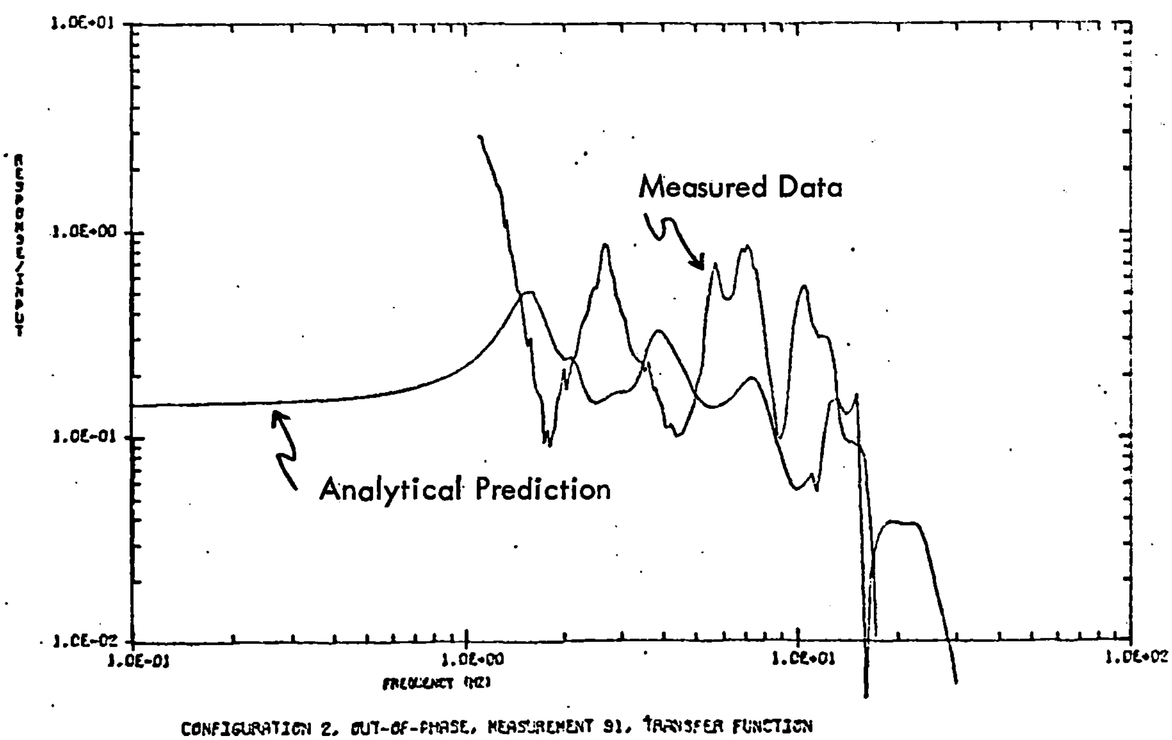

(b) 91/Input, Platform Trailer Transfer Function

Figure 6-50. Measured and Analytical Transfer Functions

CONFIGURATION 2

SHAKERS OUT OF PHASE

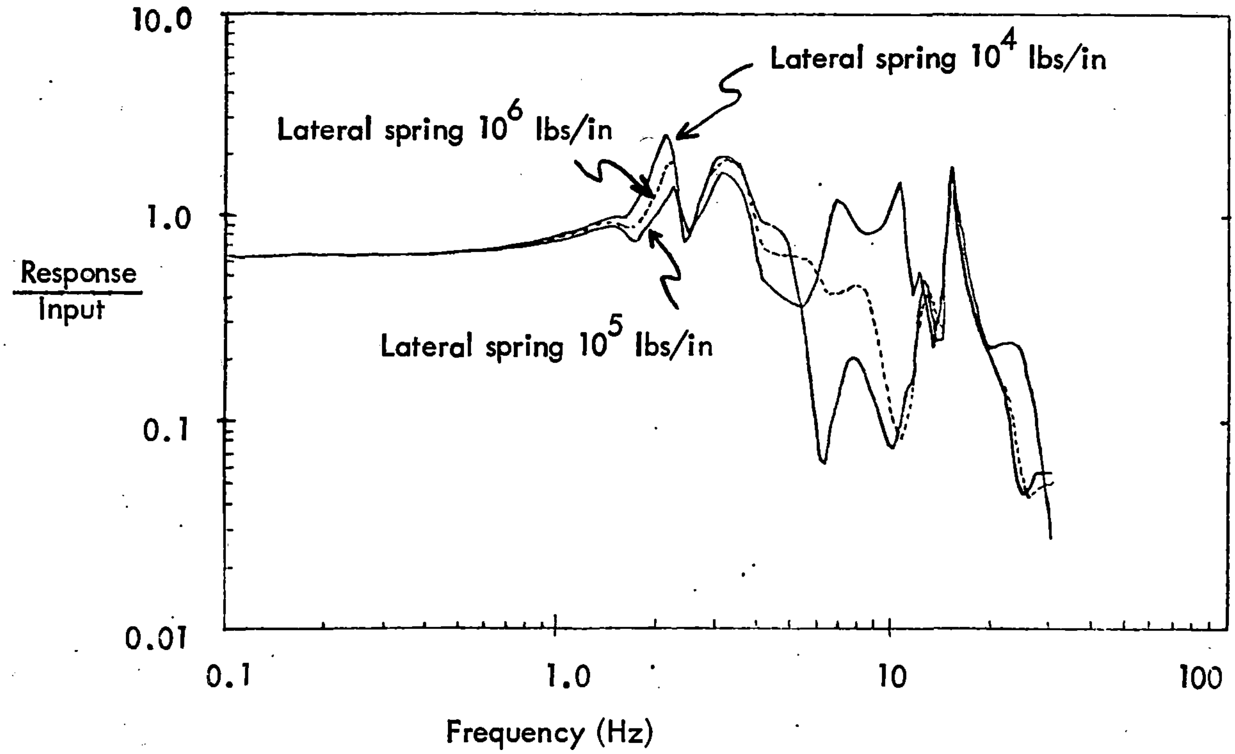

(a) Van Trailer Lateral Response

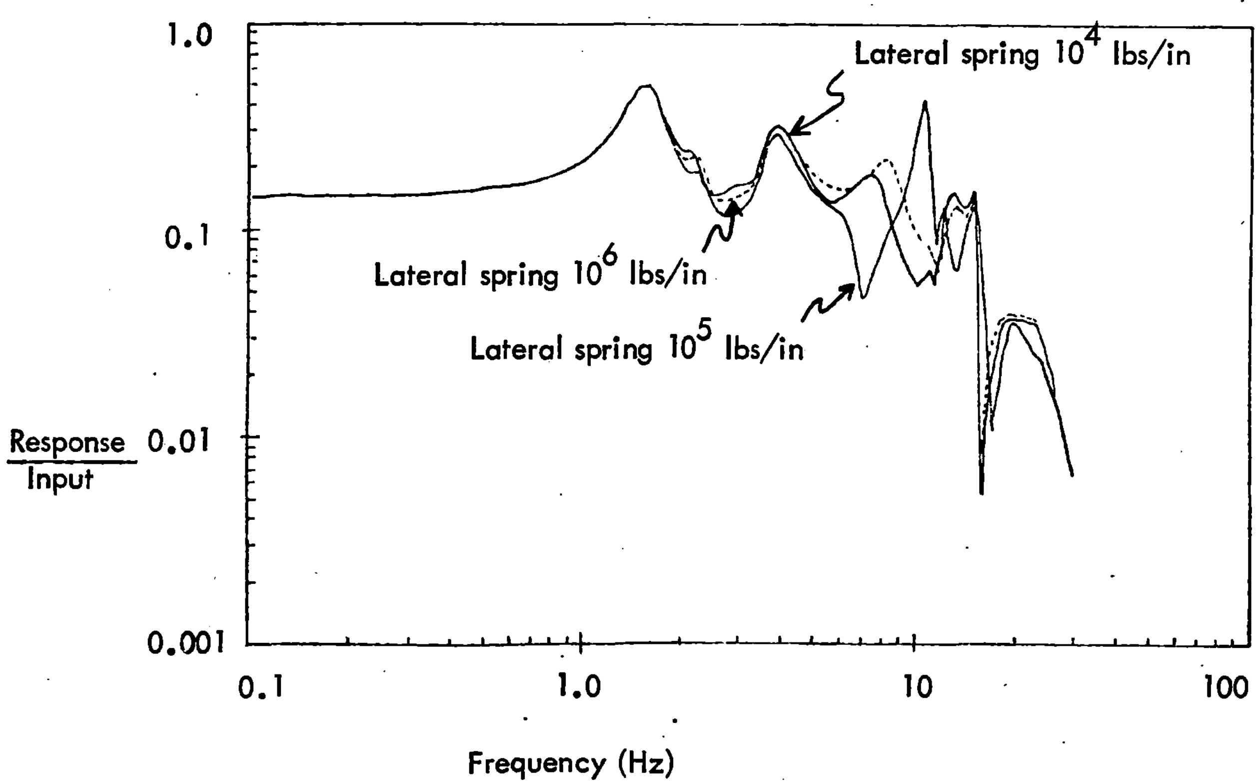

(b) Platform Trailer Lateral Response

Figure 6-51. Analytical Trailer Lateral Responses

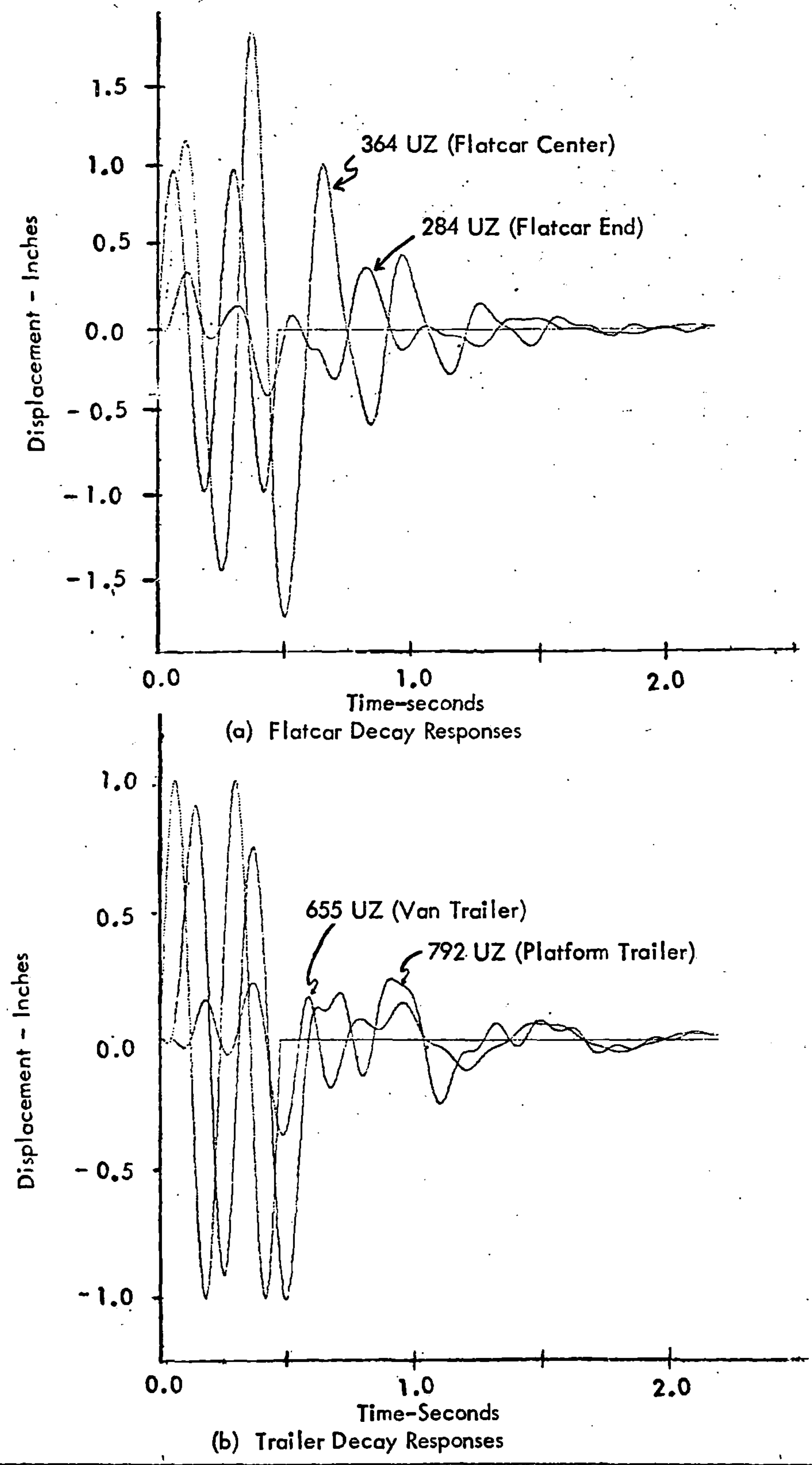

(a) Flatcar Decay Responses

(b) Trailer Decay Responses

Figure 6-52. Analytical Decay Responses

6.4 CONFIGURATION 3

6.4.1 Response Frequencies

The frequency domain plots of the configuration 3 test were examined to establish the significant resonant frequencies. Examples of this data are shown in Figures 6-53 to 6-57 for the in-phase excitation and in Figures 6-58 to 6-62 for the out-ofphase excitation. The resultant frequencies are summarized in Table 6-5. The results of the configuration 3 transfer function at the flatcar center show the same double-peak first resonant frequency as the configuration with the frequencies being less than configuration because of the added weight of the empty platform trailer as discussed in Part 1. Figure 6-53 (a) shows the flatcar center transfer function and the resonant peaks at 2.7 and 3.0 Hz. The structural amplification factor on the flatcar in Figure 6-54 (b) shows the first bending mode of the flatcar to be 3.1 Hz. The second bending mode appears to be between 6.7 and 8.7 Hz. The displacement measurement across the spring group shows predominant peaks at 2.8 and 4.1 Hz which should correspond to the rigid body bounce and pitch modes. The transfer function at the flatcar end in Figure 6-53 (b) shows its predominant response in the pitch mode at 4.1 Hz. The stress levels measured in the main sill show a peak level of 3700 psi occurring at the first flatcar resonance. The tire pressure measurement in Figure 6-55 (b) shows peak at 2.9 Hz and 5.1 Hz. The second resonance occurs at the bounce mode of the unloaded trailer. This compares with a loaded trailer bounce mode of approximately 3.2 Hz.

The out-of-phase excitation showed little change in resonant frequencies from the unloaded configuration. The transfer functions to the flatcar are shown in Figure 6-58. By looking at the phase relationship of the accelerometers at the two ends of the flatcar in Figure 6-59 (b) it is possible to identify the modes. Up to 4 Hz the flatcar ends move the in phase, indicating a rigid body rocking at 1.7 Hz. The 11.8 Hz mode has the two ends 180 degrees out of phase of the first torsional mode. At 19 Hz the two ends are back in phase indicating the second torsional mode. The flatcar lateral structural amplification factor in Figure 6-60 (a) shows the first lateral bending frequency to be 11 Hz. The amplification factor in the lateral direction is not as pronounced as for configuration 1 (Figure 6-5 (a)), which indicates that loading the flatcar tends to suppress this mode. As noted for the fully loaded flatcar the mode is completely suppressed. The displacement measurements for configuration 3 in Figure 6-61 show the rocking modes at 1.7 Hz to have considerable rocking motion on the

CONFIGURATION 3

SHAKERS IN PHASE

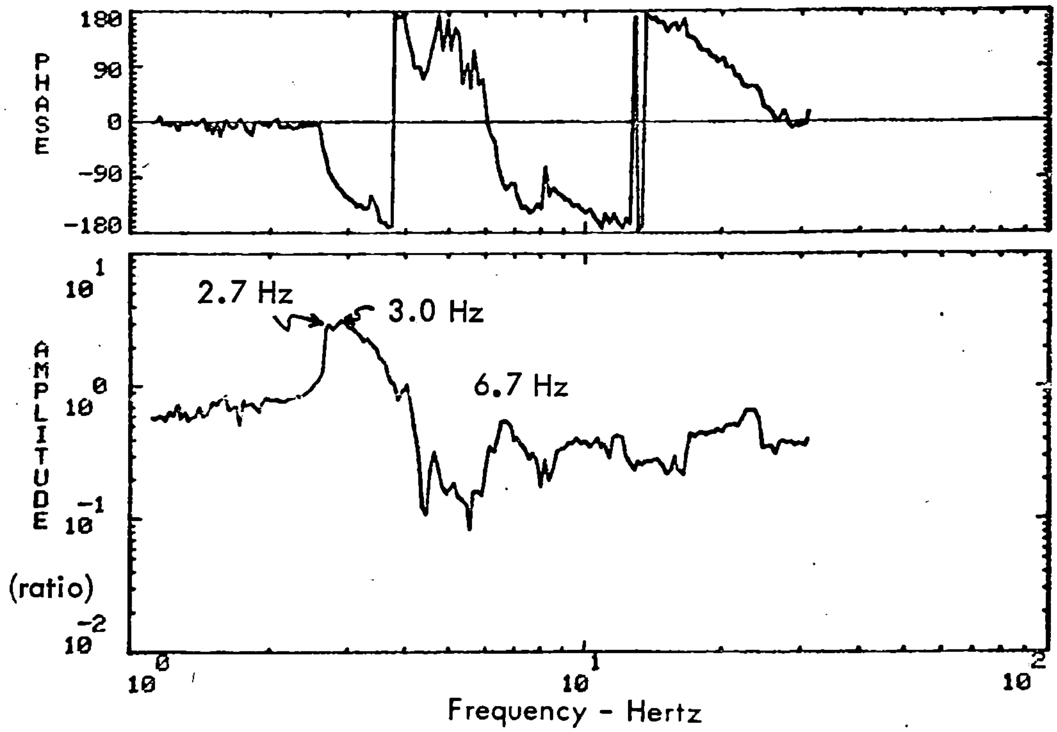

CONFIGURATION 3, HLGH LEVEL RUN, SHAKERS IN PHASE, RUN 103

(a) 89/Input, Flatcar Center Transfer Function

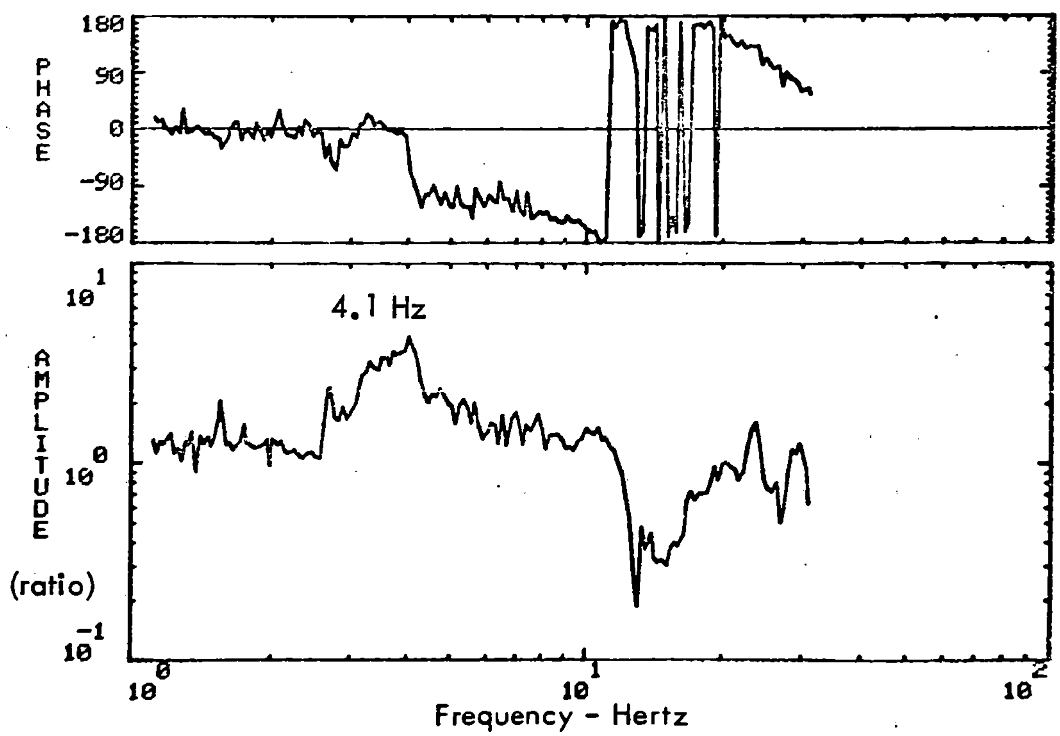

CONFIGURATION 3, HLGH LEVEL RUN, SHAKERS IN PHASE, RUN 103

(b) 123/Input, Flatcar End Transfer Function

Figure 6-53. Flatcar Transfer Functions, Configuration 3

CONFIGURATION 3

SHAKERS IN PHASE

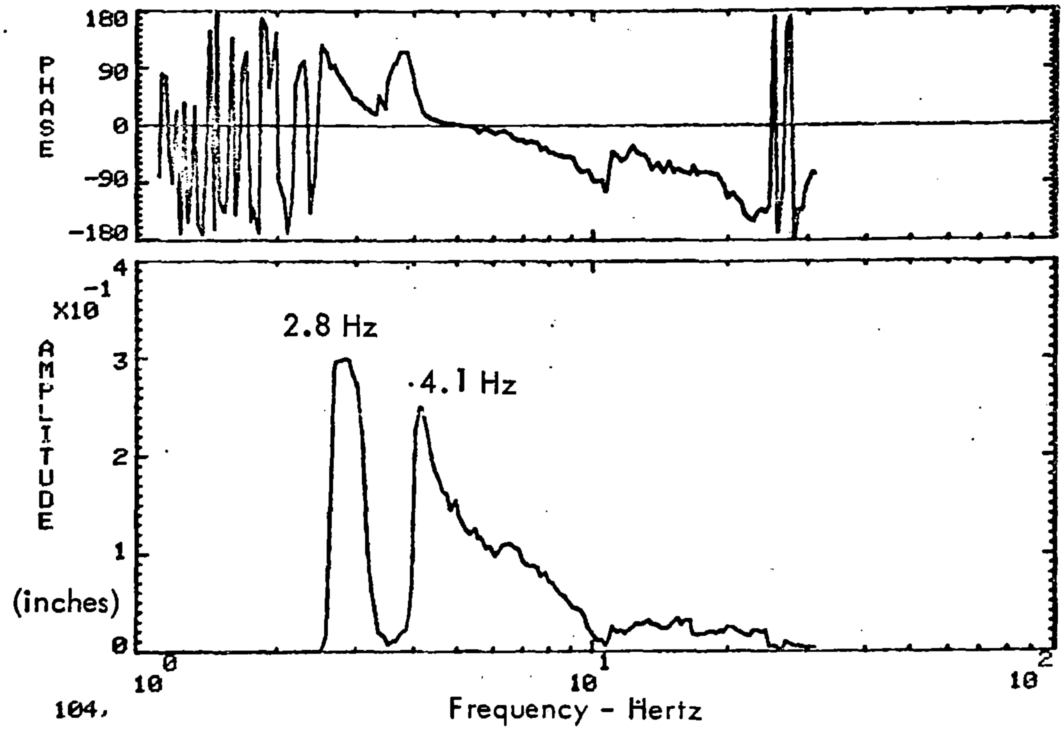

CONFIGURATION 3, HLGH LEVEL RUN, SHAKERS IN PHASE, RUN 103

(a) 104, Displacement Across Spring Group

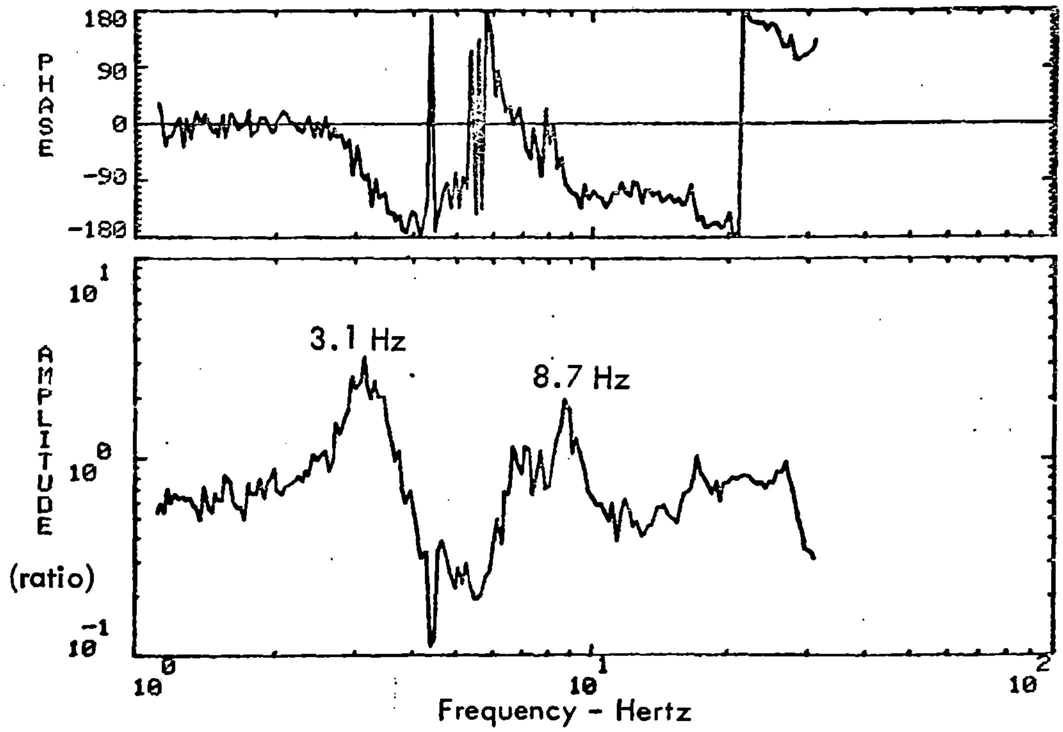

CONFIGURATION 3, HLGH LEVEL RUN, SHAKERS IN PHASE, RUN 103

(b) 89/65, Flatcar Structural Amplification

Figure 6-54. Flatcar Transfer Functions

CONFIGURATION 3

SHAKERS IN PHASE

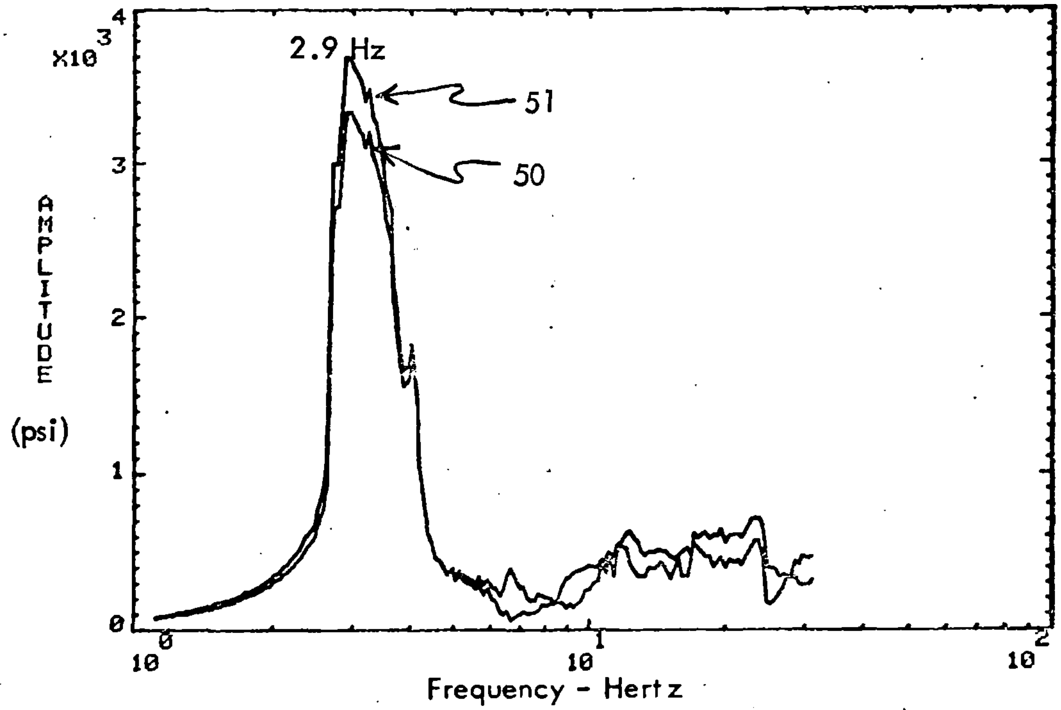

CONFIGURATION 3, HLGH LEVEL RUN, SHAKERS IN PHASE, RUN 103

(a) Stress in Flatcar Main Sill

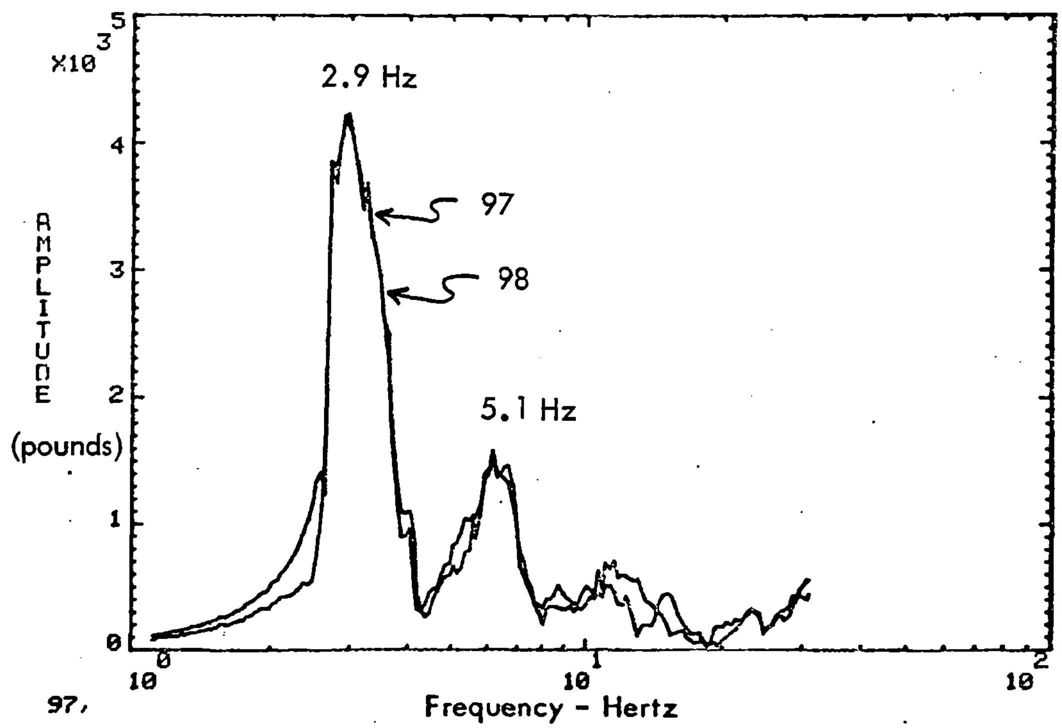

CONFIGURATION 3, HLGH LEVEL RUN, SHAKERS IN PHASE, RUN 103

(b) Tire Force Measurements

Figure 6-55. Flatcar Stress and Force Measurements

CONFIGURATION 3

SHAKERS IN PHASE

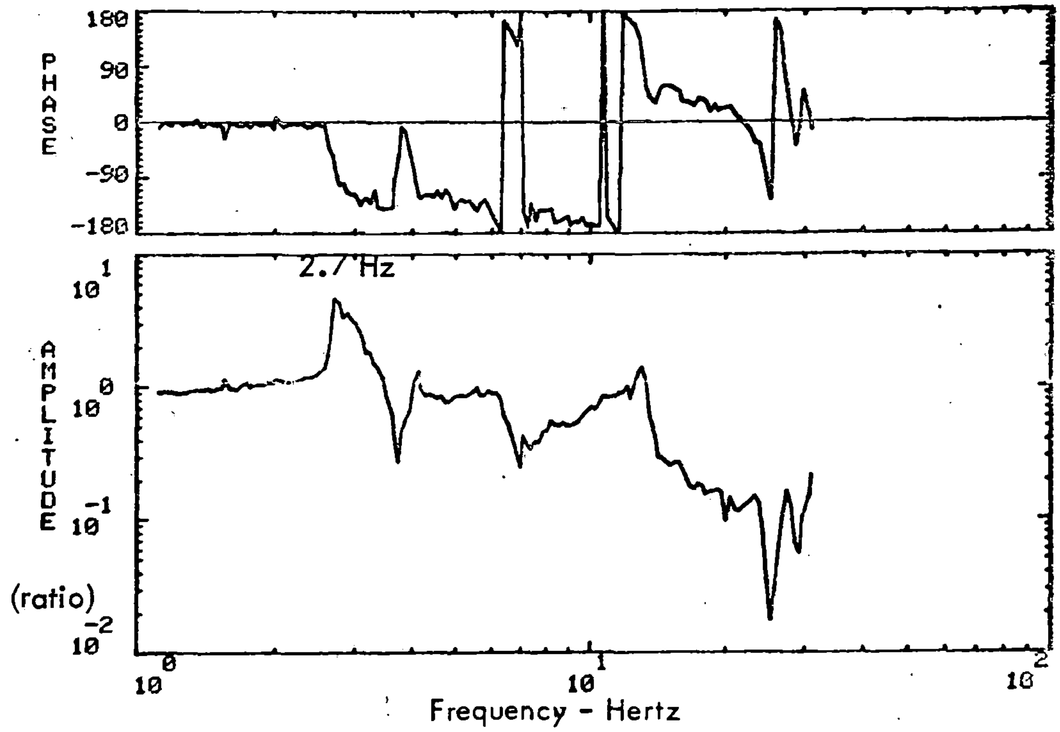

CONFIGURATION 3, HLGH LEVEL RUN, SHAKERS IN PHASE, RUN 103

(a) 81/Input, Platform Trailer Center Transfer Function

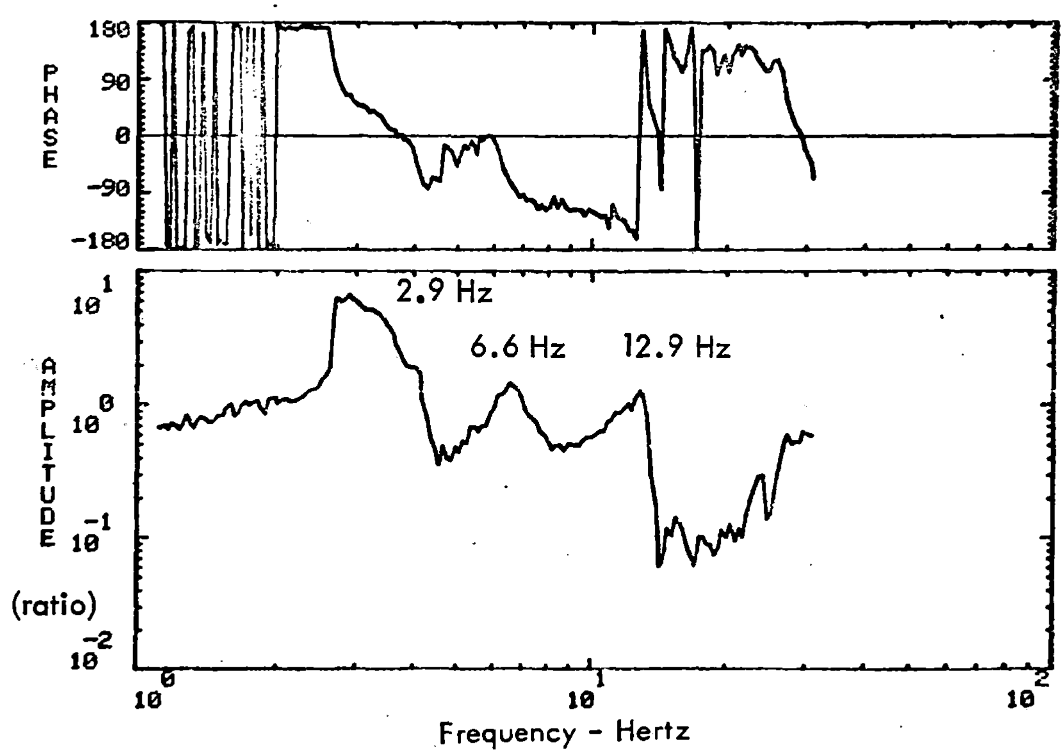

CONFIGURATION 3, HLGH LEVEL RUN, SHAKERS IN PHASE, RUN 103

(b) 128/Input, Platform Trailer Transfer Function

Figure 6-56. Platform Trailer Transfer Functions

CONFIGURATION 3

SHAKERS IN PHASE

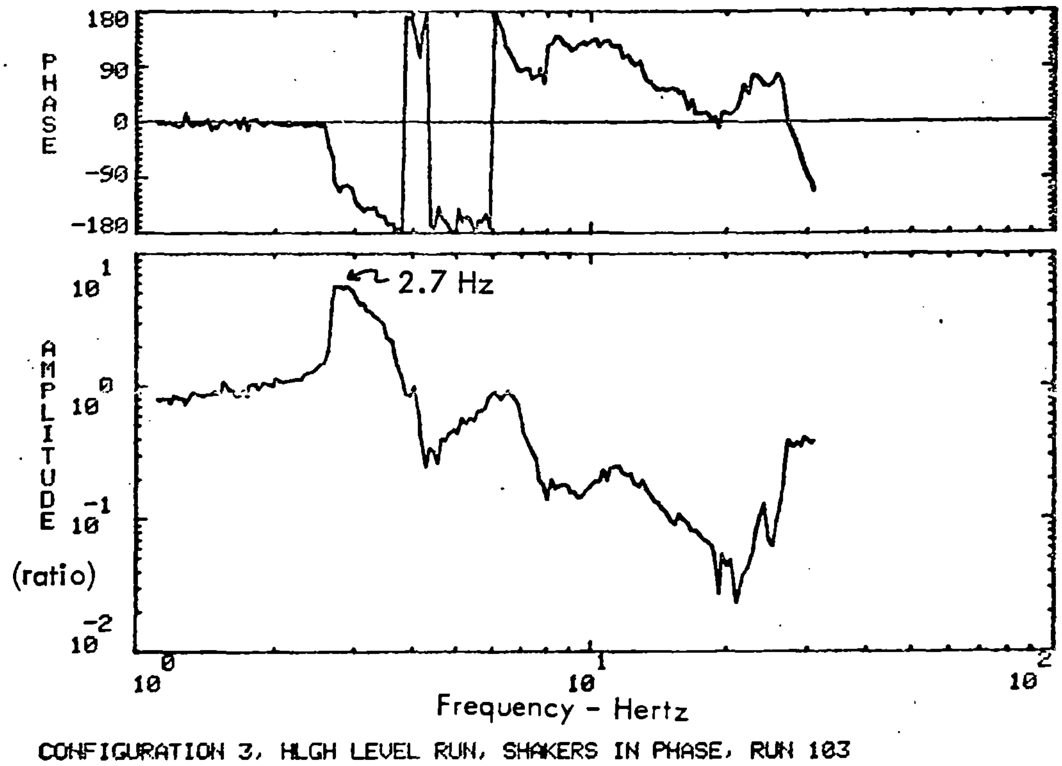

(a) 70/Input, Platform Trailer Transfer Function

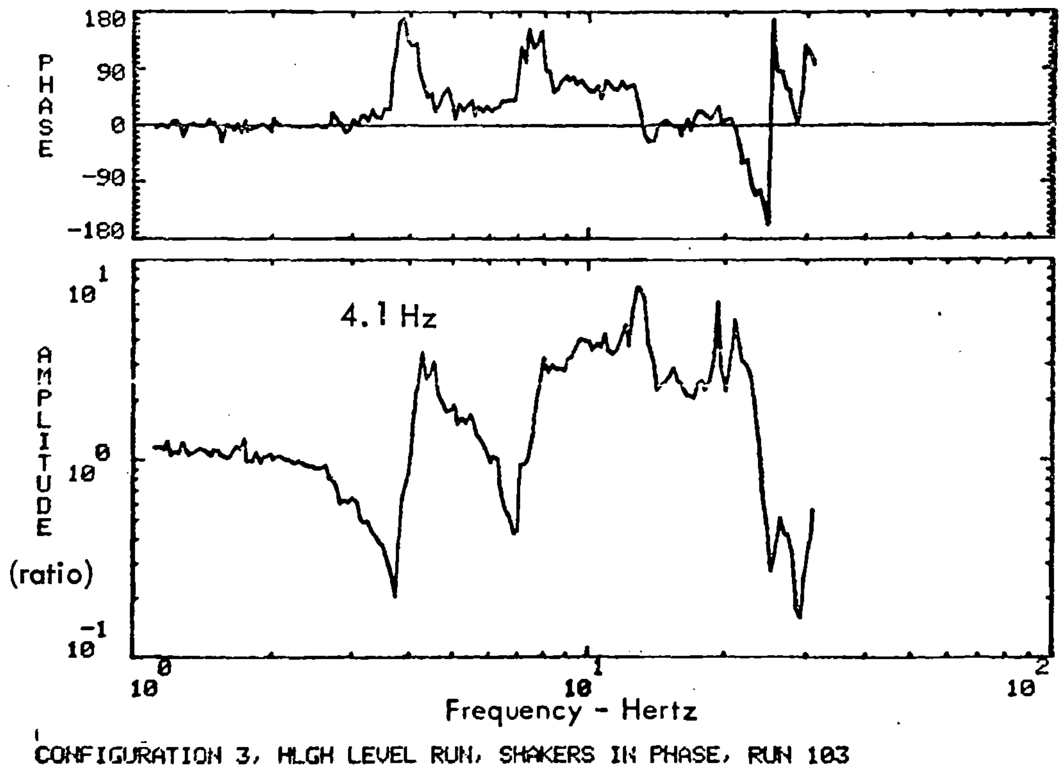

(b) 81/70, Platform Trailer Structural Amplification Factor

Figure 6-57. Platform Trailer Transfer Functions

CONFIGURATION 3

SHAKERS OUT OF PHASE

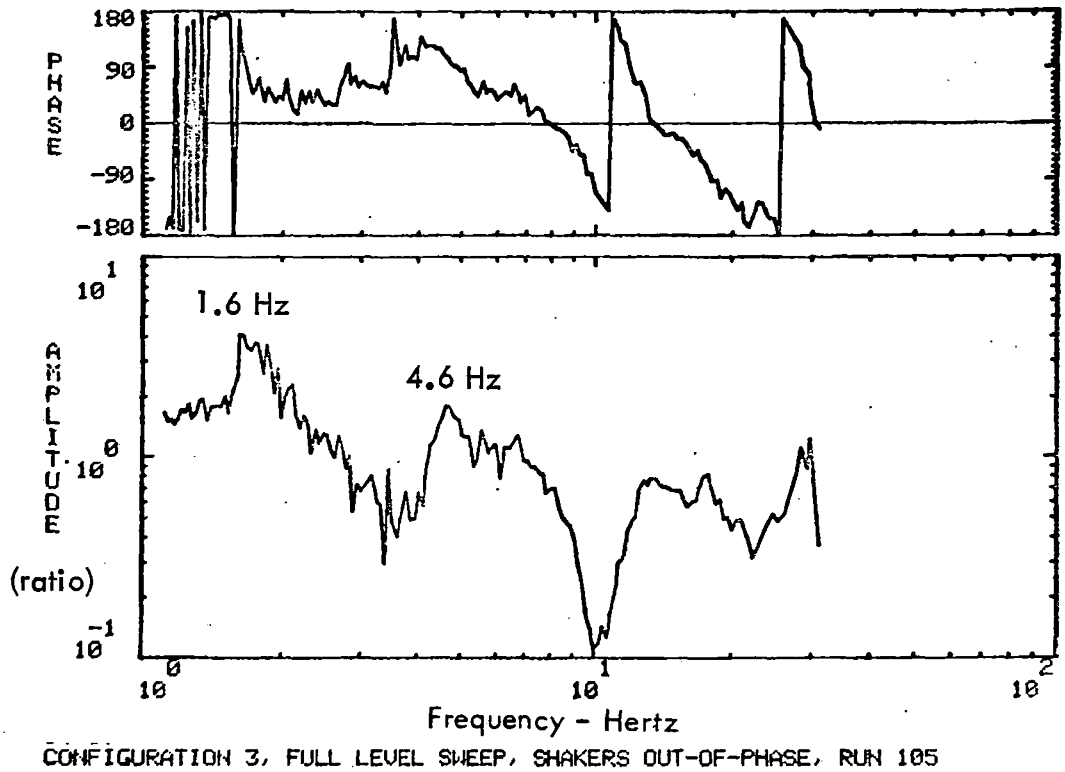

(a) 118/Input, Flatcar Transfer Function

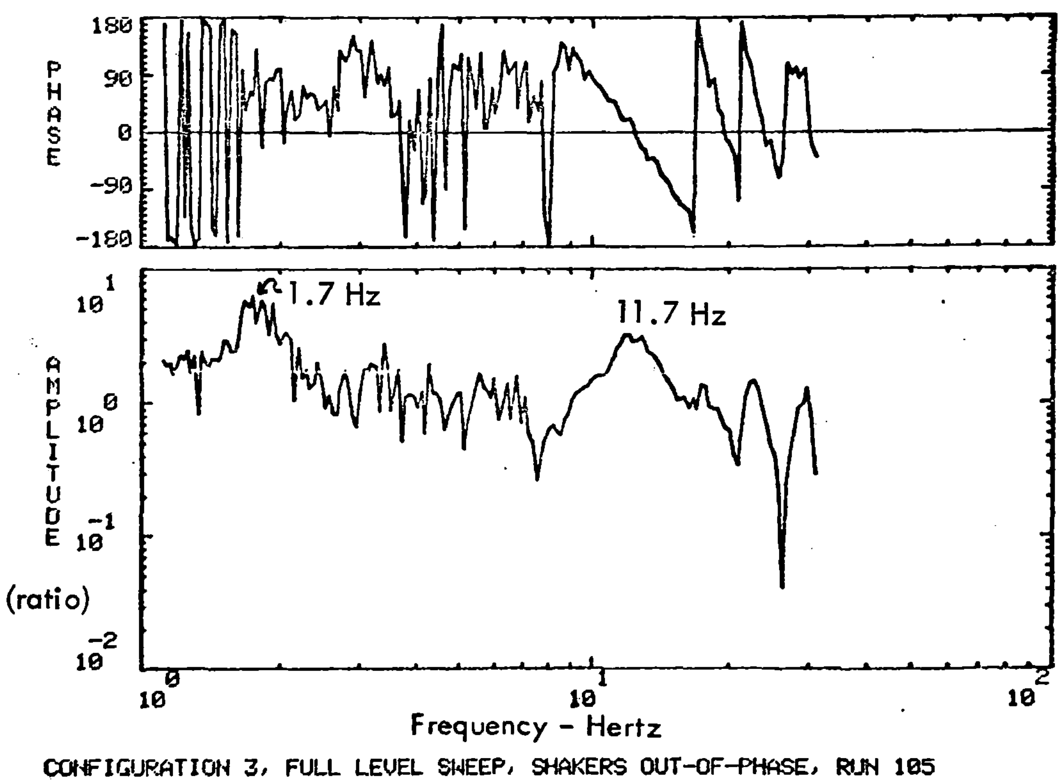

(b) 123/Input, Flatcar Transfer Function

Figure 6-58. Flatcar Transfer Function

CONFIGURATION 3

SHAKERS OUT OF PHASE

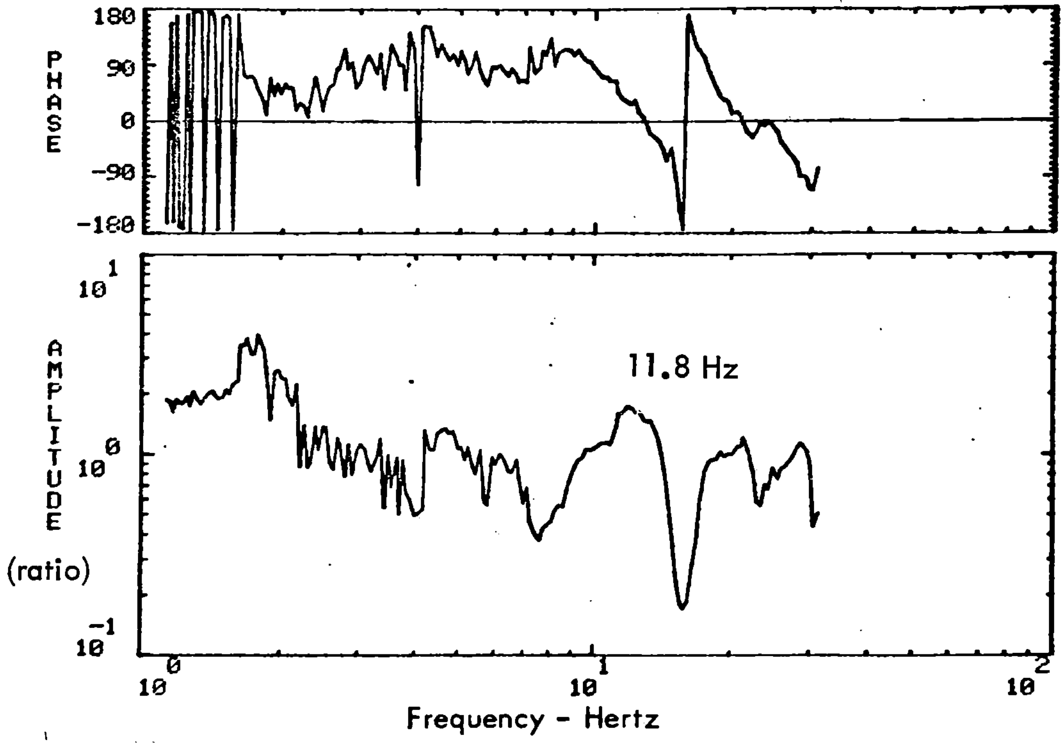

CONFIGURATION 3, FULL LEVEL SWEEP, SHAKERS OUT-OF-PHASE, RUN 105

(a) 65/Input, Flatcar Transfer Function

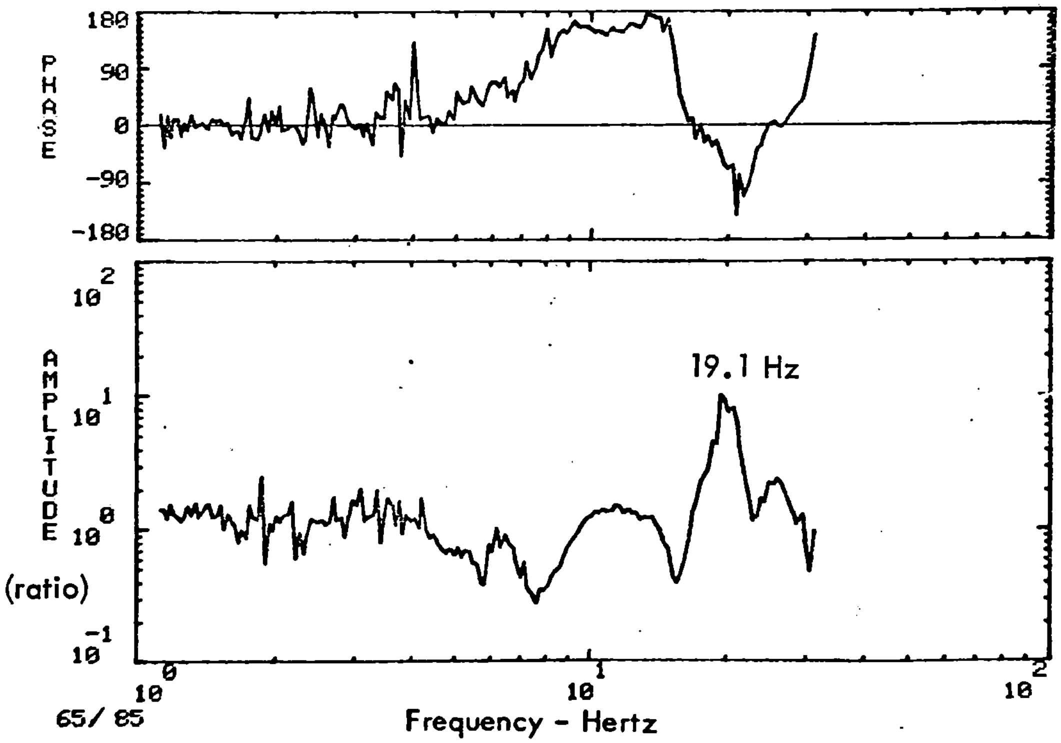

CONFIGURATION 3, FULL LEVEL SWEEP, SHAKERS OUT-OF-PHASE, RUN 105

(b) 65/85, Flatcar Torsional Transfer Function

Figure 6-59. Flatcar Transfer Function

CONFIGURATION 3

SHAKERS OUT OF PHASE

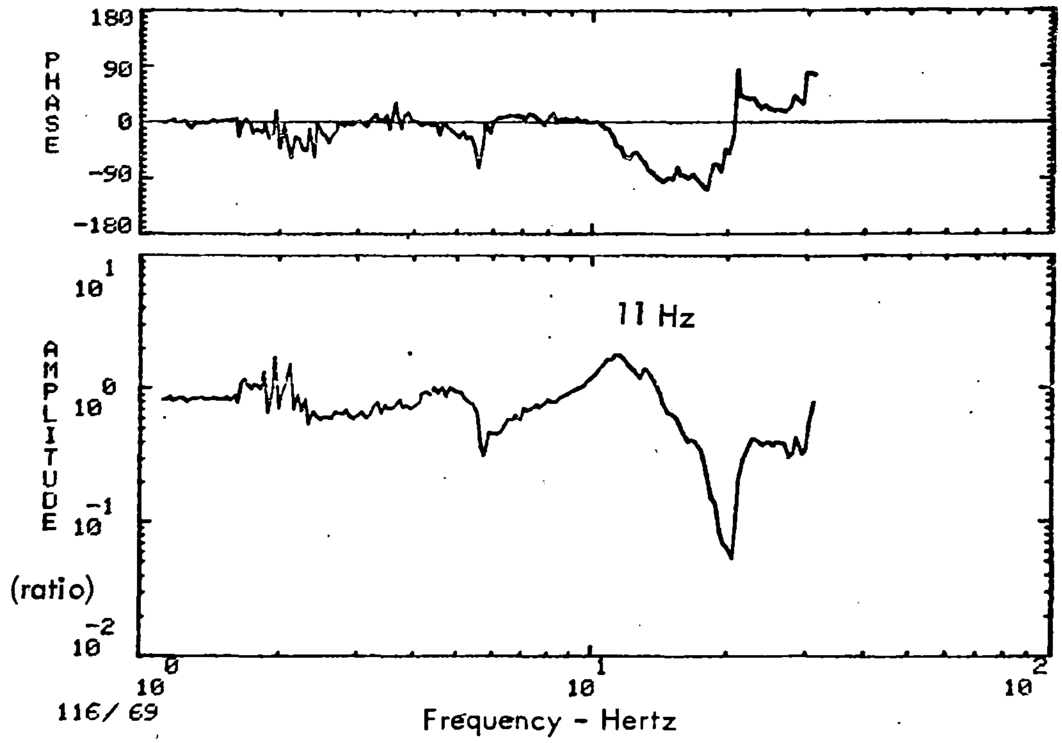

CONFIGURATION 3, FULL LEVEL SWEEP, SHAKERS OUT-OF-PHASE, RUN 105

(a) 116/69, Flatcar Lateral Structural Amplification

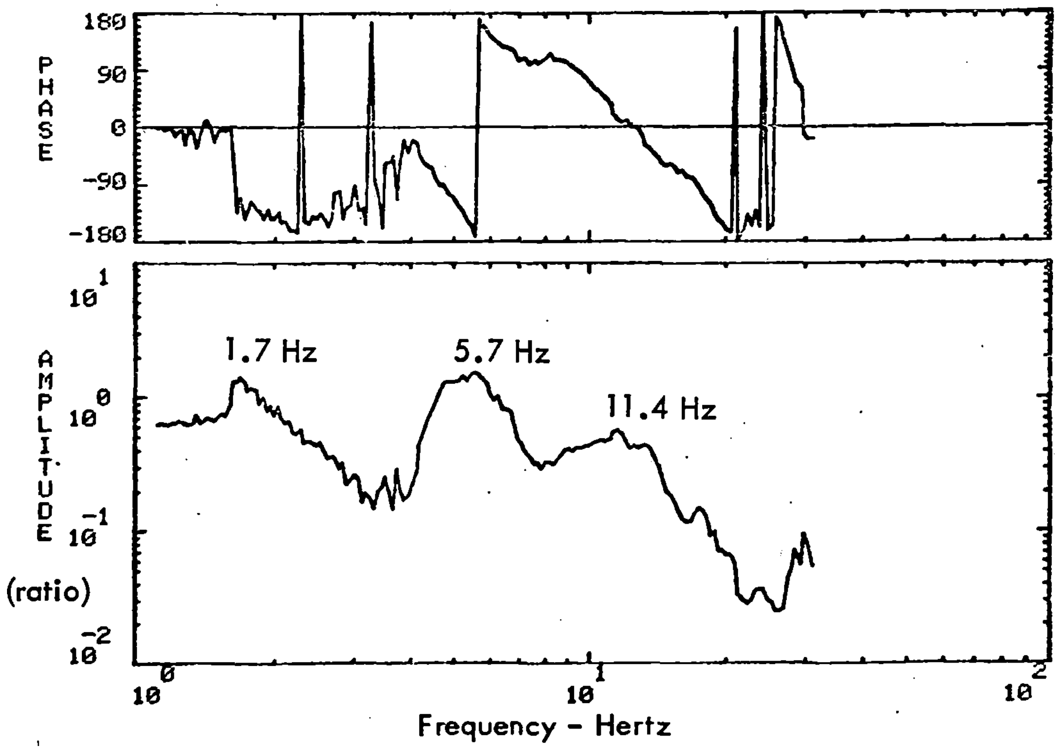

CONFIGURATION 3, FULL LEVEL SWEEP, SHAKERS OUT-OF-PHASE, RUN 105

(b) 86/Input, Flatcar Lateral Transfer Function

Figure 6-60. Flatcar Transfer Function

CONFIGURATION 3

SHAKERS OUT OF PHASE

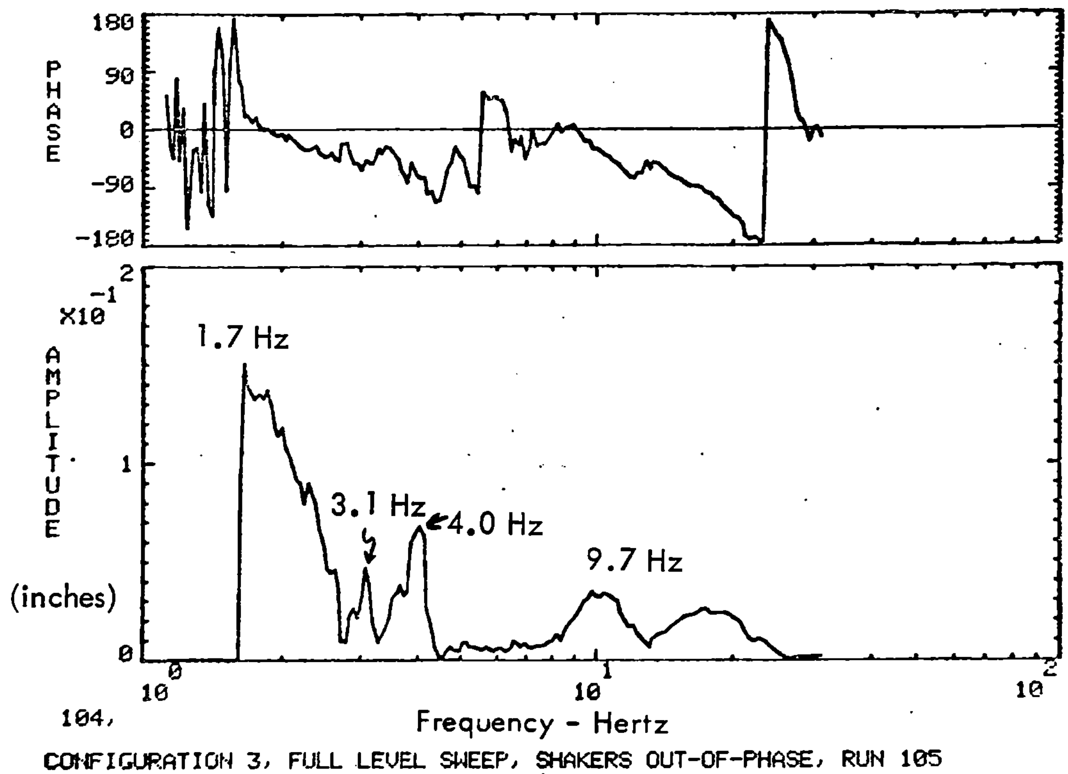

(a) 104, Spring Group Displacement

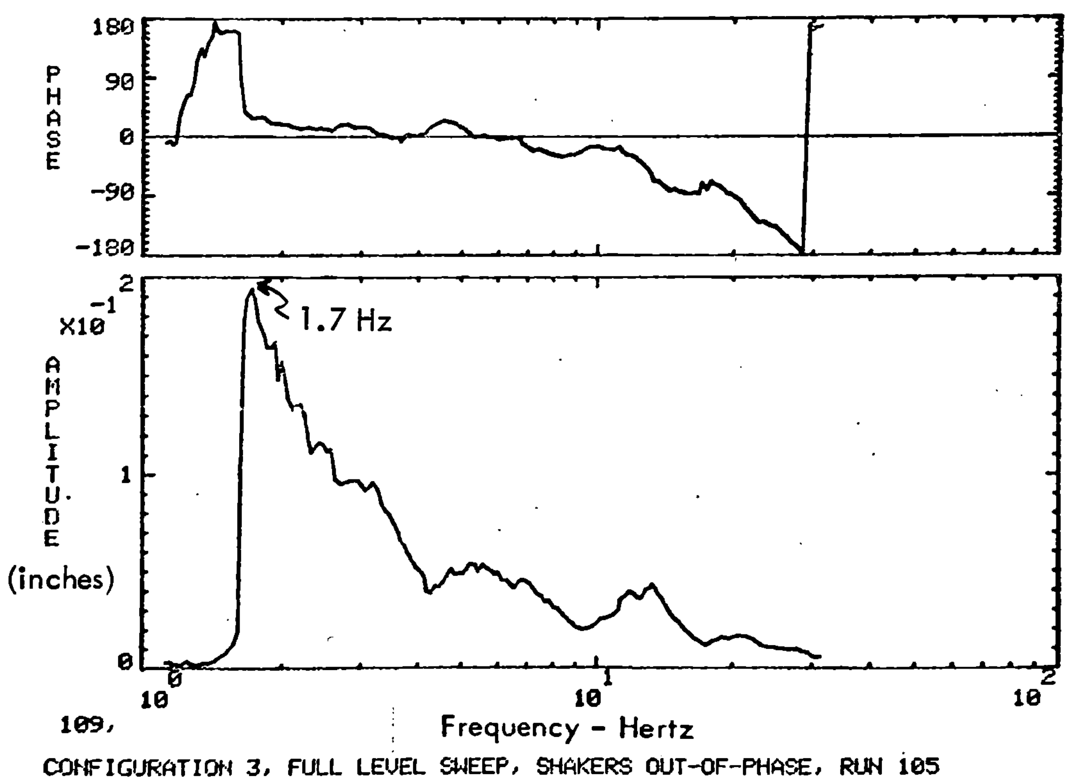

(b) Flatcar Center Plate Rocking

Figure 6-61. Flatcar Displacements

CONFIGURATION 3

SHAKERS OUT OF PHASE

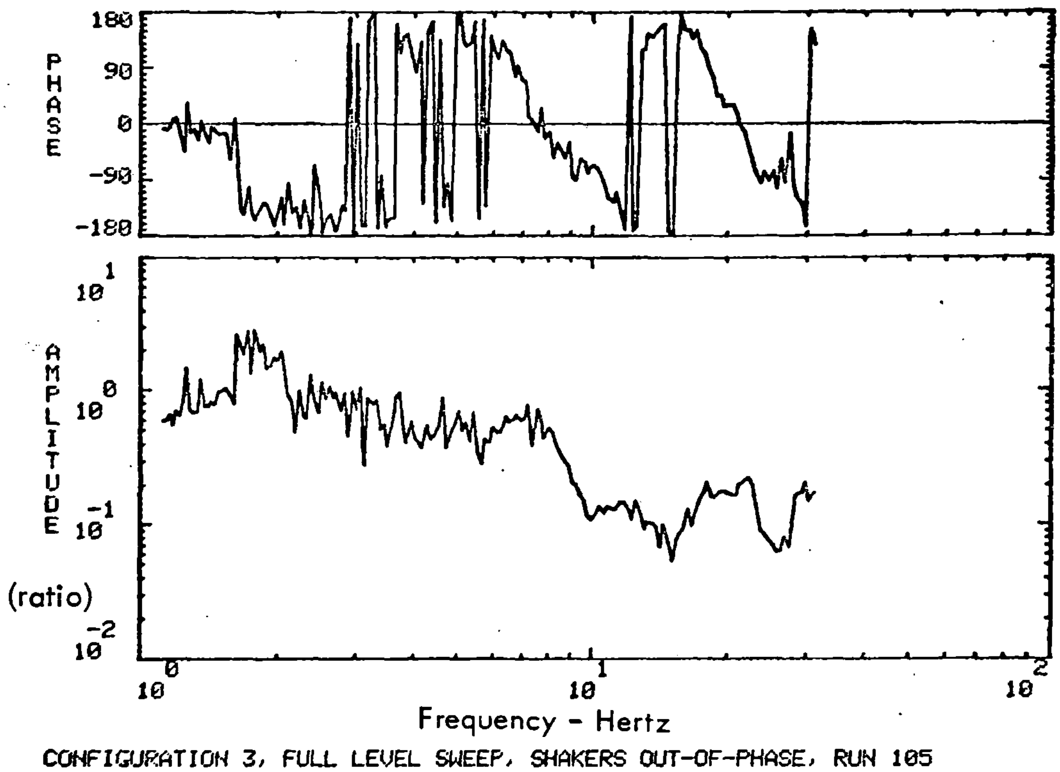

(a) 75/Input, Platform Trailer Vertical Transfer Function

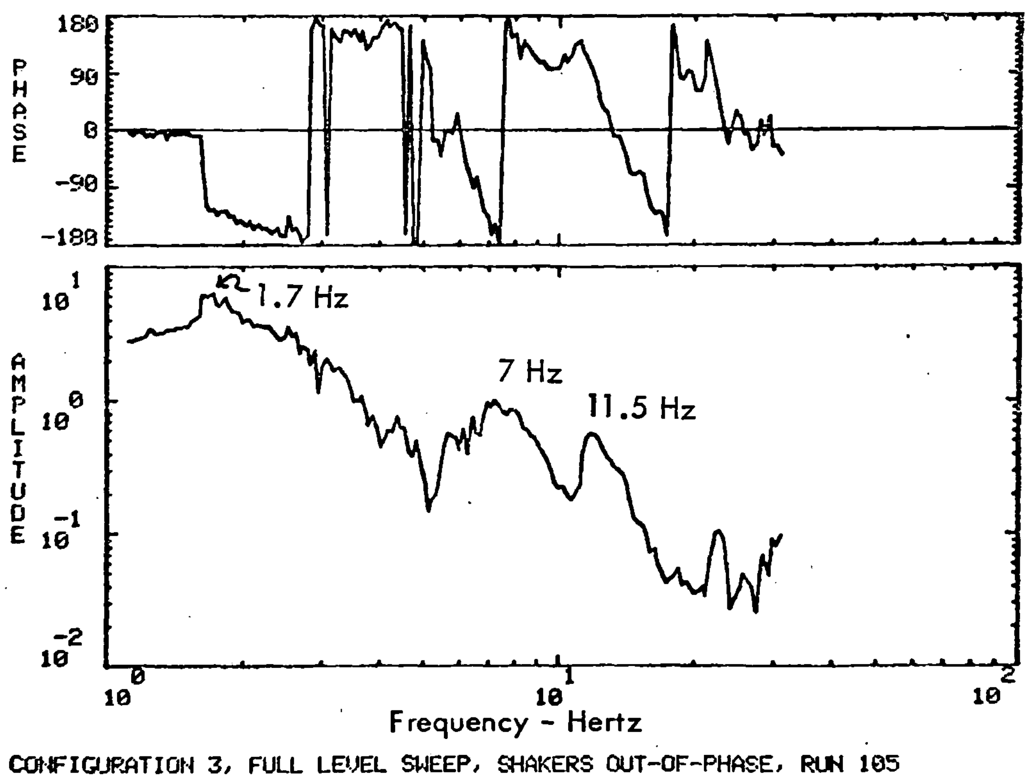

(b) 71/Input, Platform Trailer Lateral Transfer Function

Figure 6-62. Platform Trailer Transfer Function

Table 6-5. Response Frequencies, Configuration 3

Mode	Test Frequency	Analytical Prediction
Rocking	1.7 Hz	2.3 Hz
Bounce	2.8	
1st Vertical Bending	3.1	3.0 Hz
Rigid Body Pitch	4.1	
2nd Vertical Bending	8.7	10.1 Hz
Platform Trailer Bounce	5.1	4.1 Hz
Platform Trailer Bending	12.9	
1st Torsional	11.8	12.6 Hz
1st Lateral Bending	11	10.3 Hz
2nd Torsional	19.1 Hz	
3rd Vertical Bending	**	18.3

**Not identifiable

centerplate as for configuration. However, there is a considerable reduction in the rocking frequency (2.4 Hz to 1.7 Hz) with the addition of the empty platform trailer. The vertical and lateral transfer function on the empty platform trailer are shown in Figure 6-62 and have essentially the same frequencies as the flatcar.

6.4.2 Decay Responses

Due to schedule constraints it was not possible to run a full set of decay traces for configuration 3. The only decay plots available are for the strain gages shown in Figure 6-63. Configuration 3 shows the same tendency as configuration 1 to decay at its first bending frequency. However, the damping is much more than for configuration 1 (approximately 1.2% versus 0.5%).

6.4.3 Frequency Domain Responses

The comparisons between analysis and measured data for configuration 3 are shown in Figures 6-64 to 6-66. As for configuration 2, because of time limitations, no attempt was made to modify the model (as was done for configuration 1) based on the test data. The analytical predictions show good agreement with the test data.

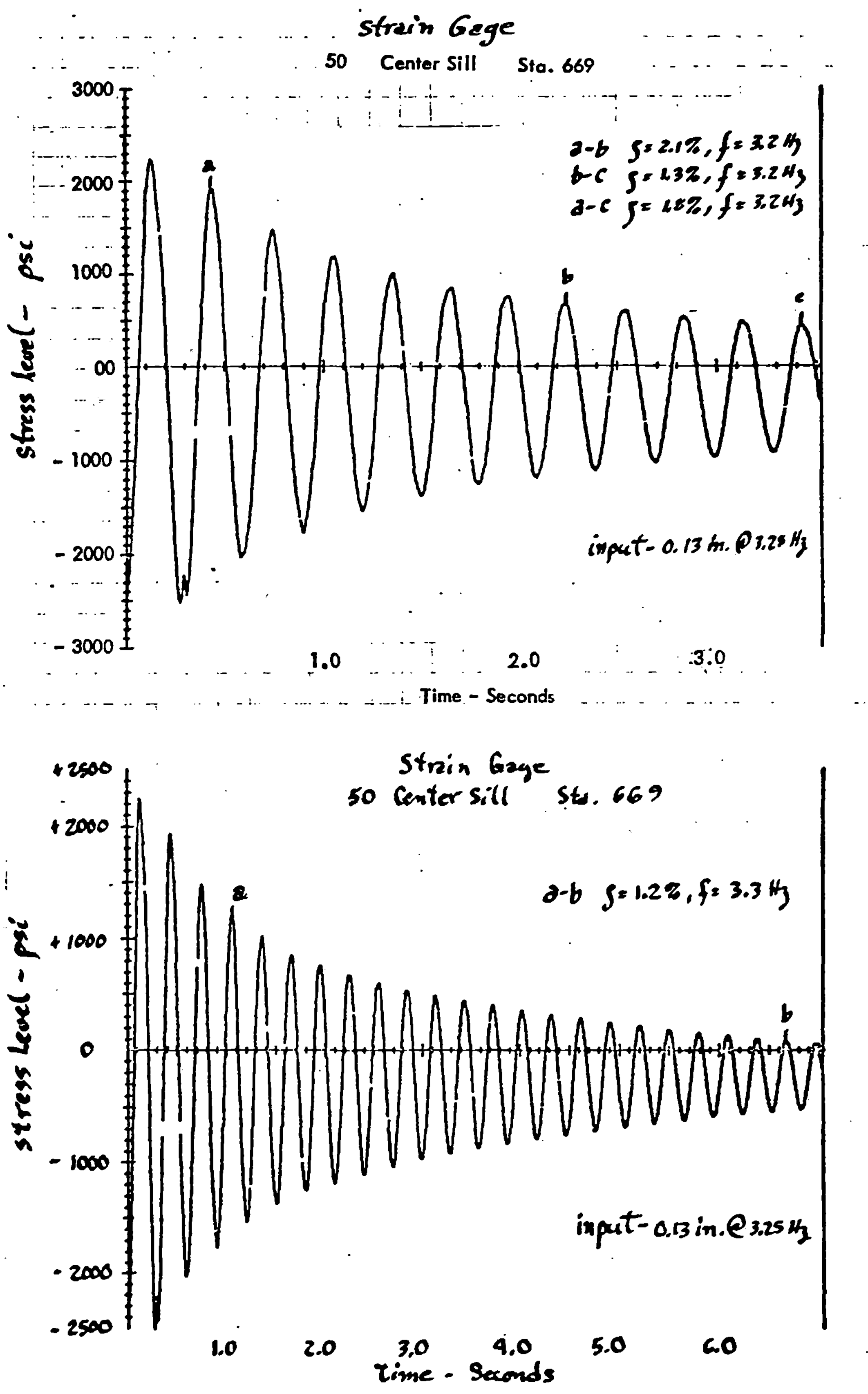

Figure 6-63. Configuration 3 Damping Data

CONFIGURATION 3

SHAKERS IN PHASE

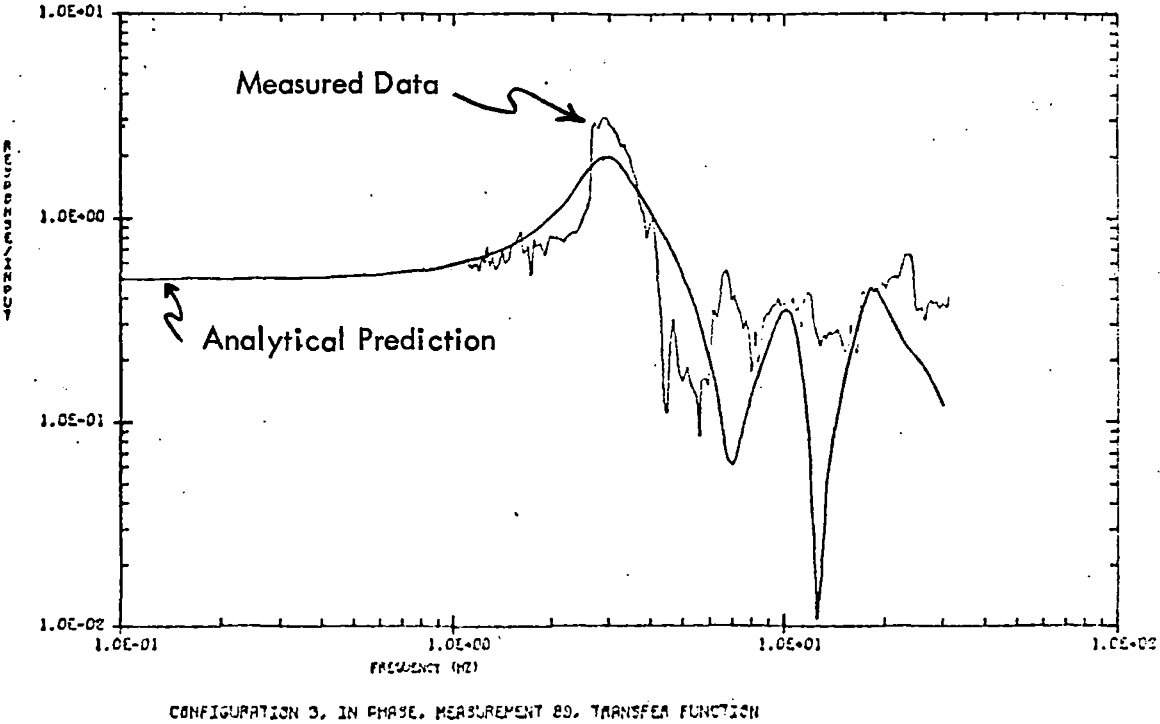

(a) 89/Input, Flatcar Transfer Function

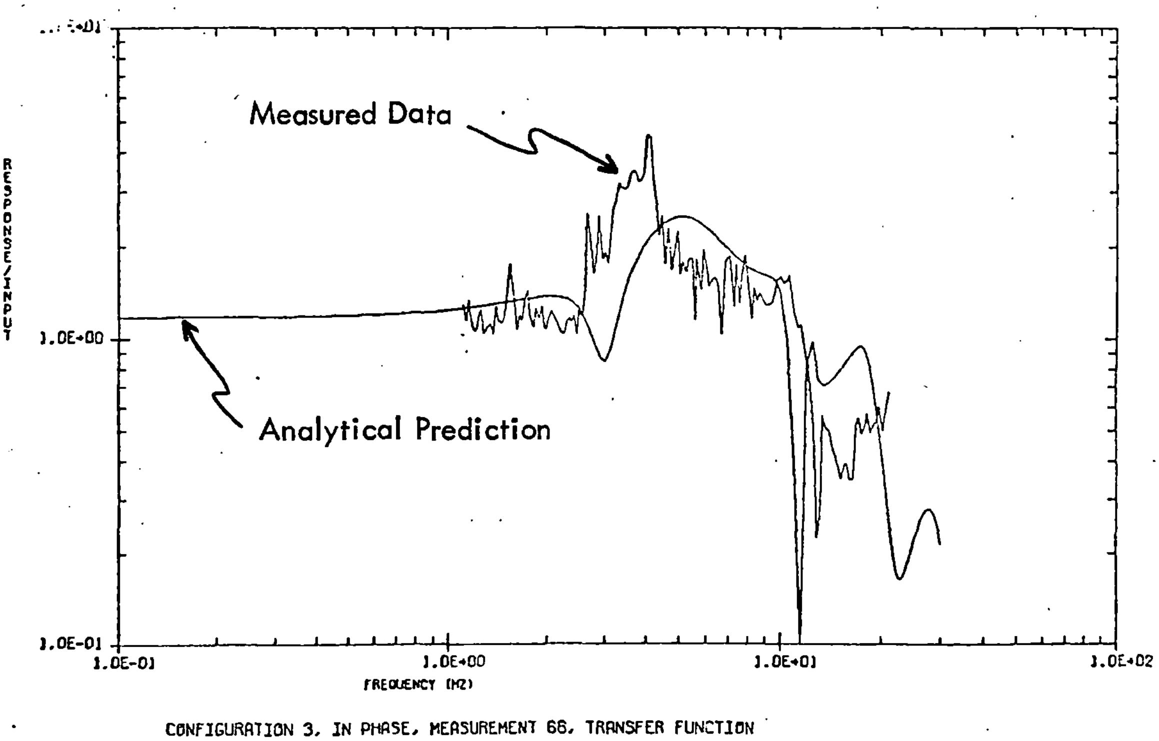

(b) 66/Input, Flatcar Transfer Function

Figure 6-64. Comparison of Measured and Analytical

CONFIGURATION 3
SHAKERS IN PHASE

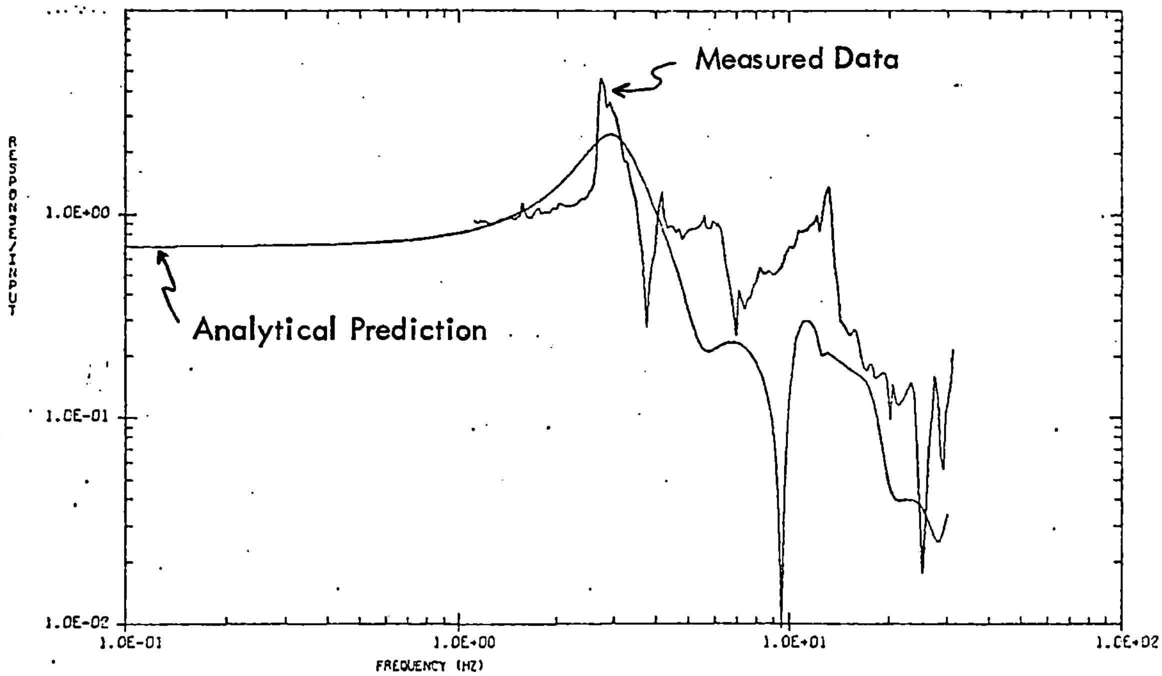

CONFIGURATION 3. IN PHASE. MEASUREMENT 81. TRANSFER FUNCTION

(a) 81/Input, Platform Trailer Transfer Function

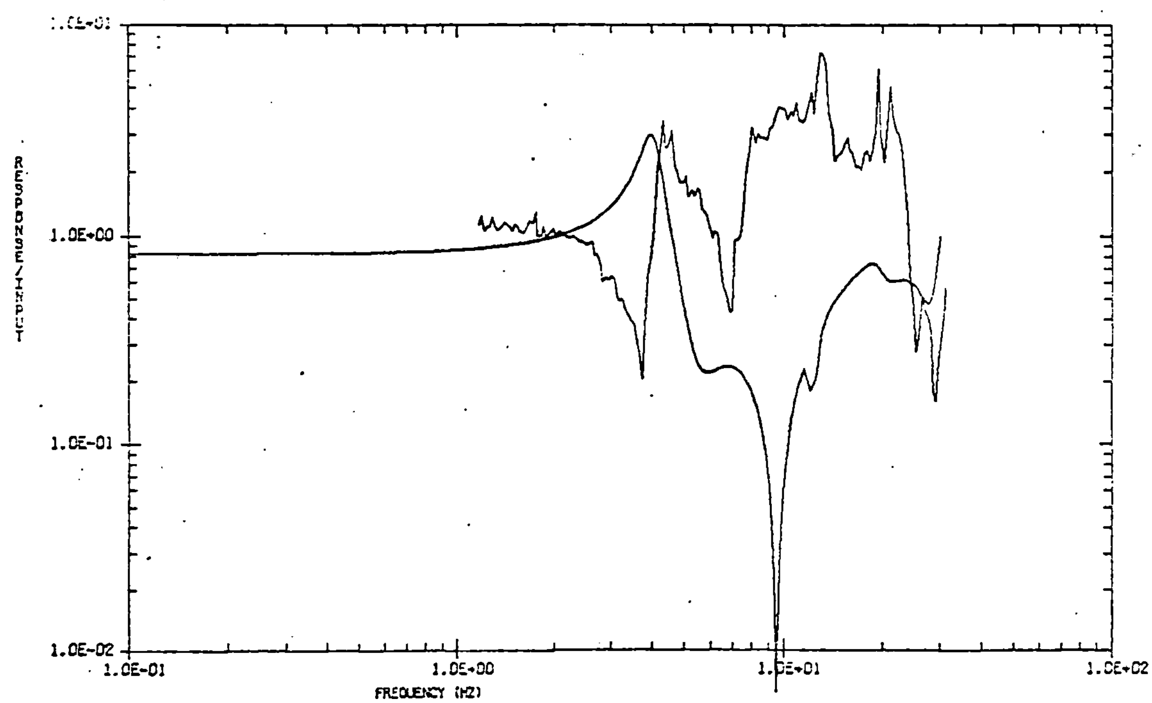

CONFIGURATION 3. IN PHASE. MEASUREMENT 81/70. TRANSFER FUNCTION

(b) 81/70, Platform Trailer Structural Amplification

Figure 6-65. Comparison of Measured and Analytical

CONFIGURATION 3

SHAKERS OUT OF PHASE

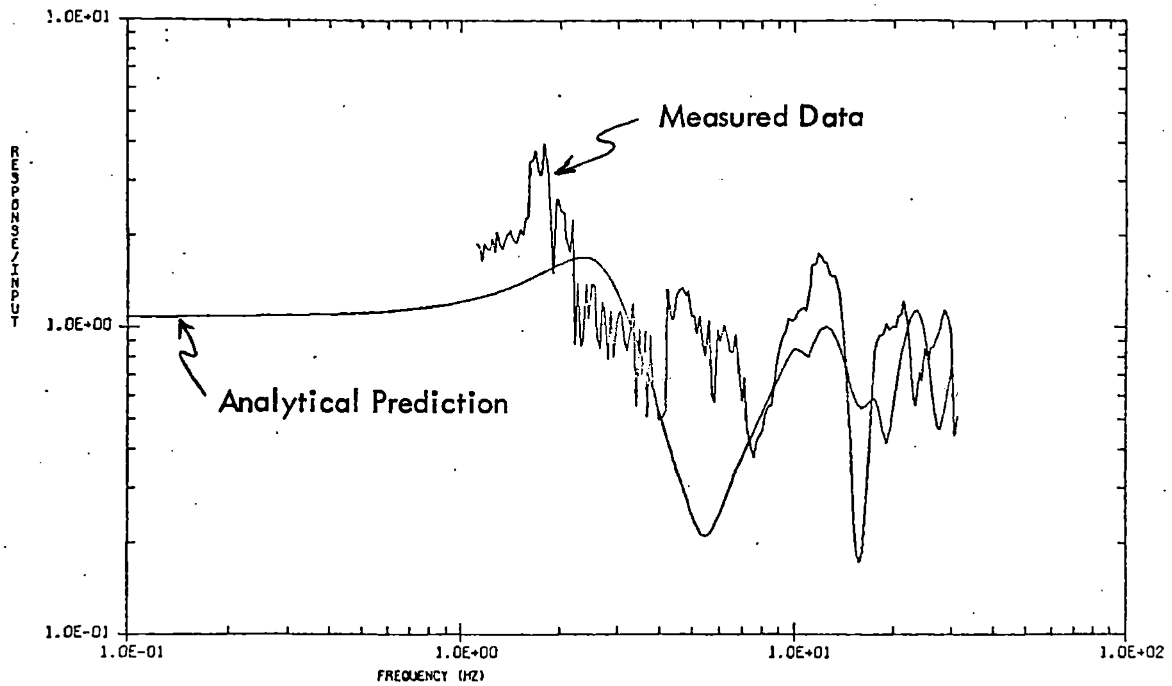

CONFIGURATION 3, OUT-OF-PHASE, MEASUREMENT 65, TRANSFER FUNCTION

(a) 65/Input, Flatcar Transfer Function

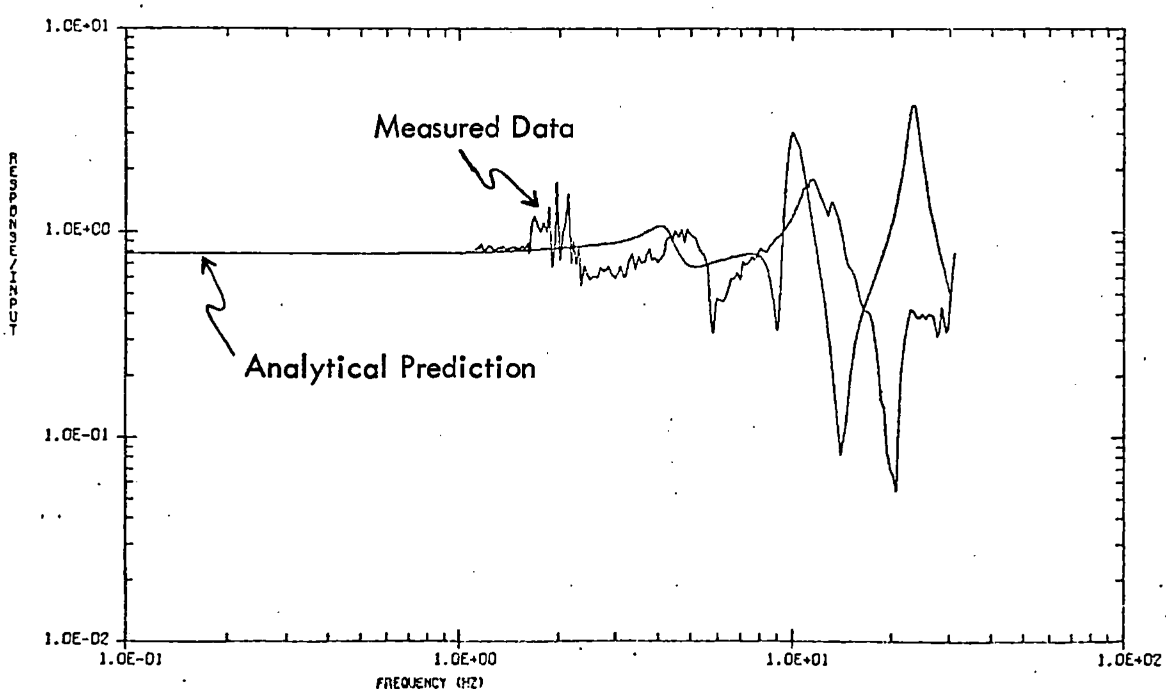

CONFIGURATION 3, OUT-OF-PHASE, MEASUREMENT 116/69, TRANSFER FUNCTION

(b) 116/69, Flatcar Lateral Amplification Factor

Figure 6-66. Comparison of Measured and Analytical

SECTION 7 - NONLINEAR PROGRAM DEVELOPMENT

7.1 ASSUMPTIONS AND LIMITATIONS

There are two types of assumptions and limitations associated with programs of this nature. The first deals with amplitude limits and poses the question: Given a specific vehicle, what are the ranges of amplitudes, frequencies, and other conditions over which reasonable simulation accuracy can be maintained? The second deals with the question: Given a program which has been written and validated for a specific vehicle, what range of vehicles can be simulated without major modifications (other than simple changes in coefficients) in the program? While these questions are interrelated to some degree, the distinction between them should not be confused.

7.1.1 Assumptions for a Specific Vehicle

There is no computer program which can predict all dynamic responses of a given math model for all conceivable conditions. However, most of the time we are concerned only with certain specific responses under a fairly narrow range of conditions. For example, we are rarely concerned with roll angles over 10 degrees Single Amplitude (20 degrees peak-to-peak), because derailment has usually occurred by the time such a large displacement is achieved.

Reference 8 discusses the assumptions and limitations of the program in detail. To summarize, however, the primary limitations are the following:

a. Choice of Degrees of Freedom. The car body has five degrees of freedom, ignoring only longitudinal translation. However, each truck mass has only three degrees of freedom. Thus, reactions associated with longitudinal, pitching, and yawing motions of the truck are ignored. The height of the car is assumed to be large relative to the height of the truck; however, a judicious selection of vehicle coefficients can compensate for this if a vehicle of small height such as a flatcar is considered.

b. Small Amplitudes. The motion of the vehicle is restricted to fairly small amplitudes. However, the assumption is less stringent than the "small angle assumptions" that are often used which limit angular deflections to less than 5 degrees. In this analysis, first order trigonometric functions are used; only second order effects are ignored.

On the basis of the validation described elsewhere in this report, it appears that the analysis is valid until roll angles exceed about 10 degrees single amplitude. The angular approximations for body yaw and pitch motions are similar, but these limits are far higher than would ever be seen in practice.

If nonlinear characteristics describing spring bottoming and separations are included in the coefficient descriptions, there is no practical limit on vertical motions. Validity of the simulation after wheel liftoff due to large rocking motions has been demonstrated as long as the roll angle limits mentioned above are not exceeded. The use of linear coefficients would invalidate simulations after spring bottoming has occurred.

If proper nonlinear lateral coefficients are given to the program, lateral excursions up to, but not greatly exceeding, flange contact can be simulated. The use of linear coefficients would restrict valid simulations to excursions where wheel/rail slippage is not involved.

c. Detailed Forces and Deflections Within Trucks. The 11 dof model will provide forces transmitted by the truck to rail and car body, but it cannot predict forces and relative motions between internal truck components. Use of the 17 dof model, Version 2, can simulate centerplate rocking conditions and associated forces as well as side bearing roller forces and specific spring nest forces. If more detailed internal truck reactions such as relative deflections between side frames and axles are required, use of a program like the Stucki program is suggested.

d. Normal Mode Assumptions. For a specific application, the flexible characteristics of the vehicle and resulting normal mode data can be as detailed as desired. Proper specification of these modes could permit analysis of inputs to the lading or could describe the interaction between a flexible lading and the vehicle structure if desired. Normally, however, assumptions will be made in the derivation of these flexible characteristics themselves. Assumptions and limitations related to vehicle and lading flexibility will be made by the user in defining and calculating the mode shapes for his specific vehicle; no inherent limitations in the program itself exist.

e. Coulomb Damping. If coulomb damping is used in the trucks, certain problems can occur when a very light vehicle is being simulated or if very small motions are occurring in the spring nests. This is discussed in some detail in Appendix D.

These problems occur to some degree in all response programs that use numerical integration methods for systems including coulomb damping even if their existence is not recognized. Several methods do exist for minimizing the effect. Further evaluation of these methods by the author is planned.

f. **Coefficients.** Coefficients independent of the math model are used to characterize the elements of the model for the specific vehicle under consideration. The use of any given coefficient always implies an assumption or limitation in the simulation, and the validity of any simulation is no better than the descriptive coefficients being used. It is up to the user of any response program to recognize the assumptions and limitations in the coefficients being used.

7.1.2 Limitations on Vehicles

No single math model can be said to apply to all possible vehicles. In the validation process, the models described have been shown to be applicable to such diverse vehicles as a rigid 100-ton hopper car loaded with coal and a more flexible unloaded 89 foot 4 inch flatcar. It may be reasonably inferred that the model can be applied to vehicles similar to these and to a wide range of vehicles in between. Further studies are suggested to determine any limitations on choice of vehicles. Until these studies are performed, we may only say that these models are applicable to a far wider range of vehicle types than is a dynamic response program which does not use the normal mode approach to calculate vehicle flexibility.

One example of a vehicle to which the model cannot be applied without modification is the loaded trailer on flatcar configuration. It cannot be applied to this configuration directly because of the many highly significant and interactive nonlinearities between the flatcar and trailers (i.e. within the vehicle structure) in this case. However, the program can be modified for this type of vehicle, and Reference 7 discusses those modifications and the resulting program.

7.2 METHODS OF SOLUTION

It is presupposed that rail vehicles are highly nonlinear and that any reasonable predictions of dynamic responses can only be generated with nonlinear programs. The method used involves numerical integration of the differential equations of motion. In contrast to the normal use of Lagrangian or energy methods for deriving these differential equations of motion, the Newtonian method for deriving these equations was used instead. Use of the Newtonian method implies a great reduction in complexity of the program and in programming costs. Conversely, it implies that the program will be applicable to a certain range of displacements. For example, in roll motions it is felt that accuracy will begin to degrade as roll motions exceed about 10 degree single amplitude. This is not expected to present a problem because larger roll motions are rarely, if ever, encountered in rail applications unless derailment occurs. The program is accurate to much larger displacements in the other modes. Reference 2 provides a detailed discussion of the methods that were available for solution, and gives more detail on the reasons for the choice of the Newtonian method.

The flexibility of the car is taken into account by the technique of superposition of normal modes. Reference 1 provides a discussion of this topic.

7.2.1 Theory of Normal Modes

It is possible to characterize a linear system in terms of its normal modes. A system with n degrees of freedom will have n natural frequencies and n mode shapes which characterize the behavior of the system. The normal mode method is characterized by the fact that the differential equations of motion are decoupled when the displacements are expressed in terms of the normal modes. Thus the system is broken down into n independent differential equations rather than a system of n simultaneous differential equations. By characterizing the system as a finite number of lumped masses, it is possible to write the differential equations of motion in matrix form:

$$M \{\ddot{x}\} + C \{\dot{x}\} + K \{x\} = 0$$

where x_i is the displacement at the ith degree of freedom. The eigenvectors of the matrix $[[M]^{-1}[K]]$ uncouple the system of equations. Let $[\phi]$ be a matrix whose columns are the eigenvectors of $[[M]^{-1}[K]]$ and define the vector η by $\{x\} = [\phi]\{\eta\}$

then the uncoupled differential equation may be written:

$$\left[\diagdown MM \diagdown\right]\{\ddot{\eta}\} + \left[\diagdown MC \diagdown\right]\{\dot{\eta}\} + \left[\diagdown MK \diagdown\right]\{\eta\} = 0$$

This results in n uncoupled differential equations with natural frequencies:

$$\omega_i = \sqrt{\frac{K_i}{M_i}}$$

The above formulation is easily handled on today's large digital computers for systems with a large number of lumped masses. Thus for a linear structure it is possible to break it down into a number of lumped masses and let the computer take care of the solution for frequencies and normal modes.

7.2.2 Superposition of Normal Modes

One advantage of the normal mode method is that the work involved in calculating the mode shapes and frequencies need be performed only once for each vehicle. A second advantage is that it is possible to selectively choose those modes which are significant to a given problem, thus taking into account the effects of a great deal of system complexity while solving only a handful of differential equations. The disadvantage of the normal mode method is that it can be applied only to regions of a model which can be considered linear and lightly damped.

Many rail vehicles themselves have structures that are quite linear, while the nonlinearities are concentrated in the trucks and perhaps in the lading. The linear portions of the model are handled by normal mode techniques while the balance of the model is handled by nonlinear techniques. In these calculations an interface is drawn between the linear and nonlinear portions of the model, and the forces across the interface are considered external force inputs to the linear portions of the model. The same concepts are applied when one portion of the model has high damping while in another portion the damping is low enough for normal mode methods to apply. Those portions of the model in which nonlinearities or high damping exist are broken down into lumped masses, and their differential equations of motion are solved directly.

7.3 TREATMENT OF NONLINEARITIES

One advantage of the method used in this approach is the ease with which nonlinearities may be handled. Two common types of nonlinearities are nonlinear forces in the elements connecting the lumped masses and nonlinear inputs to the system. Other types of nonlinearities can be handled by the program without difficulty, but these are the most frequently encountered.

7.3.1 Nonlinear Forces

The computer program described in this report is valid whether forces are linear or nonlinear. However, since rail vehicles tend to have highly nonlinear characteristics, accuracy and ranges of validity are greatly enhanced if the nonlinear elements of the vehicle are described without linear approximations.

In order to avoid the need for different programs to accomplish similar functions, the point of view taken here is that nonlinear forcing elements can be described in terms of nonlinear coefficients. The term "coefficient" then is not taken in the ordinary sense of a single parameter (e.g. a spring constant), but is taken to be a complete definition of the force versus displacement (or force versus velocity, or force versus any other response parameter) history. Nonlinear forces are then described in terms of nonlinear coefficient histories to the computer.

Reference to the listing in Appendix A shows that all forces are calculated first in terms of the ordinary linear relationship (loop 701):

$$F_i = K_i \text{ (relative displacement)} + C_i \text{ (relative velocity)}$$

For example, the force F_i is defined as:

$$F_1 = K_1 (Z_1 - Z_2) + C_1 (Z_1 - Z_2)$$

If substitution of a nonlinear expression is desired instead, one only needs to put in the desired expression after loop 701. Virtually any expression that uniquely defines the force may be used.

For example, if the force is partially a function of the relative displacement squared, the expression:

$$F_1 = C_1 (Z_1 - Z_2) + K_1 (Z_1 - Z_2) + K_1 (Z_1 - Z_2)^2$$

may be used. If the force is partially a function of the higher powers of the relative velocity,

$$F_1 = C_1\ (Z_1\ \ Z_2) + C_1\ (Z_1\ \ Z_2)^2\ +\ C_1\ (Z_1\ \ Z_2)^3 + K_1\ (Z_1\ \ Z_2)$$

is perfectly acceptable. If coulomb (slip-stick) friction is a factor, the expression might take the form:

$$F_1 = C_1\ (Z_1\ \ Z_2) + K_1\ (Z_1\ \ Z_2) + \mathrm{SIGN}\ (K_c, (Z_1\ \ Z_2)\ )$$

In this expression, the term SIGN (K_c, (Z_1 - Z_2)) is a FORTRAN expression which is evaluated as zero if (Z_1 - Z_2) is positive, and a constant - K_c if (Z_1 - Z_2) is negative. This is recognized as the form of the idealized coulomb friction force as a function of the relative velocity. (Other forms of this expression are often seen.)

A particularly useful technique involves a table look up routine to define a force. For example, if a mechanical stop is present in the vertical suspension, a graph of force versus relative displacement might look like this:

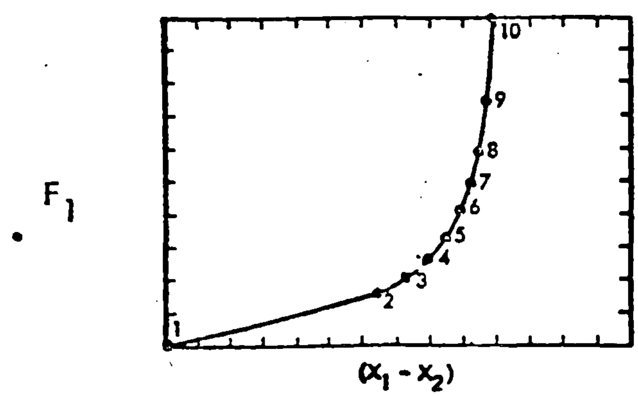

Simple routines are available which read in selected table values, such as the ten points noted in the figure, and direct the computer to connect the points by straight-line segments. When the computer needs a value for F_1, it can interpolate for the value corresponding to any (X_1 - X_2).

Naturally, any combination of the examples may be used. A more general statement of the situation is that

$$F_1 = \text{Any computer-generated function}$$

may be used. Only two exceptions to the above are known to the author, and they are not expected to present any problems in the case of rail dynamics calculations. They are:

a. The value for the force must be uniquely or singularly defined at all times. If, in the figure, two values of F_1 were possible for a single value of $(X_1 - X_2)$, difficulties should be expected unless the computer was told which to choose.

b. The values of the forces should not be defined in terms of certain inertia forces. If, for example, F_1 were defined as a function of vertical acceleration Z_1, then that definition together with the expression for Z_1 would be telling the computer that:

$$Z_1 = f\,(Z_1)$$

Such an expression would lead to serious difficulties in achieving convergence. However, such an expression, if encountered, could be modified to a more valid form.

7.3.2 Nonlinear Inputs

The usual input for a rail vehicle dynamics study performed in the time domain is a time history of accelerations, velocities, or displacements at the rail/wheel interface. While inputs can be defined as sinusoids, they can also be defined in terms of virtually any function that can be programmed on a computer. One particularly useful technique uses the subroutines available for defining tables of functions as described in the last section. Thus, if the geometry of the rail surface is available in the form of digitized data from tests, such as was the case in the American Steel Foundries (ASF) tests which are described in the section on validation, this digitized data can be used directly as a table whose given points are to be connected by straight line segments.

One note of caution should be given however. If inputs of this form are to be used, some attention should be given to the integration interval Δt. A program will "see" the input only at integer multiples of Δt regardless of the detail with which the input time history is given to the computer. If what the program "sees" does not adequately duplicate the intended input, the choice of integration intervals may have to be refined.

7.4 MATHEMATICAL MODELS

One of the advantages of the Newtonian method is the ease with which one may adapt a program to look at a related but different math model. This is in contrast to programs derived by Lagrangian methods, which can usually be applied to only one math model unless extensive modifications are made. The advantage is that one may evaluate a whole series of math models to find which model is best able to handle a given problem rather than being forced to choose a math model at the beginning of the analysis. This is especially valuable if test data is available to provide a basis for selection of math models.

Since the vehicle structure itself could be handled any number of ways using the normal mode method, the most significant part of writing a general program involves modeling of the trucks. That is to say, since the vehicle can be modeled in almost any degree of complexity desired, the success or failure of a general program depends on modeling of the truck, especially since most of the nonlinearities are concentrated in the trucks. Test data was available from rocking tests conducted by ASF with the 100 ton hopper car; typical comparisons will be discussed later in this report. The 100 ton hopper car vehicle structure itself could be considered rigid in response to crosslevel inputs whose period corresponds to the truck center-to-center distance. Consequently, the dynamic responses for this configuration could be viewed as totally determined by the trucks. By means of generating dynamic response predictions using several different truck models, and comparing these predictions with each other and with test data, the simplest truck model capable of adequate dynamic response predictions could be found. This model is applicable to all instances where ASF Ride Control Trucks are used as long as the vehicle structure is modeled in sufficient detail; use of a different type of truck would require changes in the truck model.

Five basic math models for the trucks were studied. Their equations of motion were programmed, and responses to the ASF test track input at a velocity of 18.4 mph were evaluated. Ability to predict test responses accurately was used as a basis for comparison, while factors such as simplicity, projected computer simulation costs, and degree of inherent mathematical stability were also taken into account. The models were the following:

7.4.1 Battelle Model - Fully Linear

Most of the basic information on trucks was taken from Reference 9 which was a report prepared by Battelle on various aspects of truck modeling. The model used by Battelle for roll is reproduced in Figure 7-1. This model as used by Battelle had no provisions for nonlinearities such as liftoff and separation. While Battelle used an impedance element for the rear truck, our study with this model used the full truck model in both front and rear positions.

When applied to the ASF test conditions, this model showed good agreement with test data up to the point where wheel liftoff apparently took place in the test, and very poor agreement for the remainder of the test. (Wheel liftoff here is defined as the point where the vertical force went to zero, not as a point where a large, visible, physical separation took place.) The method of mass lumping dictated a small integration interval (1-2 milliseconds), which would result in large simulation costs. It was concluded that a nonlinear model should be used instead.

7.4.2 Martin Model

Martin-Marietta (Denver) has generated a truck model (see Reference 10) which was based on a series of component tests done by ASF in 1974. Elements of this model are shown in Figure 7-2. This model emphasized the possibility of free relative motion between elements in taking up tolerances, and the coulomb nature of internal frictional forces between the truck components. Martin used the model primarily for hunting motions, but we checked to see if there were any advantages to this model when used for rolling motions.

For our particular application, little advantage was found in the use of this model. In view of its inherent complexity, its use was discontinued.

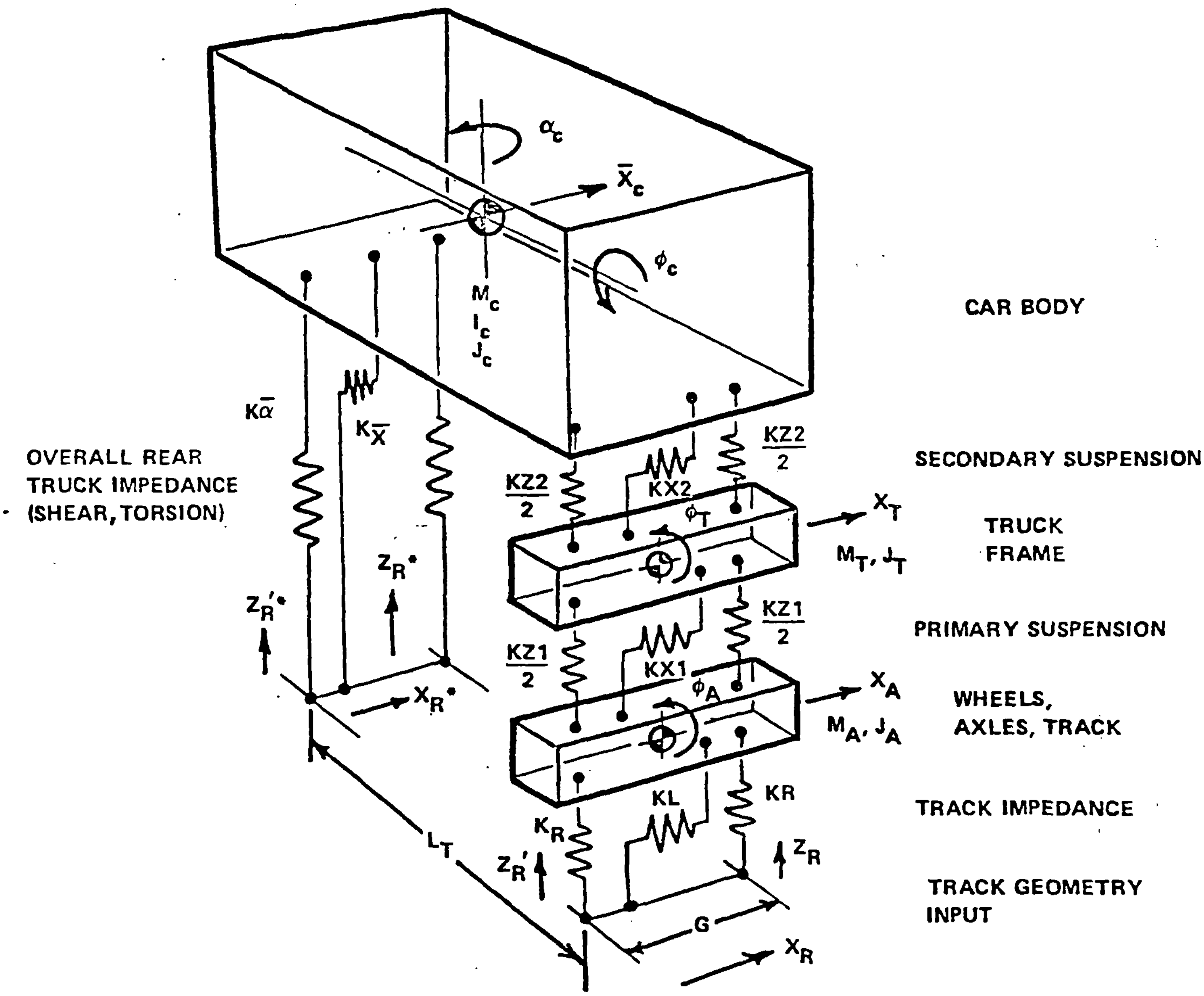

Figure 7-1. Roll/Yaw Model of Vehicle and Track Structure - Battelle

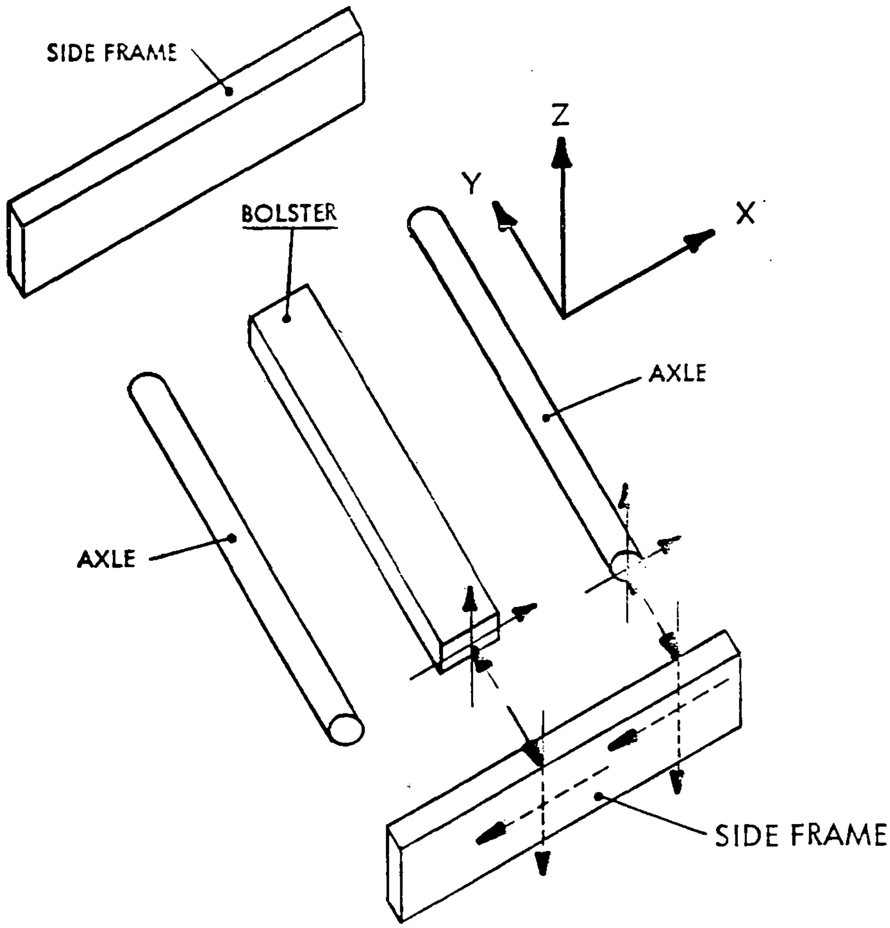

EACH JOINT MODELED AS SHOWN BELOW:

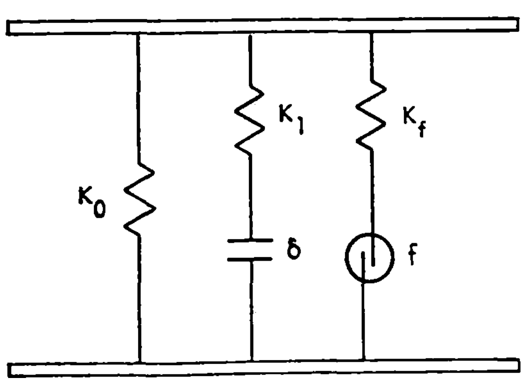

K_0 = Initial Stiffness
K_1 = Hard Stop
δ = Free Play
K_f = Friction Stiffness
f = Coulomb Friction

Figure 7-2. Martin Truck Model

7.4.3 17 dof - Version 1

Figure 7-3 shows two versions of truck math models which were used as a part of the 17 dof dynamic response computer program. Each of the two masses representing a truck is capable of moving vertically, laterally, and in roll, thus providing six degrees of freedom for truck motions. Between each mass are flexibility elements shown as simple springs, which resist relative motion. Two flexibility elements separated by a certain distance act vertically while one element acts in a horizontal direction. While shown as simple springs, these flexibility elements may be as nonlinear and complex as seems necessary. Normally, they will include damping terms which may be linear (viscous) or nonlinear (coulomb).

Version 1 of our truck model is identical to the Battelle truck model with added capability to use nonlinear flexibility elements. Separation, defined in terms of setting the force in the flexibility element to zero when the element goes into tension, was allowed at both wheel/rail interfaces and at the interfaces between spring nest and truck bolster. While separation at the top of the spring nest was not found to occur, wheel/rail separation was a frequent occurrence during the ASF tests, and inclusion of this nonlinearity greatly improved fidelity of simulation. Simulation accuracy with this and the following two models was almost identical; but this model required very small integration intervals (1-2 ms), resulting in high computer simulation costs.

7.4.4 17 dof - Version 2

Figure 7-3 shows a modified model labeled Version 2. The purpose of this model was to see if modeling of the centerplate-kingpin side bearing roller connections was beneficial. While the Version 1 model assumed the car and truck bolsters to be rigidly linked, a modeling of their rocking conditions is included in Version 2. The side bearing rollers are modeled by a spring which begins to act once the side bearing clearance is taken up. The flexibility of the wheels, axles, and bearings is included in the track flexibility.

Even under the very severe conditions encountered in the ASF shimmed track tests, no contact of the side bearing rollers took place. There was a tendency for liftoff at the wheel/rail interface to take place before side bearing contact.

As with the previous model, simulation accuracy was excellent, but the small integration intervals resulted in relatively high computer costs.

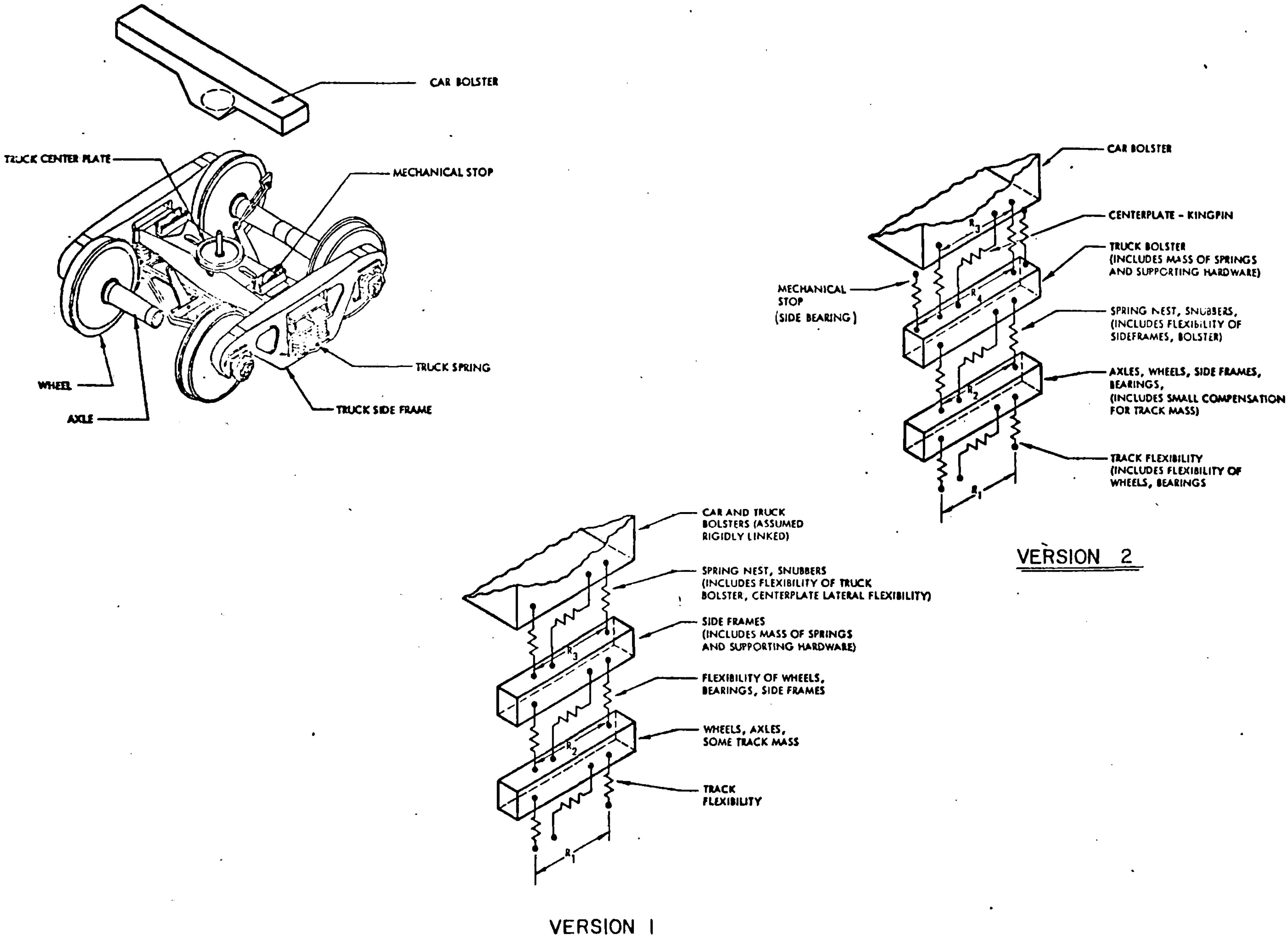

Figure 7-3. Truck Math Models

7.4.5 22 dof - Version 3

Figure 7-4 shows the 11-degree-of-freedom model. As in Version 1 of the last model, this model considered car and truck bolsters rigidly linked. All remaining truck masses are lumped together, and the flexibility of wheels, bearings, and side frames are lumped in with the track flexibility. A comparison of dynamic response predictions for the ASF test conditions made with this simplified model was virtually identical to response predictions made with the Version 1 and Version 2 models described above. However, because of the elimination of the high frequencies in the model, it was possible to increase the integration interval to 7-10 milliseconds, enabling a drastic reduction in computer costs.

The analysis demonstrated that even under the severe and varied conditions encountered in the ASF shimmed track tests, there was no need for a detailed modeling of the centerplate bolster rocking conditions or for a breakdown of the truck into more than one mass. However, later work indicated that these conclusions hold only for relatively heavy cars. A very light vehicle, such as an unloaded flatcar, would probably require the greater complexity of the Version 2 17 dof model for satisfactory simulation.

7.4.6 Detailed Description of 11 dof Model

The 11 dof model is shown in Figure 7-4. The model is comprised of three masses and twelve flexibility elements.

Masses 1 and 2 are lumped masses representing the front and rear trucks, respectively. Each has the freedom to move vertically, laterally, and in roll. The masses and moments of inertia for each comprise the side frames, wheels, and axles, with some amount of track mass and spring nest mass added in. The mass of the truck bolster is lumped with the vehicle mass in this model. The widths R_1 and R_3 are the rail gages and the widths R_2 and R_4 are the effective distances between spring nests. The longitudinal length of the truck is ignored, and both wheels on one side of a truck are assumed to act at a single point. Thus, inputs from the rail are averaged over the truck axle spacing. The height of the truck is neglected because it is often small relative to the vehicle height. For low vehicles, the truck height can be partially taken into account by using the combined vehicle-truck height as the vehicle height. Yawing motions of the truck are neglected.

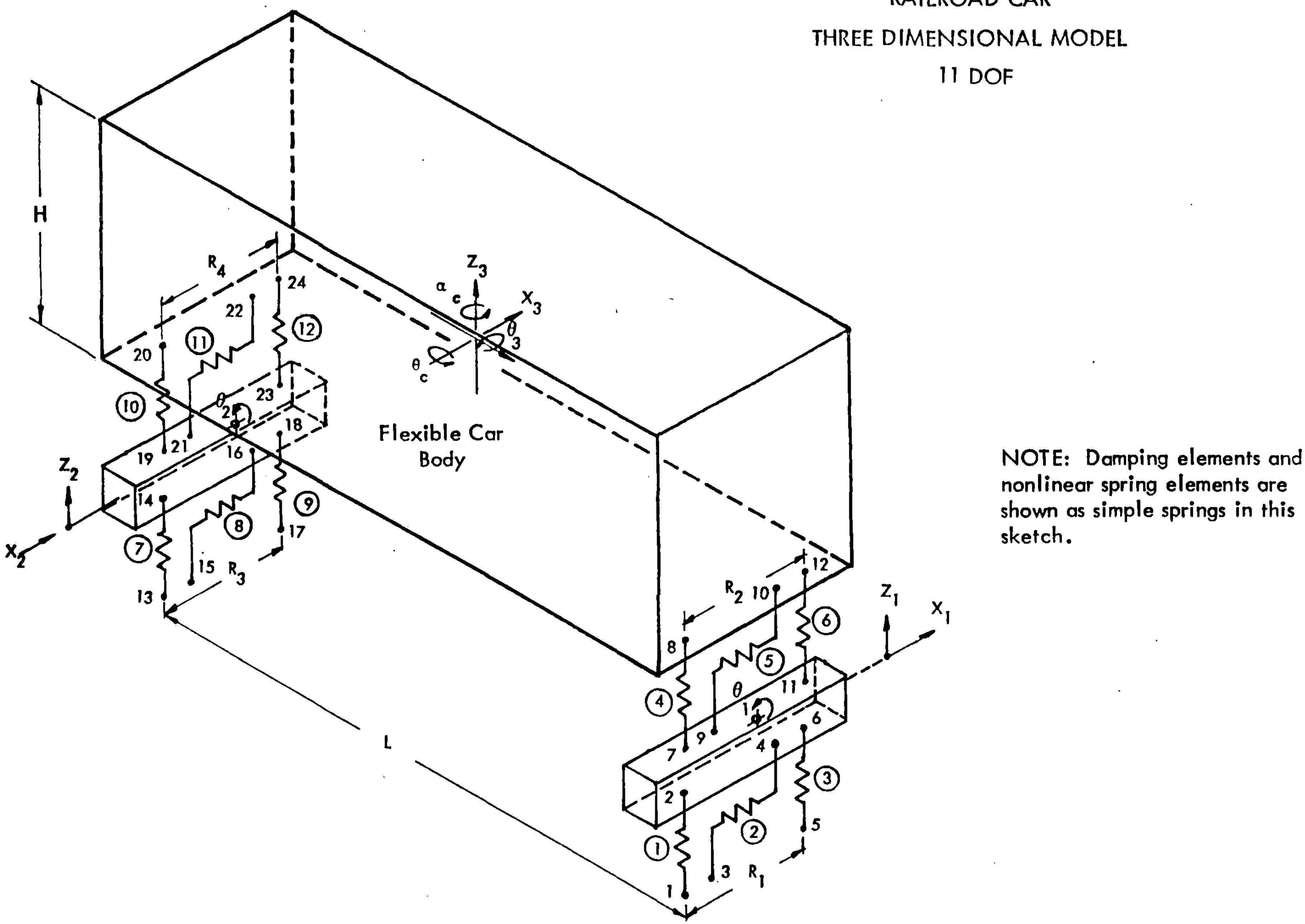

Figure 7-4. Model of Railroad Car, II Degrees of Freedom

Springs 1, 3, 7, and 9 represent the vertical flexibility of the track, wheels, bearings, and side frames. Springs 2 and 8 represent the lateral flexibility of the same items. Springs 4, 6, 10, and 12 represent the vertical flexibility of the spring nests, bolster, and centerplate, while springs 5 and 11 represent the lateral flexibility of these items. Damping characteristics are included in the above. Note that the vertical flexibility of each spring nest is modeled separately while the lateral flexibility of two nests is lumped into a single spring. Node points 1 and 5 represent the vertical wheel/rail interaction points of the front truck (averaged between the two wheels on one side of the truck). Track histories are inputted by giving these node points the vertical displacements (and velocities if desired) of the track surface as seen by a moving train. Node point 3 represents the same thing in the lateral direction, and inputs to the rear truck are handled in a similar manner.

Mass 3 represents the flexible car, which can have vertical, lateral, roll, pitch, and yaw motions. "L" is the truck center-to-center distance and "H" represents twice the vertical distance from the truck centerplate to the vehicle structure-lading combination c.g. (Alternately, for vehicles of fairly short height, this can be twice the distance between the wheel/rail interface and the c.g.) If flexible modes are superimposed on the vehicle, excitation of these modes takes place at all points where a spring interacts with the vehicle structure. This will take place at each car bolster, and influence coefficients will have to be defined at the points where an interaction occurs. Normal modes can be defined only when a vehicle is relatively linear and important nonlinearities can be concentrated in external members such as trucks. If important nonlinearities exist in the vehicle structure-lading combination itself, some modifications will be necessary. See Reference 7 for an example of how these modifications can be made.

7.5 FLEXIBLE VEHICLE

Applying the normal mode methods of Section 7.2 to the flatcar body results in the natural frequencies and mode shapes for the flatcar structure. The location for the lumped masses is based on the physical structure of the flatcar. For this model the mass was lumped at the node locations defined by the attach point of the structural elements of the flatcar. Figure 7-5 shows the structural element location for the flatcar and the resulting node point location definition. From this definition it is possible to formulate the appropriate mass and stiffness matrices for the flatcar

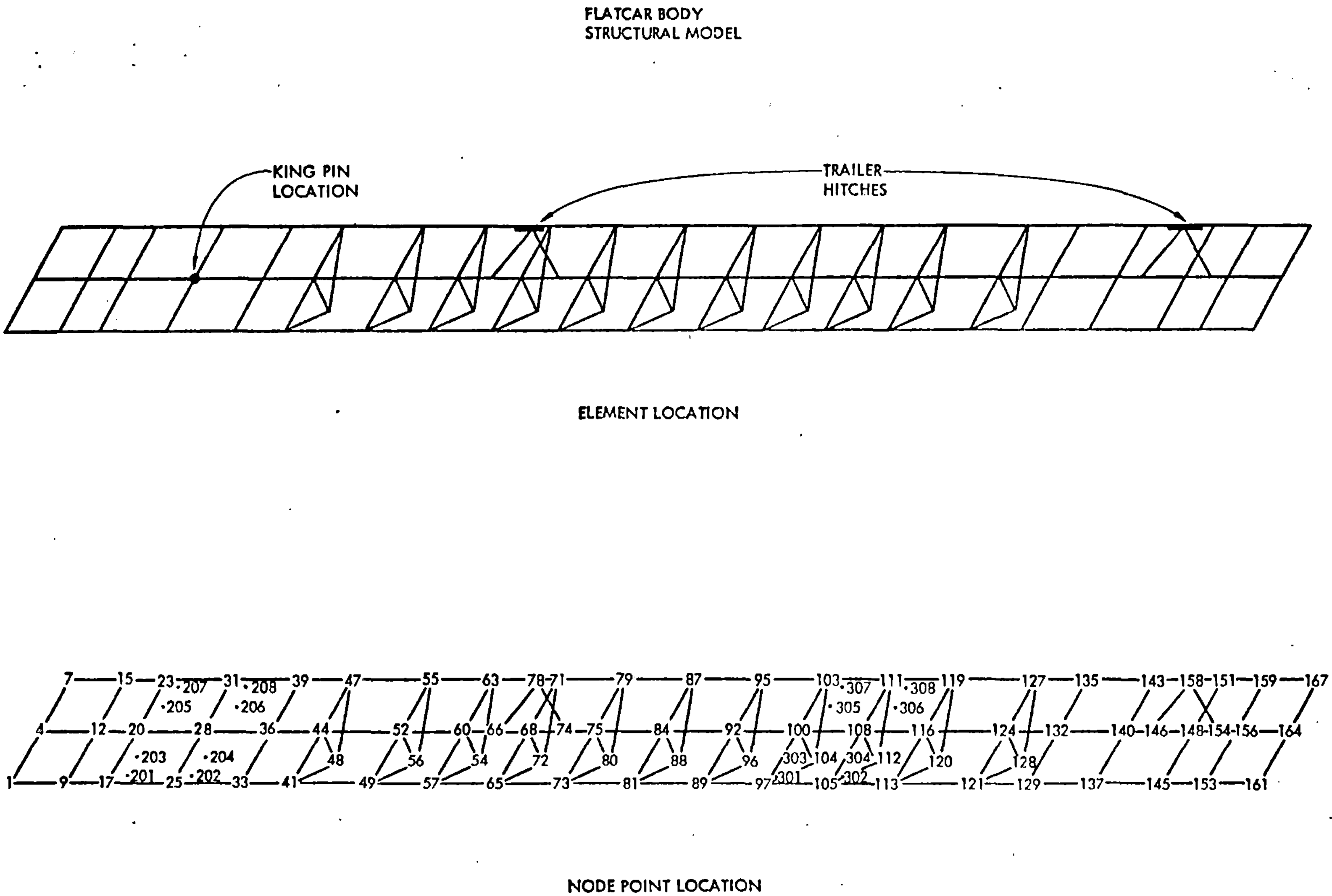

Figure 7-5. Flatcar Body Structural Model

structure. Using the normal mode technique, the natural frequencies and mode shapes can then be solved. The ANSYS computer program provides this information directly.

7.6 COMPONENT TESTS

In a nonlinear system it is extremely important to understand the characteristics of the actual components in use. Even if nominal characteristics had been available, they might have been inadequate because of normal tolerance deviations. Since even nominal characteristics are unavailable, component test data are indispensable in generating coefficients.

A list of the type of tests which are necessary is provided in Appendix C. A more complete description of the proposed use of data from these tests is given in Reference 8.

7.7 MODEL VERIFICATION

In order to verify the method in its application to rail vehicles, in order to assess the degree of complexity required in a math model, and in order to assess the need for certain nonlinearities and for higher order terms in the program, comparisons were made between simulations using the program and test results. Test data were available for two considerably different types of vehicles. The first was a rigid, loaded 100-ton hopper car moving on shimmed track designed to excite large rock and roll motions. The second was a flexible unloaded 89 foot 9 inch flatcar subjected to sinusoidal excitations at the Rail Dynamics Laboratory facility at Pueblo, Colorado.

In May, 1968 a series of tests were run by ASF near Hartford, Illinois. In these tests, a loaded 100-ton hopper car riding on two ASF Ride Control Trucks was run on a specially prepared track section at ten different velocities. Each rail joint was shimmed approximately 3/4 inch to excite the rocking mode. Approximately 15 channels of response data, including accelerations, forcers, and displacements, were recorded.

The first test was run at a very low speed, where no dynamic effects were apparent. The recorded angular displacement of the car at this speed was taken to be the angular cross-level geometry of the track as statically deflected by the weight of the vehicle.

This geometry was used as the input to the computer program for the runs at the other velocities.

The truck center-to-center distance of the test vehicle was approximately 39 feet, which coincided with the rail length and, hence, with the excitation. This implies that torsional vehicle flexibility did not have a significant effect on dynamic responses. For this reason, and because a detailed description of the specific hopper car was not available, no flexible modes were used for the calculations.

The damping properties of friction snubbers vary widely because of manufacturing tolerances and wear. No information on the condition of the friction snubbers on the trucks of the test car was available. As was done in Reference 11, damping coefficients for these snubbers were derived by iterative techniques rather than by consideration of the characteristics of the snubbers themselves. The coefficient in the model was varied until one dynamic response at one velocity agreed with measured data. The resulting model was then used to simulate the other responses at that velocity, and then to simulate responses at the other velocities.

Coefficients for damping in the friction snubbers of the trucks were obtained from comparison of theory and test results at 18.4 mph. While the damping is known to be coulomb type, the calculation was also performed with linear (viscous) damping because of its simplicity. After three or four iterations, the results shown in Figure 7-6 were obtained by using a value of c = 1400 lb - sec/in. for viscous damping while a value of 8000 lbs of coulomb-type damping produced the results shown in Figure 7-7.

Using these values for damping, similar predictions were made for responses at 17.4 mph. Figure 7-8 gives the results for viscous damping, while Figure 7-9 uses coulomb damping. Because both angular deflections and forces compared well at all simulation times, and especially because the simulation could be applied at the new velocity, the validity of the model for a 100-ton hopper car was considered proven.

As still further proof, the same comparison was made at a much different speed. The values for 15.2 mph were used. The raw data showed a shift due to a probable calibration error which was corrected. The comparisons are shown in Figures 7-10 and 7-11.

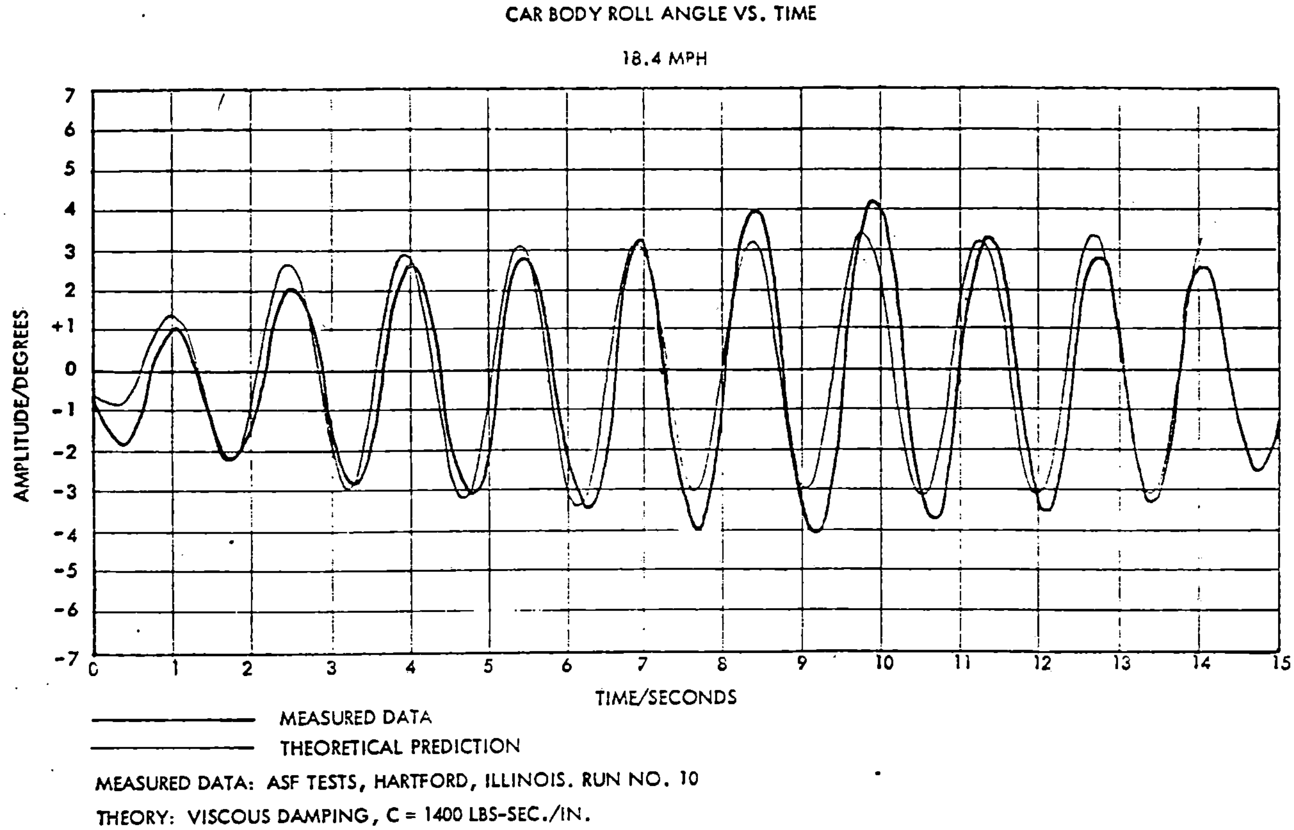

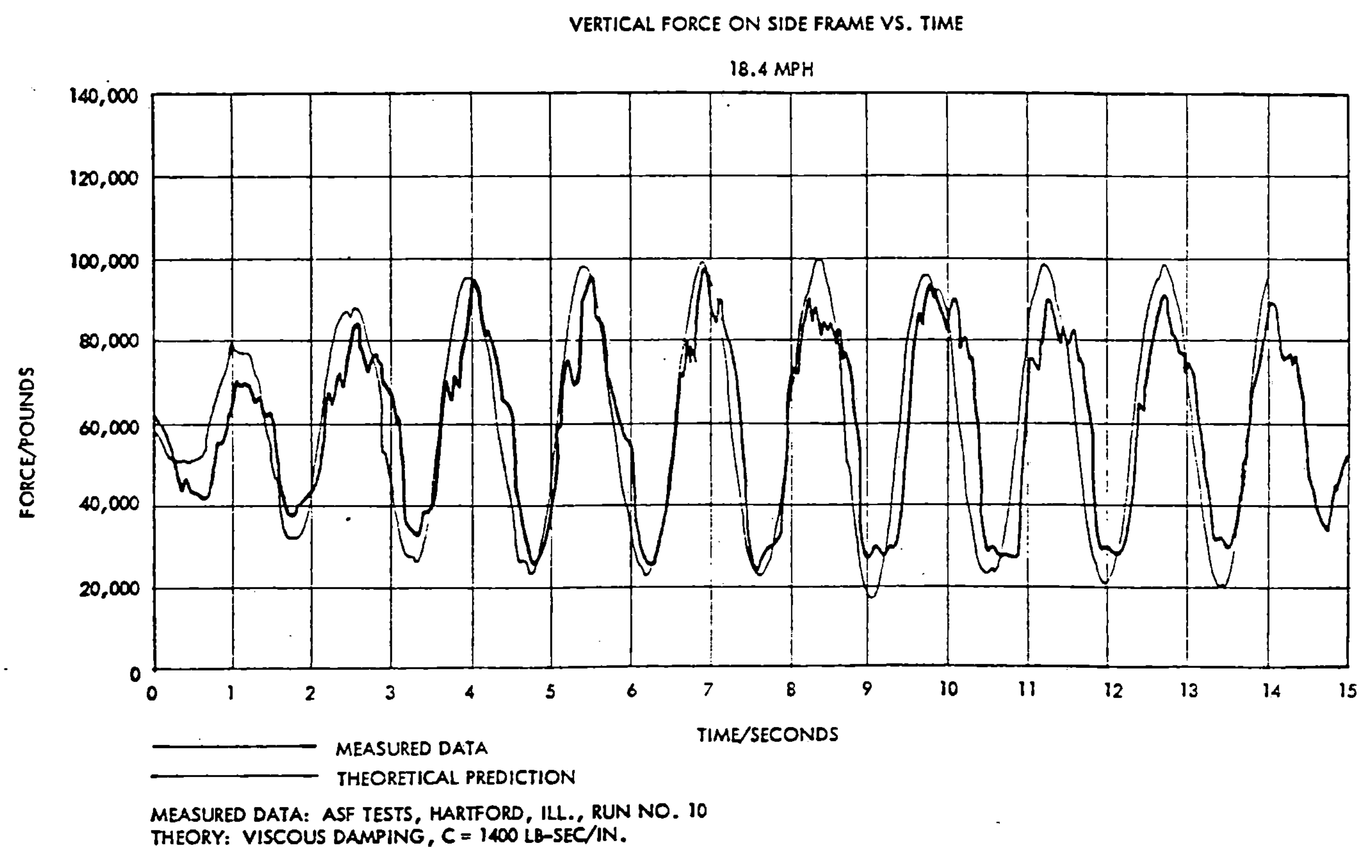

Figure 7-6. Results for Viscous Damping at 18.4 MPH

CAR BODY ROLL ANGLE VS. TIME

18.4 MPH

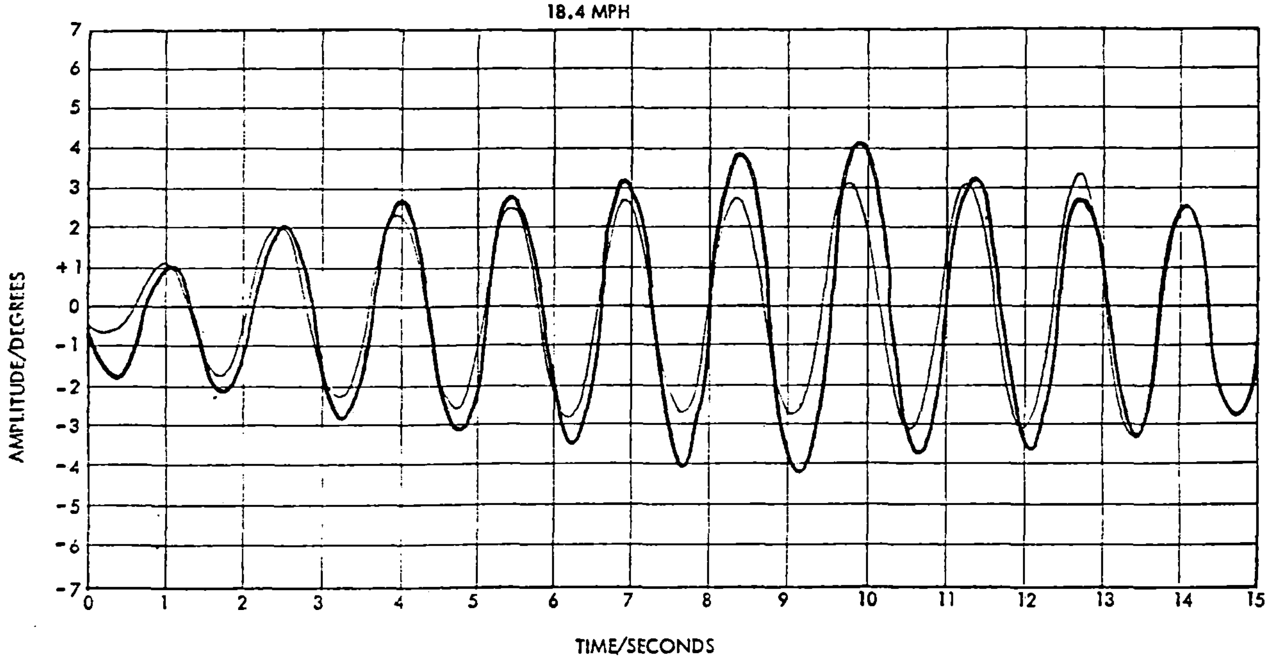

MEASURED DATA

THEORETICAL PREDICTION

MEASURED DATA: ASF TESTS, HARTFORD, ILLINOIS, RUN NO. 10
THEORY: COULOMB DAMPING, F = 8000 lbs.

VERTICAL FORCE ON SIDE FRAME VS TIME

18.4 MPH

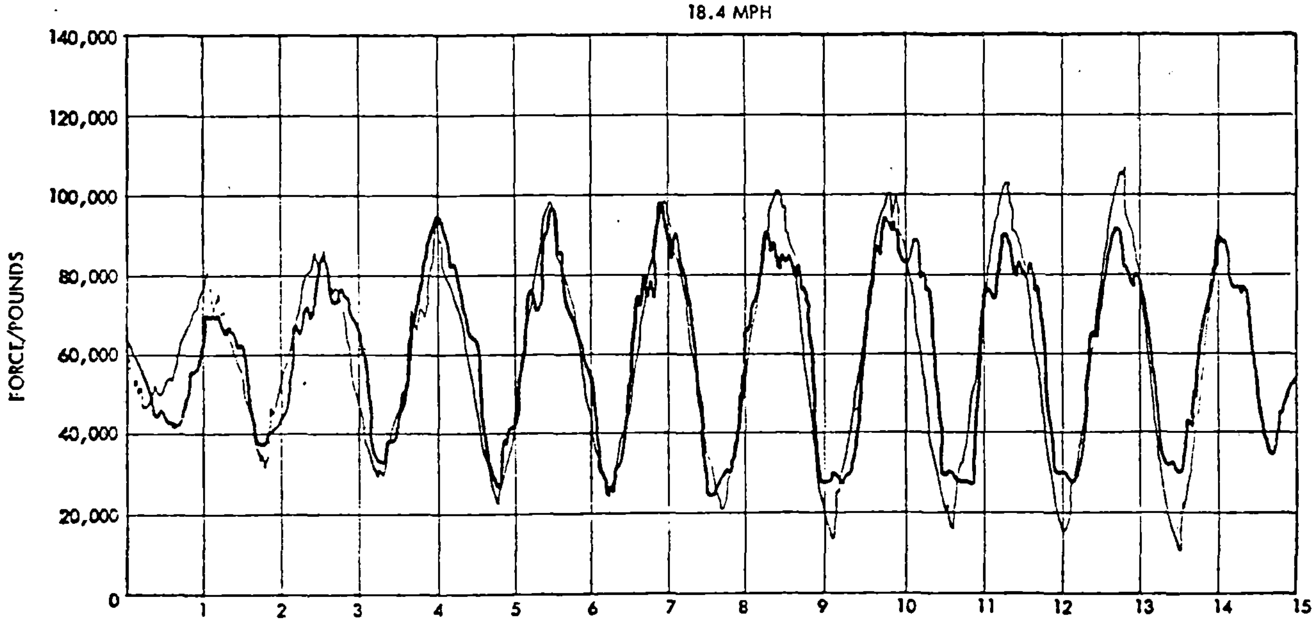

MEASURED DATA

TIME/SECONDS

THEORETICAL PREDICTION

MEASURED DATA: ASF TESTS, HARTFORD, ILLINOIS, RUN NO. 10

THEORY: COULOMB DAMPING, F = 8000 LBS.

Figure 7-7. Results for Coulomb Damping at 18.4 MPH

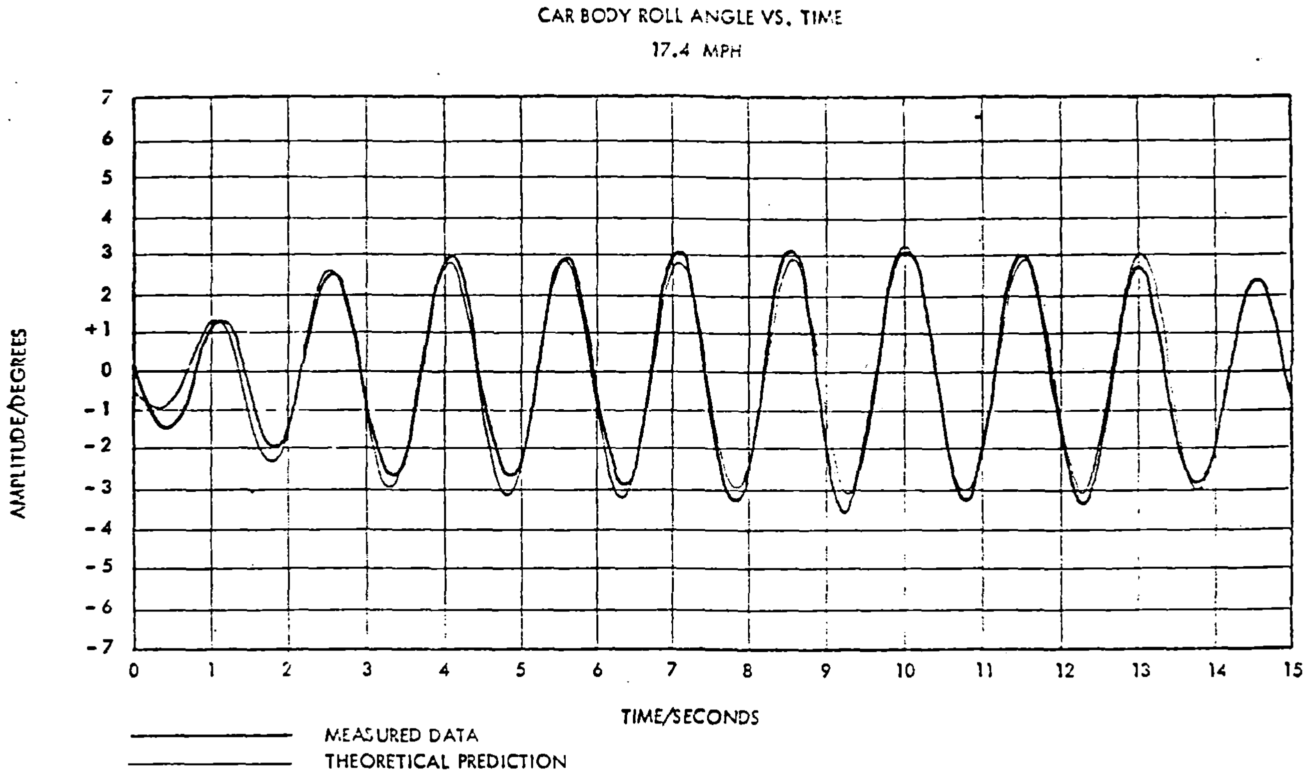

MEASURED DATA: ASF TESTS, HARTFORD, ILLINOIS, RUN NO. 4
THEORY: VISCOUS DAMPING, C = 1400 LB-SEC./IN.

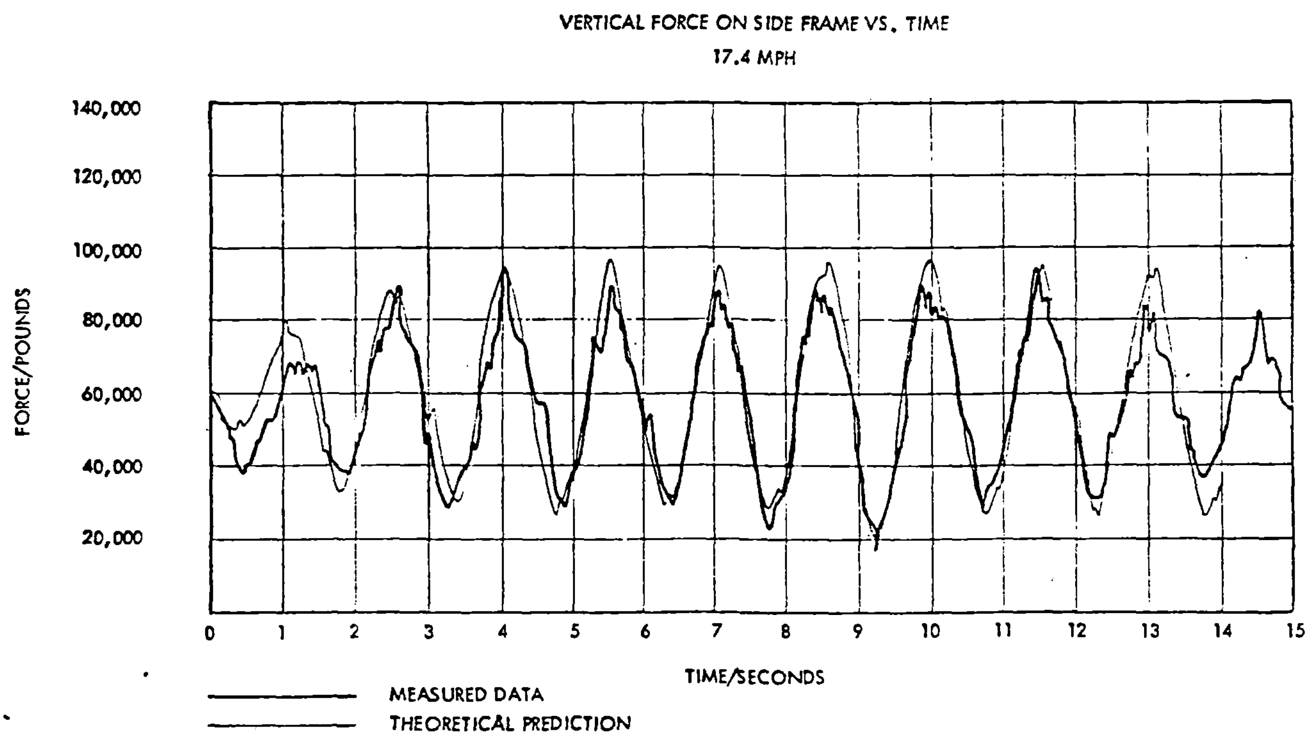

MEASURED DATA: ASF TESTS, HARTFORD, ILLINOIS, RUN NO. 4
THEORY: VISCOUS DAMPING, C = 1400 LB-SEC./IN.

Figure 7-8. Results for Viscous Damping at 17.4 MPH

CAR BODY ROLL ANGLE VS. TIME

17.4 MPH

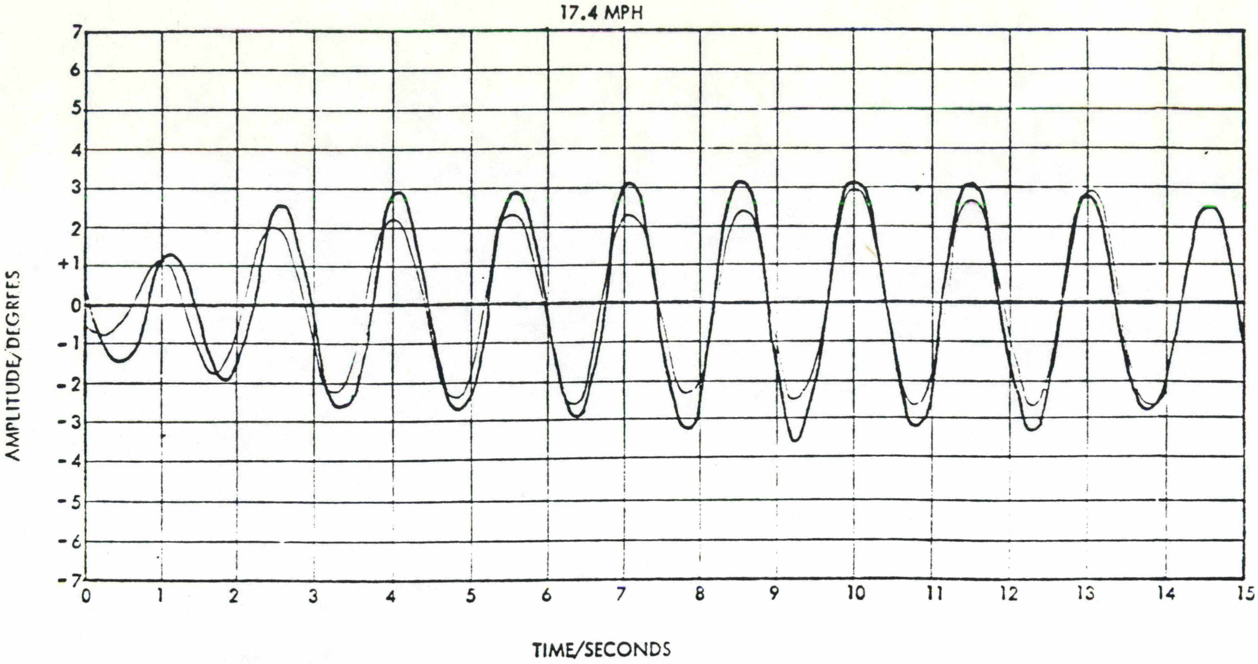

MEASURED DATA

THEORETICAL PREDICTION

MEASURED DATA: ASF TESTS, HARTFORD, ILLINOIS, RUN NO. 4

THEORY: COULOMB DAMPING, F = 8000 lbs.

VERTICAL FORCE ON SIDE FRAME VS TIME

17.4 MPH

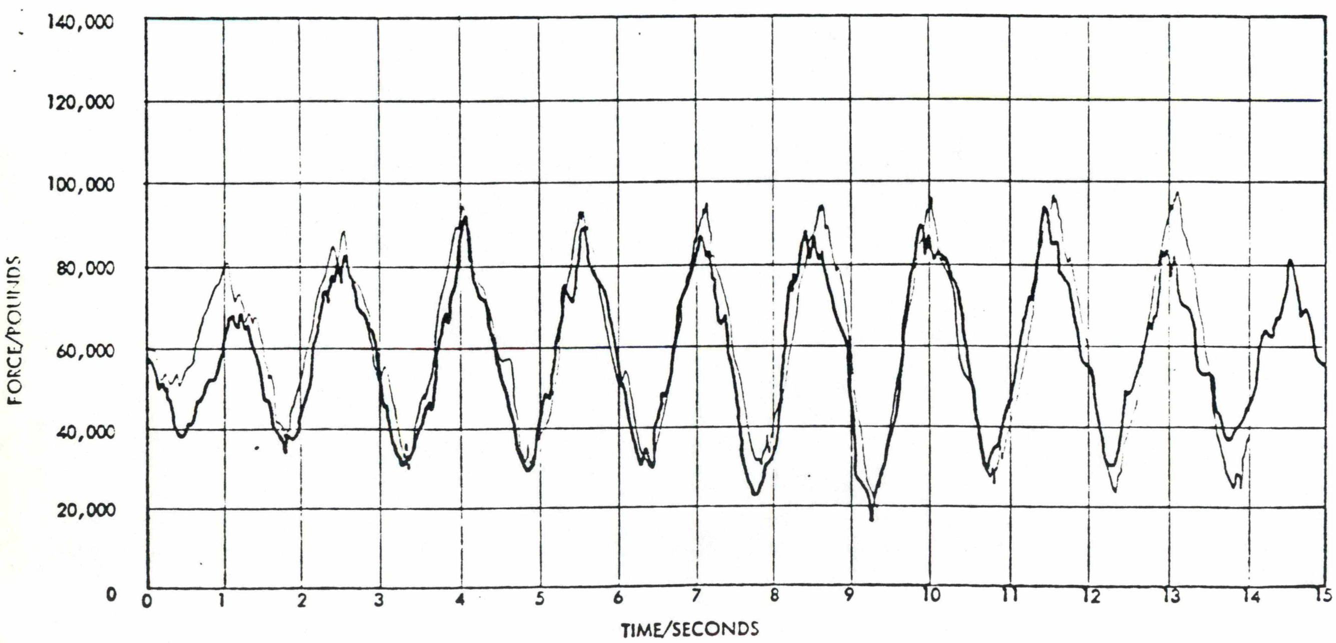

MEASURED DATA

THEORETICAL PREDICTION

MEASURED DATA: ASF TESTS, HARTFORD, ILLINOIS, RUN NO. 4

THEORETICAL DATA: COULOMB DAMPING, F = 8000 LBS.

Figure 7-9. Results for Coulomb Damping at 17.4 MPH

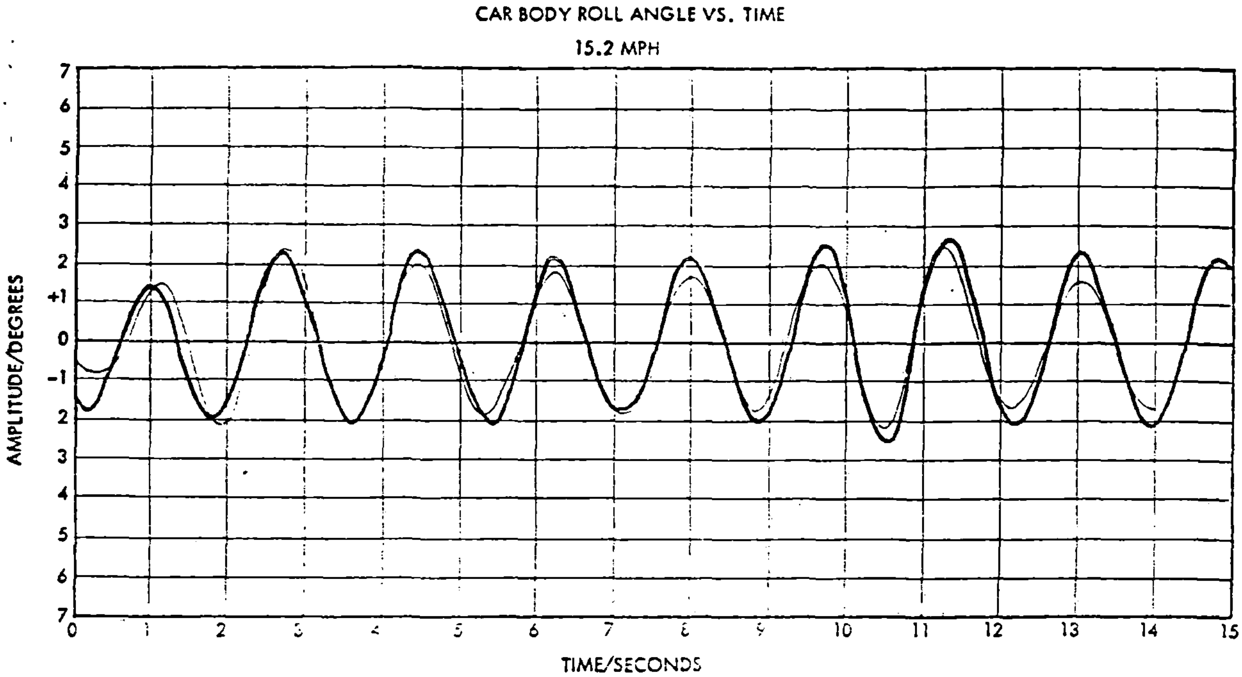

MEASURED DATA

THEORETICAL PREDICTION

MEASURED DATA: ASF TESTS, HARTFORD, ILLINOIS, RUN NO. 2

THEORY: VISCOUS DAMPING, C = 1400 LB - SEC/IN

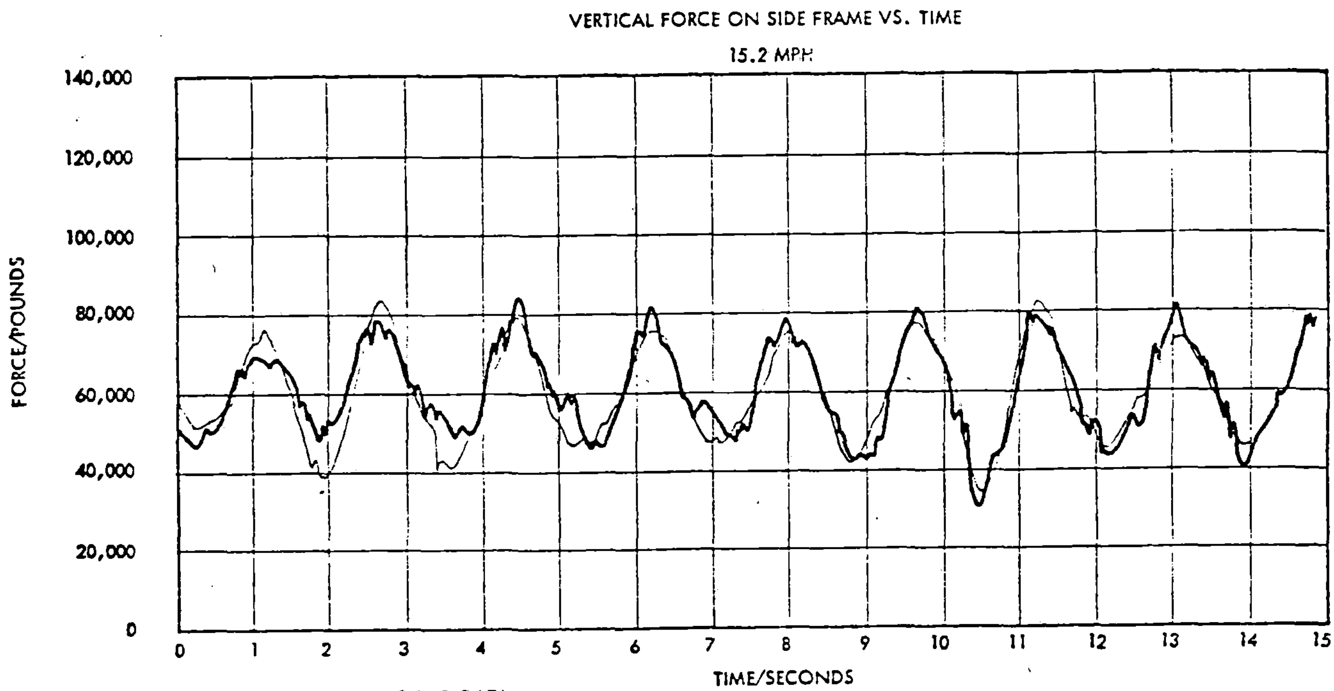

MEASURED DATA

THEORETICAL PREDICTION

MEASURED DATA: ASF TESTS, HARTFORD, ILLINOIS, RUN NO.2

THEORY: VISCOUS DAMPING, C = 1400 LB - SEC/IN.

Figure 7-10. Results for Viscous Damping at 15.2 MPH

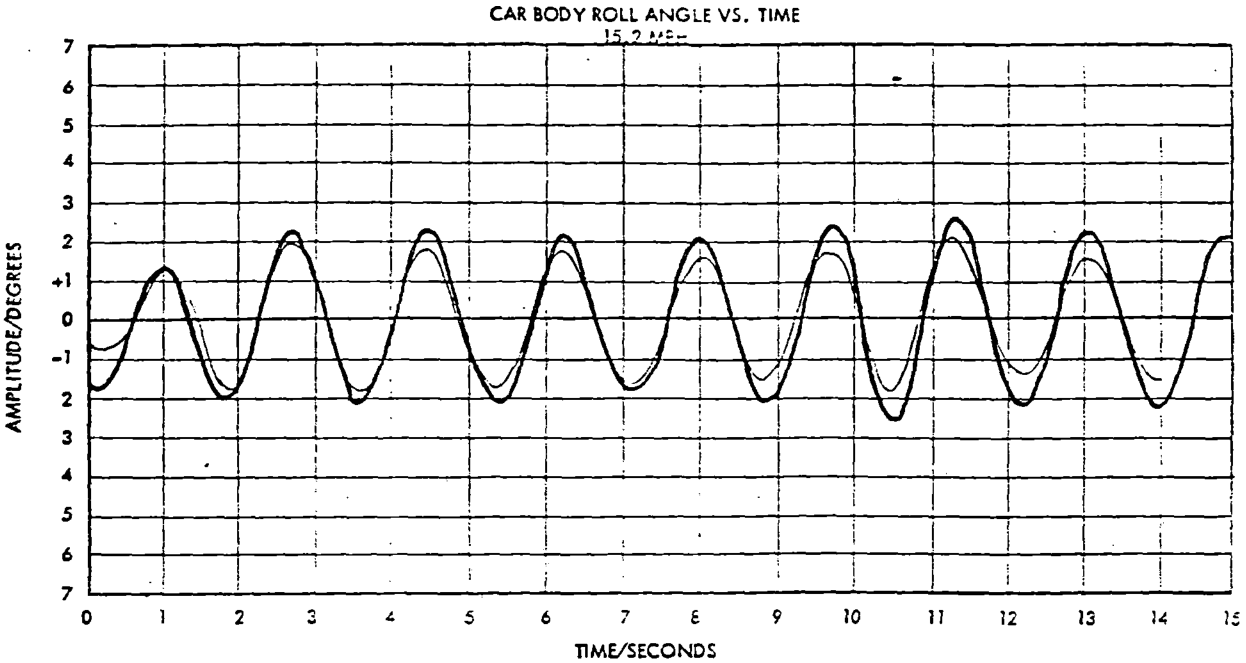

MEASURED DATA

THEORETICAL PREDICTION

MEASURED DATA: ASF TESTS, HARTFORD, ILLINOIS, RUN NO. 2

THEORY: COULOMB DAMPING, F = 8000 LBS.

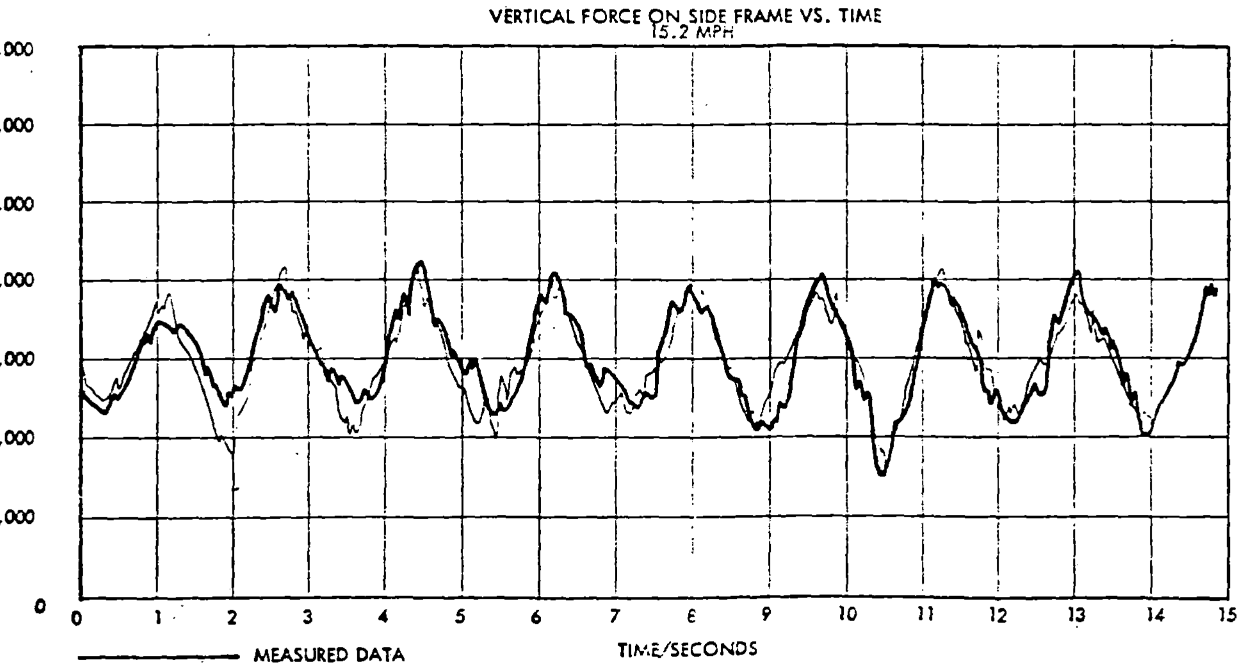

MEASURED DATA

THEORETICAL PREDICTION

MEASURED DATA: ASF TESTS, HARTFORD, ILLINOIS, RUN NO. 2

THEORY: COULOMB DAMPING, F = 8,000 LBS.

Figure 7-11. Results for Coulomb Damping at 15.2 MPH

It was concluded that the model was completely valid for a loaded hopper car subjected to this range of conditions. It was also concluded that, for this heavy a vehicle at these large amplitudes, either viscous or coulomb damping could be used at will. Additional test data (other responses and other velocities) were available, but no additional validation was felt to be necessary.

To check the model under different test conditions another comparison was made with tests run at Hollidaysburg, Pennsylvania in 1966. This comparison, which was also very satisfactory, is described in Reference 5.

Test results from the Demonstration Test Program were used to validate the TOFC Model described in Appendix B. In these tests, a highly flexible 89 foot 4 inch long unloaded trailer-on-flatcar type flatcar was subjected to sinusoidal excitation at the Pueblo, Colorado facility. In this case, responses were determined more by vehicle flexibility effects than by truck characteristics.

Since a different truck was in use in the Pueblo tests, iterative techniques were used once again to find the proper truck spring nest damping value, and a viscous value of c = 1900 lb-sec/in. was selected. For excitation applied in phase, exciting pitch and bounce type motions, comparisons between theory and test at three different locations on the flexible flatcar are shown in Figures 7-12 through 7-14. Here, channel 65 was located directly over the truck being excited. Channels 89 and 118 were located at the center of the flexible flatcar, with 89 on the centerbeam and 118 on the left side. The comparisons are of essentially steady state conditions in dwell type tests. Once again, these comparisons are felt to be excellent.

Attempts were made to repeat these simulations using coulomb representations of damping. Because of numerical stability problems which are discussed in Reference 8, some problems with coulomb damping were experienced. It is felt that this represents a temporary numerical problem which will be corrected in future work rather than any modeling problem.

Tests were also run out-of-phase, which tended to excite torsional and rolling modes of the flatcar. Since one truck was fixed while the other was rocked, the excitation was

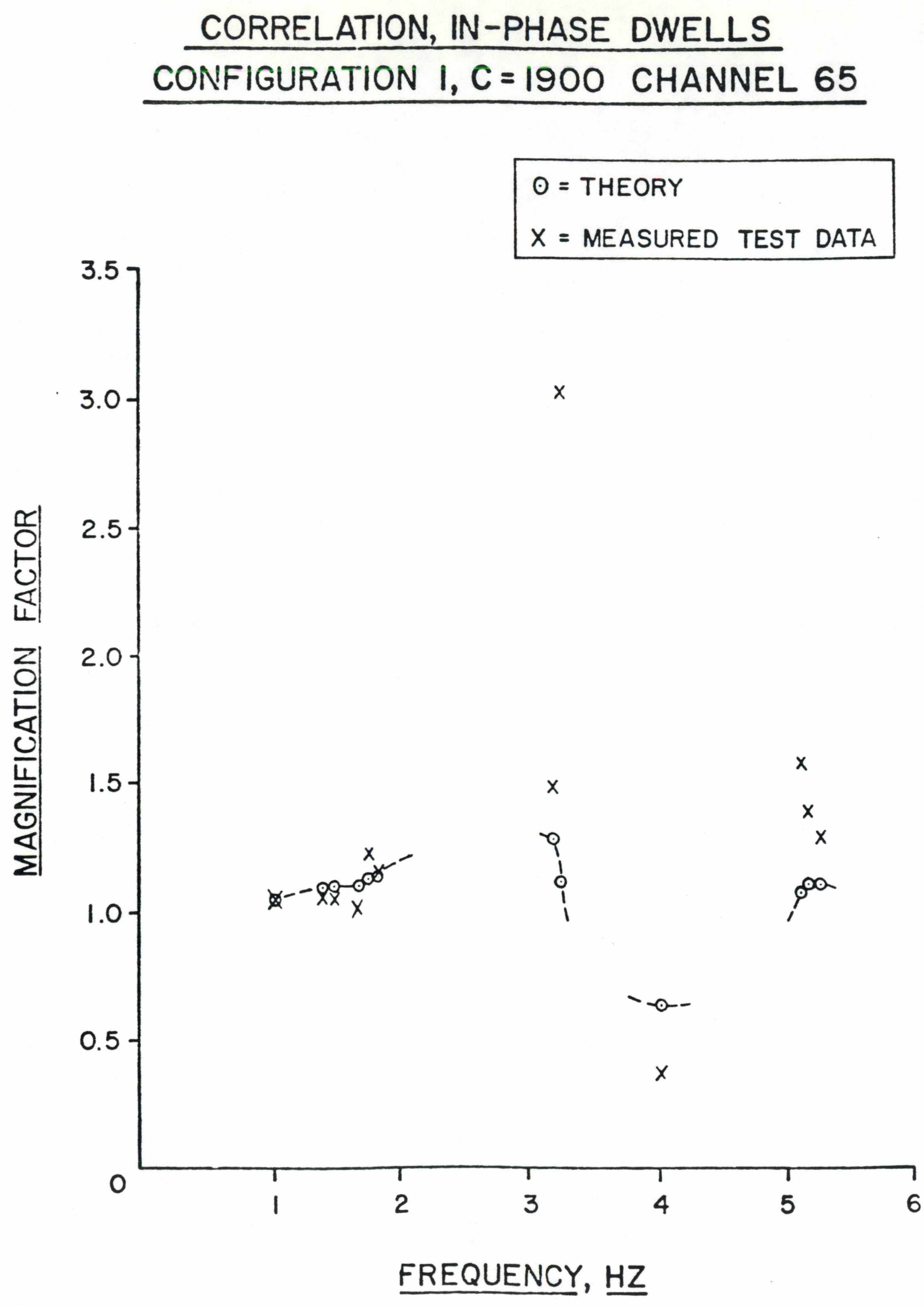

Figure 7-12. Correlation In-Phase Dwells Configuration 1, C = 1900 Channel 65

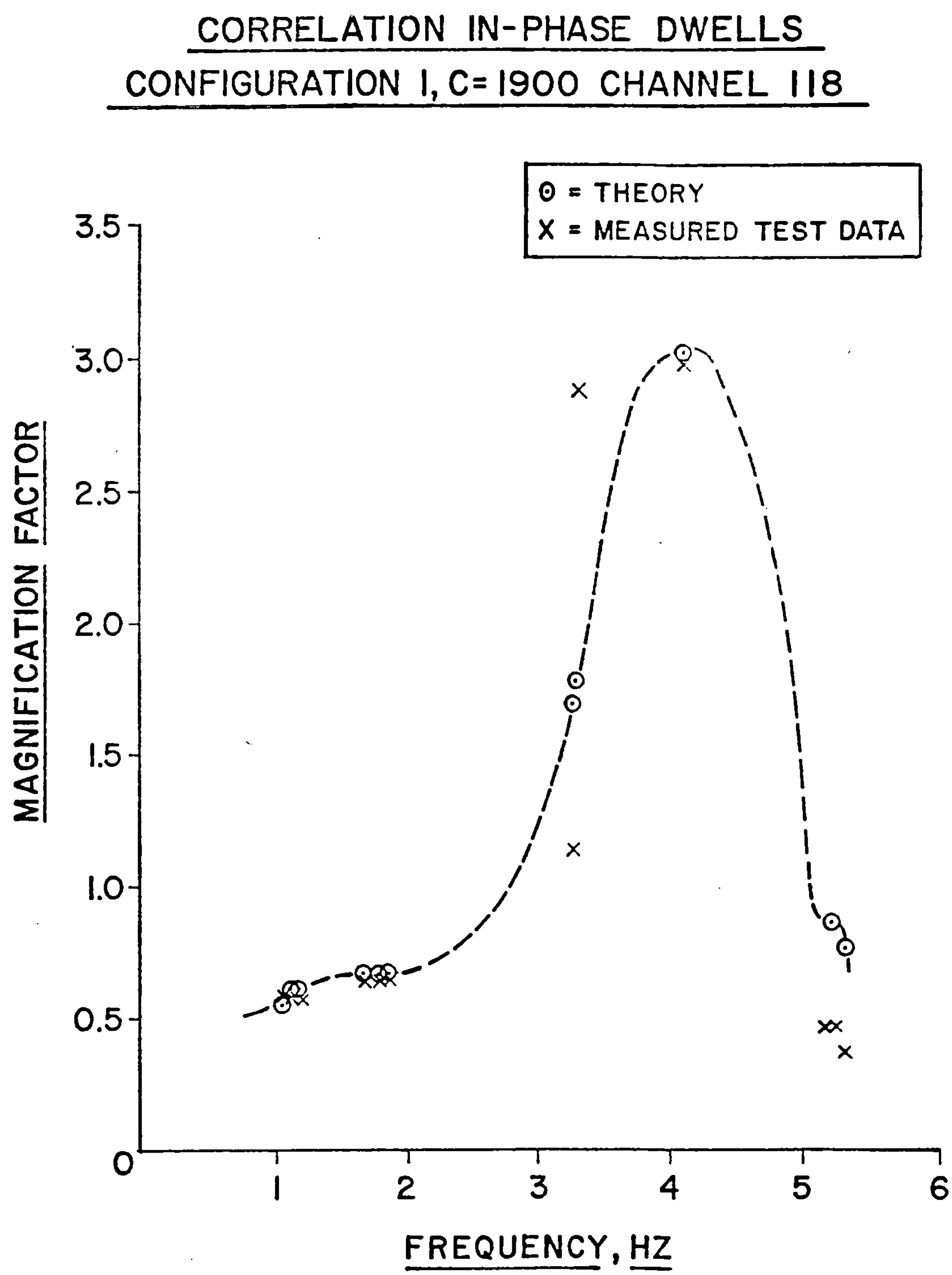

Figure 7-13. Correlation In-Phase Dwells Configuration 1, C = 1900 Channel 118

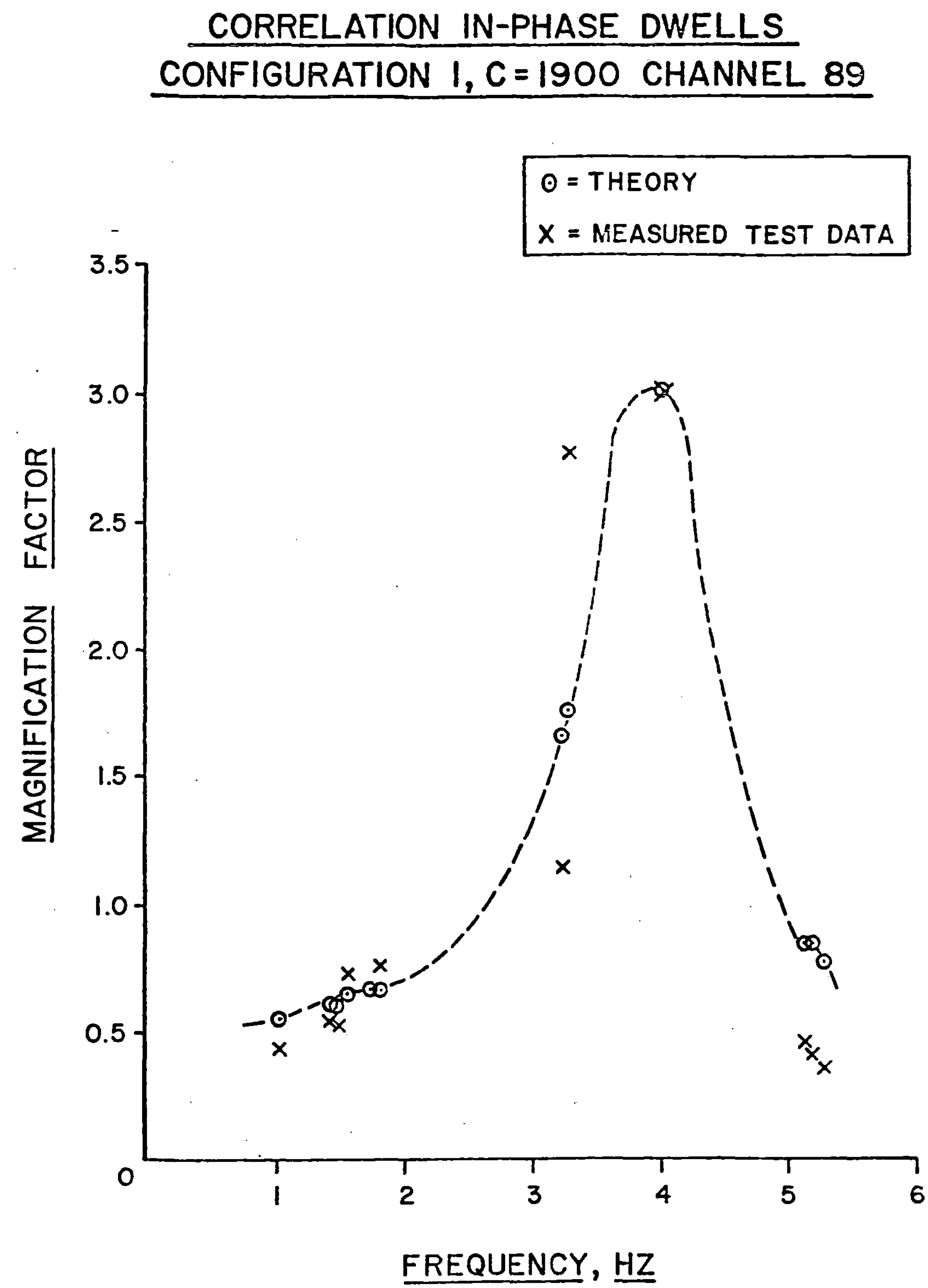

Figure 7-14. Correlation In-Phase Dwells Configuration 1, C = 1900 Channel 89

primarily of flatcar torsional modes. Because of the very light weight of the vehicle, a great deal of rocking on the centerplate took place. Clearly, the 11 dof model could not be used in this case, but the 17 dof model (Version 2) does have the capability to study centerplate rocking motions. Because of time and cost restrictions, the necessary testing required to define the nonlinear coefficients needed for this analysis could not be performed, and no comparisons could be made. It is recommended that these tests be performed at a later date.

While the torsional analysis could not be performed at this time, it is clear from the results of the bounce and pitch motion analysis that the model is applicable to the flexible flatcar as well. It was concluded that vehicle flexibility is being adequately modeled, and that the model can clearly be applied to a very wide range of different vehicle types and conditions.

7.8 COST FACTORS

One disadvantage of numerical integration is that excessive computer costs may be encountered if the programmer is not careful. Generally speaking, the costs of making a run with the type of program described in this report can be approximated by the following equation:

$$\text{COST} = C_c \, \frac{\text{NEQ}}{\Delta t} \cdot \text{TMAX}$$

where NEQ = Number of differential equations to be numerically integrated

Δt = Integration interval

TMAX = Total simulation time

C_c = Constant of proportionality involving efficiency of the computer and nature of the integration package.

In general, simulation costs will not be affected significantly by the presence or absence of nonlinearities or by the complexity of the equations describing the internal forces or the input time-histories. However, the simulation of very complex models (i.e. those with large numbers of degrees of freedom) over very long simulation times can be prohibitively expensive.

Increasing the number of degrees of freedom will have two effects on the above equation. First, costs will be directly proportional to the number of degrees of freedom. In addition, increasing the number of degrees of freedom usually increases the frequency of the highest-frequencied subcomponent. This will often necessitate a reduction in Δt, which will further increase the simulation costs. However, most of the higher frequencied degrees of freedom will contribute little or nothing to the overall response. Consequently, if computer costs are important, it is vital to eliminate the unnecessary high-frequencies from the mathematical model.

Following such an approach will usually ensure a satisfactory dynamic analysis for a reasonable cost. With the 11 dof program described in this report, simulation costs were found to be in the range of 50¢ to $1.00 per second of simulation time using the CDC Cybernet System.

It should be noted that a second of simulation time involves a significant amount of forward travel for a vehicle that is moving with a reasonably high velocity. A relatively small number of seconds of simulation time can then provide a great deal of information.

7.9 PROGRAM OUTPUT

The output from a program of this type will normally include the transient time-histories of all accelerations, velocities, and displacements associated with the degrees of freedom in the mathematical model, together with the forces and moments applied to the members as a function of time. Transient here is not used to indicate a very short time duration, but rather to differentiate from steady-state responses. Steady-state responses are not normally available from calculations of this type unless the simulation is conducted for such a long time that steady-state conditions are achieved. If a flexible vehicle body is used, then accelerations, velocities, and displacements at any point on the flexible body may be calculated by very simple expressions. Internal forces, bending moments, and stresses at any point within the flexible body are also available. Any of the above responses can be plotted by the computer.

One output which is not normally given by programs of this type is the eigenvalues and eigenvectors of the initial system. Since systems analyzed with this type of program are frequently nonlinear, this should present few real difficulties. However, when overall mode shapes are desired, they can be calculated by other programs used in conjunction with programs of this type.

SECTION 8 - CONCLUSIONS

The data acquired during the Demonstration Test Program was of good quality and could be meaningfully interpreted in understanding the physical character of the test specimen. The full range of VSS data acquisition and analysis was valuable in interpreting the test data. This included sweep analysis, dwell analysis, dwell time histories, and decay responses. The actuators were able to provide a controlled input to the test specimen which could be repeated over a range of test conditions. However, the responses on the test specimen showed some variation for the same input indicating the difficulty in characterizing a system as complex as the TOFC.

An analytical model was developed early in the test program to aid in test planning and data analysis. It proved essential in the pretest planning of actuator capability, test levels, limit checks, and expected specimen response. It was used in the post test analysis of data as an aid in interpreting test results. The finite element modeling technique used for the Demonstration Program was successful in developing the model used for the TOFC configurations.

The vast amount of data acquired from this test program made it impossible to completely assimilate and present it all in a report of this size. Thus the approach taken was to reduce and analyze only a representative sample of the data for this report in order to give some insight into the physical characteristics of the system. The primary purpose of the Demonstration Program was to demonstrate the use of the VSS, so it was not possible to structure the testing to provide a complete characterization of the TOFC. In many instances conclusions are drawn in this report on incomplete test data. This was done to provide some guidelines for future test planning on the TOFC, and the conclusions drawn are subject to revision when future data dictates.

The analytical model was developed for use in test planning and data analysis. Time was not available at the completion of the data analysis to spend a lot of time updating the model to agree with test data, so in some instances there is considerable variation between the analytical prediction and test data. However, the model proved very valuable in its primary purpose of test planning and data evaluation.

Because of the nonlinear response of the TOFC specimen as a function of input amplitude, it is recommended that future tests be planned so that runs are made at several different input amplitudes. In particular the analysis of data showed that running two series of sweeps at several amplitudes provides an extremely convenient method of acquiring and displaying the data to show the variation of transfer functions as a function of amplitude. It is also recommended that any future tests planned for the VSS have the model developed early in the test program in order to effectively plan and run the test program.

APPENDIX A - PROGRAM LISTING

All cards associated with the calculation of coulomb damping are identified by a vertical line in the left margin. Only these cards are annotated because it is assumed that the reader is already familiar with the FRATE program. Computer cards are available upon request.

The version shown is the 17 dof version of FRATE. Slight modifications will be required for the TOFC version of FRATE.

```
      PROGRAM MAIN(INPUT,OUTPUT,TAPE5=INPUT,TAPE6=OUTPUT,TAPE44)
       REAL M,INERT(10)
      REAL L
      REAL K
      DIMENSION PLOTM(3050,4),TIM(3050),VAL(3050)
      DIMENSION DISP(50),VEL(50),PHDCPH(10),SINPHI(10),R(10)
      DIMENSION F(30),DER(60),VAR(60),M(10),K(30),C(30)
      DIMENSION D(20),DI(10),WI(10),G(20),V(20)
      DIMENSION RF(10),RMM(10),OMEGA(10),ZETA(10),COEF(15,10)
      DIMENSION FORC(50),DISL(50)
      DIMENSION DTOT(15),DDTOT(15),FLEXF(10)
    1 FORMAT(≠   *** LIFTOFF *** WHEEL NO.≠,I3,≠ T=≠,G14.4)
    9 FORMAT(6G14.4)
    8 FORMAT (3F14.4,7I3)
   11 FORMAT (6G14.4//)
    7 FORMAT(3I14)
   20 FORMAT (20X,≠ THE INITIAL DEFLECTIONS ARE ≠)
   21 FORMAT (1H1)
   22 FORMAT(≠     TIME          FORCES          ACCELERATIONS   VELOCITIES
     1DISPLACEMENTS   INPUTS≠)
   23 FORMAT(≠     (SECS)          (LBS)              (GS)          (IN/SEC)
     1     (IN)        (IN)≠)
   24 FORMAT(14X,5G14.4)
   25 FORMAT(14X,5G14.4,//)
   35 FORMAT (11F9.5)
   37 FORMAT (F7.2,10F7.5)
      READ(5,7)NMAS,IPRINT,NMODES
      WRITE(6,7)NMAS,IPRINT,NMODES
      CALL READXY (DISL,FORC,NB,20)
      IP=1
      DO 100 I=1,22
      READ (5,8) K(I),C(I)
  100 CONTINUE
C *** SET THE VISCOUS COEFFICIENTS TO ZERO IF THIS HAS NOT ALREADY
C   * BEEN DONE IN THE INPUT DATA
      C(8)=0.0
      C(9)=0.0
      C(10)=0.0
      C(19)=0.0
      C(20)=0.0
      C(21)=0.0
      DO 649 I=1,22
      WRITE(6,9) K(I),C(I)
  649 CONTINUE
      DO 102 I=1,NMAS
      READ (5,8) M(I),INERT(I)
  102 WRITE(6,9) M(I),INERT(I)
      READ (5,8) INERT(6)
      WRITE(6,9) INERT(6)
      READ (5,8) INERT(7)
      WRITE(6,9) INERT(7)
      DO 103 I=1,8
      READ (5,8) R(I)
  103 WRITE(6,9) R(I)
C *** READ THE BILINEAR COEFFICIENTS COUL (SLIDING FRICTION
C   * COEFFICIENT) AND SL (SLOPE)
       READ(5,8) COUL,SL
```

```
      WRITE(6,9)COUL,SL
      READ (5,8) EPS,H
      WRITE(6,9) EPS,H
      NLOC=10
      NQ=34+2*NMODES
      EXTF=0.0
      EXTMR=0.0
      EXTMY=0.0
      EXTMT=0.0
      LIFT=0
      ICNT=NQ+2
      DO 201 I=1,ICNT
      VAR(I)=0.0
  201 DER(I)=0.0
      T=0.0
      DO 34 J=1,NMODES
      RMM(J)=1.0
      ZETA(J)=0.02
   34 CONTINUE
      READ (5,8) DT,TMAX ,FREQ
      WRITE (6,9) DT,TMAX,FREQ
      READ(5,8)AMPL,L,DELAY
      DELAY=0.5/FREQ
      WRITE(6,9)AMPL,L,DELAY
      JQ=1
      PI=3.1416
      Z01D=0.0
      Z02D=0.0
      DO 10 I=1,NMAS
   10 WT(I)=M(I)*386.
      DO 38 J=1,NMODES
       READ(5,37) RF(J),(COEF(I,J),I=1,10)
      WRITE(6,35) RF(J),(COEF(I,J),I=1,10)
   38 CONTINUE
      OMIN=2.0*PI*FREQ
      DO 33 J=1,NMODES
   33 OMEGA(J)=RF(J)*2.0*PI
      FLEXD1=0.0
      FLEXD2=0.0
      IF (NMODES .EQ. 0) GO TO 44
      DO 43 J=1,NMODES
      NM2=34+2*J
      WTA=WT(3)/4.0
      WTB=WTA*(COEF(2,J)+COEF(4,J)+COEF(7,J)+COEF(9,J))
      VAR(NM2)=-1.0/RMM(J)/OMEGA(J)/OMEGA(J)*WTB
      FLEXD1=FLEXD1+(COEF(2,J)+COEF(4,J))*VAR(NM2)/2.0
      FLEXD2=FLEXD2+(COEF(7,J)+COEF(9,J))*VAR(NM2)/2.0
   43 CONTINUE
   44 CONTINUE
      DI(1)=0.0
      DI(2)=DI(1)+(WT(2)+WT(3)/2.0)/(K(4)+K(6))
      DI(3)=DI(2)+WT(3)/2.0/(K(8)+K(10))
      DI(3)=DI(3)-FLEXD1
      DI(4)=0.0
      DI(5)=DI(4)+(WT(5)+WT(3)/2.0)/(K(15)+K(17))
      DI(6)=DI(5)+WT(3)/2.0/(K(19)+K(21))
      DI(6)=DI(6)-FLEXD2
```

```
      VAR(12)=-DI(1)
      VAR(14)=-DI(2)
      VAR(16)=-(DI(3)+DI(6))/2.0
      VAR(18)=-DI(4)
      VAR(20)=-DI(5)
      VAR(32)=(DI(6)-DI(3))/L
      EPS=VAR(16)-VAR(14)-EPS
      DI(3)=-VAR(16)
      DI(6)=-VAR(32)
  301 JPRINT=0
      WRITE(6,20)
      WRITE (6,11) (VAR(I),I=12,20,2),VAR(32)
      WRITE(6,21)
      WRITE(6,22)
      WRITE(6,23)
      DO 502 I=1,44
      DISP(I)=0.0
  502 VEL(I)=0.0
  999 CONTINUE
      Z01=SIN(OMIN *T)*AMPL
      Z02=SIN(OMIN *(T-DELAY))*AMPL
      DISP(7)=Z01
      DISP(11)=Z01
      SINTH=SIN(VAR(32))
      SINA=SIN(VAR(34))
      DO 700 I=1,5
      ICNT=20+I*2
      ICNT1=ICNT-1
      PHDCPH(I)=COS(VAR(ICNT))*VAR(ICNT1)
  700 SINPHI(I)=SIN(VAR(ICNT))
      THDCTH=COS(VAR(32))*VAR(31)
      VSA=H/2.0*(1.0-COS(VAR(26)))
      ADCA=COS(VAR(34))*VAR(33)
      DO 30 I=1,NLOC
      DTOT(I)=0.0
      DDTOT(I)=0.0
      DO 32 J=1,NMODES
      NM1=34+2*J-1
      NM2=NM1+1
      DTOT(I)=DTOT(I)+COEF(I,J)*VAR(NM2)
      DDTOT(I)=DDTOT(I)+COEF(I,J)*VAR(NM1)
   32 CONTINUE
   30 CONTINUE
      DISP(8)=VAR(14)-R(2)/2.*SINPHI(2)
      DISP(10)=VAR(4)
      DISP(12)=VAR(14)+R(2)/2.*SINPHI(2)
      DISP(15)=VAR(14)-R(3)/2.*SINPHI(2)
      DISP(16)=VAR(16)+L/2.*SINTH-R(3)/2.*SINPHI(3)-DTOT(2)+VSA
      DISP(17)=VAR(4)
      DISP(18)=VAR(6)+L/2.*SINA+H/2.*SINPHI(3)-DTOT(3)
      DISP(19)=VAR(14)+R(3)/2.*SINPHI(2)
      DISP(20)=VAR(16)+L/2.*SINTH+R(3)/2.*SINPHI(3)-DTOT(4)+VSA
      DISP(30)=VAR(20)-R(6)/2.*SINPHI(5)
      DISP(32)=VAR(10)
      DISP(34)=VAR(20)+R(6)/2.*SINPHI(5)
      DISP(37)=VAR(20)-R(7)/2.*SINPHI(5)
      DISP(38)=VAR(16)-L/2.*SINTH-R(7)/2.*SINPHI(3)-DTOT(7)+VSA
```

```
      DISP(39)=VAR(10)
      DISP(40)=VAR(6)-L/2.*SINA+H/2.*SINPHI(3)-DTOT(8)
      DISP(41)=VAR(20)+R(7)/2.*SINPHI(5)
      DISP(42)=VAR(16)-L/2.*SINTH+R(7)/2.*SINPHI(3)-DTOT(9)+VSA
      VEL(8)=VAR(13)-R(2)/2.*PHDCPH(2)
      VEL(10)=VAR(3)
      VEL(12)=VAR(13)+R(2)/2.*PHDCPH(2)
      VEL(15)=VAR(13)-R(3)/2.*PHDCPH(2)
      VEL(16)=VAR(15)+L/2.*THDCTH-R(3)/2.*PHDCPH(3)-DDTOT(2)
      VEL(17)=VAR(3)
      VEL(18)=VAR(5)+L/2.*ADCA+H/2.*PHDCPH(3)-DDTOT(3)
      VEL(19)=VAR(13)+R(3)/2.*PHDCPH(2)
      VEL(20)=VAR(15)+L/2.*THDCTH+R(3)/2.*PHDCPH(3)-DDTOT(4)
      VEL(30)=VAR(19)-R(6)/2.*PHDCPH(5)
      VEL(32)=VAR(9)
      VEL(34)=VAR(19)+R(6)/2.*PHDCPH(5)
      VEL(37)=VAR(19)-R(7)/2.*PHDCPH(5)
      VEL(38)=VAR(15)-L/2.*THDCTH-R(7)/2.*PHDCPH(3)-DDTOT(7)
      VEL(39)=VAR(9)
      VEL(40)=VAR(5)-L/2.*ADCA+H/2.*PHDCPH(3)-DDTOT(8)
      VEL(41)=VAR(19)+R(7)/2.*PHDCPH(5)
      VEL(42)=VAR(15)-L/2.*THDCTH+R(7)/2.*PHDCPH(3)-DDTOT(9)
      DO 701 I=1,22
      ICNT=2*I
      ICNT1=ICNT-1
701   F(I)=K(I)*(DISP(ICNT1)-DISP(ICNT))+C(I)*(VEL(ICNT1)-VEL(ICNT))
      RDIS1=DISP(17)-DISP(18)
      RDIS2=DISP(39)-DISP(40)
      CALL TABL(F(9),RDIS1,FORC,DISL,NB,1)
61    CALL TABL(F(20),RDIS2,FORC,DISL,NB,2)
C *** CALCULATE THE COULOMB FORCES. SPRINGS NO. 8,9,10 AND
C  * 19,20,21 ARE ASSUMED TO HAVE COULOMB DAMPING
      DO 204 I=9,20,11
      DO 205 ICNT=1,3,2
      ICNT1=I+ICNT-2
      NM=2*ICNT1
      NM1=NM-1
      NM2=I*2
      NM3=NM2-1
C *** CALCULATE RELATIVE VERTICAL AND LATERAL VELOCITIES VV AND VH
      VV=VEL(NM1)-VEL(NM)
      VH=VEL(NM3)-VEL(NM2)
C *** CALCULATE RESULTANT VELOCITY AND THE ANGLE AT WHICH IT ACTS
      VR=SQRT(VV*VV+VH*VH)
406   IF (ABS(VH) .GT. .0001) GO TO 357
      ANG=90.0/57.3
      GO TO 358
357   CONTINUE
      ANG=ATAN(VV/VH)
358   CONTINUE
C *** CALCULATION OF BILINEAR APPROXIMATION
      FR=SL*VR
      IF(FR .LT. COUL) GO TO 208
      FR=COUL
208   CONTINUE
C *** TAKE COMPONENTS OF RESULTANT FORCE. NOTE THAT THE LATERAL FORCE
C  * IS ADDED IN TWICE SINCE THE MODEL HAS ONLY ONE LATERAL
```

```
C  * SPRING FOR BOTH SNUBBERS ON EACH TRUCK.
      FH=SIGN(FR*COS(ANG),VH)
      FV=SIGN(FR*SIN(ANG),VV)
      F(I)=F(I)+FH
      F(ICNT1)=F(ICNT1)+FV
205   CONTINUE
204   CONTINUE
50    F(7)=0.0
52    F(11)=0.0
54    F(18)=0.0
56    F(22)=0.0
      DO 104 I=4,15,11
      DO 106 ICNT1=1,3,2
      ICNT2=I+ICNT1-1
      IF (F(ICNT2) .GT. 0.0) GO TO 108
      F(ICNT2)=0.
      IF (LIFT-1) 107,108,108
107   WRITE(6,1) ICNT2,T
      LIFT=1
108   CONTINUE
106   CONTINUE
104   CONTINUE
      DER(3)=(F(5)-F(9))/M(2)
      DER(5)=(F(9)+F(20)+EXTF)/M(3)
      DER(9)=(F(16)-F(20))/M(5)
      DER(13)=(F(4)+F(6)-F(7)-F(8)-F(10)-F(11))/M(2)-386.
      DER(15)=(F(7)+F(8)+F(10)+F(11)+F(18)+F(19)+F(21)+F(22))/M(3)-386.
      DER(19)=(F(15)+F(17)-F(18)-F(19)-F(21)-F(22))/M(5)-386.
      DER(23)=(R(2)/2.*(F(6)-F(4))+R(3)/2.*(F(8)-F(10))
     1+R(4)/2.*(F(7)-F(11)))/INERT(2)
      DER(25)=(R(3)/2.*(F(10)-F(8))+R(4)/2.*(F(11)-F(7))
     1 +R(7)/2.*(F(21)-F(19))+R(8)/2.*(F(22)-F(18))
     2  +H/2.*(F(9)+F(20))+EXTMR)/INERT(3)
      DER(29)=(R(6)/2.*(F(17)-F(15))+R(7)/2.*(F(19)-F(21))
     1 +R(8)/2.*(F(18)-F(22)))/INERT(5)
      DER(31)=(L/2.*(F(7)+F(8)+F(10)+F(11)-F(18)-F(19)-F(21)-F(22))
     1  +EXTMT)/INERT(6)
      DER(33)=(L/2.*(F(9)-F(20))+EXTMY)/INERT(7)
      DO 702 I=2,34,2
      ICNT=I-1
702   DER(I)=VAR(ICNT)
      DO 31 J=1,NMODES
      FLEXF(J)=0.0
      NM1=34+2*J-1
      NM2=NM1+1
      DO 60 I=1,5
      IC1=I+5
      IC2=I+6
      IC3=I+17
      FLEXF(J)=FLEXF(J)+COEF(I,J)*F(IC2)+COEF(IC1,J)*F(IC3)
60    CONTINUE
      DER(NM1)=(-2.0*ZETA(J)*OMEGA(J)*VAR(NM1)-OMEGA(J)**2.*VAR(NM2)
     1-FLEXF(J))/RMM(J)
      DER(NM2)=VAR(NM1)
31    CONTINUE
300   IF (JQ .EQ. 4) GO TO 910
      IF (T) 910,299,79
```

```
      79    JPRINT=JPRINT+1
            TIM(IP)=T
            PLOTM(IP,1)=VAR(16)
            PLOTM(IP,2)=F(4)
            PLOTM(IP,3)=VAR(32)*57.3
            D84=VAR(16)-DTOT(1)+VSA+DI(3)
            PLOTM(IP,4)=D84
            IP=IP+1
            IF (IPRINT-JPRINT) 299,299,910
     299    JPRINT=0
            DO 13 I=1,17
            ICNT=2*I
            IGNT=ICNT-1
            G(I)=DER(IGNT)/386.
            V(I)=VAR(IGNT)
      13    D(I)=VAR(ICNT)
            DO 14 I=1,5
            ICNT=I+5
      14    D(ICNT)=D(ICNT)+DI(I)
            D(16)=D(16)+DI(6)
            DO 15 I=11,17
            D(I)=D(I)*57.3
      15    G(I)=G(I)*386.
            WRITE(6,9)T,F(1),G(1),V(1),D(1),Z01
            WRITE(6,24) F(2),G(2),V(2),D(2),Z02
            DO 2 I=3,17
       2    WRITE (6,24) F(I),G(I),V(I),D(I)
            WRITE (6,25) (F(I),I=18,22)
            DO 39 J=1,NMODES
            NM1=34+2*J-1
            NM2=NM1+1
      39    WRITE (6,9) DER(NM1),VAR(NM1),VAR(NM2)
     910    IF (JQ .EQ. 3) GO TO 998
            CALL RUNKUT (JQ,VAR,DER,NQ,T,DT,TMAX)
            GO TO 999
     998    CONTINUE
            CALL EXIT
            END
```

SYMBOLIC REFERENCE MAP (R=1)

```
ENTRY POINTS
 6153  MAIN

VARIABLES      SN  TYPE             RELOCATION
10347  ADCA          REAL                              10323  AMPL       REAL
10360  ANG           REAL                              54700  C          REAL        ARRAY
55126  COEF          REAL         ARRAY                10302  COUL       REAL
54736  D             REAL         ARRAY                55537  DDTOT      REAL        ARRAY
10324  DELAY         REAL                              54510  DER        REAL        ARRAY
54762  DI            REAL         ARRAY                55436  DISL       REAL        ARRAY
54250  DISP          REAL         ARRAY                10320  DT         REAL
55520  DTOT          REAL         ARRAY                10370  D84        REAL
```

APPENDIX B - DESCRIPTION - LOADED TOFC PROGRAM

TOFC Configuration 2 consists of a van trailer and a platform trailer mounted on an 89 foot long flatcar. Any combination of vertical, lateral, yawing, rolling, and pitching motions can be simulated. The inputs may be sinusoidal or actual track histories. The program will predict all dynamic responses at any point as well as forces between elements as a function of time. The two masses representing the two trucks and the mass representing the rear suspension of the trailers can move vertically, laterally, and in roll. The mass representing the flatcar structure and the mass representing each trailer structure can have flexible modes superimposed by normal mode techniques. Each may move vertically, laterally, in roll, in pitch, and in yaw. Flexibility elements, shown as simple springs in the model, may incorporate any type of force characteristics and may be made linear or nonlinear as desired. These elements are usually specified in terms of force relationships as a function of relative velocities and relative displacements. The actual definition of one of these force relationships is considered encompassed in the nonlinear coefficient characteristic of this element. More information on the model, assumptions, limitations, and alternate modeling possibilities are given in Reference 8.

The method used was to add models for the trailers to the 11 dof general rail vehicle model described in References 6 and 7. The loaded TOFC program can be considered a specialized extension of the General Rail Vehicle program. The same methods are used in the analysis. The references quoted above provide details on analysis methods. Details on the addition of flexible modes are also provided in these references.

Supplementary sections of this appendix provide the following information on the loaded TOFC program:

1. Generalized Block Diagram
2. Listing
3. Nomenclature

4. Required Input

5. Sample Output

6. Cost Factors

This appendix shows the following example:

Configuration - Full up, TOFC, loaded van trailer front loaded platform trailer rear. One flexible mode for flatcar (for demonstration of handling flexibility only, more modes would normally be used.) Simulation of demonstration test 57: Sinusoidal in-phase input, dwell mode; Frequency = 2.04 Hz; Amplitude = -.145. Simulation time = 3 sec (6 cycles of simulated motion). Trailer flexibility has been ignored. Slight modifications to the program would be required to include trailer flexible modes.

On the following pages is a listing of the FORTRAN Computer Program.

```
      PROGRAM MAIN(INPUT,OUTPUT,TAPE5=INPUT,TAPE6=OUTPUT,TAPE44)
      REAL K,L,M,INERT(15)
      DIMENSION DISP(70),VEL(70),PHDCPH(10),SINPHI(10),R(10)
      DIMENSION F(30),DER(99),VAR(99),M(10),K(30),C(30)
      DIMENSION P(30),DT(10),WT(10),G(30),V(30)
      DIMENSION VDDTOT(10),VDTOT(10)
      DIMENSION TDDTOT(10),TDTOT(10)
      DIMENSION FF(10),RMR(10),OMEGA(10),ZETA(10),COFF(25,10)
      DIMENSION DTOT(25),DDTOT(25),FLEXF(10)
      DIMENSION IJ(27),IF(27),IG(27),L1(3),L2(4),L3(5),LL(5)
      DIMENSION IJ(27),INDF(10),JF(18),VAR1(10),SYM(18)
      DATA SYM/6*(-1.),12*(1.)/
      DATA JF/4,5,6,10,11,12,14,13,29,15,16,17,22,21,30,23,24,25/
      DATA INDF/4,5,6,10,14,15,18,22,23,26/
      DATA IJ/1,2,3,12,13,20,21,4,5,6,14,15,22,23,7,8,9,10,11,16,17,18,
     1 19,24,25,26,27/
      DATA IF/2,2,1,2,2,1,2,2,3*1,3,4,3,4,3,3*4,3,4,3,4,3,3*4/
      DATA IG/3*1,3*2,3*5,4,3,1,1,2,2,5,5,4,3,1,1,2,2,5,5,4,3/
      DATA L1/5HFRONT,4HREAR,6HFLATCA/
      DATA L2/1HR,5HTRUCK,4HAXLE,6HTRAILR/
      DATA L3/6H LAT. ,6H VERT.,6H YAW  ,6H PITCH,6H ROLL /
      DATA LL/5HTHETA,5HALPHA,3HVAN,7HFLATCAR,8HPLATFORM/
    1 FORMAT(≠   *** LIFTOFF *** WHEEL NO.≠,I3,≠ T=≠,G14.4)
    4 FORMAT(6G14.4)
    8 FORMAT (3F14.4,2I3)
   11 FORMAT (6G14.4//)
    7 FORMAT(4I14)
   20 FORMAT(//1X,≠INITIAL DEFLECTIONS≠)
   24 FORMAT(14X,5G14.4)
   25 FORMAT(14X,6G14.4,//)
   26 FORMAT(/)
   35 FORMAT(8F8.2)
  705 FORMAT(9G13.4)
  307 FORMAT(≠1NO. OF MASSES=≠,I3,≠    PRINT INTVL=≠,I3,≠    NO. OF MODES=
     1≠,I3,≠    NO. OF LOCS=≠,I3/)
  309 FORMAT(≠1FLATCAR HEIGHT≠,G14.4//T33,     ≠LENG. FROM CENT. OF GRAV.
     1≠,T77,≠LOCATION ON FLATCAR≠/T18,≠BODY HEIGHT≠,T36,≠TO AXLE≠,T49,≠T
     2O HITCH≠,T59,≠HITCH HEIGHT≠,T74,≠FRONT HITCH≠,T89,≠REAR HITCH≠)
  310 FORMAT(1X,2A6,5X,6G14.4)
  311 FORMAT(≠ INT.INTVL=≠,E10.3,T25,≠SIM.TIME=≠,F7.3,T45,≠FREQ=≠,F7.3)
  312 FORMAT(6X,≠AMPL=≠,F7.3,T27,≠LENGTH=≠,F8.2,T44,≠DELAY=≠,F7.4)
  313 FORMAT(T16,≠K≠,T29,≠C≠)
  314 FORMAT((6,3G14.4)
  315 FORMAT(//≠  MOD.≠,I13,≠MASS≠,T28,≠INERT≠)
  316 FORMAT(6X,A6,A8,G14.4)
  317 FORMAT(//≠  MODE  MODAL ACCEL.  MODAL VELOC.  MODAL DISPL.≠)
  318 FORMAT(/≠ FIGTHS=≠,8F7.2/)
  319 FORMAT(/≠ FLATCAR FLEXIBLE MODES≠)
  320 FORMAT(10G13.4/(13X,9G13.4))
  323 FORMAT(≠1TIME≠,F7.3,≠ SEC≠//T8,≠FORCE (LBS)≠,T43,≠ACCEL (GS)≠,T57,
     1 ≠V (IN/SEC)≠,T72,≠DISP (IN)≠,T86,≠INPUT≠)
  324 FORMAT(I4,G14.4,2X,3A6,5G14.4)
  325 FORMAT(/I4,G14.4,T43,≠RAD/SEC**2≠,T57,≠V(RAD/SEC)≠,T71,≠DISP (RAD)
     1≠)
```

```
 325    FORMAT(1X,3A6,2X,G14.4)
        READ(5,7)NMAS,IPRINT,NMODES,NLOC
        WRITE(6,307) NMAS,IPRINT,NMODES,NLOC
        WRITE(6,313)
        IP=1
        DO 100 I=1,24
        READ (5,8) R(I),C(I)
        WRITE(6,314) I,R(I),C(I)
 100    CONTINUE
        WRITE(6,315)
        DO 102 I=1,
        READ (5,8)  (I),INERT(I)
 102    WRITE(6,314) I, (I),INERT(I)
C  I8=ITV,I9=IAV,I10=ITF,I11=IAF,I12=ITP,I13=IAP,/T=THETA,A=ALPHA,F=FLATCAR,
C  V=VAN,P=PLATFORM
        ICNT=NMAS+1
        DO 203 I=I  T,13
        J=MOD(I,2)+1
        N=(I-2)/2
        READ (5,8)  INERT(I)
 203    WRITE(6,316) LI(J),LI(N),INERT(I)
        READ (5,4) R
        WRITE(6,3   ) R
        READ (5,4)V  ,VL  ,VL4
        READ(5,8)  V 1,VL1,VL2
        WRITE(6,31 ) L1(1),L2(4),VH,VL3,VL4,VH1,VL1,VL2
        READ (5,9)  VHR,VL3R,VL4R
        READ (5,9)  VH1R,VL1R,VL2R
        WRITE(6,31 ) L1(2),L2(4),VHR,VL3R,VL4R,VH1R,VL1R,VL2R
        DO 103 I=1,
 103    READ(5,8) R(I)
        WRITE(6,318)(R(I),I=1,R)
        NU=54+2*NMODES
        EXTF=0.0
        EXT  =0.0
        EXT Y=0.0
        EXT T=0.0
        XZMOM=113000000.
        XRMOM=113000000.
        XZ   M=50000.
        XR  MOM=50000.
        LIFT=0
        ICNT=NU+2
        DO 201 I=1,ICNT
        VAR(I)=0.0
 201    DER(I)=0.0
        DO 34  J=1,NMODES
        RMM(J)=1.0
        ZETA(J)=0.02
 34     CONTINUE
        READ (5,8) DT,TMAX ,FREQ
        WRITE(6,311) DT,TMAX,FREQ
        READ(5,8)AMPL,L,DELAY
        DELAY=0.5/FREQ
        WRITE(6,312) AMPL,L,DELAY
```

```
      J0=1
      T=0.0
      PI=3.1416
      Z010=0.0
      Z020=0.0
      DO 10 I=1,NMAS
10    WT(I)=W(I)*386.
      WRITE(6,315)
      DO 36 J=1,NMODE
      READ(5,35) RF(J)
      READ(5,35) (COEF(I,J),I=1,NLOC)
      WRITE(6,320) RF(J),(COEF(I,J),I=1,NLOC)
36    CONTINUE
      OMIN=2.0*PI*FREQ
      DO 33 J=1,NMODE
33    OMEGA(J)=RF(J)*2.0*PI
      FLFX01=0.0
      FLFX02=0.0
      FLFX03=0.0
      FLFX04=0.0
      FLFX05=0.0
      FLFX06=0.0
      C1=WT(3)/2.+WT(4)*(L/2.+VL2)/L+WT(5)*(L/2.+VL2+VL3)/L
     1   +WT(6)*(L/2.+VL2R)/L+WT(7)*(L/2.+VL2R+VL3R)/L
      C2=WT(3)/2.+WT(4)*(L/2.-VL2)/L+WT(5)*(L/2.-VL2-VL3)/L
     1   +WT(6)*(L/2.-VL2R)/L+WT(7)*(L/2.-VL2R-VL3R)/L
      C3=WT(4)+WT(5)*VL4/(VL3+VL4)
      C4=WT(5)*VL3/(VL3+VL4)
      C5=WT(6)+WT(7)*VL4R/(VL3R+VL4R)
      C6=WT(7)*VL3R/(VL3R+VL4R)
      IF (NMODES .EQ. 0) GO TO 44
      DO 43 J=1,NMODE
      NM2=54+2*J
      WT =C1/2.*COEF(1,J)+C1/2.* COEF(3,J)+C2/2.*COEF(4,J)+C2/2.
     1   *COEF(6,J)-C3/2.*COEF(10,J)-C3/2.*COEF(12,J)-C4*COEF(8,J)
     2 -C5/2.*COEF(16,J)-C5/2.*COEF(18,J)-C6*COEF(14,J)
      VAR(NM2)=-1.0/WMM(J)/OMEGA(J)/OMEGA(J)*WTB
      FLFX01=FLFX01+(COEF(1,J)+COEF(3,J))*VAR(NM2)/2.0
      FLFX02=FLFX02+(COEF(4,J)+COEF(6,J))*VAR(NM2)/2.0
      FLFX03=FLFX03+(COEF(10,J)+COEF(12,J))*VAR(NM2)/2.0
      FLFX04=FLFX04+COEF(8,J)*VAR(NM2)
      FLFX05=FLFX05+(COEF(16,J)+COEF(18,J))*VAR(NM2)/2.0
      FLFX06=FLFX06+COEF(14,J)*VAR(NM2)
43    CONTINUE
44    CONTINUE
      DI(1)=-(WT(1)+C1)/(K(1)+K(3))
      DI(2)=-(WT(2)+C2)/(K(7)+K(9))
      DI(3)=DI(1)-C1/(K(4)+K(6))+FLFX01
      DI(4)=DI(2)-C2/(K(10)+K(12))+FLFX02
      VAR(8)=DI(1)
      VAR(10)=DI(2)
      VAR(12)=(DI(3)+DI(4))/2.
      VAR(20)=(DI(3)-DI(4))/L
      DI(5)=VAR(12)-C3/(K(15)+K(17))+VAR(20)*VL2-FLFX03
      DI(6)=VAR(12)+VAR(20)*(VL1)-C4/K(13)-FLFX04
```

```
      DI(7)=DI(6)-(WT(5)*VL4/(VL3+VL4)/(K(18)+K(20)))
      VAR(28)=DI(6)
      VAR(30)=(VL3*DI(6)+VL4*DI(7))/(VL3+VL4)
      VAR(36)=(DI(6)-DI(7))/(VL3+VL4)
      DI(8)=VAR(12)-C5/(K(23)+K(25))+VAR(20)*VL2R-FLEXD5
      DI(9)=VAR(12)+VAR(20)*VL1R-C6/K(21)-FLEXD6
      DI(10)=DI(8)-(WT(7)*VL4R/(VL3R+VL4R)/(K(26)+K(28)))
      VAR(44)=DI(8)
      VAR(46)=(VL3R*DI(9)+DI(10)*VL4R)/(VL3R+VL4R)
      VAR(52)=(DI(9)-DI(10))/(VL3R+VL4R)
301   JPRINT=0
      WRITE(6,20)
      DO 302 J=1,10
      I=INDE(J)
      I1=I1(I)
      I2=I2(I)
      I3=I3(I)
      I=I*2
      VARI(J)=VAR(I)
302   WRITE(6,326) L1(I1),L2(I2),L3(I3),VAR(I)
      DO 502 I=1,60
      DISP(I)=0.0
502   VEL(I)=0.0
      DO 202 I=1,8
      TOTDT(I)=0.0
      TODTDT(I)=0.0
      VDTDT(I)=0.0
202   VDDTDT(I)=0.0
999   CONTINUE
      Z01=SIN(OMIN*T)*AMPL
      Z02=SIN(OMIN*(T-DELAY))*AMPL
      DISP(1)=Z01
      DISP(5)=Z01
      SINTH=SIN(VAR(20))
      SINA=SIN(VAR(22))
      VSINTH=SIN(VAR(36))
      VSINA=SIN(VAR(38))
      TSINTH=SIN(VAR(52))
      TSINA=SIN(VAR(54))
      DO 700 I=1,3
      ICNT=12+I*2
      ICNT1=ICNT-1
      PHDCPH(I)=COS(VAR(ICNT))*VAR(ICNT1)
700   SINPHI(I)=SIN(VAR(ICNT))
      DO 703 I=4,5
      ICNT=24+I*2
      ICNT1=ICNT-1
      PHDCPH(I)=COS(VAR(ICNT))*VAR(ICNT1)
703   SINPHI(I)=SIN(VAR(ICNT))
      DO 704 I=6,7
      ICNT=36+I*2
      ICNT1=ICNT-1
      PHDCPH(I)=COS(VAR(ICNT))*VAR(ICNT1)
704   SINPHI(I)=SIN(VAR(ICNT))
      VSA=H/2.0*(1.0-COS(VAR(18)))
```

```
      THDCTH=COS(VAR(20))*VAR(19)
      ADCA=COS(VAR(22))*VAR(21)
      VTHDCT=COS(VAR(36))*VAR(35)
      VADCA=COS(VAR(38))*VAR(37)
      TTHDCT=COS(VAR(52))*VAR(51)
      TADCA=COS(VAR(54))*VAR(53)
      DO 30 I=1,NLOC
      DTOT(I)=0.0
      DDTOT(I)=0.0
      DO 32 J=1,NMODES
      NM1=54+2*J-1
      NM2=NM1+1
      DTOT(I)=DTOT(I)+COEF(I,J)*VAR(NM2)
      DDTOT(I)=DDTOT(I)+COEF(I,J)*VAR(NM1)
32    CONTINUE
30    CONTINUE
      DISP(2)=VAR(8)-R(1)/2.*SINPHI(1)
      DISP(4)=VAR(2)
      DISP(6)= VAR(8)+R(1)/2.*SINPHI(1)
      DISP(7)=VAR(8)-R(2)/2.*SINPHI(1)
      DISP(8)=VAR(12)+L/2.*SINTH-R(2)/2.*SINPHI(3)-DTOT(1)+VSA
      DISP(9)=VAR(2)
      DISP(10)=VAR(6)+L/2.*SINA+H/2.*SINPHI(3)-DTOT(2)
      DISP(11)=VAR(8) +R(2)/2.*SINPHI(1)
      DISP(12)=VAR(12)+L/2.*SINTH+R(2)/2.*SINPHI(3)-DTOT(3)+VSA
      DISP(14)=VAR(10)-R(3)/2.*SINPHI(2)
      DISP(16)=VAR(4)
      DISP(18)=VAR(10)+R(3)/2.*SINPHI(2)
      DISP(19)=VAR(10)-R(4)/2.*SINPHI(2)
      DISP(20)=VAR(12)-L/2.*SINTH-R(4)/2.*SINPHI(3)-DTOT(4)+VSA
      DISP(21)=VAR(4)
      DISP(22)=VAR(6)-L/2.*SINA+H/2.*SINPHI(3)-DTOT(5)
      DISP(23)=VAR(10)+R(4)/2.*SINPHI(2)
      DISP(24)=VAR(12)-L/2.*SINTH+R(4)/2.*SINPHI(3)-DTOT(6)+VSA
      DISP(25)=VAR(12)+VL1*SINTH-DTOT(8)+VSA
      DISP(26)=VAR(30)+VL4    *VSINTH-VDTOT(1)
      DISP(27)=VAR(6)+VL1*SINA-H/2.*SINPHI(3)-DTOT(7)-VH1/2.*SINPHI(3)
      DISP(28)=VAR(26)+VL4*VSINA+VH/2.*SINPHI(5)-VDTOT(2)+VH1/2.*
     1 SINPHI(5)
      DISP(29)=VAR(12)-R(5)/2.*SINPHI(3)+ VL2*SINTH-DTOT(10)+VSA
      DISP(30)=VAR(28)-R(5)/2.*SINPHI(4)
      DISP(31)=VAR(6)+VL2*SINA-H/2.*SINPHI(3)-DTOT(11)
      DISP(32)=VAR(24)
      DISP(33)=VAR(12)+VL2*SINTH+R(5)/2.*SINPHI(3)-DTOT(12)+VSA
      DISP(34)=VAR(28)+R(5)/2.*SINPHI(4)
      DISP(35)=VAR(28)-R(6)/2.*SINPHI(4)
      DISP(36)=VAR(30)-R(6)/2.*SINPHI(5)-VL3    *VSINTH-VDTOT(3)
      DISP(37)=VAR(24)-VH1/2.*SINPHI(4)
      DISP(38)=VAR(26)-VL3*VSINA+(VH+VH1)/2.*SINPHI(5)-VDTOT(4)
      DISP(39)=VAR(28)+R(6)/2.*SINPHI(4)
      DISP(40)=VAR(30)+R(6)/2.*SINPHI(5)-VL3    *VSINTH-VDTOT(5)
      DISP(41)=VAR(12)+VL1R*SINTH-DTOT(14)+VSA
      DISP(42)=VAR(46)+VL4R   *TSINTH-TDTOT(1)
      DISP(43)=VAR(6)+VL1R*SINA-(H/2.+VH1R/2.)*SINPHI(3)-DTOT(13)
      DISP(44)=VAR(42)+VL4R*TSINA+VHR/2.*SINPHI(7)-TDTOT(2)+VH1R/2.*
```

```
     1 SINPHI(7)
      DISP(45)=VAR(12)-R(7)/2.*SINPHI(3)+VL2R*SINTH-DTOT(16)+VSA
      DISP(46)=VAR(44)-R(7)/2.*SINPHI(6)
      DISP(47)=VAR(6)+VL2R*SINA-H/2.*SINPHI(3)-DTOT(17)
      DISP(48)=VAR(43)
      DISP(49)=VAR(12)+VL2R*SINTH+R(7)/2.*SINPHI(3)-DTOT(18)+VSA
      DISP(50)=VAR(44)+R(7)/2.*SINPHI(6)
      DISP(51)=VAR(44)-R(8)/2.*SINPHI(6)
      DISP(52)=VAR(46)-R(8)/2.*SINPHI(7)-VL3R   *TSINTH-TDTOT(3)
      DISP(53)=VAR(43)-VH1R/2.*SINPHI(6)
      DISP(54)=VAR(42)-VL3R*TSINA+(VHR+VH1R)/2.*SINPHI(7)-TDTOT(4)
      DISP(55)=VAR(44)+R(8)/2.*SINPHI(6)
      DISP(56)=VAR(46)+R(8)/2.*SINPHI(7)-VL3R   *TSINTH-TDTOT(5)
      XZMOM=XZKMOM*(VAR(16)-DTOT( 9)-VAR(34))
     1 +XZCMOM*(VAR(17)-DDTOT( 9)-VAR(33))
      XRMOM=XRKMOM*(VAR(18)-DTOT(15)-VAR(50))
     1 +XRCMOM*(VAR(17)-DDTOT(15)-VAR(49))
      VEL(2)=VAR(7)-R(1)/2.*PHDCPH(1)
      VEL(4)=VAR(1)
      VEL(6)=VAR(7)+R(1)/2.*PHDCPH(1)
      VEL(7)=VAR(7)-R(2)/2.*PHDCPH(1)
      VEL(8)  =VAR(11)+L/2.*THDCTH-R(2)/2.*PHDCPH(3)-DDTOT(1)
      VEL(9)=VAR(1)
      VEL(10)=VAR(5)+L/2.*ADCA+H/2.*PHDCPH(3)-DDTOT(2)
      VEL(11)=VAR(7)+R(2)/2.*PHDCPH(1)
      VEL(12)=VAR(11)+L/2.*THDCTH+R(2)/2.*PHDCPH(3)-DDTOT(3)
      VEL(14)=VAR(9)-R(3)/2.*PHDCPH(2)
      VEL(16)=VAR(3)
      VEL(18)=VAR(9)+R(3)/2.*PHDCPH(2)
      VEL(19)=VAR(9)-R(4)/2.*PHDCPH(2)
      VEL(20)=VAR(11)-L/2.*THDCTH-R(4)/2.*PHDCPH(3)-DDTOT(4)
      VEL(21)=VAR(3)
      VEL(22)=VAR(5)-L/2.*ADCA+H/2.*PHDCPH(3)-DDTOT(5)
      VEL(23)=VAR(9)+R(4)/2.*PHDCPH(2)
      VEL(24)=VAR(11)-L/2.*THDCTH+R(4)/2.*PHDCPH(3)-DDTOT(6)
      VEL(25)=VAR(11)+VL1*THDCTH-DDTOT(8)
      VEL(26)=VAR(29)+VL4   *VTHDCT-VDDTOT(1)
      VEL(27)=VAR(5)+VL1*ADCA-H/2.*PHDCPH(3)-DDTOT(7)-VH1/2.*PHDCPH(3)
      VEL(28)=VAR(25)+VL4*VADCA+(VH+VH1)/2.*PHDCPH(5)-VDDTOT(2)
      VEL(29)=VAR(11)-R(5)/2.*PHDCPH(3)+VL2*THDCTH-DDTOT(10)
      VEL(30)=VAR(27)-R(5)/2.*PHDCPH(4)
      VEL(31)=VAR(5)+VL2*ADCA-H/2.*PHDCPH(3)-DDTOT(11)
      VEL(32)=VAR(23)
      VEL(33)=VAR(11)+R(5)/2.*PHDCPH(3)+VL2*THDCTH-DDTOT(12)
      VEL(34)=VAR(27)+R(5)/2.*PHDCPH(4)
      VEL(35)=VAR(27)-R(6)/2.*PHDCPH(4)
      VEL(36)=VAR(29)-R(6)/2.*PHDCPH(5)-VL3   *VTHDCT-VDDTOT(3)
      VEL(37)=VAR(23)-VH1/2.*PHDCPH(4)
      VEL(38)=VAR(25)-VL3*VADCA+(VH+VH1)/2.*PHDCPH(5)-VDDTOT(4)
      VEL(39)=VAR(27)+R(6)/2.*PHDCPH(4)
      VEL(40)=VAR(29)+R(6)/2.*PHDCPH(5)-VL3   *VTHDCT-VDDTOT(5)
      VEL(41)=VAR(11)+VL1R*THDCTH-DDTOT(14)
      VEL(42)=VAR(45)+VL4R *TTHDCT-TDDTOT(1)
      VEL(43)=VAR(5)+VL1R*ADCA-H/2.*PHDCPH(3)-DDTOT(13)-VH1R/2.*
     1 PHDCPH(3)
```

```
      VEL(44)=VAR(41)+VL4R*TADCA+(VHR+VH1R)/2.*PHDCPH(7)-TDDTOT(2)
      VEL(45)=VAR(11)-R(7)/2.*PHDCPH(3)+VL2R*THDCTH-DDTOT(16)
      VEL(46)=VAR(43)-R(7)/2.*PHDCPH(6)
      VEL(47)=VAR(5)+VL2R*ADCA-H/2.*PHDCPH(3)-DDTOT(17)
      VEL(48)=VAR(39)
      VEL(49)=VAR(11)+R(7)/2.*PHDCPH(3)+VL2R*THDCTH-DDTOT(18)
      VEL(50)=VAR(43)+R(7)/2.*PHDCPH(6)
      VEL(51)=VAR(43)-R(8)/2.*PHDCPH(6)
      VEL(52)=VAR(45)-R(8)/2.*PHDCPH(7)-VL3R *TTHDCT-TDDTOT(3)
      VEL(53)=VAR(39)-VH1R/2.*PHDCPH(6)
      VEL(54)=VAR(41)-VL3R*TADCA+(VHR+VH1R)/2.*PHDCPH(7)-TDDTOT(4)
      VEL(55)=VAR(43)+R(8)/2.*PHDCPH(6)
      VEL(56)=VAR(45)+R(8)/2.*PHDCPH(7)-VL3R *TTHDCT-TDDTOT(5)
      DO 701 I=1.28
      ICNT=2*I
      ICNT1=ICNT-1
701   F(I)=K(I)*(DISP(ICNT1)-DISP(ICNT))+C(I)*(VEL(ICNT1)-VEL(ICNT))
      DO 105 J=1.7.6
      DO 104 I=1.4.3
      DO 106 ICNT1=1.3.2
      ICNT2=J+ICNT1+I-2
      IF (F(ICNT2) .GT. 0.0) GO TO 108
      F(ICNT2)=0.
      IF (LIFT-1) 107.108.108
107   WRITE(6.1) ICNT2.T
      LIFT=1
108   CONTINUE
106   CONTINUE
104   CONTINUE
105   CONTINUE
      DO 52 IC1=1.9.8
      DO 50 IC2=14.16.2
      I=IC1+IC2
      IF (F(I) .GT. 0.0) GO TO 51
      F(I)=0.0
      WRITE(6.1) I.T
51    CONTINUE
50    CONTINUE
52    CONTINUE
      DER(1)=(F(2)-F([illegible]))/M(1)
      DER(3)=(F([illegible])-F(11))/M(2)
      DER(5)=(F(5)+F(11)-F(14)-F(16)-F(22)-F(24)+EXTF)/M(3)
      DER(7)=(F(1)+F(3)-F(4)-F(6))/M(2)-386.
      DER(9)=(F(7)+F(9)-F(10)-F(12))/M(2)-386.
      DER(11)=(F(4)+F(6)+F(10)+F(12)-F(13)-F(15)-F(17)-F(21)-F(23)
     1 -F(25))/M(3)-386.
      DER(13)=(R(1)/2.*(F(3)-F(1))+R(2)/2.*(F(4)-F(6)))/INERT(1)
      DER(15)=(R(3)/2.*(F(9)-F(7))+R(4)/2.*(F(10)-F(12)))/INERT(2)
      DER(17)=(R(2)/2.*(F(6)-F(4))+R(4)/2.*(F(12)-F(10))+H/2.*(F(5)
     1 +F(11)+F(14)+F(16))-XZMOM+R(5)/2.*(F(15)-F(17))+EXTMR+F(14)*
     2  VH1/2.+(H+VH1 )/2.*F(22)+H*F(24)-XRMOM+R(7)/2.*(F(23)-F(25))
     3  )/INERT(3)
      DER(19)=(L/2.*(F(4)+F(6)-F(10)-F(12))-VL2*(F(15)+F(17))
     1 -VL1*F(13)-VL2R*(F(23)+F(25))-VL1R*F(21)+EXTMT)/INERT(10)
      DER(21)=(L/2.*(F(5)-F(11))-F(16)*VL2-F(14)*VL1-F(24)*VL2R
```

```
     1   -F(22)*VL1R+FXTMY)/INERT(11)
      DER(23)=(F(16)-F(14))/M(4)
      DER(25)=(F(19)+F(14))/M(5)
      DER(27)=(F(15)+F(17)-F(18)-F(20))/M(4)-386.
      DER(29)=(F(16)+F(2?)+F(13))/M(5)-386.
      DER(31)=(R(6)/2.*(F(17)-F(15))+R(6)/2.*(F(18)-F(20)))/INERT(4)
      DER(33)=(R(6)/2.*(F(20)-F(18))+(F(14)+F(19))*(VH+VH1)/2.+XZMOM)/
     1 INERT(5)
      DER(35)=(F(13)*VL4-F(18)*VL3-F(20)*VL3)/INERT(8)
      DER(37)=(F(14)*VL4-F(19)*VL3)/INERT(9)
      DER(39)=(F(24)-F(27))/M(6)
      DER(41)=(F(22)+F(27))/M(7)
      DER(43)=(F(23)+F(25)-F(26)-F(28))/M(6)-386.
      DER(45)=(F(21)+F(26)+F(28))/M(7)-386.
      DER(47)=(R(7)/2.*(F(25)-F(23))+R(8)/2.*(F(26)-F(28)))/INERT(6)
      DER(49)=(XRMOM+R(9)/2.*(F(28)-F(26))+(F(22)+F(27))*(VHR+VH1R)/2.
     1     )/INERT(7)
      DER(51)=(F(21)*VL4R-(F(26)+F(28))*VL3R)/INERT(12)
      DER(53)=(F(22)*VL4R-F(27)*VL3R)/INERT(13)
      DO 702 I=2,54,2
      ICNT=I-1
702   DER(I)=VAR(ICNT)
      F(  )=XZMOM
      F(50)=XRMOM
      DO 31 J=1,NMODE
      FLEXF(J)=0.0
      NM1=54+2*J-1
      NM2=NM1+1
      DO 60 I=1,1?
      N=IF(I)
60    FLEXF(J)=FLEXF(J)-COFF(I,J)*F(N)*SYN(I)
      DER(NM1)=(-2.0*ZETA(J)*OMEGA(J)*VAR(NM1)-OMEGA(J)**2.*VAR(NM2)
     1-FLEXF(J))/AMM(J)
      DER(NM2)=VAR(NM1)
31    CONTINUE
300   IF (JQ .EQ. 4) GO TO 910
      IF (T) 910,299,79
79    JPRINT=JPRINT+1
      IF (IPRINT-JPRINT) 299,299,910
299   JPRINT=0
      DO 13 I=1,27
      ICNT=2*I
      IGNT=ICNT-1
      G(I)=DER(IGNT)
      IF(IG(I).LT.3) G(I)=G(I)/386.
      V(I)=VAR(IGNT)
13    D(I)=VAR(ICNT)
      DO 14 J=1,1
      I=INDF(J)
14    D(I)=D(I)-VARI(J)
      WRITE(6,323) T
      I=1
      I5=15
      WRITE(6,324) I,F(1),L1(1),L2(2),L3(1),G(1),V(1),D(1),Z01
      DO 2 J=2,27
```

```
      I=IJ(J)
      JJ=J
      I1=I0(I)
      I2=IF(I)
      I3=IS(I)
      IF (J.GT.14)  JJ= IJ+1
      WRITE(6,324)  JJ,F(J),L1(I1),L2(I2),L3(I3),S(I),V(I),D(I)
      IF(J.EQ.14)  WRITE(6,325)  15,F(15)
    2 CONTINUE
      WRITE(6,317)
      DO 34  J=1,NMODE
      NM1=54+2*J-1
      NM2=NM1+1
   34 WRITE(6,314)  J,DER(NM1),VAR(NM1),VAR(NM2)
      WRITE(6,26)
  910 IF (IW .EQ. 3)  GO TO 998
      CALL RUNKUT (JQ,VAR,DER,NQ,T,DT,TMAX)
      GO TO 999
  998 CONTINUE
      CALL EXIT
      END
```

NOMENCLATURE

The variables used in the Configuration 2 program are defined as follows:

ADCA = ALPHA DOT (Yaw angular velocity of flatcar) times cosine of alpha

AMPL = Amplitude of input (if sinusoidal)

C = Array of damping coefficients

COEF = Array of influence coefficients in flexible modes

C1-C6 = Load on individual points at time zero (used to calculate initial deflections)

D = Array of deflections for printout

DDTOT = Velocity contributions of flexibility at specific flatcar locations $(\sum_j \mu_{ij} \dot{v}_j)$

DELAY = Time delay between input at the front truck and the same input at the rear truck

DER = Array of derivatives to be integrated (see explanation table next page)

DI = Array of initial deflections at time zero

DISP = Array of deflections at 56 locations as numbered in Figure

DT = Integration Interval

DTOT = Displacement contributions of flexibility at specific flatcar locations $(\sum_j \mu_{ij} v_j)$

EXTF = Provision for external lateral force acting on flatcar (unused)

EXTMR = Provision for external moment causing flatcar roll (unused)

EXTMT = Provision for external moment causing flatcar pitch (unused)

EXTMY = Provision for external moment causing flatcar yaw (unused)

F = Array of 28 forces given by circled numbers in Figure

FLEXD1-FLEXD6 = Initial displacement contributions from flatcar flexible modes

FLEXF = Storage array for force inputs to flexible modes

FREQ = Frequency associated with input, Hertz

G = Array of accelerations for printout

H = Height of flatcar

I, ICNT, ICNT1, ICNT2, IC1, IC2, ID, IE, IG, IGNT, IJ, INDF = Integer Counters

INERT = Array of moments of inertia

IP = Counter associated with plots (if used)

IPRINT = Print interval specification

I1-I5 = Integer counters

J, JF, JJ = Integer counters

JPRINT = Print interval counter

JQ = Output of RUNKUT that tells main program the status of the calculation

K = Array of spring constants

L = Length of flatcar body

LIFT, LL, L1, L2, L3 = Miscellaneous integers

M = Mass

N = Integer counter

NLOC = Number of locations on flatcar at which influence coefficients are defined

NMAS = Number of masses in math model

NMODES = Number of flexible modes

NM1-NM2 = Integer counters, mode number

NQ = Number of differential equations to be integrated by RUNKUT

OMEGA = Modal frequencies in radians

OMIN = Input frequency in radians

PHDCPH = PHI DOT (roll angular velocity) times cosine of PHI

PI = 3.1416

R = width of elements

RF = Modal frequencies in hertz

RMM = Modal masses (normalized to one)

SINA = Sine of alpha (flatcar yaw angle)

SINPHI = Sine of phi (roll angle)

SINTH = Sine of theta (pitch angle)

SYN = Matrix of signs

T = Time

TADCA = ADCA term for rear trailer

TDDTOT = Provision for trailer flexible velocity contributions (unused)

TDTDT = Provision for trailer flexible displacements (unused)

THDCTH = Theta dot (pitch angular velocity of flatcar) times cosine of theta

TMAX = Desired simulation time

TSINA = Sine term for trailer

TSINTH = SINTH term for trailer

TTHDCT = THDCTH term for trailer

V = Array of velocities for output

VADCA = ADCA term for van (i.e. front trailer)

VAR = Array of integrated values (see explanation next page)

VARI = Value of VAR at time zero (initial condition)

VDDTOT = Provision for van flexible velocity contribution (unused)

VDTOT = Provision for van flexible displacement contribution (unused)

VEL = Array of velocities at 56 locations as numbered in Figure

VH = Height of van trailer (i.e. front trailer)

VHR = Height of rear trailer

VH1 = Distance from top of flatcar to bottom of van (assumed same front and rear of trailer)

VH1R = Distance from top of flatcar to bottom of rear trailer (assumed same front and rear of trailer)

VL1 = Distance, flatcar c.g. to front trailer hitch

VL1R = Distance, flatcar c.g. to rear trailer hitch (use negative value if rear hitch is behind c.g. of flatcar)

VL2 = Distance, flatcar c.g. to rear suspension of front trailer

VL2R = Distance, flatcar c.g. to rear suspension of rear trailer (use negative value if behind c.g. of flatcar)

VL3 = Distance, c.g. to rear suspension, front trailer

VL3R = Distance, c.g. to rear suspension, rear trailer

VL4 = Distance, c.g. to hitch, front trailer

VL4R = Distance, c.g. to rear suspension, rear trailer

VSA = "Vertical Small Angle" term, one of the second order terms equal to H/2 (i−cos φ)

VSINA = SINA term for van trailer (front trailer)

VSINTH = SINTH term for van trailer

VTHDCT = THDCTH term for van trailer

WT = Weight of mass

WTB = Storage value used for calculating initial condition of each mode

XRCMOM = Damping coefficient, moment spring simulating hitch, rear trailer

XRKMOM = Moment spring constant, hitch simulation, rear trailer

XRMOM = Bending moment, hitch, rear trailer

XZCMOM = Damping coefficient, moment spring simulating hitch, front trailer

XZKMOM = Moment spring constant, hitch simulation, front trailer

XZMOM = Bending moment, hitch, front trailer

ZETA = Damping ratio, flatcar flexible modes

Z01−Z02 = Input displacements at wheel/rail interface

Z01D,Z02D = Provision for time derivative of input displacements at wheel/rail interface (unused)

The elements in the VAR and DER arrays are as follows. The descriptions refer to the math model of Figure . Dots over a symbol indicate differentiation with respect to time.

DER (1)	$= \ddot{X}_1$	VAR (1)	$= \dot{X}_1$
DER (2)	$= \dot{X}_1$	VAR (2)	$= X_1$
DER (3)	$= \ddot{X}_2$	VAR (3)	$= \dot{X}_2$
DER (4)	$= \dot{X}_2$	VAR (4)	$= X_2$
DER (5)	$= \ddot{X}_3$	VAR (5)	$= \dot{X}_3$
DER (6)	$= \dot{X}_3$	VAR (6)	$= X_3$
DER (7)	$= \ddot{Z}_1$	VAR (7)	$= \dot{Z}_1$
DER (8)	$= \dot{Z}_1$	VAR (8)	$= Z_1$
DER (9)	$= \ddot{Z}_2$	VAR (9)	$= \dot{Z}_2$
DER (10)	$= \dot{Z}_2$	VAR (10)	$= Z_2$
DER (11)	$= \ddot{Z}_3$	VAR (11)	$= \dot{Z}_3$
DER (12)	$= \dot{Z}_3$	VAR (12)	$= Z_3$
DER (13)	$= \ddot{\varphi}_1$	VAR (13)	$= \dot{\varphi}_1$
DER (14)	$= \dot{\varphi}_1$	VAR (14)	$= \varphi_1$
DER (15)	$= \ddot{\varphi}_2$	VAR (15)	$= \dot{\varphi}_2$
DER (16)	$= \dot{\varphi}_2$	VAR (16)	$= \varphi_2$
DER (17)	$= \ddot{\varphi}_3$	VAR (17)	$= \dot{\varphi}_3$
DER (18)	$= \dot{\varphi}_3$	VAR (18)	$= \varphi_3$
DER (19)	$= \ddot{\theta}$	VAR (19)	$= \dot{\theta}$
DER (20)	$= \dot{\theta}$	VAR (20)	$= \theta$
DER (21)	$= \ddot{\alpha}$	VAR (21)	$= \dot{\alpha}$
DER (22)	$= \dot{\alpha}$	VAR (22)	$= \alpha$

DER (23) $= \ddot{X}_4$

DER (24) $= \dot{X}_4$

DER (25) $= \ddot{X}_5$

DER (26) $= \dot{X}_5$

DER (27) $= \ddot{Z}_4$

DER (28) $= \dot{Z}_4$

DER (29) $= \ddot{Z}_5$

DER (30) $= \dot{Z}_5$

DER (31) $= \ddot{\varphi}_4$

DER (32) $= \dot{\varphi}_4$

DER (33) $= \ddot{\varphi}_5$

DER (34) $= \dot{\varphi}_5$

DER (35) $= \ddot{\theta}_v$

DER (36) $= \dot{\theta}_v$

DER (37) $= \ddot{\alpha}_v$

DER (38) $= \dot{\alpha}_v$

DER (39) $= \ddot{X}_6$

DER (40) $= \dot{X}_6$

DER (41) $= \ddot{X}_7$

DER (42) $= \dot{X}_7$

DER (43) $= \ddot{Z}_6$

DER (44) $= \dot{Z}_6$

VAR (23) $= \dot{X}_4$

VAR (24) $= X_4$

VAR (25) $= \dot{X}_5$

VAR (26) $= X_5$

VAR (27) $= \dot{Z}_4$

VAR (28) $= Z_4$

VAR (29) $= \dot{Z}_5$

VAR (30) $= Z_5$

VAR (31) $= \dot{\varphi}_4$

VAR (32) $= \varphi_4$

VAR (33) $= \dot{\varphi}_5$

VAR (34) $= \varphi_5$

VAR (35) $= \dot{\theta}_v$

VAR (36) $= \theta_v$

VAR (37) $= \dot{\alpha}_v$

VAR (38) $= \alpha_v$

VAR (39) $= \dot{X}_6$

VAR (40) $= X_6$

VAR (41) $= \dot{X}_7$

VAR (42) $= X_7$

VAR (43) $= \dot{Z}_6$

VAR (44) $= Z_6$

DER (45)	$= \ddot{Z}_7$	VAR (45)	$= \dot{Z}_7$
DER (46)	$= \dot{Z}_7$	VAR (46)	$= Z_7$
DER (47)	$= \ddot{\varphi}_6$	VAR (47)	$= \dot{\varphi}_6$
DER (48)	$= \dot{\varphi}_6$	VAR (48)	$= \varphi_6$
DER (49)	$= \ddot{\varphi}_7$	VAR (49)	$= \dot{\varphi}_7$
DER (50)	$= \dot{\varphi}_7$	VAR (50)	$= \varphi_7$
DER (51)	$= \ddot{\theta}_T$	VAR (51)	$= \dot{\theta}_T$
DER (52)	$= \dot{\theta}_T$	VAR (52)	$= \theta_T$
DER (53)	$= \ddot{\alpha}_T$	VAR (53)	$= \dot{\alpha}_T$
DER (54)	$= \dot{\alpha}_T$	VAR (54)	$= \alpha_T$

REQUIRED DATA INPUT

The following page summarizes the inputs that are required. An explanation follows.

NO. OF MASSES= 7 PRINT INTVL= 30 NO. OF MODES= 1 NO. OF LOCS= 18

	K	C
1	.1820E+06	250.0
2	.9500E+05	333.0
3	.1820E+06	250.0
4	.2250E+05	1400.
5	.1000E+06	1400.
6	.2250E+05	1400.
7	.1820E+06	250.0
8	.9500E+05	333.0
9	.1820E+06	250.0
10	.2250E+05	1400.
11	.1000E+06	1400.
12	.2250E+05	1400.

HERE PUT CONSTANTS AND COEFFICIENTS FOR FLEXIBILITY ELEMENTS 13-28 WHEN THEY BECOME AVAILABLE.

NUM.	MASS	INERT
1	22.33	.22[illegible]E+05
2	22.33	.22[illegible]E+05
3	155.2	.10[illegible]E+05
4	6.174	.200[illegible]E+0[illegible]
5	152.5	.255[illegible]E+06
6	7.13	.171[illegible]E+05
7	148.9	.102[illegible]E+06
THETA VAN		.294[illegible]E+07
ALPHA VAN		.31[illegible]E+07
THETA FLATCAR		.10[illegible]0E+0[illegible]
ALPHA FLATCAR		.10[illegible]0E+0[illegible]
THETA PLATFORM		.131[illegible]E+07
ALPHA PLATFORM		.131[illegible]E+07

FLATCAR HEIGHT 16.00

	BODY HEIGHT	LENG. FROM CENT. OF GRAV. TO AXLE	TO HITCH	HITCH HEIGHT
FRONT TRAILER	56.40	131.4	189.7	47.00
REAR TRAILER	37.80	115.4	2[illegible]3.6	47.00

LOCATION ON FLATCAR

FRONT HITCH	REAR HITCH
469.0	148.0
-89.00	-413.0

WIDT-S= 58.00 79.00 58.00 79.00 62.25 43.50 52.25 43.50

INT.INTVL= .4000E-02 SIM.TIME= 3.000 FREQ= 2.044
AMPL= .145 LENGTH= 742.00 DELAY= .2446

FLATCAR FLEXIBLE MODES

4.620	.6846E-01	0.		.6846E-01	.8248E-01	0.
	.8248E-01	0.		.1391	0.	
	-.6265E-01	0.		-.6265E-01	0.	-.7692E-01
	0.		.9251E-01	0.	.9251E-01	

EXPLANATION:

No. of masses = >as shown in math model

Print Interval - optional. If this is set to 30, the dynamic responses for every 30th time step (i.e. - 30 times the integration interval) will be printed out. If the number is smaller, information will be provided for more time points.

No. of Modes = Number of flexible flatcar modes. At least 4 or 5 modes should normally be used.

No. of Locations = Number of points or the flexible flatcar for which influence coefficients are specified. Influence coefficients must be specified for each point where a force or moment is applied to the flexible mode (minimum of 18) as well as unit point on the flatcar structure itself where responses or internal stresses are desired.

Constants for flexibility elements - The math model shows 28 elements as simple springs. As was explained, any characteristics may be used for each of these elements, and any required constants, coefficients, or tables are inputted at this point. The first 12 elements model the trucks, and the linear approximations (spring constants - lbs/in - and damping coefficients lb-sec/in) from Reference are shown here. Coefficients for elements 13-28, representing coefficients for the trailer suspensions, will be provided here when they become available.

Masses, Moments of Inertia. Masses (>slugs) and moments of inertia in roll (slug-in^2) for the seven masses shown in the model are required here. Moments of inertia in pitch (THETA) and yaw (ALPHA) for the front trailer, flatcar, and rear trailer follow.

Dimensions - In sequence, the following dimensions as shown in the math model are required: H, VH, VL3, VL4, VH1, VL1, VL2, VHR, VL3R, VL4R, VH1R, VL1R, VL2R. See Reference for a discussion on use of VH1 and VH1R. Note also that dimensions VL1R and VL2R, which represent distances from the c.g. of the flatcar to the hitch and midpoint of the rear suspension of the trailer in the rear should be specified as negative numbers since they are located behind the flatcar c.g. The flatcar c.g. is assumed to be at the center (L/2 from each truck kingpin), but slight modifications could relocate this if desired.

Widths - In sequence, the following values as shown in the math model are read in: R1 (track gage, front truck), R2 (distance between spring nests, front trucks) R3, R4 (same, rear truck), R5 (Nominal axle width, front trailer), R6 (nominal distance between leaf springs, front trailer) R7, R8 (same, rear trailer).

Integration Interval. Time step for integration. See Reference for an explanation of the choice of this value. One should use here the largest interval for which numerical convergence is achieved. 0:004 seconds was used, but this might have to be modified if masses or characteristics of the flexibility elements change drastically.

Simulation Time - Total desired length of time for which the simulation is desired, seconds.

Frequency, Amplitude - Sinusoidal inputs were used for this run, and the frequency and amplitude of these inputs are specified here. External inputs may be specified for nodes (shown as uncircled numbers in the math model) 1, 5, 13, 17 representing vertical displacements of the respective wheel/rail interface points, and at nodes 3 and 15 representing averaged lateral displacements at each truck (gage variations are neglected). The inputs are specified in the lines following statement 999 in the program (see listing). An alternate specification of actual measured track geometrical deviations from nominal values could be made here in the form of a table if desired. Out of phase sinusoidal inputs at the front truck, for example, could be specified by the substitution of"disp (5) = - Z01" for the fourth card after statement 999 in the listing.

Length = Flatcar length, distance "L" on math model. This is the truck center to center distance.

Delay = Not used for sinusoidal inputs. When measured track geometry is used, there is a delay between the time when the front truck sees a given section of track and the time when the rear truck sees the same input. This is a function of the vehicle speed. The time delay may be inputted or calculated as desired.

Flatcar Flexible Modes - One set of these cards must be used for each flatcar mode that is included. The first number represents the frequency of the mode in hertz. Following this are the influence coefficients for the mode. The sequence of influence coefficients corresponding to the forces are as follows:

For Location of Force	Use Coefficient #
F_4	1
F_5	2
F_6	3
F_{10}	4
F_{11}	5

For Location of Force	Use Coefficient #
F_{12}	6
F_{14}	7
F_{13}	8
X2MOM	9 (slope)
F_{15}	10
F_{16}	11
F_{17}	12
F_{22}	13
F_{21}	14
VRMOM	15 (slope)
F_{23}	16
F_{24}	17
F_{25}	18

Additional coefficients should be added if outputs at specific locations on the flexible flatcar are desired.

SAMPLE OUTPUT

One page of output will be printed for each time point. The print interval is specified in the input.

The first column gives the force in each of the 28 flexibility elements in pounds. Following this are the accelerations, velocities, and displacements associated with each of the degrees of freedom. The acceleration, velocity, and displacement in each mode follows.

If additional outputs, such as responses at specific flatcar locations, are desired, they may be printed out at this point.

TIME 0.000 SEC

	FORCE (LBS)			ACCEL (GS)	V (IN/SEC)	DISP (IN)
1	.4720E+05	FRONT TRUCK	LAT.	0.	0.	0.
2	0.	REAR TRUCK	LAT.	0.	0.	0.
3	.4720E+05	FLATCAR	LAT.	0.	0.	0.
4	.4289E+05	FRONT AXLE	LAT.	0.	0.	0.
5	0.	FRONT TRAILR	LAT.	0.	0.	0.
6	.4289E+05	REAR AXLE	LAT.	0.	0.	0.
7	.4883E+05	REAR TRAILR	LAT.	0.	0.	0.
8	0.	FRONT TRUCK	VERT.	-.1087E-07	0.	0.
9	.4883E+05	REAR TRUCK	VERT.	.1087E-07	0.	0.
10	.4452E+05	FLATCAR	VERT.	-.1123E-02	0.	0.
11	0.	FRONT AXLE	VERT.	.6846E-03	0.	0.
12	.4452E+05	FRONT TRAILR	VERT.	.9666E-03	0.	0.
13	.2417E+05	REAR AXLE	VERT.	-.8337E-06	0.	0.
14	0.	REAR TRAILR	VERT.	-.1357E-05	0.	0.
15	.1898E+05			RAD/SEC**2	V(RAD/SEC)	DISP (RAD)
16	.1898E+05	FRONT TRUCK	ROLL	0.	0.	0.
17	0.	REAR TRUCK	ROLL	0.	0.	0.
18	.1898E+05	FLATCAR	ROLL	0.	0.	0.
19	.1740E+05	FLATCAR	PITCH	-.2412E-02	0.	0.
20	0.	FLATCAR	YAW	0.	0.	0.
21	.1740E+05	FRONT AXLE	ROLL	0.	0.	0.
22	.2047E+05	FRONT TRAILR	ROLL	0.	0.	0.
23	0.	FRONT TRAILR	PITCH	.3411E-02	0.	0.
24	.1986E+05	FRONT TRAILR	YAW	0.	0.	0.
25	0.	REAR AXLE	ROLL	0.	0.	0.
26	.1986E+05	REAR TRAILR	ROLL	0.	0.	0.
27	.1850E+05	REAR TRAILR	PITCH	-.1300E-04	0.	0.
28	0.	REAR TRAILR	YAW	0.	0.	0.

MODE	MODAL ACCEL.	MODAL VELOC.	MODAL DISPL.
1	6.229	0.	-12.04

TIME .120 SEC

	FORCE (LBS)				ACCEL (GS)	V (IN/SEC)	DISP (IN)
1	.4590E+05	FRONT	TRUCK	LAT.	0.	0.	0.
2	0.	REAR	TRUCK	LAT.	0.	0.	0.
3	.4590E+05	FLATCAR		LAT.	0.	0.	0.
4	.4189E+05	FRONT	AXLE	LAT.	0.	0.	0.
5	0.	FRONT	TRAILER	LAT.	0.	0.	0.
6	.4189E+05	REAR	AXLE	LAT.	0.	0.	0.
7	.4899E+05	REAR	TRAILER	LAT.	0.	0.	0.
8	0.	FRONT	TRUCK	VERT.	-.6610E-01	.2507	.1517
9	.4899E+05	REAR	TRUCK	VERT.	.4718E-03	-.8807E-02	-.8647E-03
10	.4468E+05	FLATCAR		VERT.	-.1401E-01	.4243	.4902E-01
11	0.	FRONT	AXLE	VERT.	.4363E-02	.6964	.4688E-01
12	.4468E+05	FRONT	TRAILER	VERT.	-.1769E-01	1.110	.8853E-01
13	.2266E+05	REAR	AXLE	VERT.	-.1572E-02	-.5167E-01	-.6822E-02
14	0.	REAR	TRAILER	VERT.	.1446E-02	.1111E-01	.9079E-03
15	.1919E+05				RAD/SEC**2	V(RAD/SEC)	DISP (RAD)
16	.1919E+05	FRONT	TRUCK	ROLL	0.	0.	0.
17	0.	REAR	TRUCK	ROLL	0.	0.	0.
18	.1919E+05	FLATCAR		ROLL	0.	0.	0.
19	.1761E+05	FLATCAR		PITCH	-.2724E-01	.1597E-02	.1848E-03
20	0.	FLATCAR		YAW	0.	0.	0.
21	.1761E+05	FRONT	AXLE	ROLL	0.	0.	0.
22	.2054E+05	FRONT	TRAILER	ROLL	0.	0.	0.
23	0.	FRONT	TRAILER	PITCH	-.1118	.1971E-02	.4206E-03
24	.1966E+05	FRONT	TRAILER	YAW	0.	0.	0.
25	0.	REAR	AXLE	ROLL	0.	0.	0.
26	.1966E+05	REAR	TRAILER	ROLL	0.	0.	0.
27	.1851E+05	REAR	TRAILER	PITCH	.9112E-02	.5642E-03	.6895E-04
28	0.	REAR	TRAILER	YAW	0.	0.	0.

MODE	MODAL ACCEL.	MODAL VELOC.	MODAL DISPL.
1	64.81	-1.904	-12.26

TIME .240 SEC

	FORCE (LBS)			ACCEL (GS)	V (IN/SEC)	DISP (IN)
1	.4565E+05	FRONT TRUCK	LAT.	0.	0.	0.
2	0.	REAR TRUCK	LAT.	0.	0.	0.
3	.4565E+05	FLATCAR	LAT.	0.	0.	0.
4	.4137E+05	FRONT AXLE	LAT.	0.	0.	0.
5	0.	FRONT TRAILR	LAT.	0.	0.	0.
6	.4137E+05	REAR AXLE	LAT.	0.	0.	0.
7	.4875E+05	REAR TRAILR	LAT.	0.	0.	0.
8	0.	FRONT TRUCK	VERT.	-.8155E-02	-1.969	.1982E-01
9	.4875E+05	REAR TRUCK	VERT.	.1076E-02	.3920E-01	.3954E-03
10	.4443E+05	FLATCAR	VERT.	-.1642E-01	-.2867	.5812E-01
11	0.	FRONT AXLE	VERT.	-.3386E-01	.5353E-01	.1103
12	.4443E+05	FRONT TRAILR	VERT.	-.4309E-01	-.9650	.1087
13	.2302E+05	REAR AXLE	VERT.	.1182E-01	.7691E-01	-.1227E-01
14	0.	REAR TRAILR	VERT.	.4759E-02	.2265	.1316E-01

				RAD/SEC**2	V(RAD/SEC)	DISP (RAD)
15	.1820E+05					
16	.1820E+05	FRONT TRUCK	ROLL	0.	0.	0.
17	0.	REAR TRUCK	ROLL	0.	0.	0.
18	.1820E+05	FLATCAR	ROLL	0.	0.	0.
19	.1668E+05	FLATCAR	PITCH	-.2429E-01	-.2804E-02	.1086E-03
20	0.	FLATCAR	YAW	0.	0.	0.
21	.1668E+05	FRONT AXLE	ROLL	0.	0.	0.
22	.2045E+05	FRONT TRAILR	ROLL	0.	0.	0.
23	0.	FRONT TRAILR	PITCH	-.5359E-02	-.9354E-02	-.1600E-03
24	.2002E+05	FRONT TRAILR	YAW	0.	0.	0.
25	0.	REAR AXLE	ROLL	0.	0.	0.
26	.2002E+05	REAR TRAILR	ROLL	0.	0.	0.
27	.1865E+05	REAR TRAILR	PITCH	-.2948E-01	.1695E-02	.2536E-03
28	0.	REAR TRAILR	YAW	0.	0.	0.

MODE	MODAL ACCEL.	MODAL VELOC.	MODAL DISPL.
1	-2.184	7.955	-11.81

TIME .360 SEC

	FORCE (LBS)				ACCEL (GS)	V (IN/SEC)	DISP (IN)
1	.4847E+05	FRONT	TRUCK	LAT.	0.	0.	0.
2	0.	REAR	TRUCK	LAT.	0.	0.	0.
3	.4847E+05	FLATCAR		LAT.	0.	0.	0.
4	.4389E+05	FRONT	AXLE	LAT.	0.	0.	0.
5	0.	FRONT	TRAILR	LAT.	0.	0.	0.
6	.4389E+05	REAR	AXLE	LAT.	0.	0.	0.
7	.4797E+05	REAR	TRAILR	LAT.	0.	0.	0.
8	0.	FRONT	TRUCK	VERT.	.6443E-01	-.2948	-.1510
9	.4797E+05	REAR	TRUCK	VERT.	-.2506E-02	.3227E-02	.4737E-02
10	.4367E+05	FLATCAR		VERT.	-.6973E-03	-.8351	-.1641E-01
11	0.	FRONT	AXLE	VERT.	-.2118E-01	-1.639	.9638E-02
12	.4367E+05	FRONT	TRAILR	VERT.	.2251E-01	-1.426	-.6627E-01
13	.2610E+05	REAR	AXLE	VERT.	-.5689E-02	.4740	.2929E-01
14	0.	REAR	TRAILR	VERT.	-.1543E-01	.6522E-02	.3736E-01
					RAD/SEC**2	V(RAD/SEC)	DISP (RAD)
15	.1862E+05						
16	.1862E+05	FRONT	TRUCK	ROLL	0.	0.	0.
17	0.	REAR	TRUCK	ROLL	0.	0.	0.
18	.1862E+05	FLATCAR		ROLL	0.	0.	0.
19	.1707E+05	FLATCAR		PITCH	.3983E-01	-.1533E-02	-.2326E-03
20	0.	FLATCAR		YAW	0.	0.	0.
21	.1707E+05	FRONT	AXLE	ROLL	0.	0.	0.
22	.1997E+05	FRONT	TRAILR	ROLL	0.	0.	0.
23	0.	FRONT	TRAILR	PITCH	.1583	.3254E-02	-.7352E-03
24	.1964E+05	FRONT	TRAILR	YAW	0.	0.	0.
25	0.	REAR	AXLE	ROLL	0.	0.	0.
26	.1964E+05	REAR	TRAILR	ROLL	0.	0.	0.
27	.1824E+05	REAR	TRAILR	PITCH	-.4216E-01	-.5381E-02	.5150E-04
28	0.	REAR	TRAILR	YAW	0.	0.	0.

MODE	MODAL ACCEL.	MODAL VELOC.	MODAL DISPL.
1	-14[illegible].2	-5.41[illegible]	-11.47

TIME .480 SEC

	FORCE (LBS)		ACCEL (GS)	V (IN/SEC)	DISP (IN)
1	.4892E+05	FRONT TRUCK LAT.	0.	0.	0.
2	0.	REAR TRUCK LAT.	0.	0.	0.
3	.4892E+05	FLATCAR LAT.	0.	0.	0.
4	.4456E+05	FRONT AXLE LAT.	0.	0.	0.
5	0.	FRONT TRAILR LAT.	0.	0.	0.
6	.4456E+05	REAR AXLE LAT.	0.	0.	0.
7	.4913E+05	REAR TRAILR LAT.	0.	0.	0.
8	0.	FRONT TRUCK VERT.	.1144E-01	1.899	-.2921E-01
9	.4913E+05	REAR TRUCK VERT.	-.2106E-03	-.8933E-01	-.1548E-02
10	.4483E+05	FLATCAR VERT.	.2896E-01	-.8558E-01	-.8609E-01
11	0.	FRONT AXLE VERT.	.5917E-01	-.6997	-.1698
12	.4483E+05	FRONT TRAILR VERT.	.4573E-01	.4037	-.1386
13	.2469E+05	REAR AXLE VERT.	-.2584E-01	-.5259	.3635E-01
14	0.	REAR TRAILR VERT.	-.6731E-02	-.7475	-.1132E-01
			RAD/SEC**2	V(RAD/SEC)	DISP (RAD)
15	.2014E+05				
16	.2014E+05	FRONT TRUCK ROLL	0.	0.	0.
17	0.	REAR TRUCK ROLL	0.	0.	0.
18	.2014E+05	FLATCAR ROLL	0.	0.	0.
19	.1847E+05	FLATCAR PITCH	.1949E-01	.2979E-02	-.1198E-03
20	0.	FLATCAR YAW	0.	0.	0.
21	.1847E+05	FRONT AXLE ROLL	0.	0.	0.
22	.2071E+05	FRONT TRAILR ROLL	0.	0.	0.
23	0.	FRONT TRAILR PITCH	-.5781E-01	.1152E-01	.4253E-03
24	.1951E+05	FRONT TRAILR YAW	0.	0.	0.
25	0.	REAR AXLE ROLL	0.	0.	0.
26	.1951E+05	REAR TRAILR ROLL	0.	0.	0.
27	.1819E+05	REAR TRAILR PITCH	.5404E-01	-.1465E-02	-.5336E-03
28	0.	REAR TRAILR YAW	0.	0.	0.

MODE	MODAL ACCEL.	MODAL VELOC.	MODAL DISP.
1	98.20	-4.025	-12.65

COST FACTORS

Computer simulation costs and the factors that tend to increase or decrease these costs are discussed in Reference

For the example shown, for all three seconds of simulation, costs are as follows:

Computer: CDC Cybernet System, CDC-6600 Computer, P-2, 25¢/second.

COSTS:

	Compilation	Calculation	Loading	Total
Seconds	8.8	19.8	5.	33.6
Dollars	2.20	4.95	1.25	8.40

Calculation costs/second of simulation = $1.65

APPENDIX C - POSSIBLE COMPONENT TESTS

1.0 INTRODUCTION

2.0 TRAILER-FLATCAR-TRUCK ASSEMBLY

2.1 Rocking Interface, Car Bolster - Truck Bolster Connection

Procedure: Clamp truck bolster relative to a rigid foundation. Apply very slow (pseudo-staic) force to car body. (e.g. constant applied force to top of car body above c.g.) Rock body statically in positive direction until mechanical stop is contacted solidly, then reverse force until the other stop is contacted.

Record: Force or applied moment vs. rigid body car body angular deflection.

2.2 Yawing Friction, Kingpin - Bolster

Procedure: If a simple method can be devised to rotate the truck bolster relative to the kingpin in yaw with the normal weight of the car applied, slowly (pseudo-statically) make this rotation through the maximum yaw angle ($\pm$) achievable in practice. Repeat test at a constant angular velocity (say, 0.25 rad/sec).

Record: Required moment or force vs. relative angular displacement.

3.0 TRUCK ASSEMBLY

3.1 Vertical Direction

Procedure: Place the unloaded truck on rails. Pseudo-statically apply a vertical load at the centerplate until spring bottoming is achieved. Pseudo-statically release the load.

Record: Vertical deflections at several points, and angular deflection of side frames, vs. load.

3.2 Lateral Direction

Procedure: Take unloaded truck and restrain the wheel at the wheel-rail interfaces. Apply a lateral force pseudo-statically at the truck bolster. Deflect laterally as far as possible without damaging truck. Reverse directions.

Record: Lateral deflections at several locations, and angular deflections of side frames, vs. load.

4.0 TRUCK COMPONENTS

4.1 Spring Rests

Procedure: Remove the entire spring rest from one side. Pseudo-statically deflect the springs with an applied vertical load until solid bottoming is achieved, then release the load. Repeat the cycle at two constant velocities (e.g. 1 inch per second and 1 inches per second). Repeat laterally.

Record: Deflection vs. force.

4.2 Friction Snubbers

Procedure: Isolate the friction snubber joint (e.g., remove the spring rest). At several constant or sinusoidal velocities, move the two plates through the normal travel expected in service. Test both lateral and vertical relative motions, do not exceed one cycle, and intersperse lateral and then vertical cycles. About 4-5 velocities will be required.

Record: Displacements, velocities, forces.

5.0 TRAILER SUSPENSION

5.1 Vertical Frequencies and Damping

Step a.

Procedure: Deflect the trailer body vertically downward by means of an applied force. Suddenly release the force. Repeat with progressively larger deflections until normal range of travel under service conditions has been achieved.

Record: Trailer body motions vs. time until all motion dies out.

Step b.
Procedure: Pseudo-statically load the trailer so as to deflect the suspension. Increase the load until the normal range of travel is achieved. Slowly release the load.

Record: Deflections at several locations on the suspension vs. load.

Step c.
Procedure: Repeat the load test in Step b at constant or sinusoidal velocities. Test at 4-5 different velocities.

Record: Velocities, displacements, forces.

5.2 Lateral Frequencies and Damping

Procedure: Repeat Steps a, b, and c in the lateral direction.

Record: Data as in Steps a, b, and c.

5.3 Components

a. Leaf springs - stiffness
Procedure: Jack up trailer and remove the wheels on both sides. Restrain the trailer bed. Applying a vertical symmetric load to both sides of an axle, vertically raise the axle relative to the bed pseudo-statically. Deflect through the normal range of travel, then release the load psuedo-statically.

Record: Deflections on several points on the leaf springs vs. force.

b. Leaf springs - damping
Procedure: Repeat the cycle described in a. above at several constant or sinusoidal velocities. About 4-5 velocities will be required.

Record: Velocities, axle displacement, forces.

c. Tires

Procedure: Remove one wheel and tire. Mount to a short bar representing the axle so that a symmetric vertical load can be applied simulating normal axle loading. Pseudo-statically deflect vertically with the tire resting on a flat plate. Pseudo-statically release the load. Repeat the above at several constant or sinusoidal velocities. About 4-5 velocities will be required. Achieve a deflection equal to maximum normal service deflection under worst conditions.

Record: Deflection, velocities, loads.

Note: In all tests above, pseudo-static means so slowly that no dynamic effects are apparent. Constant velocities are to be preferred to sinusoidal velocities.

APPENDIX D - MODELING METHODS FOR COULOMB DAMPING

1.0 INTRODUCTION

The dynamic responses of rail vehicles are highly dependent on the frictional characteristics of the vehicle isolation system. Many vehicles employ frictional snubbing devices to obtain desired damping characteristics. These vehicles display highly nonlinear coulomb (slip-stick) damping characteristics. An understanding of this type of damping is essential if dynamic responses are to be simulated.

While coulomb damping is simple in form and concept, serious problems are encountered in the use of this mathematical concept in simulation. In linear frequency domain types of analysis, coulomb damping cannot be used directly, and quasi-linear on describing functions approximations are often employed. While these approximations can be very accurate and satisfactory in some types of analysis, they leave much to be desired in other cases.

In nonlinear or time domain analysis, the direct use of coulomb damping will lead to a numerical instability. This instability is normally neither convergent nor divergent. The greatest danger associated with this numerical problem is that its presence may not be recognized, because the direct use of coulomb damping will yield an apparently reasonable, but incorrect, solution. On the other hand, nonlinear analyses can incorporate approximations of greater generality and utility than is possible using linear techniques.

This report will consider the bilinear approximation in some detail. This approximation is directed towards the FRATE programs[1] where vehicle flexibility is handled by normal mode methods, and the truck is viewed as a nonlinear isolator which directly inputs energy into the vehicle.

The objective here is to provide a method which can be incorporated into the FRATE programs without major modifications, and which retains the transparency and close

1. FRATE-11 (11 DOF) Rock & Roll Program, FRATE-17, (17 DOF Rock & Roll Program), FRATE (TOFC Analysis Program), HUNTCT (Hunting Analysis Program).

relation to physical reality that FRATE emphasizes. Thus, techniques such as use of a variable time step integration routine or approximations that treat the coulomb relationship as an exponential series have not been considered despite their obvious applicability to the problem.

2.0 STATEMENT OF THE PROBLEM

The coulomb damping relationship is usually approximated by a constant retarding force whose sign is that of the relative velocity across the isolator.

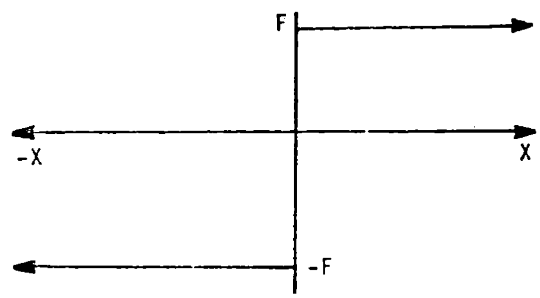

Figure D-1. Coulomb Damping Relationship

where: F = Assumed constant friction force

X = Relative velocity

As with all mathematical idealizations, nothing in the real world displays these characteristics exactly. However, many real pieces of hardware that utilize rubbing or sliding friction can be characterized in this fashion with reasonable accuracy. For the purposes of this report, we will assume that friction snubbers always follow these characteristics exactly.

If linear techniques are used, this characterization cannot be used directly because of its nonlinear nature. An approximation is used instead. There are several problems involved in this approximation which will be discussed later.

Most nonlinear methods utilize numerical integration. Whether stated or not, most of these methods rely on convergence upon a valid point after several intermediate calculations. Thus, these techniques (including the fourth-order Runge-Kutta methods used in the FRATE class of programs) rely on essentially trial and error methods of approaching or converging on a valid point during a series of intermediate calculations. As an example, consider the numerical integration process involved in the motion of a mass on a linear spring. The numerical integration process will begin at an assumed "initial condition" (usually the last previous valid point). A force is calculated, corresponding to these conditions, and a force balance performed in accordance with Newton's equation:

$$F = M\ddot{X}$$

This force balance implies a new set of conditions, and a corresponding force is calculated. This process is repeated in a series of intermediate steps until convergence (as defined according to whatever criteria was originally set up) is achieved, and the final set of conditions is considered a valid point. The key to this whole process is that each succeeding intermediate calculation must bring us closer to the final correct value. The process can be illustrated by noting the relative deflections on a force-deflection curve. If the initial cut is noted as position 1 , and the following intermediate steps are labeled 2 , 3 , and so forth, this could be illustrated as follows:

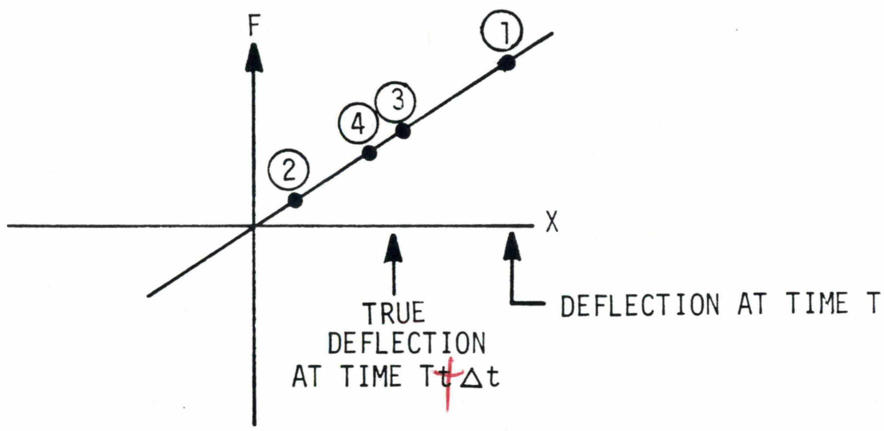

If, for some reason, (such as inappropriate selection of the integration interval Δ t), point 2 is farther from the "true deflection at time TtΔt" than is point 1 , the "solution" will continue to diverge until the numbers involved exceed the capacity of the computer. If point 2 is closer to the actual point than is point 1 , the solution will normally continue to converge until we are sufficiently close to the true deflection. Each of the above processes, however, depends upon the conditions of relative velocity and relative deflection affecting the magnitude of the force, which in turn dictates a new relative velocity or relative deflection.

Consider now the case of the coulomb damper. If we begin relatively close to the transition region, so that the sign of the retarding force changes from step 1 to step 2 , there will be only two possible force levels for all subsequent intermediate calculations, + F and - F. That is to say, if the transition region has an infinite slope, the convergence process can never work properly. Unless disturbed by the action of another mass, the computer can never converge upon any solution other than + F or - F, regardless of how many attempts are made. An illustration of this process follows.

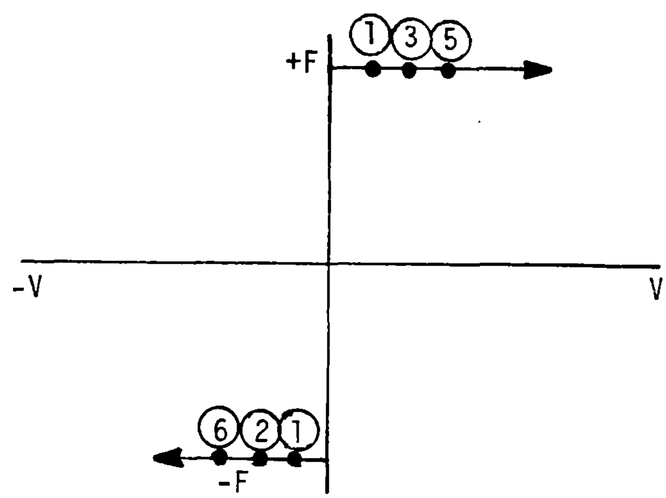

In the real world, of course, the true force will be somewhere between + F and - F. But, because of the numerical methods employed, convergence on the true force is not possible. There will be two errors introduced into the simultation by this process. First, the magnitude of the force can be incorrect whenever the relative velocity is within a certain distance of the transition region, where this distance is determined partially by the integration interval. Secondly, since the selection between + F and - F occurs essentially on a random basis, spurious frequency excitations will be introduced into the dynamic system where these frequencies are themselves partially a function of the integration interval. If the frequency of these spurious excitations coincides with one of the resonances of the system, serious errors may result. If this coincidence effect does occur, it can be detected by halving the integration interval and comparing the results. If it does not occur, overall errors are usually small unless one is primarily concerned with actual forces in the friction element or with actions of adjacent, small masses. Other than these localized effects, errors introduced into the overall solution tend to be small.

It is clear that the problem can be solved, at least theoretically, by introducing a finite slope into the transition region. Then, the force-velocity curve will look like this:

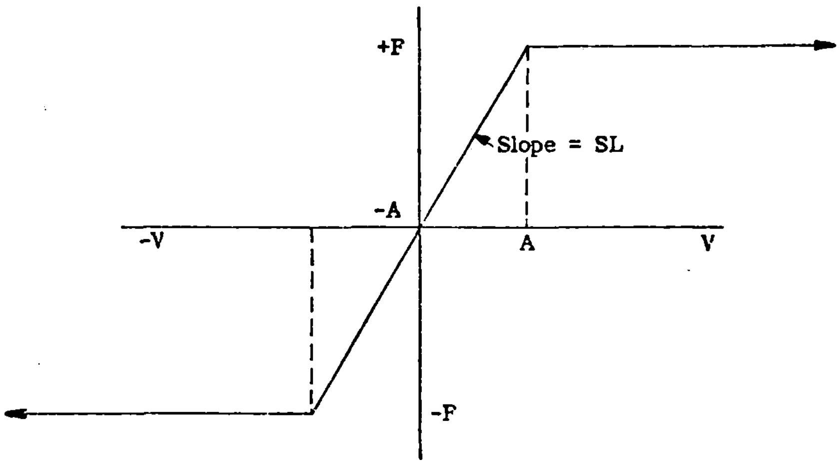

In practice, this will not always solve the problem. If the slope is too large, the process will continue as before unless velocities between + A and - A are involved. If the slope is too small, severe distortion of the true force - velocity curve can result. It will be found that the concepts of "too large" and "too small" must be judged relative to the integration interval. Thus, if this approximation is to be used, our objective is to maximize the slope in order to minimize distortions of the true coulomb waveform while minimizing the slope more to minimize distortions due to numerical problems. These mutually contradictory objectives imply an optimal slope for any given analysis type and integration interval. The purpose of this report, then, is to provide guidelines for achieving this optimal value.

3.0 LINEAR APPROXIMATIONS

3.1 Describing Functions

If linear solution techniques are to be employed, some method must be found to approximate the coulomb relationship by a linear expression. The technique often employed, quasi-linearization, uses a describing function or equivalent viscous damping relationship. This relationship has been derived in a number of ways, of which the Fourier Series is the most transparent.

If a mass isolated from ground by a coulomb damper undergoes a sinusoidal oscillation, the force history will be a square wave of amplitude F_o (the coulomb coefficient) as shown below:

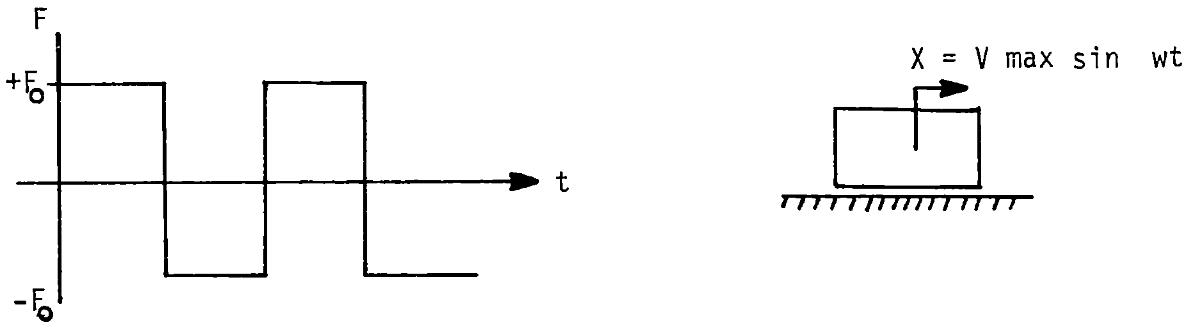

Figure D-2. Force History

where: F_o = Magnitude of retarding friction force,

V_{max} = Maximum velocity

w = Fundamental frequency, rad/sec

t = Time

This force history can be represented (Ref. 12) by the following series:

$$f(t) = \frac{4F_o}{\pi}\left(\sin \omega t + \frac{1}{3}\sin 3\omega t + \frac{1}{5}\sin 5\omega t + \cdots\right)$$

The approximation that is made in the describing function analysis is that the nonlinear force history can be adequately represented by the fundamental term only, and that all higher order terms can be neglected. The describing function is defined as the ratio of the fundamental component of the output to the amplitude of the sinusoidal input. Thus, we can approximate the coulomb damping of Figure D-2 by use of an "quivalent viscous coefficient" of:

$$Ceq = \frac{4Fo}{\pi V max}$$

and the damping force becomes:

$$F = \frac{4Fo}{\pi V max} \quad \dot{X}$$

Expression 3 has been derived by several other methods, such as minimization of the mean square error between the nonlinear and quasi-linear responses in Reference 13. Equating the energy dissipation through one complete cycle caused by the actual coulomb damper to the energy loss associated with the idealized equivalent viscous damper in Reference 14 does not make the fact that all but the fundamental term has been neglected as obvious, even though the latter derivations make more physical sense.

There are several problems involved in the application of the describing function approach to rail vehicle dynamic simulations. They include:

a. Neglecting the higher order terms results in a distortion of the force versus velocity signal.
b. The peak force in the damping element will be overestimated by approximately 30%.
c. The accuracy of the approximation is extremely sensitive to the amplitude of the resultant motion, which must normally be assumed.

Problem c is usually handled by performing the calculation on a trial and error basis within an iterative loop. This will require substantially more computer time for a given analysis effort.

Problem b is important only if we are primarily interested in the force in the damping element, or in the motions of small adjacent masses. This problem may be compensated for by applying a correction factor.

If we are primarily concerned with overall motions of large rigid vehicles, or with forces transmitted to the rail by a large, rigid vehicle, Problem a is unimportant as well. For example, Reference 5 demonstrates that the overall rock and roll responses of a 100ton hopper car may be predicted equally well using coulomb or viscous damping methods.[2]

---

2. In Reference 5, the damping coefficient representing the friction snubbers was varied until theory and test data agreed. It was found that similar predictions were made with a coulomb coefficient of 8000 lbs. and with a viscous coefficient of 1400 lb.-sec/in. It is interesting to note that eq. 3 would require an "equivalent viscous coefficient" of about 1200 lb.-sec/in. at 17.7 mph, and about 1600 lb.-sec/in. at 15.5 mph, with the coulomb value noted above.

On the other hand, if we are dealing with a light, flexible vehicle, or if we are dealing with lading environments or lading responses, these higher order terms may be of paramount importance. Consider for example, a hypothetical flexible rail vehicle with a fundamental roll mode of 2 Hz whose friction snubbers display the typical coulomb characteristics. If we simulate dynamic roll responses using the describing function approach, the vehicle model will see an excitation at the 2 Hz fundamental frequency. However, according to equation 2 , a real excitation at 6 Hz, with an input amplitude equal to 1/3 that of the fundamental, will be entirely ignored. If the flexible vehicle itself has a relatively undamped resonance near 6 Hz, this excitation could be far more important than that of the fundamental excitation itself. Similarly, a 10 Hz resonance, with an input amplitude of 1/5 that of the fundamental, is neglected.

With a particularly flexible vehicle, such as a long flatcar, important vehicle resonances typically occur at frequencies between perhaps 4 Hz and 20 Hz. Clearly, then, if we are dealing with a highly flexible vehicle or we are concerned with lading environments and lading responses, these higher frequency components cannot be neglected.

The describing function approach can be used to great advantage in linear programs that do not consider vehicle flexibility effects in detail. However, for the FRATE class of programs which handle vehicle flexibility in some detail using the normal mode methods, an approximation which does not distort the coulomb waveform at frequencies in the range of the vehicle modes is felt to be important.

3.2 The Bilinear Approximation

The bilinear approximation utilizes a finite slope to permit mathematical stability. The general shape of this curve is as shown below:

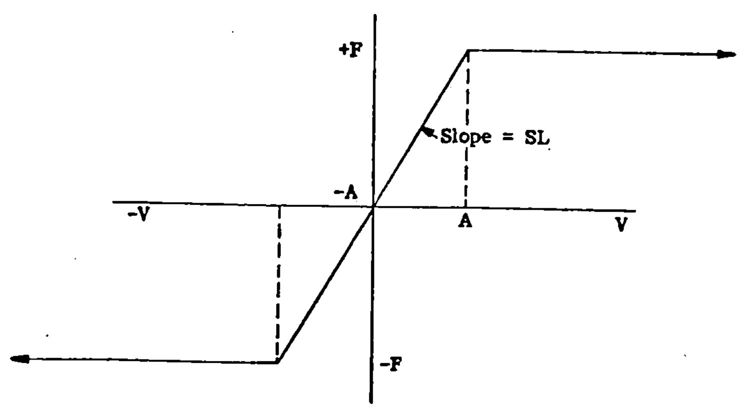

Figure D-3. Bilinear Approximation

where: F is the coulomb coefficient.

It can be seen there will be less dissipated energy than in the case of an ideal coulomb damper when this approximation is used. In this section we will show that this difference in dissipated energy is not important in most applications, although it might be important in isolated cases of very low frequencies and low amplitudes.

We could adjust the curve to a slightly higher force to compensate for the energy lost in the triangular (sloped) portion as shown:

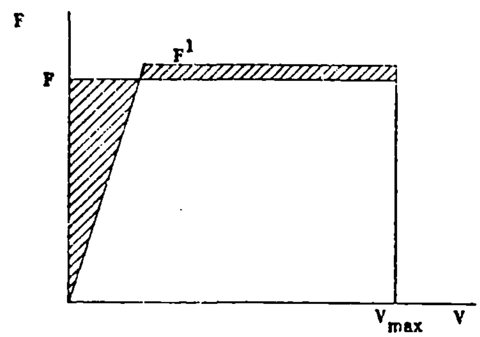

Figure D-4. Adjusted Curve

Thus, by selecting the proper F^1, we might be able to effect equal energy dissipation per cycle between actual and approximated coulomb dampers.

Unfortunately, energy dissipation is the area under the force versus displacement curve rather than under the force versus velocity curve, and the author was not able to come up with any reasonable way to manipulate this relationship to obtain dissipated energy directly. However, the area under the force versus velocity curve is essentially energy dissipated per unit time, and is closely related. Our objective, then, is to choose a value for F^1 so that the area of the two shaded regions shown in Figure D-4 are equal.

If we consider the two total areas

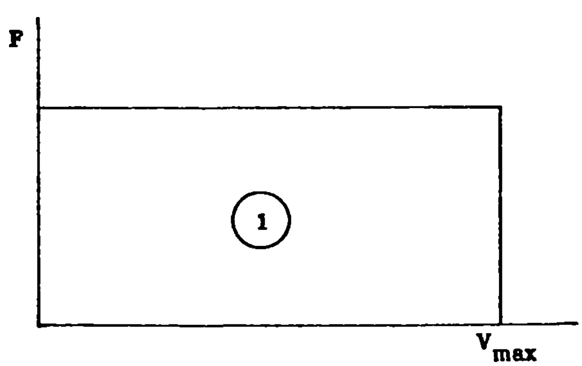

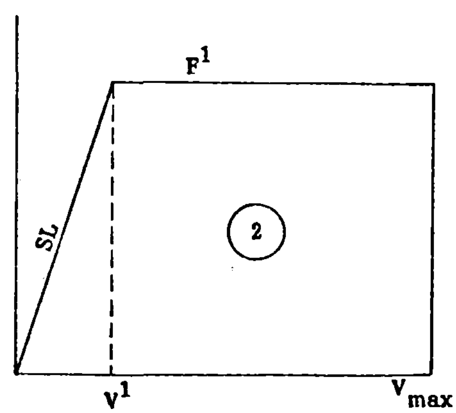

The area of the first is:

$$A_1 = F\,V max = F\,Aw$$

The area of the second is:

$$A_2 = 1/2\ F^1 V^1 + F^1\ (V max - V^1)$$

But, $V^1 = F^1/SL$

$$\text{So, } A_2 = 1/2\ (F^1)^2/SL + F^1 Aw - (F^1)^2/SL$$

Equating the areas,

$FAw = F^1 Aw - 1/2\ (F^1)^2/SL$

or,

$$(F^1)^2 - 2\ SL\ (F^1)\ Aw + 2\ SL\ F\ Aw = 0.$$

If we assume some typical characteristics, such as F = 8000 lbs, A = 2 inches, and a frequency of 2 Hz., we can solve for the following tabular data of F^1 as a function of slope:

SLOPE (SL)	F^1
1,000	9981. lbs.
2,000	8763.
5,000	8272.
10,000	8131.
20,000	8065.
50,000	8025.
100,000	8013.

In normal applications of this approximation, the slope will be about 5000 or more. But the difference between the coulomb coefficient and F^1 is very small, and is rarely known to be anywhere near this accuracy. Consequently, except in unusual cases of very small amplitudes and frequencies, it is suggested that the energy differential be ignored and the coulomb coefficient be used directly.

4.0 SIGNAL DISTORTION

4.1 Basic Concept

Use of the bilinear approximation described in the last section will, for any finite slope, distort the basic square-wave signal of the coulomb damper, although to a far lower extent than by use of describing function approximation. In order to evaluate the extent of this distortion, a purely theoretical study was undertaken utilizing PSD (power spectral desntiy) analyses of the waveform shown in Figure D-3 with different slopes. Comparison of these PSD's to PSD's of the same form using a nearly-vertical slope will reveal the extent to which the higher frequency contributions have been distorted. The force versus velocity curves were first converted to a time base by assuming a sinusoidal motion across the snubber. The frequency of this motion was set to 2 Hz for the analyses discussed in this section. That is to say, the curves in this section show the frequency content of the approximated force output signal when the relative motion across the snubber joint is sinusoidal at 2 Hz.

Figure D-5 shows a typical PSD plot with a slope of 10,000 (SL = 10000), while Figure D-6 shows the same with SL = 100,000. The horizontal axis is frequency in Hz. The vertical axis is essentially the content of the force signal at this frequency. The square root of the PSD has been shown for convenience (i.e. the discrete fast fourier transform). An alternate interpretation of these curves is that they show the coefficients of the Fourier series representation of the curve shown in Figure D-4 (basically the series shown in equation 2), where w = 2 Hz. By analogy with equation 2 , these curves, for a very high slope, start at the point ($4F_0/\pi$, 2 Hz), then go to (0, 4 Hz) where 4 Hz is 2 w, then to (1/3 $\frac{4\,Fo}{\pi}$, 6 Hz), and so forth. The plotting routine connects these points with straight lines.

We are concerned here with the envelope of the peaks, as an indication of the frequency content of the signal. Figure D-6, using SL = 100,000, can be taken to be the equivalent of a perfect square wave or ideal coulomb damper. The difference between the envelope of the peaks of the perfect square wave of Figure D-6, and the envelope of the peaks of the bilinear approximation with a slope SL = 10,000 from Figure D-5, can be taken as a measurement of the distortion of the signal resulting from use of this

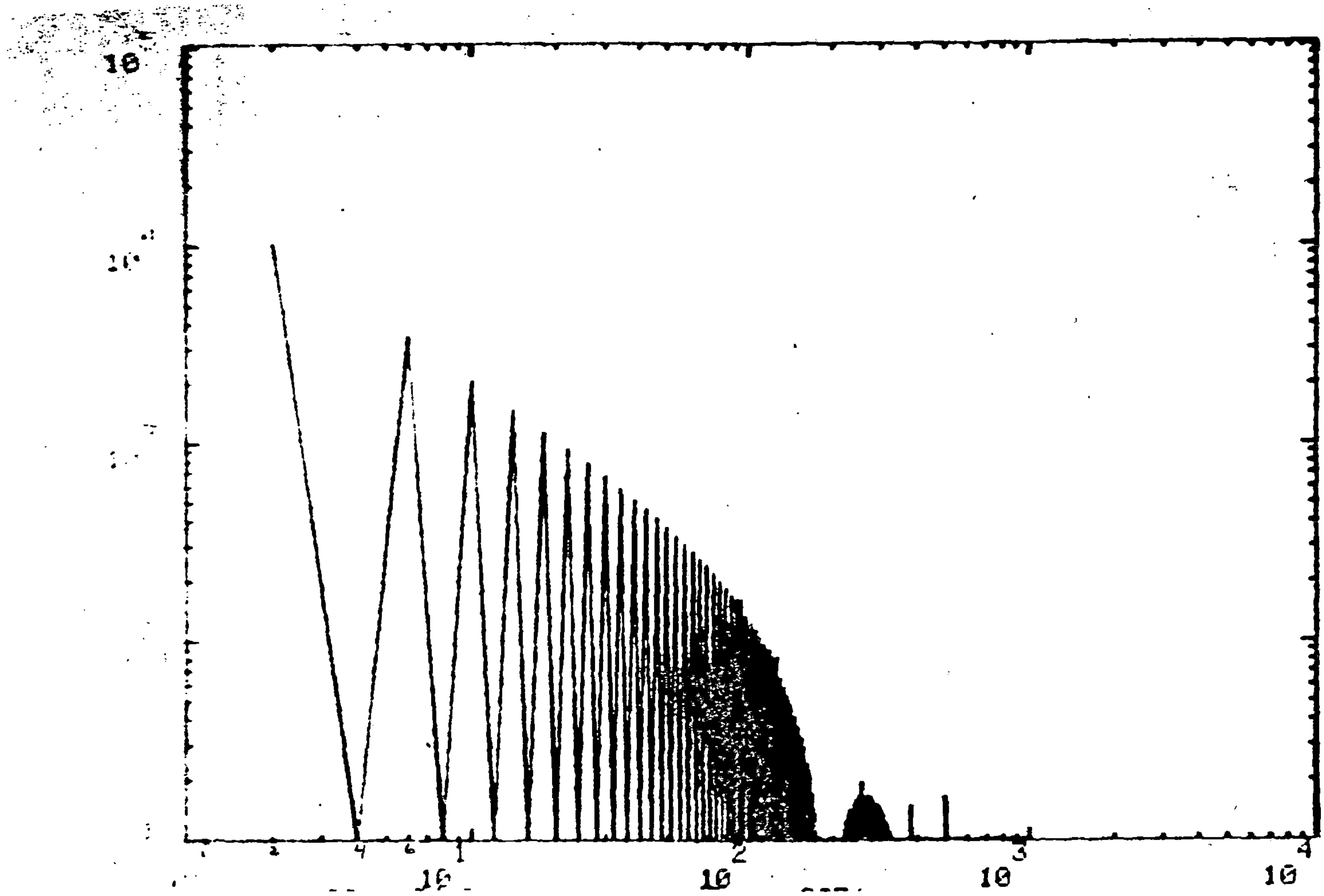

Figure D-5. Typical PSD Plot with SL = 10,000

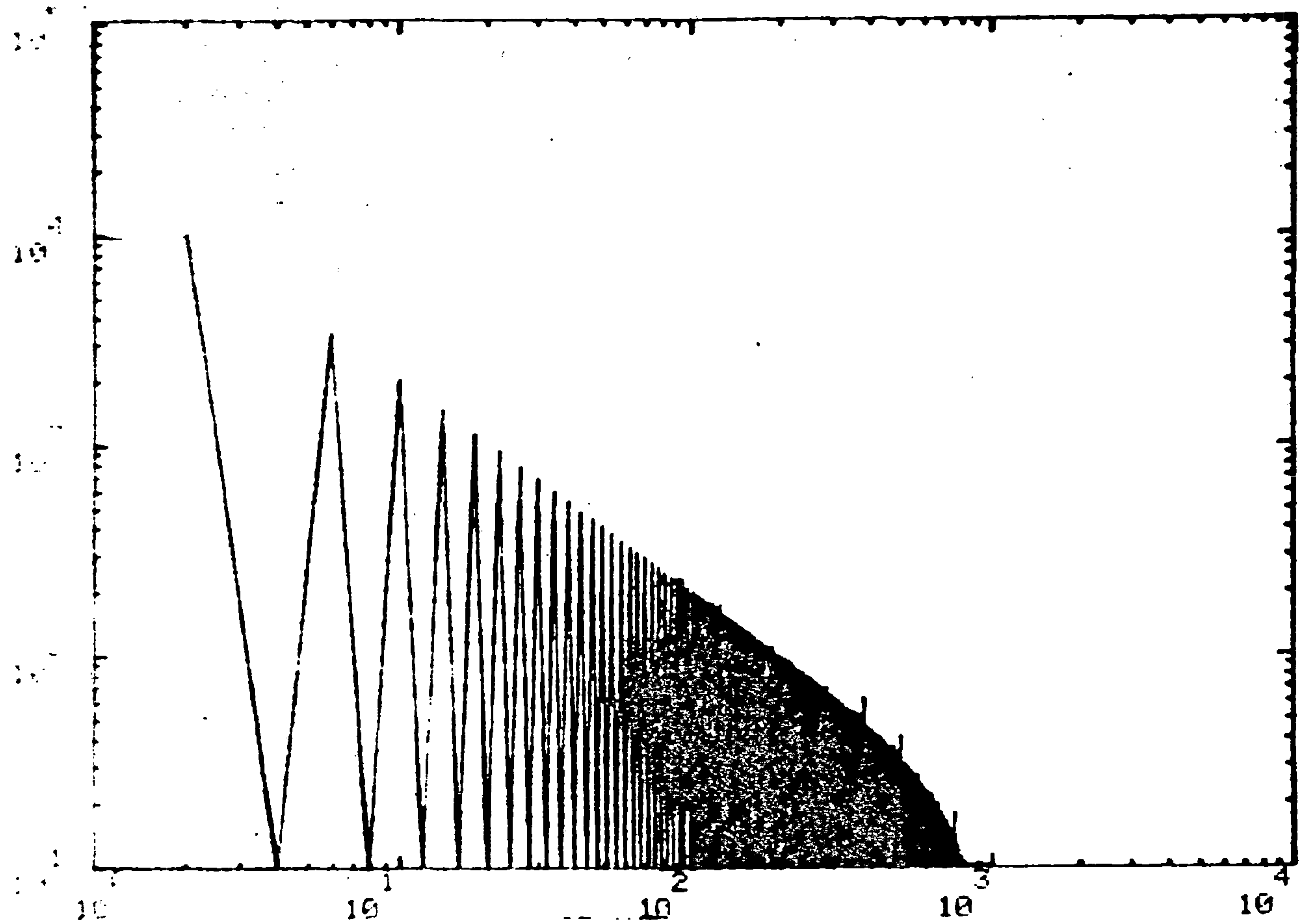

Figure D-6. Typical PSD Plot with SL = 100,000 bilinear approximation. An alternate interpretation of these envelopes is that they are a measure of the energy available to excite any system resonance that may exist at or near the frequency shown on the horizontal axis. The difference between the envelope of the peaks of Figure D-6 and the envelope of the peaks of Figure D-5 is, therefore, an indication of the energy that is available to excite resonances on the real system but which has been neglected by using the bilinear approximation with a slope SL = 10,000.

Figure D-7 compares these envelopes directly. A comparison of the envelopes with SL = 10,000 and SL = 100,000 shows that the frequency contents are almost identical in the low frequency range, and that differences begin to be significant only at frequencies above 55 Hz. Thus, if we have no significant system resonances above, say, 50 Hz, use of the bilinear approximation with SL = 10,000 will be perfectly acceptable and result in no noticeable signal distortion.

In a typical rail vehicle application, significant resonances above 20 Hz are rare. Thus, for most applications, lower values of SL will be acceptable.

4.2 Generalization

Figures D-7 and D-8 compare envelopes for a wide range of slopes. The procedure that should be followed in using the information presented in these figures is the following:

a. Determine the highest significant frequency in the mathematical model.

b. Increase this frequency by 10% to 20% to allow for the tendency to excite adjacent modes.

c. Find, from Table D-1 or Figures D-7 and D-8, the lowest slope for the bilinear approximation that will ensure minimal distortion of the waveform at all frequencies below that determined in step b.

Figure D-7 shows a comparison of the envelopes with SL = 50,000 and SL = 100,000. A glance at this comparison will reveal the reason for the statement, made earlier, that use of a slope SL = 100,000 can be considered a perfect square wave.

Table D-1 summarizes the information contained in Figures D-7 and D-8, and gives the slope that should be used in the approximation as a function of highest significant

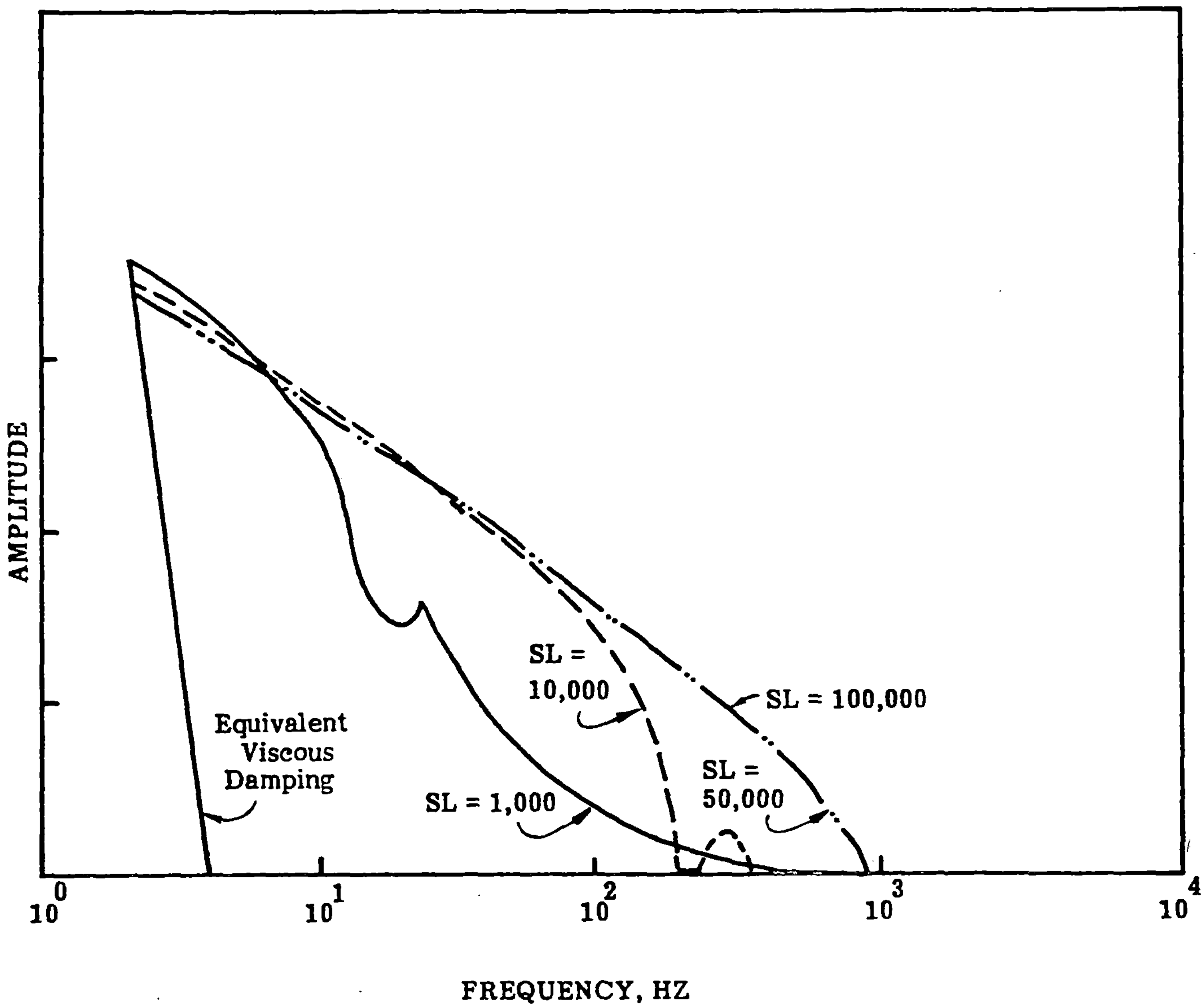

Figure D-7. Comparison of Envelopes, 2 Hz Base

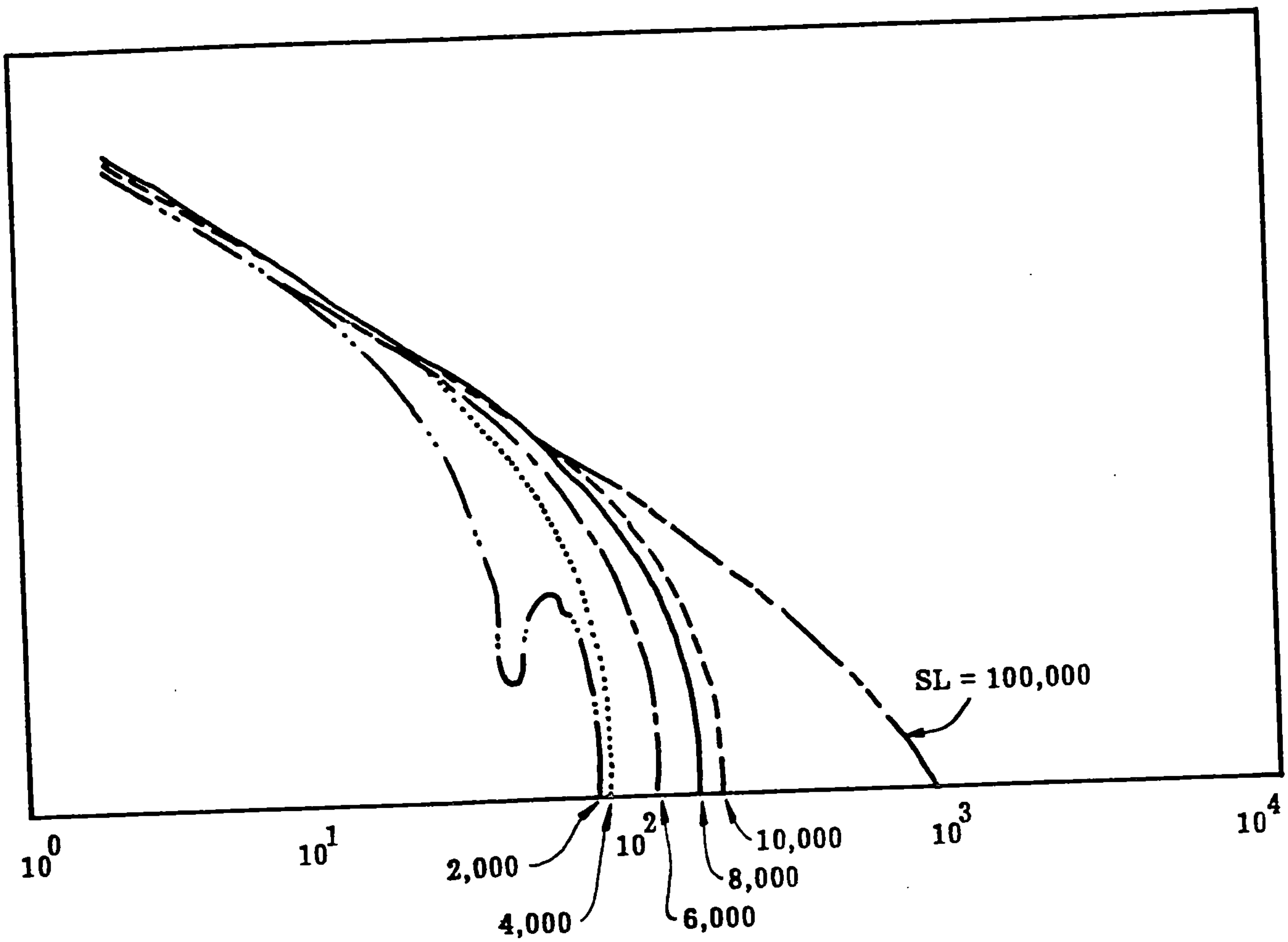

Figure D-8. Comparison of Envelopes, 2 Hz Base

Table D-1. Signal Distortion

SLOPE IN BILINEAR APPROXIMATION (SL)	FREQUENCY WHERE SIGNIFICANT SIGNAL DISTORTION BEGINS TO OCCUR	HIGHEST SIGNIFICANT MODE IN MATH MODEL
Equivalent Viscous Damping	2 Hz	Note #3
SL = 1000	6 Hz	Note #3
2000	9 Hz	8 Hz
4000	20 Hz	18 Hz
6000	30 Hz	27 Hz
8000	40 Hz	36 Hz
10000	55 Hz	50 Hz
50000	500 Hz	450 Hz

Notes:

1. These values are based on a 2 Hz input excitation. If higher inputs are involved, the frequencies should be increased proportionately.

2. To use this table, determine the highest significant mode in the math model. If vehicle flexibility is important in the calculation, or if we are mostly concerned with the lading, this will be the highest flexible mode. If we are concerned mostly with overall vehicle responses, or have a relatively rigid vehicle, it should be the vehicle fundamental, or, at most, the first or second mode. Find the corresponding slope.

3. The first two approximations are not recommended if vehicle flexibility has an important role.

frequency. It should be noted that the highest significant frequency is a function of the objective of the analysis as well as of the highest mode included in the math model.

Strictly speaking, Figures D-7 and D-8 apply only to a fundamental input vehicle excitation (e.g. - track geometry, VTU shaker input, etc.) of 2 Hz. However, further studies show that signal distortion at any given output frequency decreases as the input frequency increases. Figures D-9 and D-10, for example, show peak envelope comparisons when the input frequency is 10 Hz and 20 Hz respectively. In rail vehicle dynamic simulation we are rarely concerned with input frequencies below about 1-2 Hz, and the information already presented will yield conservative results when input frequencies are above 2 Hz. For these reasons, it is felt that the results using a 2 Hz base (Table D-1) should be used for general rail vehicle applications. In an unusual case where extremely low input frequencies are involved and where extremely high frequency modes are important in determining required dynamic responses, further study may be appropriate.

5.0 NUMERICAL DISTORTION

It was noted in the discussion on the nature of the numerical instability that the use of a finite slope will not necessarily solve the stability problems. The slope used in the approximation must be small enough, relative to the integration interval, to allow good definition of the actual waveform as the force is viewed at several sequential intermediate calculations. If we use a finite slope that is too large, the result will be unstable until a certain maximum slope is reached. This instability will have the effect of distorting the waveform, although the distortion will be more random than the signal distortion discussed in the last section. The pattern of the distortion will be dependent on both slope and integration interval.

In order to study the nature of this distortion, the 11 degree-of-freedom mathematical model of a flexible rail vehicle was used. The specific model used was set up to study the responses of a flexible, unloaded TOFC flatcar to a sinusoidal bounce excitation at one end. All runs discussed in this section include six flexible modes for the flatcar, and deal with a 4.5 Hz input at an amplitude of 0.1 inches. This model was selected because the velocity, amplitude, and nature of the motion are felt to be fairly typical

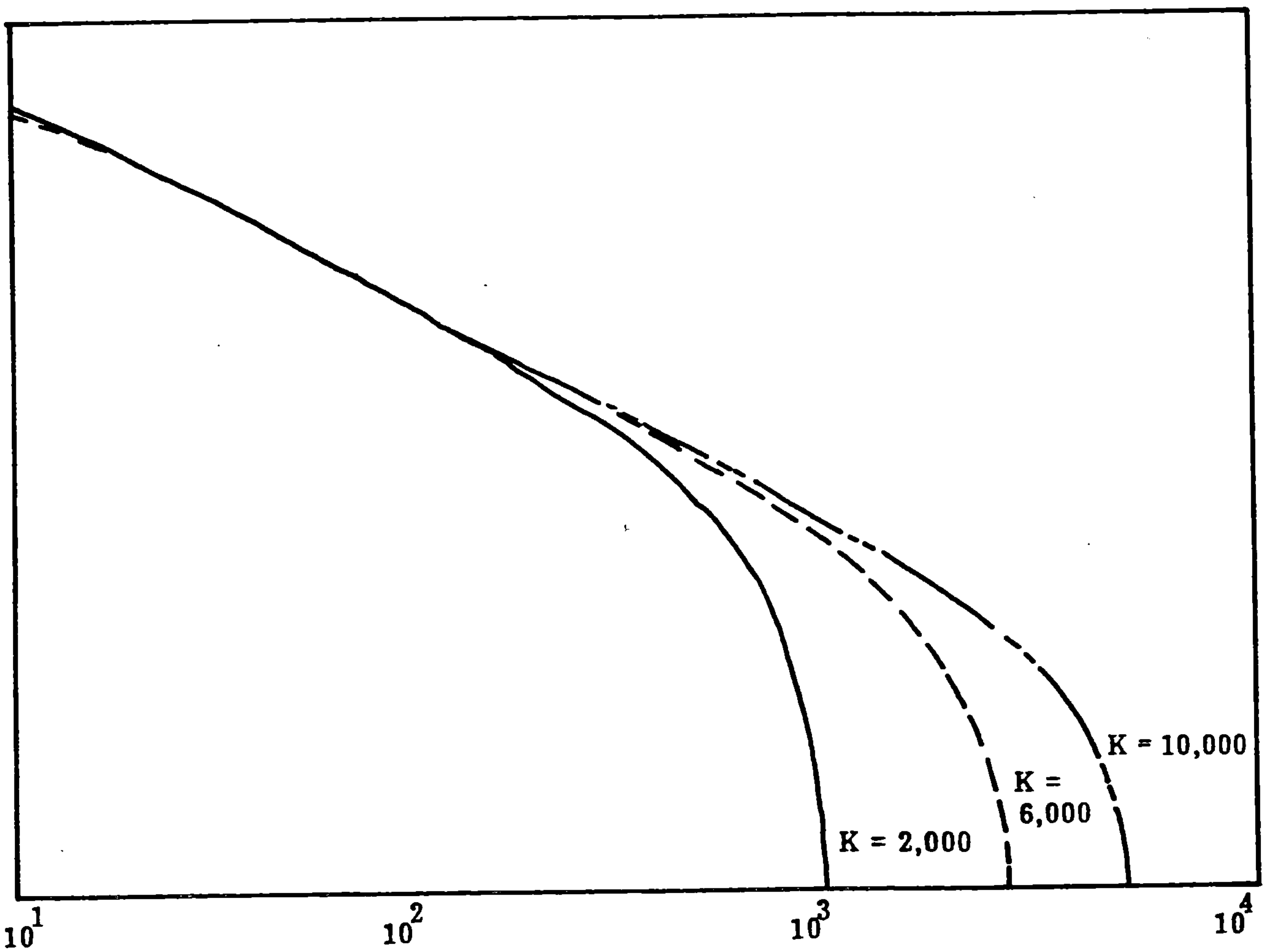

Figure D-9. Comparison of Envelopes, 10 Hz Base

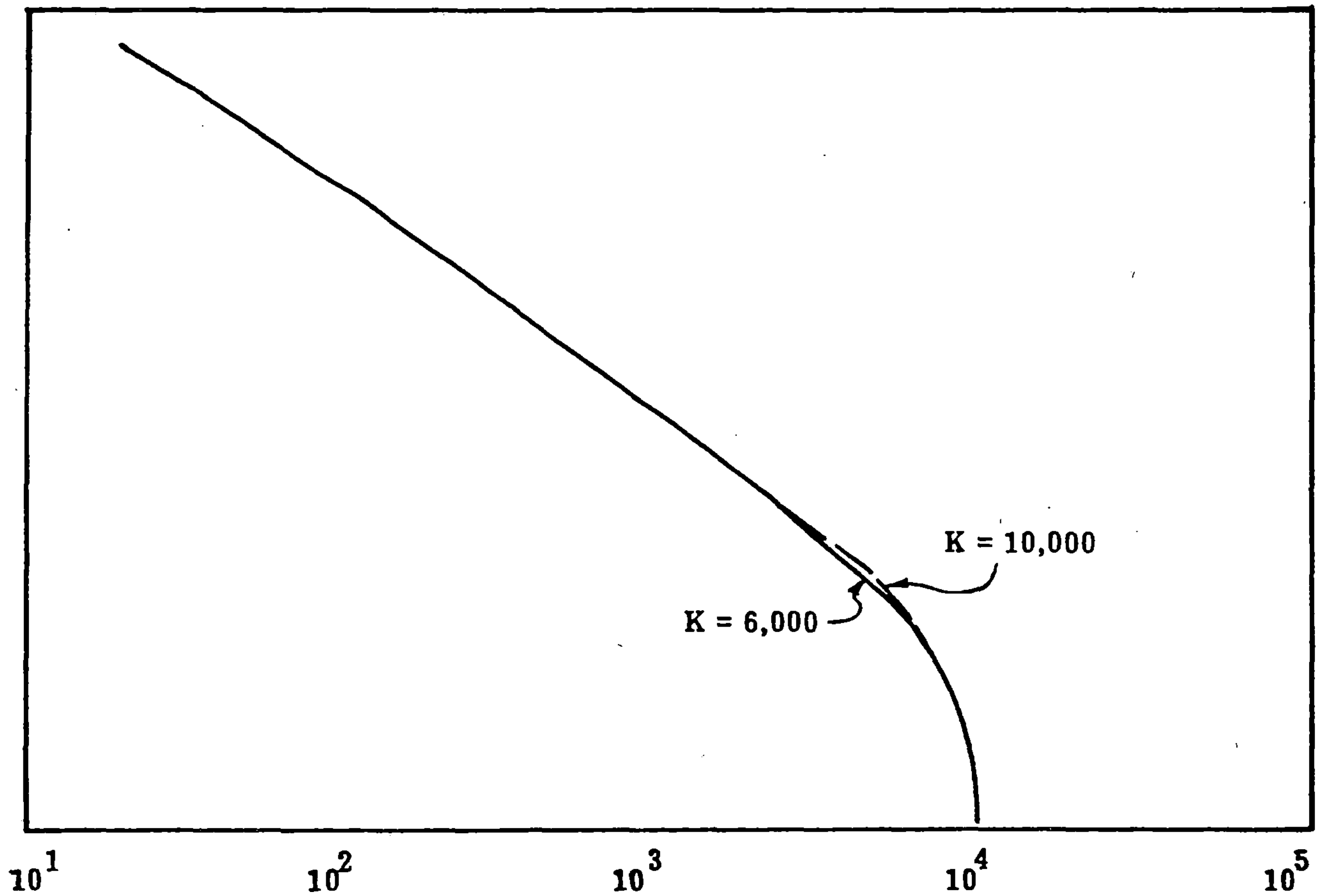

Figure D-10. Comparison of Envelopes, 20 Hz Base

of what is to be expected in many applications, and because the light, extremely flexible vehicle could best illustrate the instability being considered. While, in theory, the results quoted here apply only to this one specific case, the results are felt to be generally applicable to a wide range of normal rail vehicle applications.

Coulomb damping in the snubbers was approximated by the bilinear approximation, and a wide range of slopes and time steps were investigated. The predictions of snubber forces were recorded over several cycles, and PSD analyses were made of these force histories.

Figure D-11 shows the PSD analysis of the snubber force with an almost infinite (SL = $1x10^{10}$) slope comparison of this curve with the stable pattern shown in Figure D-14 shows several spurious frequency peaks. These spurious peaks are generated by the essentially random nature of the process of selection of a force value at a particular time point when conditions are unstable. As the slope is decreased, less of the force points will be randomly selected and more of the force points will be selected according to the logical pattern of the equations of motion. Consequently, the PSD plot will begin to converge on a stable pattern.

To illustrate this process, a slope SL = 4000 was selected. The calculation described above was performed with an integration interval of 0.005 seconds, and the time step progressively cut in half until a stable pattern was achieved. Figures D-12, D-13, D-14, and D-15 show these calculations for time steps of 0.005, 0.0025, 0.001, and 0.0005 seconds respectively. These figures show the progressive convergence onto a stable PSD form. It may be stated conclusively that the calculation with a time step of 0.001 was stable, because halving the time step had no significant effect. Alternately, we can look at the force value at a given time point to see if stability has been achieved. For example, if we consider the vertical force in a spring-snubber combination at a time of 1 second after the excitation begins, we find the following for the four runs noted above:

SL	time step	F_{10} at 1 second, lb.
4000	0.005	6888.
4000	0.0025	15,540.
4000	0.001	12,970.
4000	0.0005	12,970.

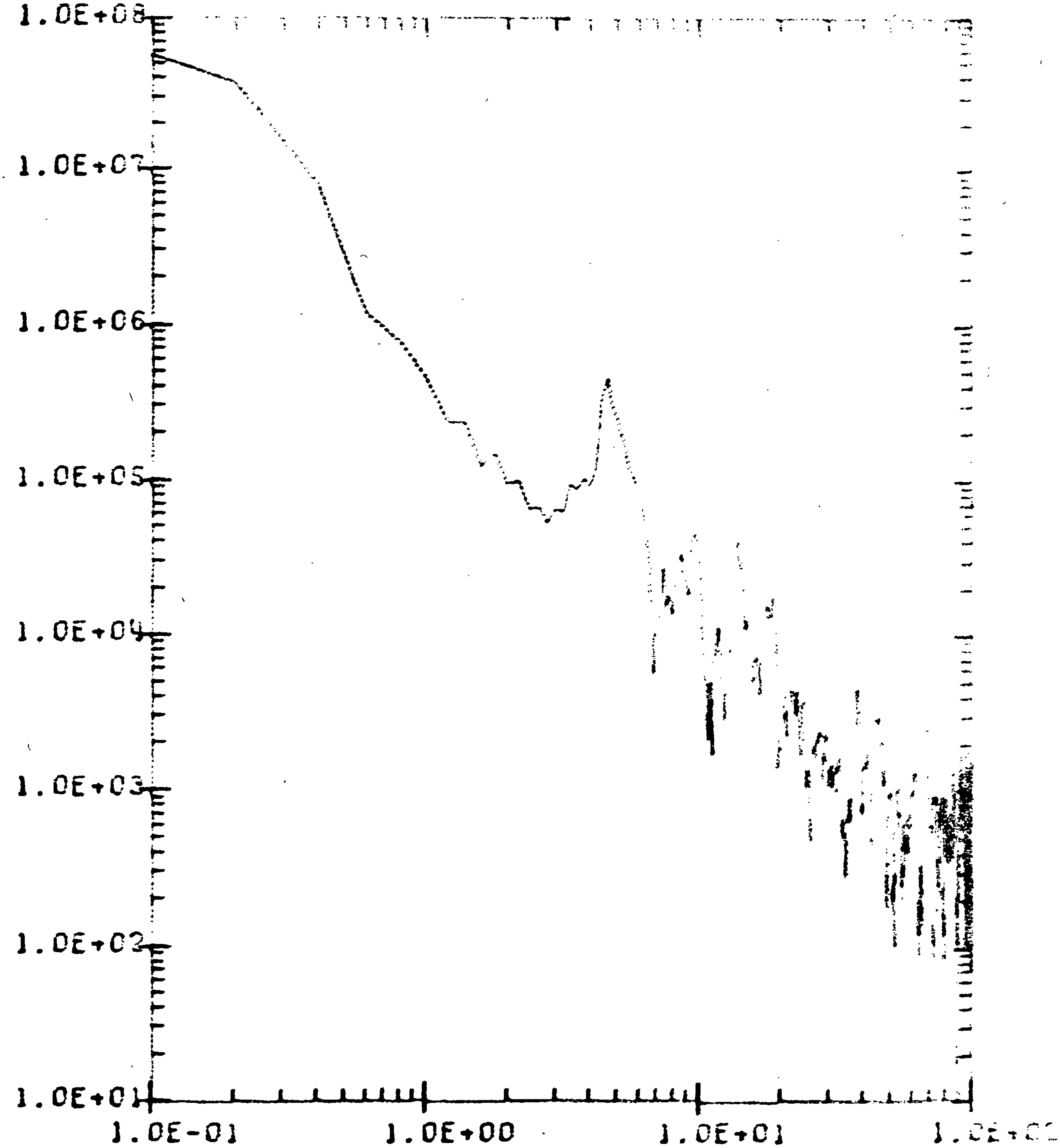

Figure D-11. PSD Analysis of Snubber Force with Almost Infinite Slope

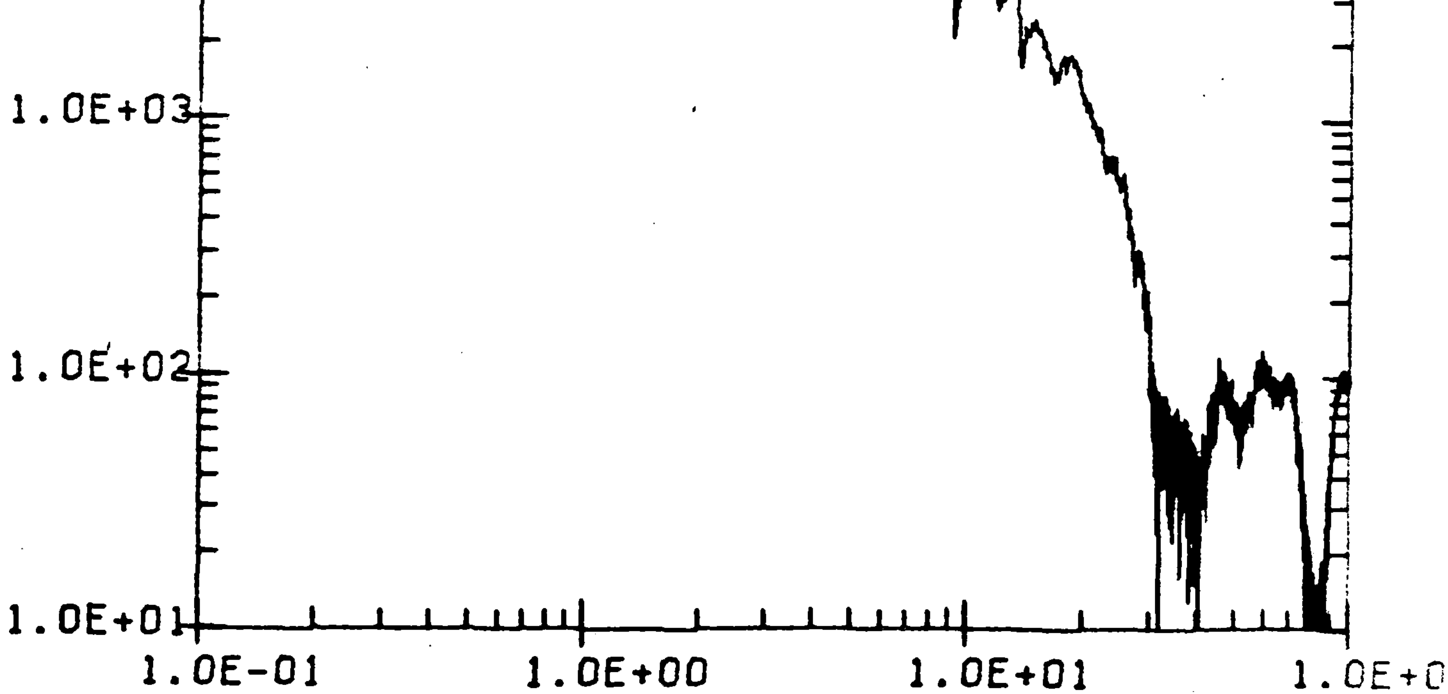

Figure D-12. Spurious Force Peaks, SL = 4000 dT = 0.005

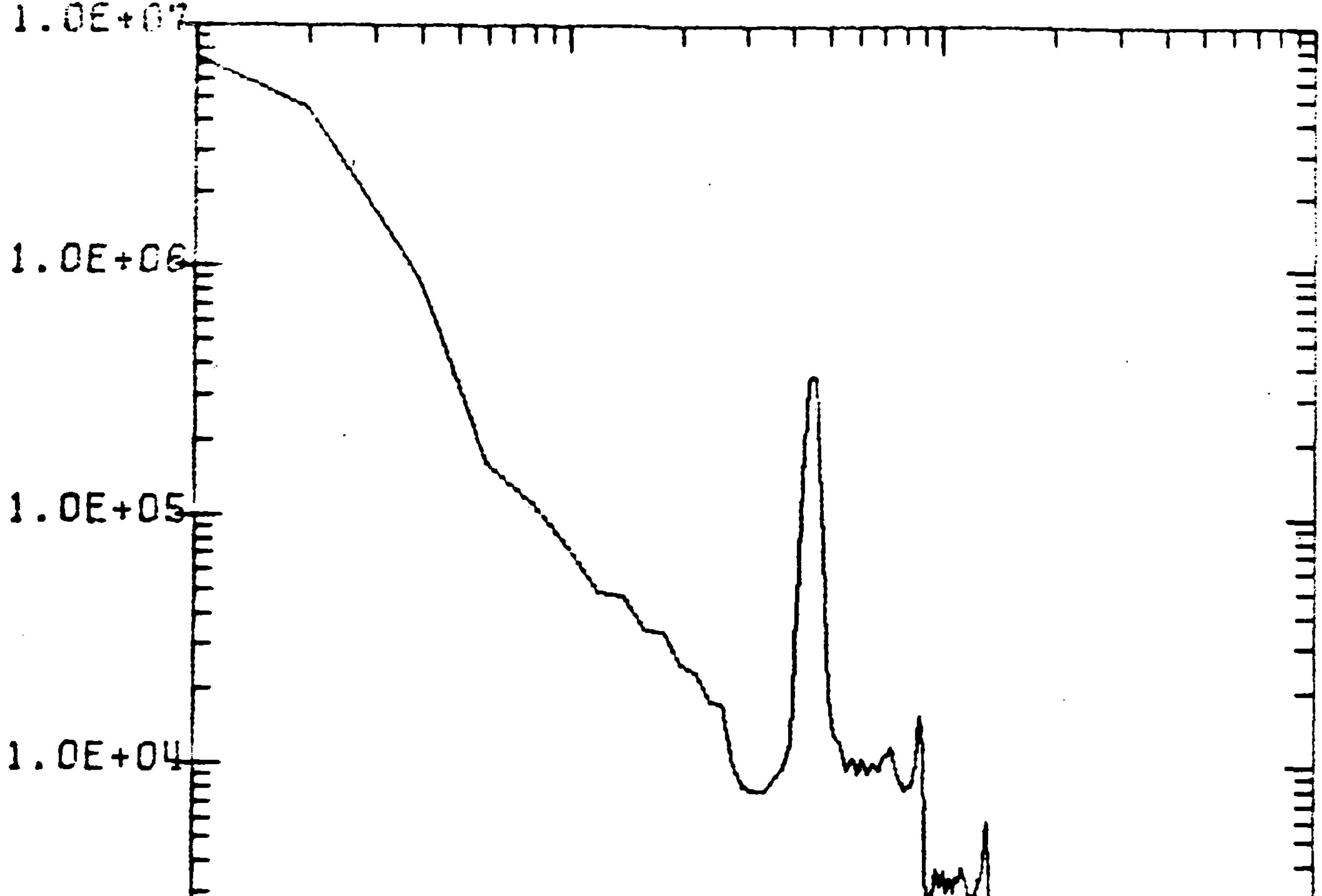

1.0E+07
1.0E+06
1.0E+05
1.0E+04

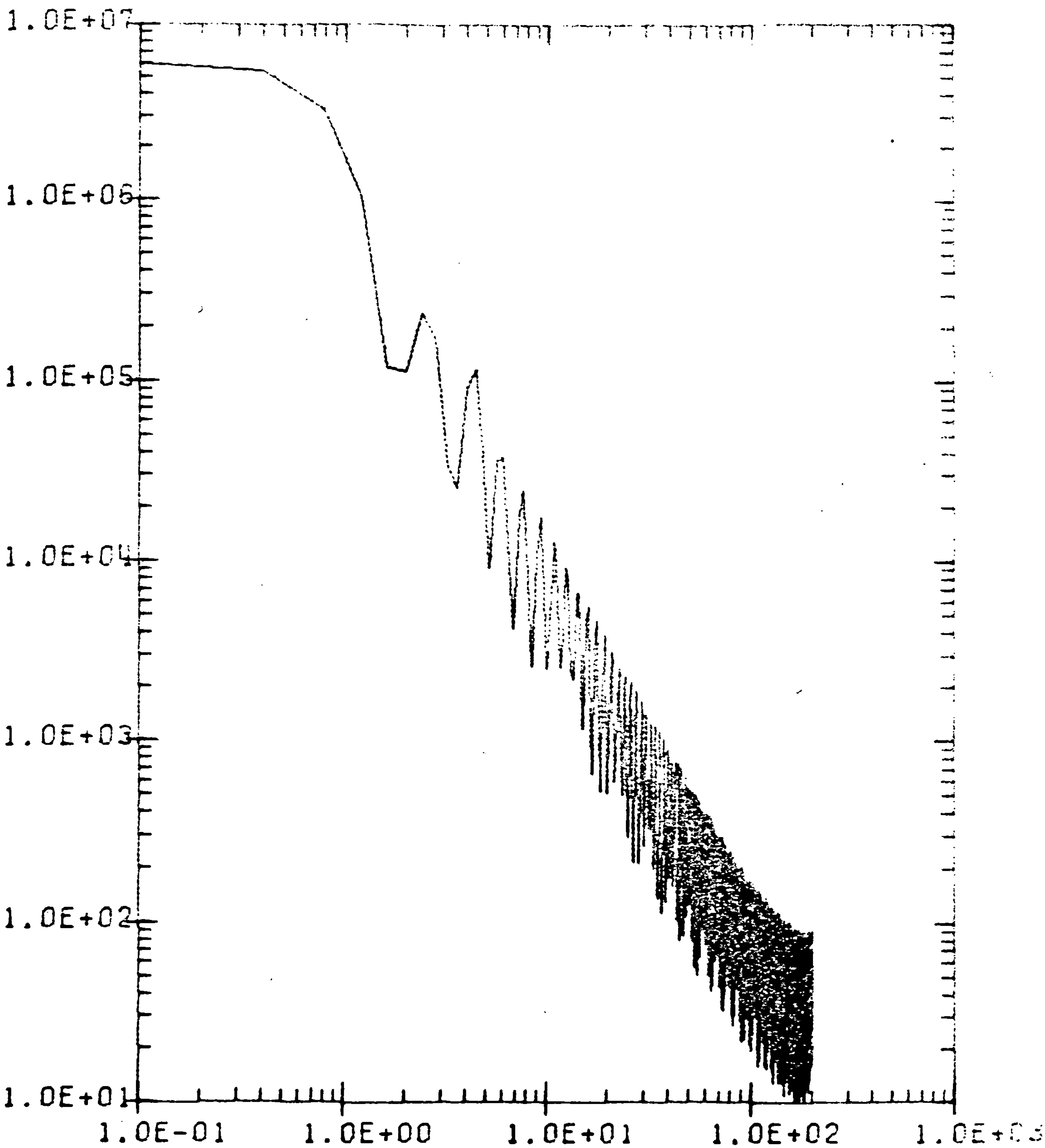

Figure D-13. Spurious Force Peaks, SL = 4000 dT = 0.0025

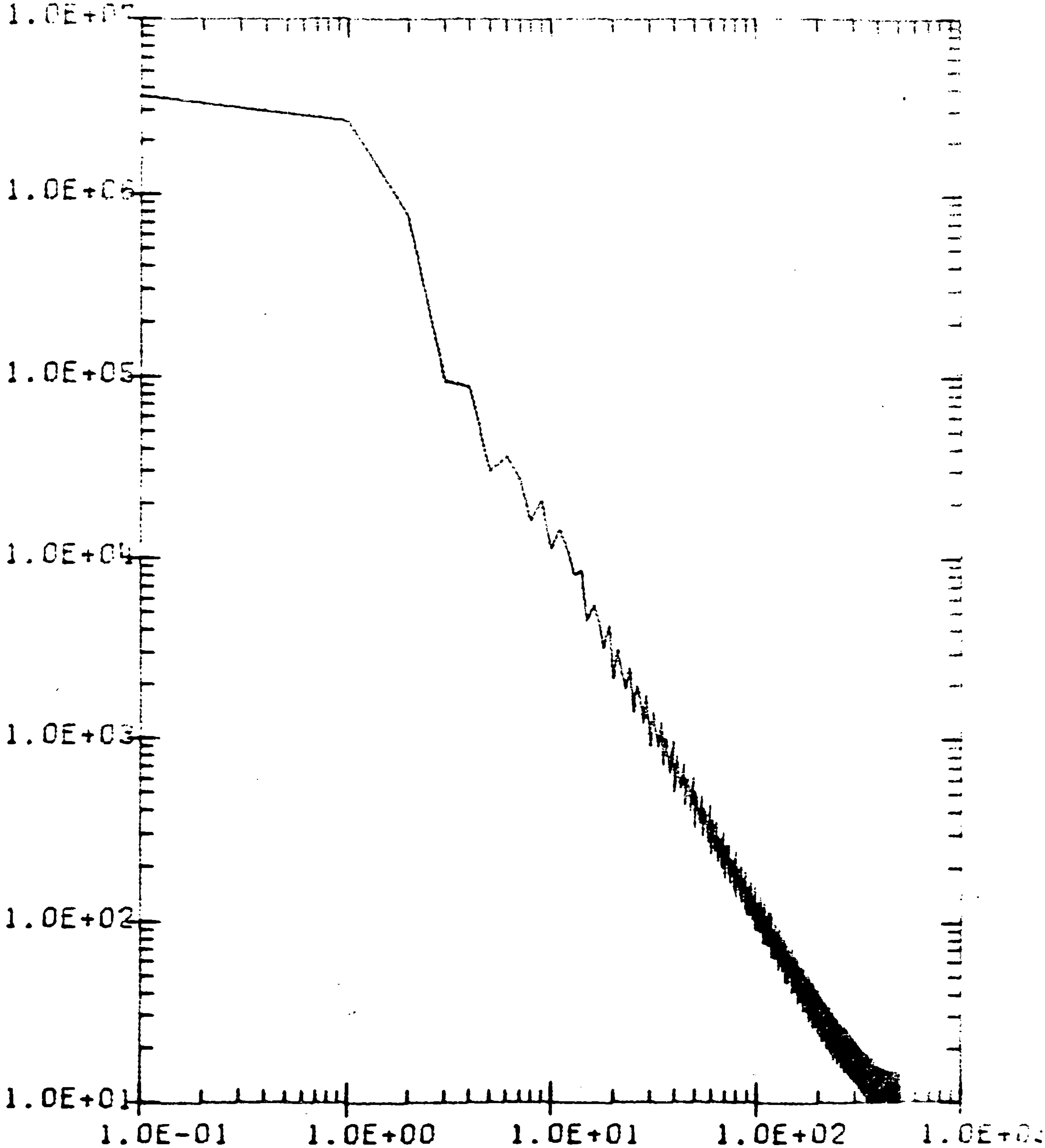

Figure D-14. Spurious Force Peaks, SL = 4000 dT = 0.001

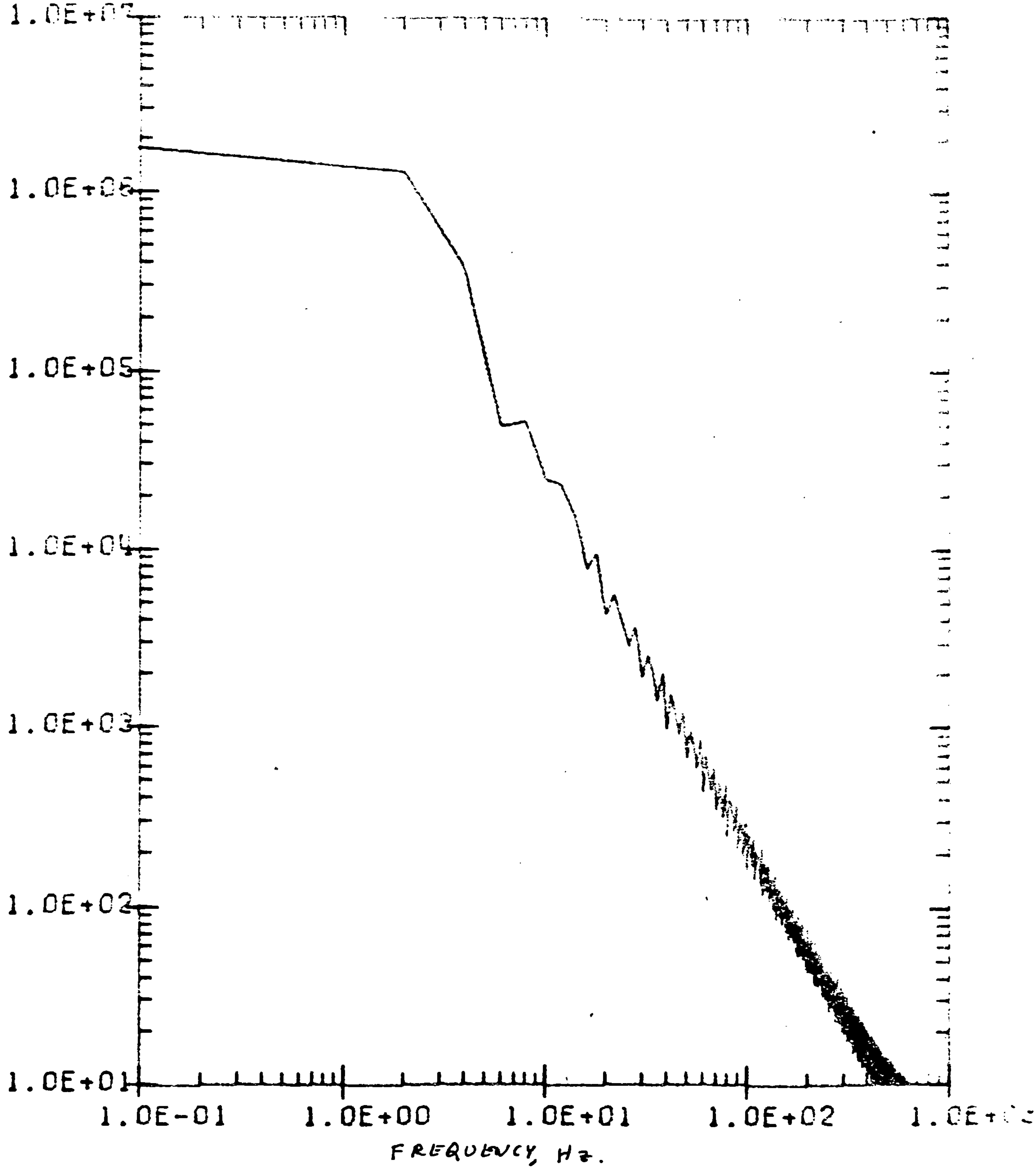

Figure D-15. Spurious Force Peaks, SL = 4000 dT = 0.0005

The tabular data above clearly indicates that stability was achieved with a time step of 0.001 seconds. This method is a much more practical way of seeing when stability has been achieved.

If we are concerned primarily with the magnitude of the force in the snubber, it is clear that we will have to achieve complete stability. On the other hand, if we are concerned with overall responses or even the response at a point on the flexible body, complete stability is unnecessary. That is to say, the spurious force peaks shown in Figure D-12 or Figure D-13 will not normally have a noticeable effect on any response other than the actual snubber force itself. With a little engineering judgment and experience, this fact can be used to permit adequate simulations without the cost penalty associated with very small time steps. Very inaccurate results will be attained only if a large spurious peak (such as those shown in Figure D-11) coincides precisely with an important flexible mode.

Further study reveals that we can characterize the relative stability of a calculation by the product of the slope and the time step. This product, which we will call the stability factor (SF), can then be used to characterize the required stability.

For example, Figure D-12 shows the PSD of the calculation with SL = 4000 and dT = 0.005, while Figure D-16 shows the calculation with SL = 8000 and dT = 0.0025. The SF, or product of SL and dT, is the same (20) in each case, and a comparison of Figure D-12 and Figure D-16 shows that the pattern, or relative instability, is practically identical. Table D-2 summarizes stability factor requirements for several types of analyses. Analyses with differing objectives will require differing amounts of relative stability. Thus, given the minimum slope requirement for adequate signal fidelity from Table D-1, and an estimate of the required stability factor from Table D-2, we can estimate the integration interval that will be required. Given this information, we can also estimate the computer costs for a proposed analytical effort, and perhaps, obtain a clearer picture of the true analytical objectives.

Table D-2 is based strictly on the judgment of the author and the limited number of computer runs performed in this effort. Any attempt to generalize is risky, and any

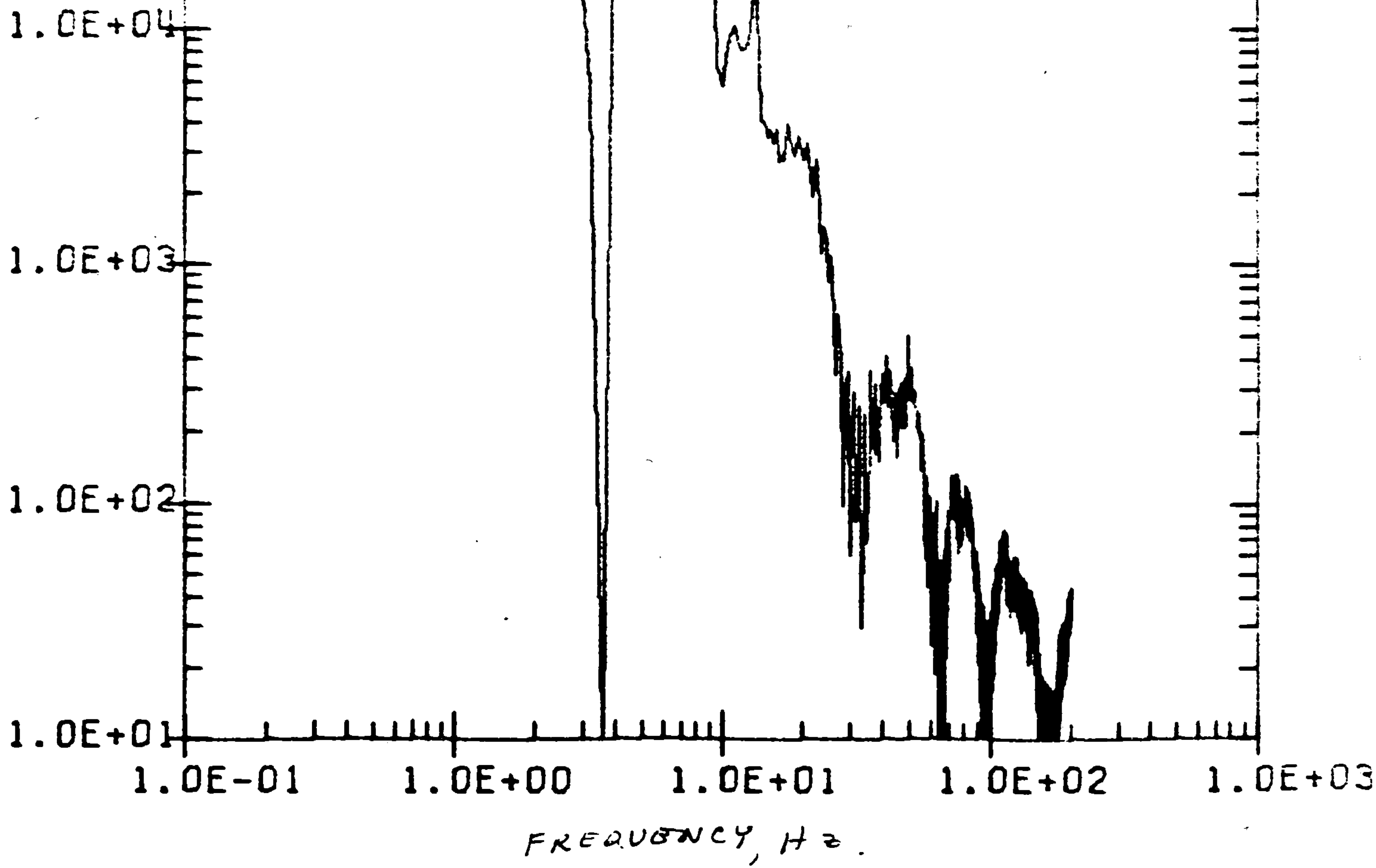

Figure D-16. Spurious Force Peaks, SL = 8000 and dT = 0.0025

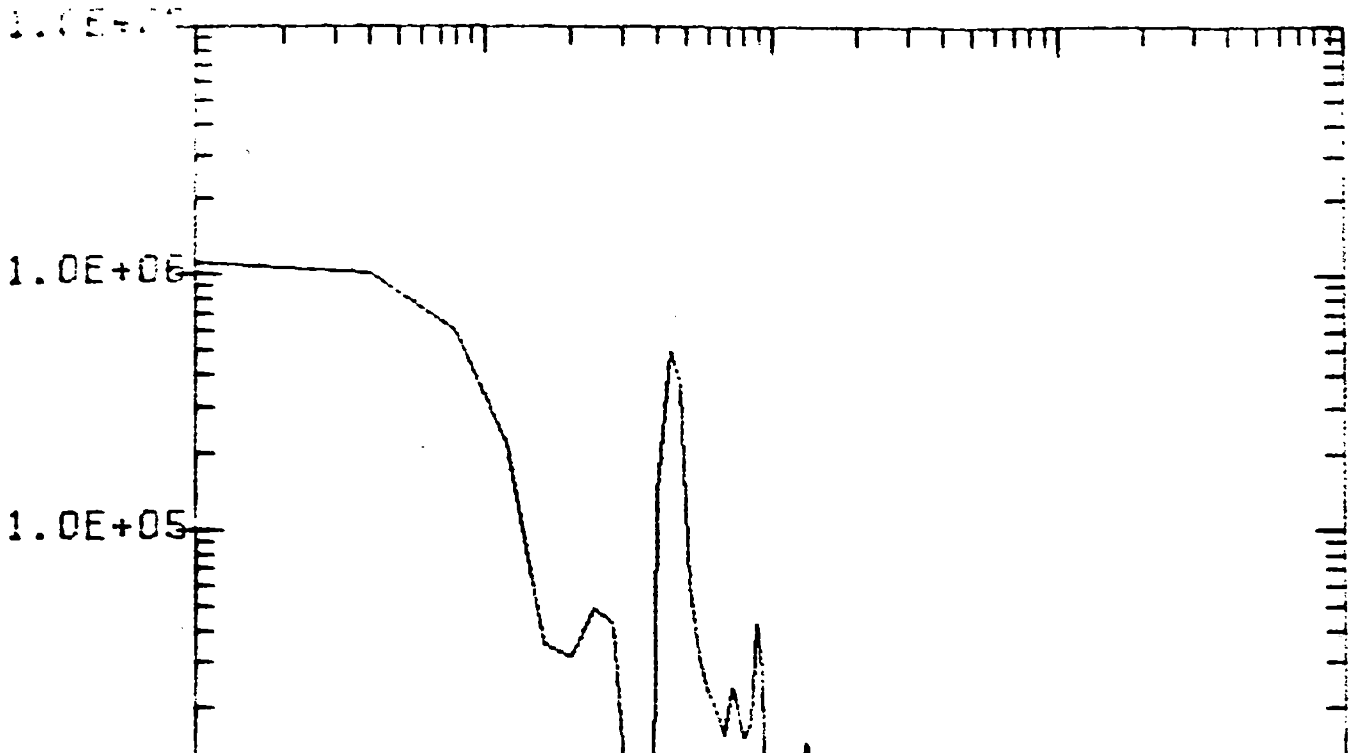

1.0E+06
1.0E+05

Table D-2. Estimated Stability Factor Requirements

ANALYTICAL OBJECTIVE	REQUIRED STABILITY FACTOR
Prediction of gross overall motions of large, rigid vehicles	20 - 100
Prediction of overall motions (or forces transmitted to rails) of flexible vehicles	10 - 20
Analysis of lading responses or lading environments, very flexible vehicle	5 - 10
Analysis of forces within friction snubbers	2 - 4
Extremely precise analysis of forces within friction snubbers	1 - 2

Note: Stability Factor = (Slope SL) x (Time Step).

attempt to apply this information should be checked by the normal procedure of repeating a typical analysis at several integration intervals and comparing the results.

Summary - Procedure

If coulomb damping is to be used with the FRATE class of programs, the following procedure is suggested:

a. Clearly establish the analytical objectives and the required outputs.

b. Estimate the highest significant frequency in the mathematical model.

c. Using Table D-1, estimate the minimum slope (SL) that will give adequate fidelity.

d. Using Table D-2, estimate the maximum acceptable time step or integration level.

e. Perform a typical analysis.

f. Cut the time step in half and verify that the required outputs do not change significantly.

g. If necessary, adjust the time step and proceed.

REFERENCES

1. DOT-FR-64200 "VSS Demonstration Program, Part 1, System Performance Evaluation," April 1976. FRA report #1

2. ANSYS Engineering Analysis System User's Manual, dated 1 March 1975.

3. O & M Manual for C/VPES

4. Hurty and Rubinstein, "Dynamics of Structures," Prentice-Hall, Inc.: 1964

5. Healy, M.J., "A Computer Method for Calculating Dynamic Responses of Non-linear Flexible Rail Vehicles," ASME Paper 76-RT-5, April 1976.

6. Healy, M.J., "A Computer Approach for the Analysis of the Dynamic Response of Linear or Nonlinear Rail Vehicles," Wyle Report 6.2.1.1, 1975.

7. Healy, M.J., "Math Modeling of TOFC Vehicles for the Demonstration Test Program," Wyle Laboratories, Colorado Springs Facility Report WR-76-003C.

8. Healy, M.J., "Assumptions in the Dynamic Response Computer Programs for Flexible, Nonlinear Rail Vehicles," Wyle Laboratories, Colorado Springs Facility Report WR-76-002C.

9. Ahlbeck, D.R. et al, "Comparative Analysis of Dynamics of Freight and Passenger Rail Vehicles," Battelle - Columbus, Report FRA-ORD&D, 74-39, March 1974.

10. "Truck and Carbody Characterization," Report on the Track-Train Dynamics Program, AAR, 1976.

11. Liepins, A.A., "A Digital Computer Simulation of Railroad Freight Car Rocking," ASME Paper 68-RR-3.

12. Harrison, H.L. and J.G. Bollinger, "Introduction to Automatic Controls", International Textbooks in Mechanical Engineering, 1963.

13. Hull, R. and N.K. Cooperider, "Influence of Nonlinear Wheel/Rail Contact Geometry on Stability of Rail Vehicles", ASME Paper 76 - WA/RT-2, December 1976.

14. "Freight Car Truck Design Optimization Project", Mathematical Modeling Report - Volume 1, Phase 1, Southern Pacific Transportation Company, July 1976.